Theoretical Modeling and Lateral Load Testing of Driven Steel Pile Bridge Bents

by

Zachary C. Skinner

A thesis submitted to the Graduate Faculty of
Auburn University
in partial fulfillment of the
requirements for the Degree of
Master of Science

Auburn, Alabama
May 4, 2019

Keywords: Lateral Load Tests, Deep Foundations, Driven Piles, Theoretical Modeling

Approved by

J. Brian Anderson, Chair, Ph.D., P.E. Associate Professor of Civil Engineering
Justin D. Marshall, Ph.D., Associate Professor of Civil Engineering
Robert W. Barnes, Ph.D., Associate Professor of Civil Engineering

Abstract

In this thesis, multiple lateral load tests on bridge bents were modeled and performed. FB Multipier models were created for eight load tests: four load tests conducted on a bridge bent under construction in an Alabama Macon County Road 9 bridge, two load tests on an in-service bridge on US Highway 331, and two load tests on battered and vertical pile bents constructed at the AUNGES site in Opelika, Alabama. These models were used to predict pile bent behavior under lateral loading conditions. The initial models predicted deflection amounts under load conditions selected to prevent in-service bridges from failing, and to ensure that failure could be reached for standalone bridge bents constructed for the project. After modeling was completed, full scale load tests were conducted on the bridge bents. The Macon County Road 9 bridge was subjected to four separate load tests: without the deck, with the deck and no load truck, with the deck and a load truck centered on the bent, and with the deck and a load truck centered over the edge girder. During each load test, the bent was loaded to approximately 75 kips. The US 331 bridge was tested with no load truck and with a load truck centered over the edge girder to approximately 90 kips. Two load tests were conducted at the AUNGES site, one on a battered pile bent and one on a vertical pile bent. Both bents were tested to failure at loads approaching 140 kip. Failure was seen in both cases at the pile to cap connection where the battered pile bent experienced rotation inducing a tensile pull out failure at the cap and the vertical pile bent drifted laterally until yielding occurred in the pile flanges. Models were then calibrated to match the observed pile behavior. Results show that vertical pile bents perform comparably to battered pile bents under lateral loads though they are less stiff. Vertical pile bents, however, do not experience the significant increases in axial load to the interior piles. Vertical pile bents should

be the preferred ALDOT bridge bent design due to their constructability and performance under lateral load.

Acknowledgments

I would like to take this space to thank everyone who played a role in the production of this thesis and in the completion of this degree. I would like to thank God and my family for continued support through my time in school and for all the opportunities that have been afforded to me. I would like to thank Johnathon Campbell for being a great partner and friend in the process to complete the various load tests required for this thesis. I would like to thanks Dr. Anderson and Dr. Marshall for their patience and guidance through the many challenges of this project. Thanks to Dan Jackson, Patrick Koch, Will Childs, Lester Lee, Billy Wilson, Pavel Voitenko, Joseph Broderick, and Taylor Rawlinson for their advice, friendship, and their time and energy on the long load test days in both the blazing heat and freezing cold. Thank you to the Alabama Department of Transportation for providing this research opportunity, Murphree Bridge for their cooperation in the Macon County Road 9 Bent testing, Scott Bridge Company, LLC. For the construction of the AUNGES test bents, and Skyline Steel for the donation of the piles used in the AUNGES tests.

Table of Contents

List of Tables

List of Illustrations

List of Abbreviations

AISC	American Institute of Steel Construction
ALDOT	Alabama Department of Transportation
AUNGES	Auburn University National Geotechnical Experimentation Site
NCAT	National Center for Asphalt Technology
PVC	Polyvinyl Carbonate
SPT	Standard Penetration Test

Chapter 1 Introduction

1.1 Introduction

This research was conducted to better understand the impact of lateral load on the axial capacity and overall behavior of driven steel piles used in a bridge foundation capacity. This research includes theoretical modeling and analysis of steel piles, and field load testing the modeled pile structures. Model results and field test results were compared to determine the accuracy of traditional modeling practice. Field test results were also used to calibrate the theoretical models so that future designs could better reflect the behavior observed in the full scale lateral load tests.

1.2 Defining the Problem

This research was focused on conducting preliminary models for the sizing and planning of full scale load tests, selection and instrumentation of full scale test bents, and the calibration of theoretical models to better understand the behavior of bridge bents under lateral load and advise what assumptions should be made during design.

1.3 The Proposed Solution

Detailed modeling and field load testing were selected as the best methods to produce the desired information. Representative ALDOT bridge bents were modeled and tested. Lateral load test results were compared to calibrated model results to determine if the theoretical models were able to accurately predict bent behavior.

1.4 Scope of Work

The research for this project was broken up into three phases: preliminary modeling, full-scale testing, and model calibration. Three test sites were selected for full scale load testing with detailed

modeling conducted prior to the execution of the lateral load tests. Modeling was conducted to predict cap deflections and pile forces during lateral testing. The models were used to select the maximum force for the lateral load tests so that in service bents would not suffer permanent damage. The first site was a bridge under construction located in Shorter, Alabama on Macon County Road 9. The selected bent was subjected to two lateral load tests, one prior to the casting of the deck, and one after the deck was cast. The bent featured four HP 14x89 piles with battered exterior piles and 30in diameter concrete encasements. The second bent tested was an existing bridge on U.S. Highway 331 in southern Montgomery County. The bent tested was constructed with six HP 10x42 piles with 16in square concrete encasements. The final test site featured two bents constructed for research only. Both bents were constructed with four HP 12x42 piles. The first bent was designed based on the standard ALDOT detail featuring battered exterior piles and 12 inches of embedment in the pile cap. The second bent was an experimental bent featuring all vertical piles embedded 18 inches into the pile cap. These two pile bents were tested to failure. After all field tests were complete, the resulting data was reduced to produce moment diagrams and deflection profiles. The field test results were compared to the initial model results. The models were the then calibrated to more closely match the observed behavior of the piles.

Chapter 2 Literature Review

2.1 Introduction

The literature review for this research covered various subjects used pertinent to the research project. The topics covered include finite element modeling using FB Multipier and the various inputs required to produce accurate models. Research on single and group pile capacity was reviewed to understand pile behavior under lateral loads, specifically the effect of lateral load on the axial capacity of piles. The lateral behavior of soil (p-y curves) and in situ tests used to determine the p-y curves were investigated for use in theoretical and calibrated modeling. Pile group effects were also reviewed to determine if the effects should be taken into account when determining the capacities of the bent piles. The connection of pile to pile cap was also researched to better compare the predicted and observed pile behavior. Limited research is available on the full-scale lateral testing of bridge bents. Most research focuses on single pile or group pile tests. For this research both single and group tests are pertinent as the piles in the bent are grouped together, but are often spaced far enough apart as to ignore group effects. Field load test procedures for both single piles and grouped piles were reviewed to prepare the load procedure for the field load tests conducted in this research.

2.2 FB Multipier

FB Multipier is modeling software used to analyze various types of geotechnical structures. The software requires the input of soil profiles and properties, structural geometries, and pertinent structural properties.

2.2.1 Soil Properties

Soil properties of the in place soil are required to produce accurate FB Multipier models. Each soil type modeled requires the input of different soil properties from unit weight to axial and lateral strength parameters. Strength parameters for cohesive soils included the undrained shear strength

and principal strain values under lateral loads. Strength parameters for cohesionless soils include the friction angle and the subgrade modulus, K_0.

2.2.2 Soil Structure Interaction

FB Multipier models break down soil behavior into lateral, axial, torsional, and tip categories. These categories have built in models derived from spring behavior. Lateral behavior is defined by a series of p-y curves that define the lateral deflection, y, a pile experiences under a certain amount of load, p.

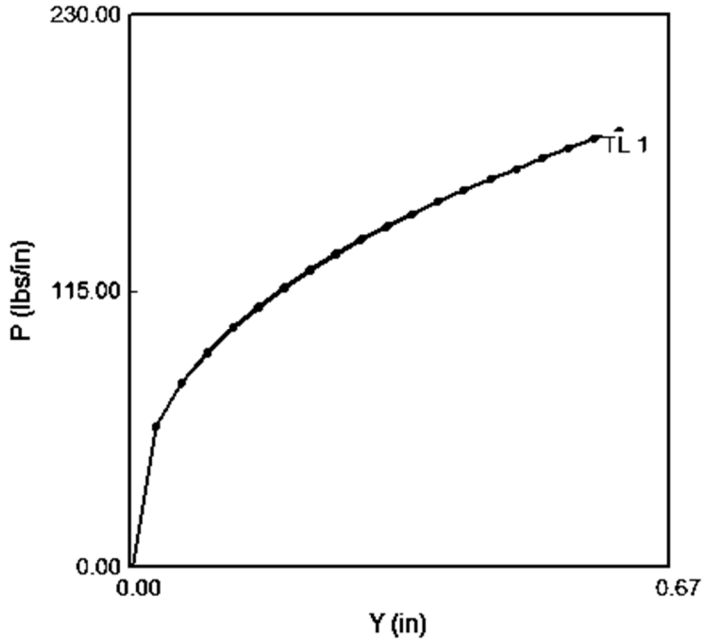

Figure 2-1 – O'Neill p-y Curve for Lateral Soil Behavior (McCarthy, 2007)

The axial behavior is defined by the type of structural element analyzed. T-z curves that define the amount of axial force required to move the structural element in a downward direction model the soil behavior during the installation process of the structural element.

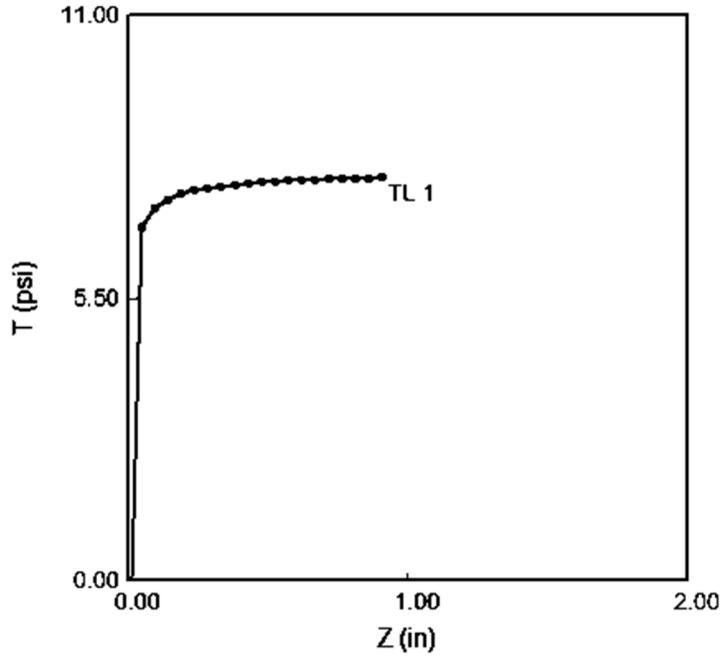

Figure 2-2 – Driven Pile T-z Curve for Axial Soil Behavior (McCarthy, 2007)

The torsional behavior is described by T-Theta curves that are defined as the force required to rotate a structural element.

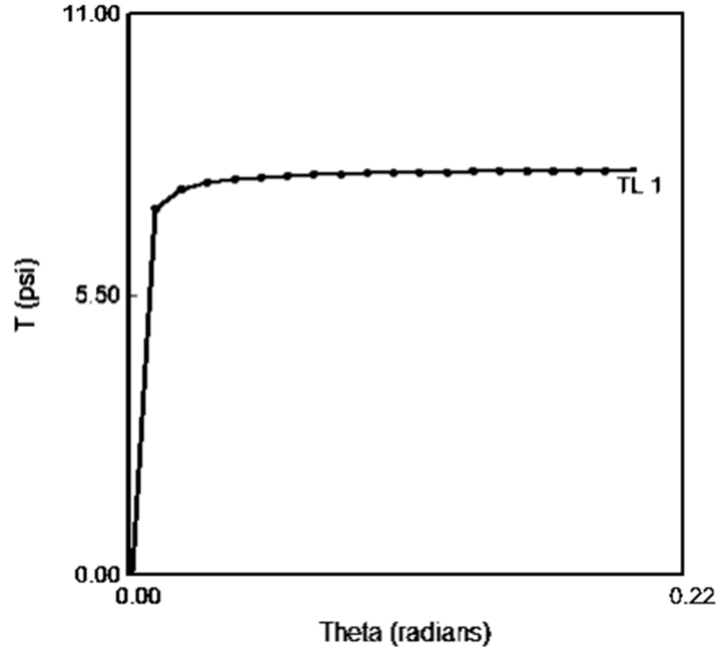

Figure 2-3 –Hyperbolic T-Theta Curve for Torsional Soil Behavior (McCarthy, 2007)

The tip model reflects the type of structural element analyzed. The built in Q-z models are used to simulate the installation process of the selected structural element.

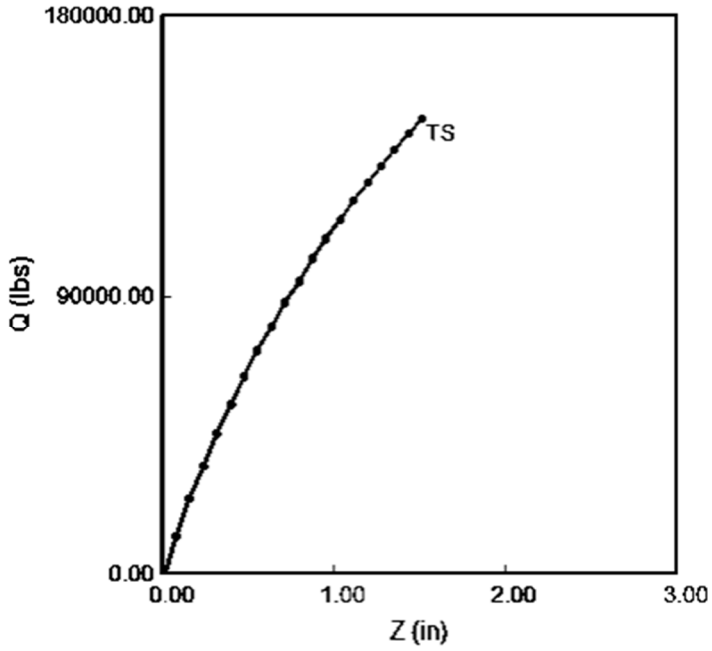

Figure 2-4 – Driven Pile Q-z Curve for Tip Soil Behavior (McCarthy, 2007)

2.2.3 Structural Behavior

The structural elements in FB Multipier can be analyzed by considering either gross section properties or full cross section properties. The software analyzes the structural elements as linear elastic elements until yielding is determined. Yielding is considered as failure when the software analyzes the bent model. The concrete elements modeled in the software include the bent caps and encasements. Concrete elements require the following data for analysis: unit weight, compressive strength (fc'), and young's modulus. The software also generates the reinforcement layout in the bent cap to accurately model the bent cap behavior. The steel elements modeled include the steel reinforcement and driven piles. The steel properties required for analysis include: unit weight,

yield stress, and elastic modulus. The piles modeled also required the input of section properties such as depth, web thickness, flange width, and flange thickness.

2.2.4 Pushover Analysis

FB Multipier contains built in programming to test a bent to failure. This program requires two load cases. The first load case is used to specify the initial conditions. The second load case specifies what condition increases. The amount of load on the bent increases in each load case by the amount of load specified in the second load case. The number of load cases allowed to run is specified prior to running the analysis. FB Multipier will then run the analysis for each specified load case until the bent fails.

2.3 Soil Structure Interaction

Geotechnical structures interact axially and laterally with the soil surrounding them. Geotechnical design focuses on understanding, quantifying, and predicting these behaviors. The following sections detail the general methods used to calculate axial capacity and predict lateral behavior of driven piles in cohesive and cohesionless soil.

2.3.1 Axial Capacity

Pile capacity is developed through end bearing and side friction. Figure 2-5 shows a graphical representation of the components of pile capacity.

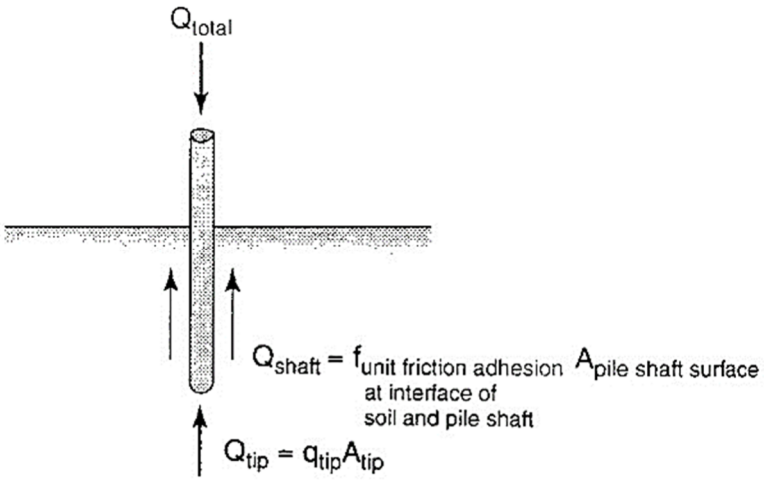

Figure 2-5 – Pile Capacity Theory (McCarthy, 2007)

The end bearing capacity for piles is a function of the pile's end area and the strength of the soil itself. Equation 1 shows the equation used for the calculation of end bearing pressure adapted from the calculation of bearing capacity for shallow foundations (McCarthy, 2007).

Equation 1: $\boldsymbol{q_{tip} = cN_c + 0.4\gamma BN_\gamma + \sigma'_v N_q}$

Where

$q_{tip} = End\ bearing\ capacity\ at\ pile\ tip$

$c = Cohesion\ shear\ strength\ of\ soil$

$N_c = N_\gamma = N_q = Bearing\ capacity\ factors\ for\ deep\ foundations$

$B = Pile\ tip\ diameter$

$\gamma = Unit\ weight\ of\ soil$

$\sigma'_v = Effective\ vertical\ Stress$

Equation 2 shows how the bearing capacity of the soil is used to determine the contribution of end bearing capacity to the overall capacity of the pile.

Equation 2: $Q_{tip} = q_{tip}A_{tip}$

Where

$Q_{tip} = Pile\ end\ bearing\ capacity$

$A_{tip} = Area\ of\ pile\ tip$

The second portion of pile capacity is developed through friction between the pile and the soil. The friction force is developed as the pile is driven through soil. Figure 2-6 shows graphically the theory behind the calculation of side friction. The side friction is derived from a pile sliding against soil particles. The amount of friction is dependent on the type of pile and the horizontal stress condition of the soil.

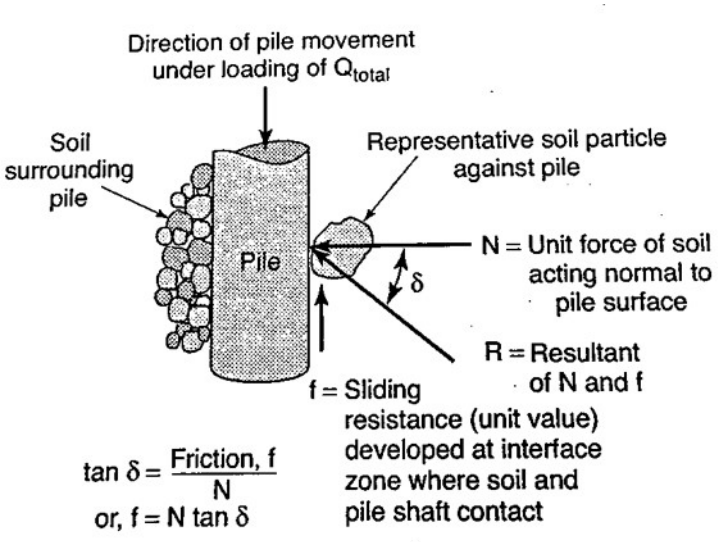

Figure 2-6 – Side Friction Theory (McCarthy, 2007)

The Beta method is a technique used to calculate the unit friction adhesion between the surface of the pile and the soil and the friction contribution to the overall pile capacity. Equation 3 shows the calculation of the unit side friction created by the pile being driven into soil.

Equation 3: $f_{soil} = \beta\sigma'_v$

Where

$f_{soil} = \ Unit\ friction\ adhesion\ between\ the\ surface\ of\ the\ pile\ and\ soil$

$\beta = Beta\ coefficient$

The Beta coefficient takes into account the horizontal strength of the soil and the type of pile analyzed. The calculation of the coefficient is shown in Equation 4.

Equation 4: $\beta = Ktan(\delta)$

Where

$K \ = \ Lateral\ earth\ pressure\ coefficient$

$tan(\delta) = Interface\ coefficient$

Once the unit skin friction has been calculated, it is used with the embedded area of the pile to calculate the side friction capacity. The calculation is shown in Equation 5.

Equation 5: $Q_{shaft} = \ f_{soil}A_{shaft}$

Where

$Q_{shaft} = \ Side\ friction\ capacity\ of\ the\ pile$

$A_{shaft} = Effective\ surface\ area\ of\ pile\ embedded\ in\ soil$

The total capacity of the pile is determined using Equation 6.

Equation 6: $\boldsymbol{Q_{Total} = \ Q_{tip} + \ Q_{shaft}}$

Where

$Q_{Total} = \ Total\ axial\ pile\ capacity$

2.3.2 Lateral Load Transfer

P-y curves are used to characterize the lateral behavior of soil. The soil is modeled as a series of nonlinear springs acting at various locations along the depth of the pile. Figure 2-7 shows a series of theoretical nonlinear springs acting on a driven pile. As the pile deflects, the soil resistance increases as the theoretical springs compress. As lateral load increases the soil will push back until the shear strength of the soil is overcome or the structural element fails. Figure 2-8 shows a p-y curve developed during this research from dilatometer data to illustrate the typical lateral behavior of soils.

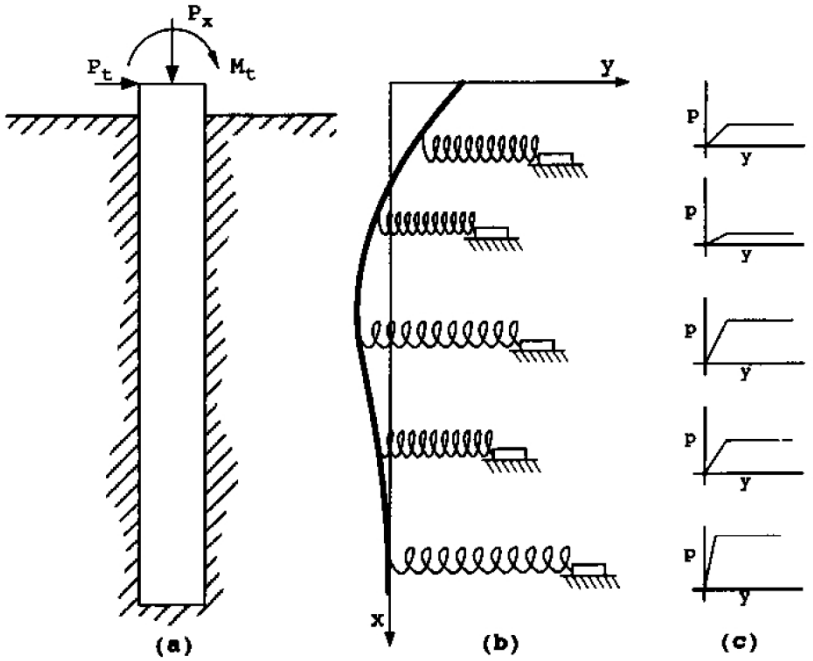

Figure 2-7 –Nonlinear Springs Acting on a Driven Pile (Reese & Wang, 2006)

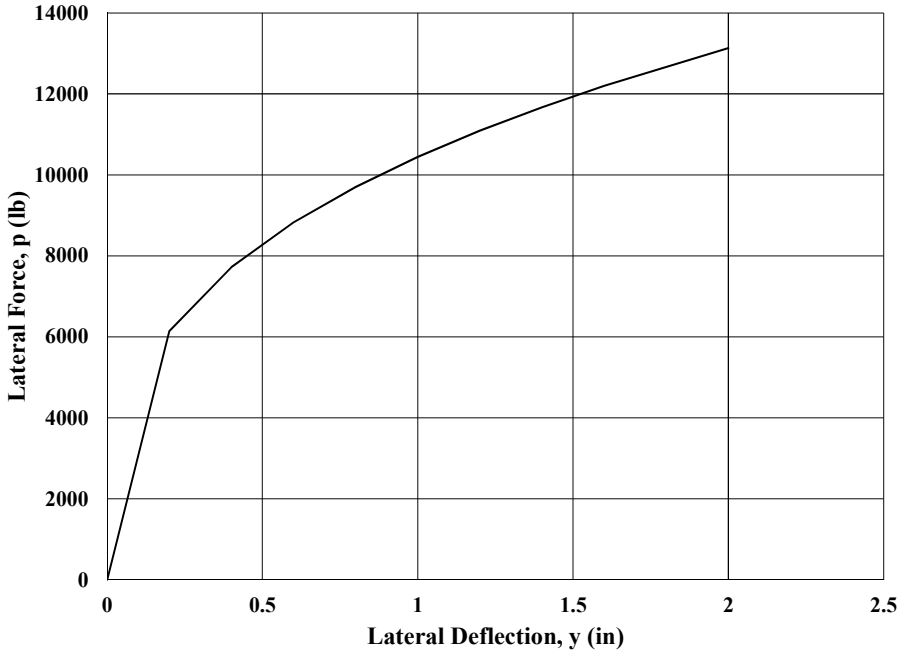

Figure 2-8 – Sample p-y Curve

2.3.3 Dilatometer Developed p-y Curves

The dilatometer is a tool for in place exploration of soil conditions and is used to determine soil properties. The test is run by pushing the blade-like probe into the ground at a measured pace.

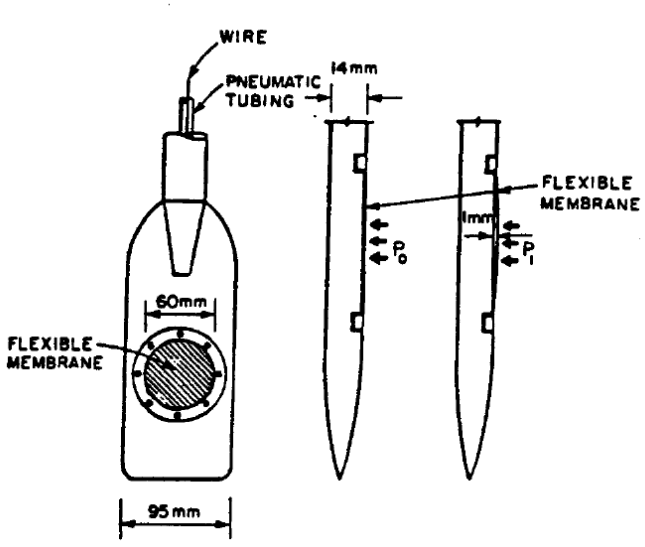

Figure 2-9 – Dilatometer Blade (Robertson, Davies, & Campanella, 1989)

Figure 2-10 – Dilatometer in Use

Every 20 centimeters a pressure membrane is inflated with compressed nitrogen until the membrane touches the soil. The pressure required to inflate the membrane and the force required to push the probe are recorded for each test depth. The data recorded is used to create a soil profile. The readings are used to determine the soil type, unit weight, and pertinent strength parameters. Dilatometer test data has been used to create p-y curves for use in soil modeling software such as FB Multipier. The dilatometer p-y curves are particularly useful and accurate for driven pile analysis since the dilatometer can be considered a small-scale model of a driven pile (Robertson, Davies, & Campanella, 1989). The following method is used to determine the p-y curves of cohesive soils. Equation 7 is the cubic parabola used to model the soil spring behavior of the soil proposed by Matlock.

Equation 7: $\frac{P}{P_u} = 0.5\left(\frac{y}{y_c}\right)^{0.33}$

Where

$$\frac{P}{P_u} = Ratio\ of\ soil\ resistance$$

$$\frac{y}{y_c} = Ratio\ of\ Pile\ deflection$$

Equation 8 is used to calculate the reference deflection for the soil based on the soil and pile properties.

Equation 8: $y_c = \frac{23.67 S_u D^{0.5}}{F_c E_D}$

Where

$y_c = Reference\ deflection$

$S_u = Undrained\ shear\ Strength$

$D = Pile\ diameter\ in\ cm$

$F_c = 10, an\ approximation\ for\ cohesive\ soils$

$E_D = Dilatometer\ modulus$

Equation 9 is used to calculate the ultimate lateral resistance for use in Matlock's cubic parabola approximation.

Equation 9: $P_u = N_P S_u D$

Where

$P_u = Ultimate\ static\ lateral\ resistance$

$N_P = Nondimensional\ ultimate\ resistance\ coefficient$

Equation 10 is used to calculate the nondimensional ultimate resistance coefficient which is a function of depth and effective stress.

Equation 10: $N_P = 3 + \frac{\sigma'_{vo}}{S_u} + \left[J\frac{x}{D}\right]$

Where

$\sigma'_{vo} = Effective\ vertical\ stress\ at\ depth\ x$

$J = Empirical\ coefficient$

$x = Depth$

The above equations are used to calculate deflections based on the load applied to a pile. The y_c and P_u values are plugged into Equation 7. The resulting relationship is used to define the lateral behavior of the soil. To calculate the profile, discrete deflection values are chosen, and the resulting force values represent the force required to cause the input deflection.

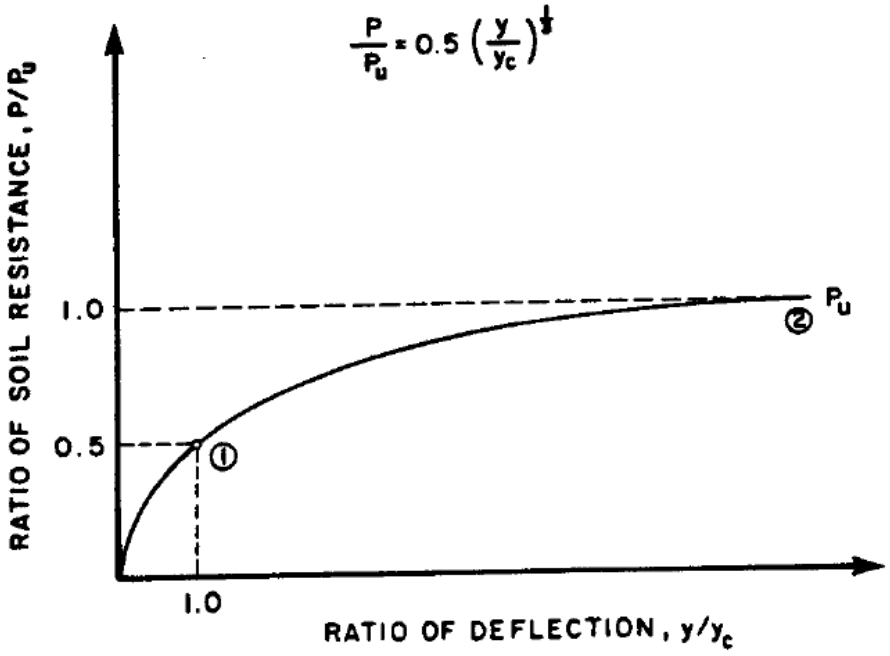

Figure 2-11 – Matlock's Cubic Parabola Approximation of Soil Spring Behavior (Robertson, Davies, & Campanella, 1989)

2.3.4 Pile Group Effects

The spacing of piles affects the capacity of the entire group. As pile spacing decreases, the load carrying capacity for each individual pile decreases for piles behind the leading pile. This affect is known as pile shadowing. Modification factors known as p-multipliers are used to reduce the pile capacity in modeling software. Figure 2-12 shows the standard p-multipliers used for pile group capacity analysis.

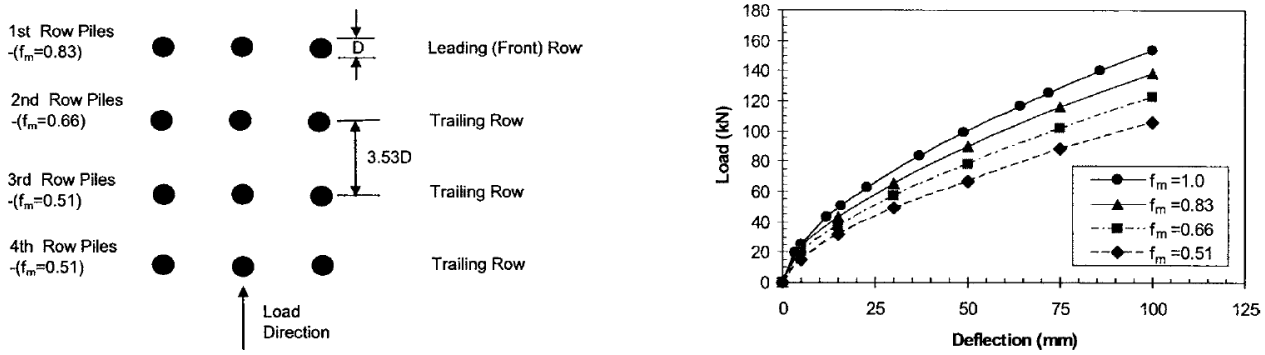

Figure 2-12 – Pile Group Configuration and Corresponding p-Multipliers for each Row of Piles (Rollins, et al., 2006)

Research suggests that when the pile spacing approaches 5 pile diameters the p-multipliers begin to approach 1 quickly, but do not actually reach 1 until reaching 6.5 to 7 pile diameters (Rollins, et al., 2006). Calculations show that the p-multipliers calculated when pile spacing approaches 5 pile diameters can be neglected as they begin to approach 1.

2.4 Pile to Cap Connection

The pile to cap connection is an important consideration when modeling pile bent behavior. The fixity of the pile head is a major factor in the lateral response of the piles. The more fixed the pile head the less rotation at each individual pile head and the less overall bent cap deflection the group of piles experiences. As pile head fixity increases, the bent deflection decreases. The fixity also affects the load transfer from the bent to the pile. A fixed connection creates more moment

development in the piles whereas a pinned connection allows for more rotation at the pile heads which induces for more sway for the bent and potentially higher axial loads in the piles. Understanding the nature of the connection allows for a better understanding of the bent behavior under lateral load. Modeling software requires that the connection be considered either fixed or pinned, but research shows that the connection is neither completely fixed nor completely pinned. The degree of fixity varies, but the added restraint of the cap increases the stiffness of the pile group above the stiffness of a single pile (Gerber & Rollins, 2009). Figure 2-13 Shows data from a Gerber and Rollins research project. The figure shows that the measured behavior of the pile cap falls between the theoretical calculations for the fixed head and free head (pinned) conditions.

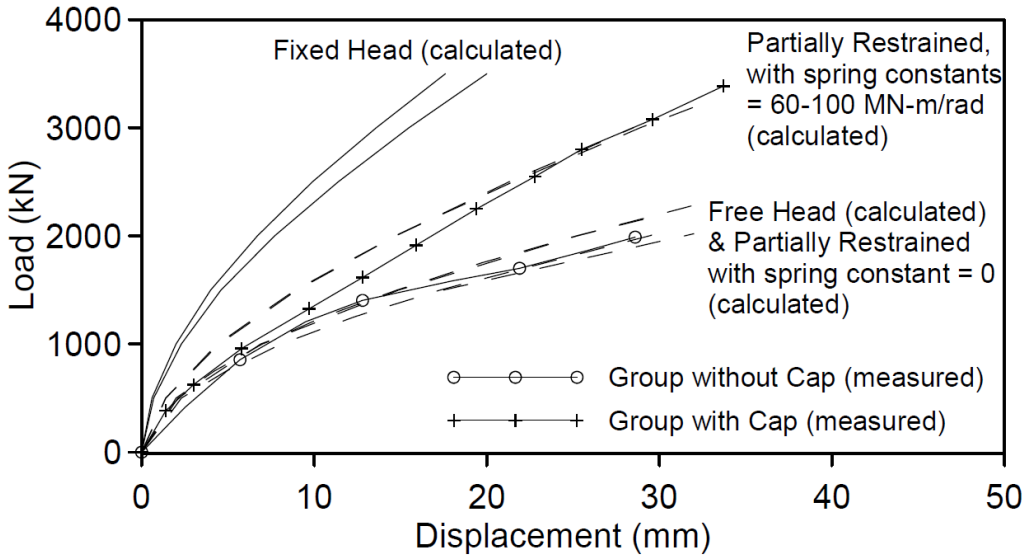

Figure 2-13 – Behavior of Pile Group with and without Cap (Gerber & Rollins, 2009)

2.5 Lateral Load Testing Procedure

Lateral load test procedures are outlined in ASTM D 3966 (American Society For Testing And Materials, 1995). Load tests are conducted by applying a load to a structure for a specified amount of time. The load procedure follows a load schedule that steps up the load on the structure.

Table 2.1 – ASTM D 3966 Suggested Loading Schedule

Standard Loading Schedule	
Percent of Design Load	Load Duration, min
0	—
25	10
50	10
75	15
100	20
125	20
150	20
170	20
180	20
190	20
200	60
150	10
100	10
50	10
0	—

Traditional load tests are conducted on single piles and pile groups where the pile head is at the ground surface. Figure 2-14 shows the typical loading schematic for a single pile lateral load test.

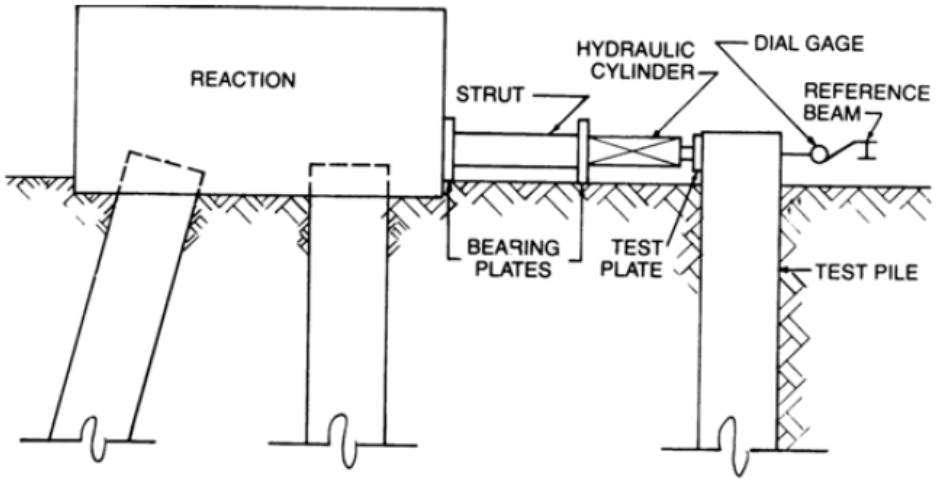

Figure 2-14 – ASTM D 3966 Lateral Load Test Load Schematic

Lateral load tests require the presence of a reaction pile and or reaction bent to apply the lateral load into the test bent. Generally hydraulic jacks are used to generate the lateral load for field testing. These jacks can be placed between the test and reaction bent and push the two apart, or the jack can be place on the outside of the reaction bent and used to pull the test and reaction bents together. Rods, struts, or high strength cables can be used to transfer the lateral load from the jacks

and the reaction bent to the test bent depending on the location of the hydraulic jacks. Bearing pads and plates are used to spread the load to the test bent to prevent localized failures in the test bents and to assure even distribution of load to prevent eccentricity in the loading process. Deflections are measured by establishing a reference point that does not move during testing. Instrumentation is used to measure the movement of the test system in reference to the established reference point. This is used to monitor and record the lateral response behavior during load testing.

2.6 Inclinometer Theory

Inclinometer probes are used to determine the deflected shape of geotechnical structures. The inclinometer probe is comprised of two gyroscopes situated a fixed distance apart. Profiles are created by running the inclinometer probe down to the bottom of a casing attached to the geotechnical structure. The probe is pulled back up the casing and readings are taken at every two foot interval. Two gyroscopes measure the slope of the pile. The difference in slope between the two gyroscopes is used to calculate the average curvature at discrete points along the pile length. This is used to create a deflected shape profile for the piles. The profile is taken in one direction and then rotated 180 degrees to account for any error in the reading. Figure 2-15 illustrates the theory behind the data reduction used to calculate the deflected shape of the structural element. The readings are used to determine the radius to a reference circle, R. deflections are calculated by subtracting the initial observed R value for the unloaded condition from R values calculated under loaded conditions. This produces deflection profiles from the observed baseline test.

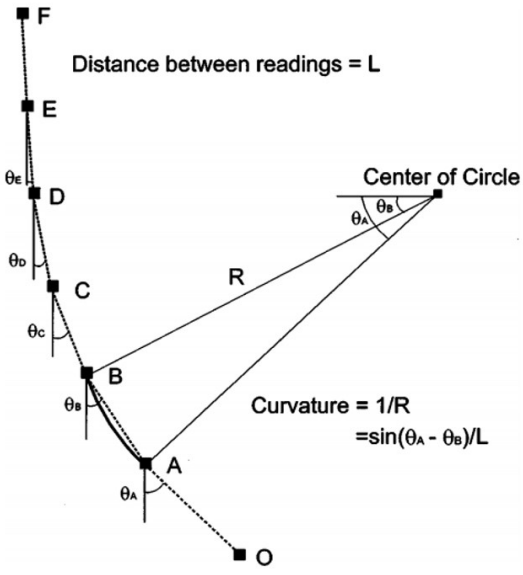

Figure 2-15 – Inclinometer Theory (Ooi & Ramsey, 2003)

Deflected shape profiles for the structural elements are created by building a profile for the unloaded condition and creating a profile at each subsequent load. The deflected shape for each load case is created by calculating the difference in the shape of the subsequent load cases and the baseline case. The deflected shape can be used to calculate the corresponding bending moment profile for the tested structural element. These bending moment profiles can be used to calibrate analytical models to accurately reflect the actual behavior of the structural element.

2.7 Group Load Test Case Studies

With few load tests on bridge bents available, research was focused instead on full scale load tests deep foundation groups. The load tests studied had many similarities with the research conducted for this thesis. They featured deep foundations grouped together and encased in a concrete cap. The main difference was that the pile groups tested had pile caps on or at the ground surface. A few of the load tests will be discussed in this literature review with emphasis place on the elements of the load tests that were incorporated into this research.

The first load test reviewed was conducted at two sites, Wilmington, North Carolina, and the AUNGES test site in Opelika, Alabama (Brown, O'Neill, McVay, El Naggar, & Chakraborty, 2001). For these load tests, 10.75 inch outside diameter piles were used. The pipe piles were ½ inch thick. Load testing was conducted to understand the effect of pile spacing on group behavior under static and dynamic loading scenarios and to better understand the dynamic behavior of pile groups. Static load tests were conducted using hydraulic jacks and load frames. These methods, and indeed the piles themselves would be used for the research conducted in this thesis. The first load tests were conducted at the Wilmington, North Carolina site. The piles were instrumented and tested as a group without a concrete cap. A steel load frame was used to induce group behavior. At the AUNGES site, the piles were tested first in a 4 by 3 configuration, and then a 3 by 3 configuration. The 3 by 3 configuration also featured a full concrete cap and was the last load test conducted. The piles were left in place. This pile group would later be used as a reaction bent for the AUNGES testing of this research. Soil properties included in the report used when developing soil profiles for initial models of the AUNGES test bents.

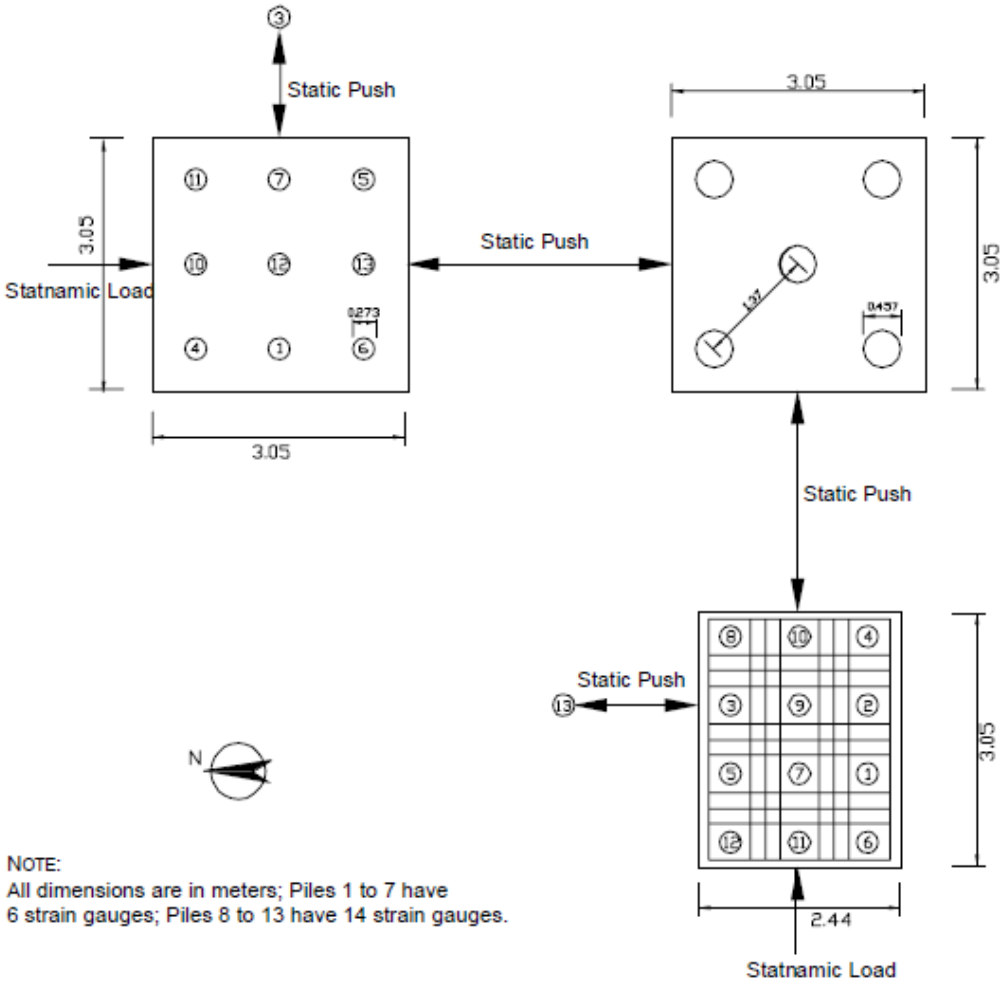

Figure 2-16 – AUNGES Load Test Configuration (Brown, et al)

The piles in the Brown AUNGES research were instrumented along the pile length. The same method was used for the AUNGES tests of this thesis. Loading increments were held for around 5 minutes each for static loading. Data reduction used all the data points recorded in the time frame to account for load creep and the loss of jack pressure during the loading process. Results from these load tests suggested that the group effects could not be ignored during modeling and data reduction for piles installed at the AUNGES site specifically (Brown, et al).

The next load testing case study was conducted to better understand the pile to cap connection details (Rollins & Stenlund, 2010). Rollins and Stenlund constructed four pile groups.

Each pile group featured different connection and cap details. Two pile caps relied on rebar and embedment depths of 6 and 12 inches. The third and fourth pile caps only relied on embedment. The piles tested were 12.75 inch outside diameter pipe piles. Cyclic loads were applied to the pile caps until failure of the pile caps. Data collected was used to determine the effect of embedment and rebar on the fixity of the pile to cap connection. Results of Rollins and Stenlund's research showed that the best model for pile group behavior is a fixed connection. Load test results were accurately predicted at lower levels of deflection. These results were used in this thesis as all piles were modeled with a fixed connection due to the embedment depth of the piles and the presence of a reinforcing cage within the cap. Rollins and Stenlund also showed that the compressive strength of the concrete would often be a limiting factor in the moment capacity of the pile to cap connection. In this thesis, concrete cylinders were used to determine the in place compressive strength of the AUNGES test bents so that models would more accurately predict the behavior of the piles and pile cap during full scale load tests.

Eberhard and Marsh conducted full scale load tests on existing bridge bents (Eberhard & Marsh, 1997). Testing was conducted on a bridge scheduled for demolition. The testing intended to investigate the capacity and stiffness of the bent, and to determine the effectiveness of analytical models. Eberhard and Marsh's test was significant to the research presented in this thesis because the load test was conducted on a full size and in-service bridge bent. Figure 2-17 shows the load configuration of the Eberhard and Marsh bent tests. Prestress reinforcing cables and hydraulic jacks were used to load the bent. The bent and bridge were to remain open to traffic during testing. Principles from this load test would be used in the Highway 331 bridge testing presented in this thesis. Results from Eberhard and Marsh showed that the common analytical methods were

effective in creating models that reflected the behavior of the bent. Similar standard analytical methods were used to produce the models and structure properties presented in this thesis.

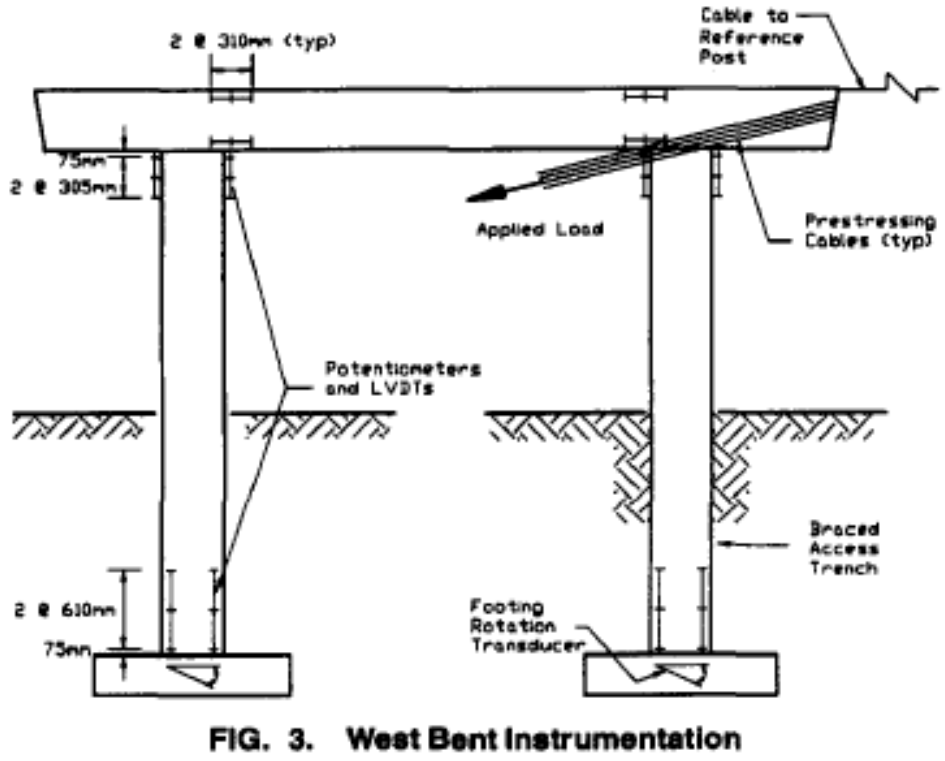

Figure 2-17 – Eberhard and Marsh Bent Load Test Configuration (Eberhard & Marsh, 1997)

In Possiel's 2008 thesis on pile fixity, several pile caps were tested in a laboratory setting, and multiple bridges were modeled using FB Multipier. Possiel's thesis sought to understand how the depth of the pile effected the fixed behavior of the pile. Single pile pile caps were constructed and tested with an actuator. The piles were fitted with gauges and the resulting data was used to determine the fixed behavior of the pile. The data was used to calibrate FB Multipier models and determine stiffness factors for use in modelling actual bridges. Possiel used field determined shear factors to model the load test behavior of the pile. Per Possiel, the fixity of the pile cap connection affected the fixed behavior of the pile in the ground (Possiel, 2008). All FB Multipier models for

this research assumed that the piles behaved in a fixed manner due to the fixed connection of the pile to cap connection and the depth to which the piles were driven.

Ruesta and Towsend also conducted load tests on pile groups. They investigated the behavior of prestressed piles on the Roosevelt Bridge in Stuart, Florida (Ruesta & Townsend, 1997). These load tests were conducted on a 4x4 pile group. Initial testing was done on a single pile identical to the piles installed in the pile group. Load testing was conducted to determine the observed p-y curves and compare them to theoretically computed curves. Also, testing of the initial pile would be compared to the overall performance of the pile group. This would provide insight into any group effects that reduce the capacity of a single pile within a pile group. Group effects could be modeled and predicted effectively using p-multipliers that assume a percentage of the capacity of a single pile. These principles would factor into the research presented in this thesis. When modeling the bents for this research, p-multipliers were used to produce calibrate models of bent behavior to match full-scale load testing results. Ruesta and Townsend also observed that outer piles experienced the most load during lateral loading. This trend would continue in the research presented in this thesis as the outer pile in the bents experienced greater bending moments than the inner piles.

Chapter 3 Preliminary Modeling and Behavior Prediction

3.1 Purpose

Comprehensive modeling using FB Multipier was conducted prior to full-scale field lateral load testing. Models simulated the existing soil conditions and the pile properties to predict the bent behavior during load testing. The models were used to predict the axial forces, flexural moment, and lateral deflection caused by the application of lateral load. The models were used to simulate loading schedules of the full-scale lateral load tests. The models were also used to determine the maximum load to apply to the bents and to size the jacks needed to test the bents. Model predictions for axial load profiles, moment profiles, and lateral deflection were compiled for each pile and compared to data gathered from field load tests. The comparison of results is shown in Chapter 6 of this thesis. After load testing, the models were refined and calibrated to the results of the field load tests. These calibrated models were used to determine the load path of lateral load in bridge bents for the effective prediction of behavior in lateral loading scenarios.

3.2 Overview

FB Multipier models were created for each bridge bent and reaction bent studied in this project. Soil properties from site specific soil exploration reports were used to determine the soil properties for each layer of soil in the FB Multipier soil profile. The geometries and properties of the structural elements of the bents were acquired from design documents provided by ALDOT. Where available, field data such as concrete compressive strength was used in the models to make more accurate predictions of bent behavior.

Initial models were run to assess the magnitude of deflection expected to occur under lateral load testing. A target load was determined and simulated on each bent cap. In the case of the in-service bridges, the resulting prediction was used to determine if the target load created a sufficient,

but not excessive, amount of force to be accurately measured in the field load testing operations. The AUNGES bents were designed to be tested to failure. Initial models were run to predict the amount of force required to fail the bents. The target values were used to create a loading schedule to be used in the field load tests. The target values were analyzed in FB Multipier to produce detailed profiles of behavior prediction for each pile during each load test. The results of these simulated load tests are presented in this chapter. The profiles were compared to the values determined from the data reduction of the load test data.

3.3 Macon County Road 9 Bridge

The Macon County Road 9 bridge was a bridge project under construction in the summer of 2014. The model bent featured four 31.5 feet long HP 14x89 piles with 5 feet of clear height above ground. The exterior piles were battered at 1.5/12 slope. All piles were encased with 30 inch diameter concrete encasements from the bottom of the pile cap to 5 feet below the expected ground surface. The piles were oriented for weak axis bending in the direction of lateral loading. The cap was modeled as a 31.75 inch by 31.75 inch square cap to approximate trapezoidal cap shown in the construction documents.

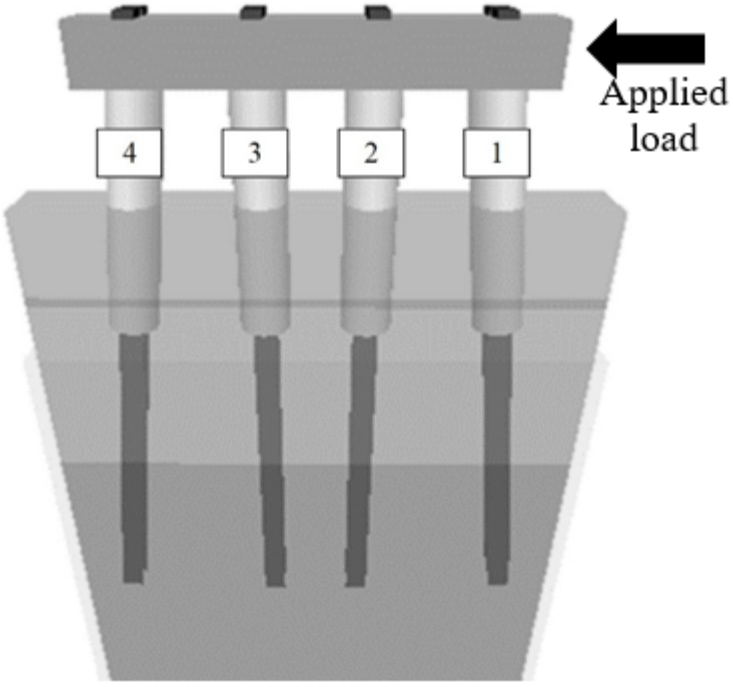

Figure 3-1 – FB Multipier Rendering of Macon County Road 9 Bridge Bent

The preliminary model was created using the bridge design plans and the boring logs provided by ALDOT. The geometric pile properties were taken from the AISC Steel Construction Manual (American Institute of Steel Construction, 2011). An initial estimate of 5,000 psi was used for the compressive strength of the concrete encasements. The steel piles were modeled using the FB Multipier default elastic modulus of 29,000 ksi and yield stress of 60 ksi. The p-y, q-z, and t-z curves for each soil layer were constructed from default FB Multipier options. The simulated load test featured ten load increments. The increments were as follows: 10 kips, 20 kips, 30 kips, 40 kips, 50 kips, 55 kips, 60 kips, 65 kips, 70 kips, and 80 kips. The axial load and bending moment predictions were compiled at node locations along the length of each pile for the distinct loading increments. The centerline horizontal displacement of the pile cap was also recorded at each loading increment. The first model created simulated the initial construction condition of the bent

without the bridge deck in place. The second model simulated the bent with additional stiffness due to the addition of a bridge deck. It was assumed that the addition of a bridge deck created additional stiffness in the test bent due to the weight of the deck resisting lateral movement and the incorporation into the completed bridge which would create alternate load paths for the resistance of lateral load. The third model included the loading of an LC-5 ALDOT load truck centered over the roadway and bent. The fourth model included the load truck with the outer wheel centered over the exterior girder opposite of the applied lateral load. A fifth model was created to simulate the reaction bent needed to field test the bent. The reaction model was subjected to the expected maximum magnitude of loading to ensure the design had sufficient strength and did not experience excessive deflection. Piles were named Pile 1, Pile 2, Pile 3, and Pile 4. Pile 4 was the leading pile, furthest away from the applied load and was battered. Pile 1, also battered, was the trailing pile closest to the load application point. Piles 2 and 3 were both vertical interior piles. This naming convention was used in every model simulation for the Macon County Road 9 bent. The piles were spaced at 8 feet center to center at the top of pile. This spacing was greater than five times the diameter of the pile. Therefore, p-multipliers to reduce the lateral capacities of the piles were not needed and were not included in any model simulations.

3.3.1 Soil Properties

Boring logs were provided in the design drawings from ALDOT. SPT N-counts were used to construct a soil profile representative of the soil the piles were driven into. The soil was modeled in four discrete layers. Correlations of N-count values to soil properties such as friction angle and undrained shear strength were used. Figure 3-2 shows the pertinent soil parameters developed from the provided boring logs.

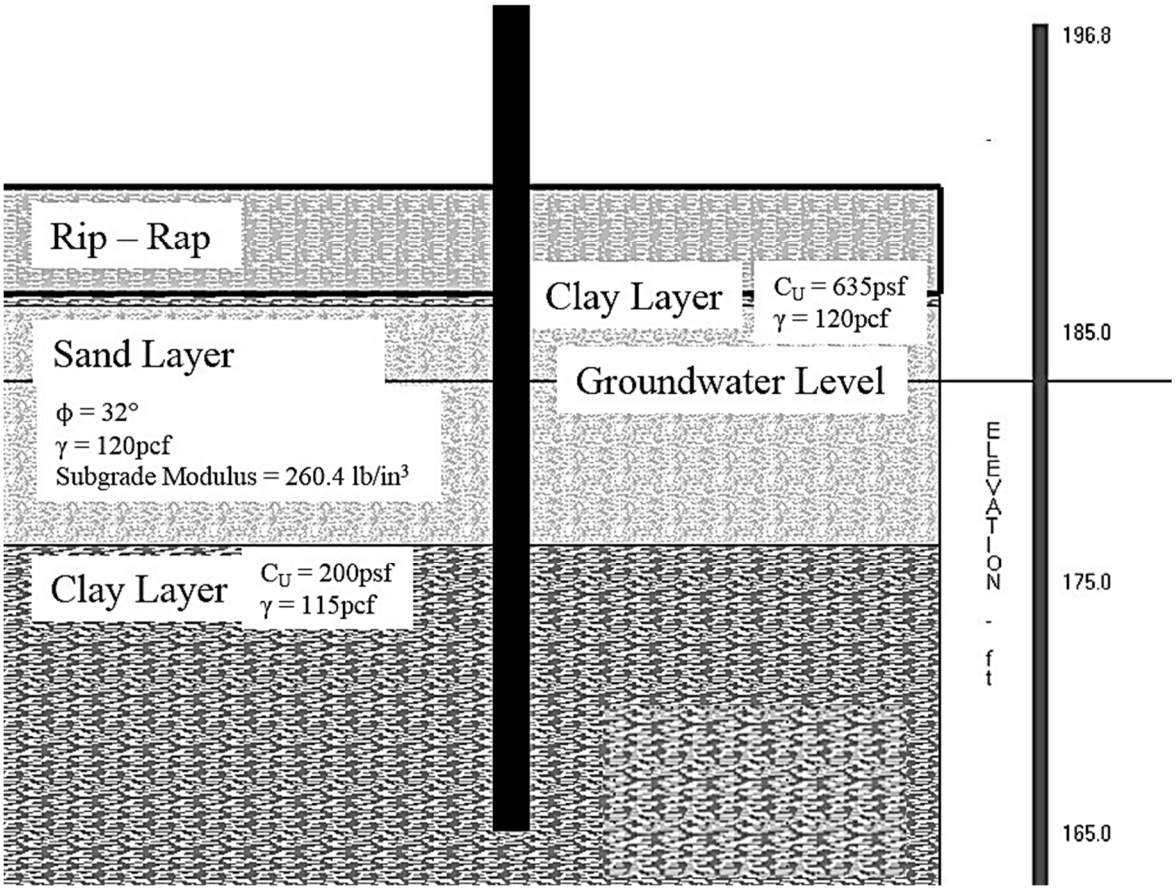

Figure 3-2 – Macon County Road 9 Bridge Soil and Pile Profile (Adapted from FB Multipier)

The top layer of clay was removed and replaced with rip-rap for scour resistance. The remaining soil was a small clay layer, a sand layer, and a bearing layer of clay. The rip-rap was neglected during the model simulation due to the uncertainty in accurately modeling rip-rap properties during simulation. The soil profile and properties discussed above were used for each load test simulation of the test bent and the reaction bent model.

3.3.2 Pre-Deck Bent Model and Behavior Prediction

The initial model was designed to simulate the first load test, which would occur prior to the casting the bridge deck. The bent was modeled as a single, stand-alone bent. Figure 3-3 shows the predicted load versus deflection behavior of the bent without added deck stiffness.

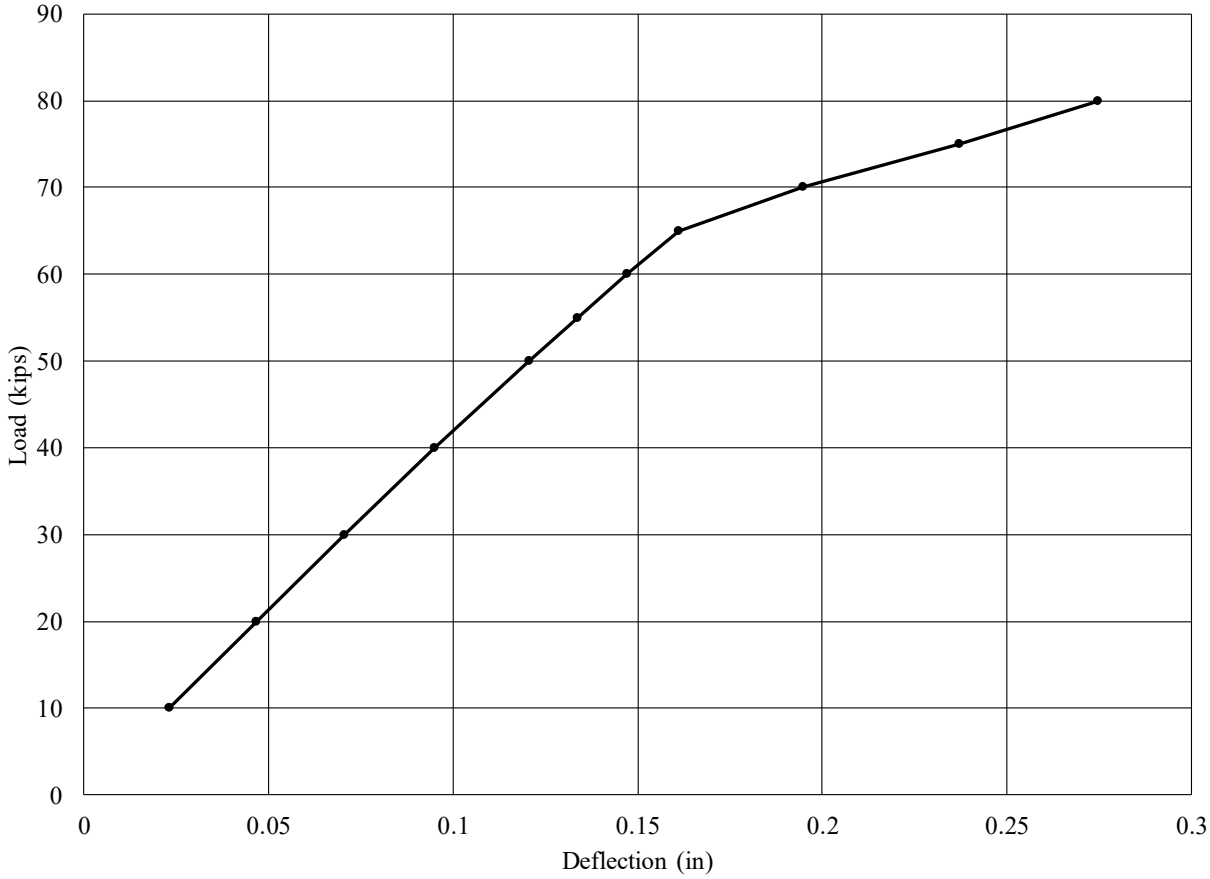

Figure 3-3 – Predicted Load versus Deflection Chart without Deck

Figure 3-4 and Figure 3-5 show the pertinent results from model simulations. Load cases of 20k, 40k, 60k, and 80k are the only cases shown for clarity. The figures show the theoretical distribution of axial load and bending moment with depth for each individual pile. Axial load profiles were used to analyze the effect of lateral load on the distribution of axial loads in the piles and bending moment profiles were used to verify the accuracy of model predictions. Results showed that after the 65 kip load, some portion of the system began to yield. Axial forces more than doubled in the central two piles between the 60 and 80 kip load cases. The outer piles were still increasing in axial

load in a linear fashion. This increase in axial load for the central piles is likely a factor of the battered outer piles. The batter induces additional tensile and compressive forces on the central piles and their connections to the pile cap due to the deflection of the pile cap under lateral load.

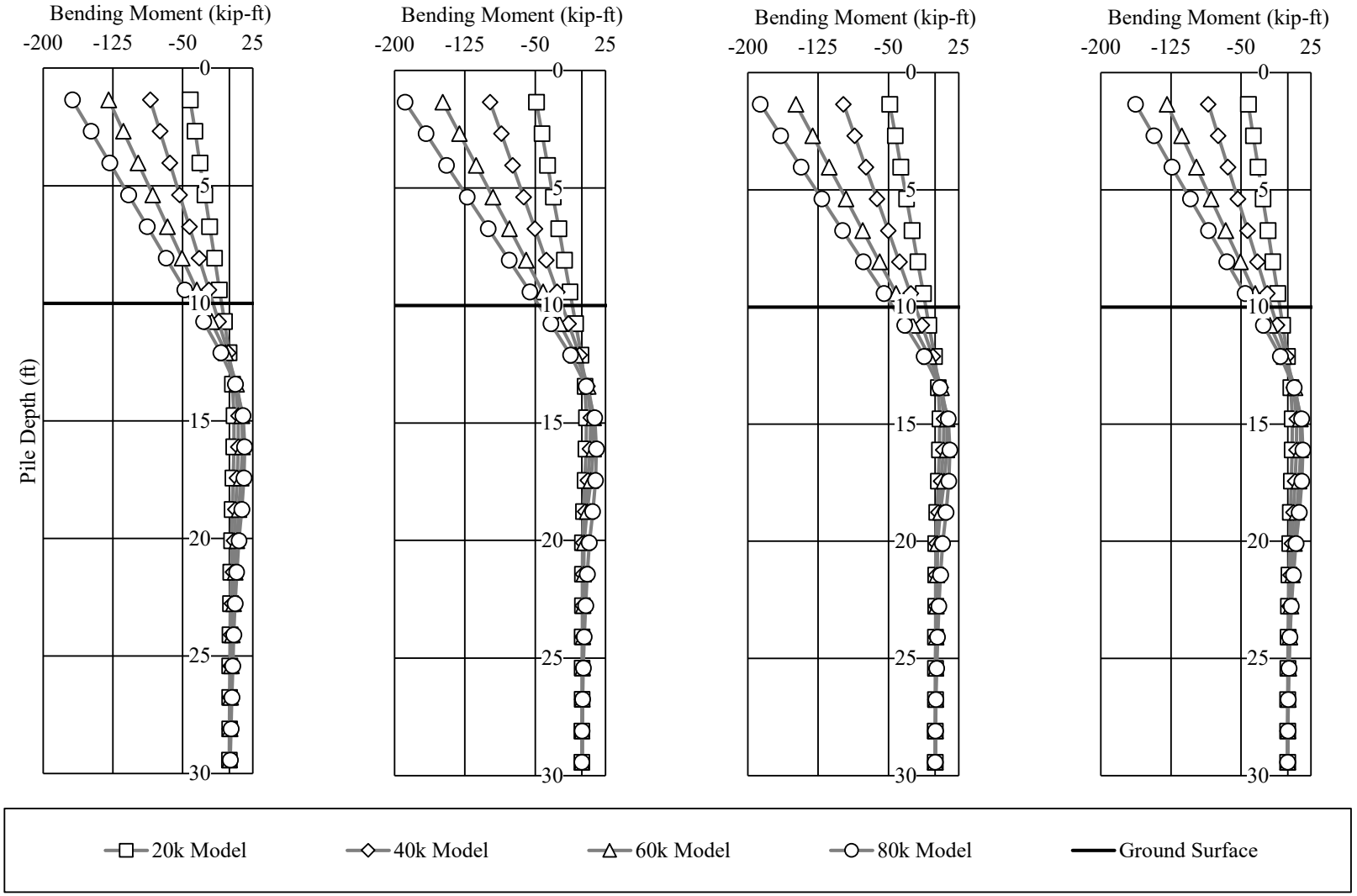

Figure 3-4 – Predicted Bending Moment Profiles with No Deck

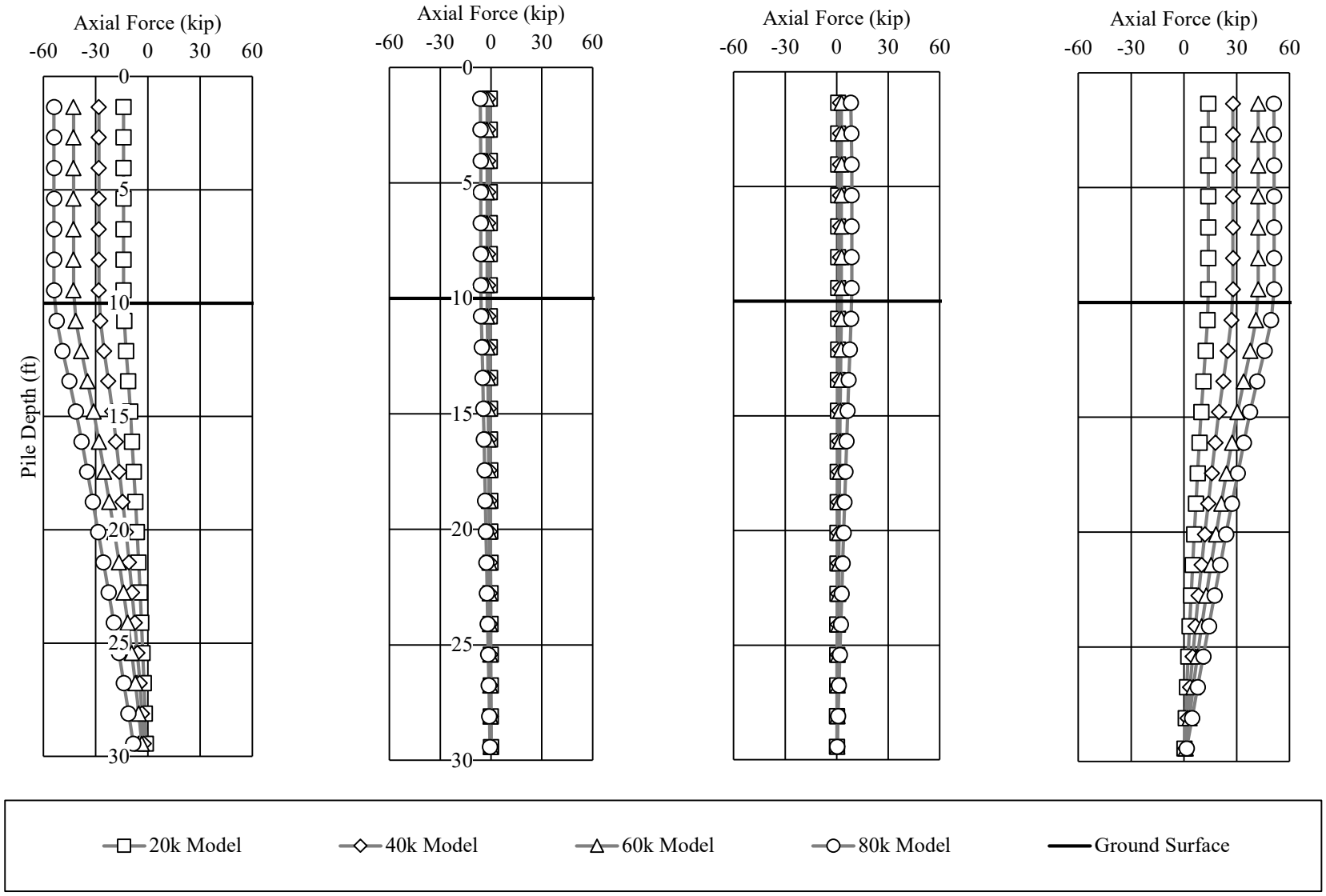

Figure 3-5 – Predicted Axial Load Profiles with No Deck

3.3.3 Post-Deck Bent Model and Behavior Prediction

Three models were created to simulate the load tests that would occur after casting the bridge deck. The models were subjected to the same loading schedule as the model for the bent without a deck. The first model simulated the load test of the bent with only the added stiffness of the deck. Initial models assumed a spring value that was applied at the centerline of the cap opposite the point of load application. After load testing, a more refined value for this spring constant was determined by comparing the observed load versus deflection charts with and with the bridge deck to determine the theoretical amount of added stiffness provided by the bridge deck. This spring value was used in all subsequent models as a baseline for added deck stiffness. All soil properties and structural parameters were the same as the model without the added bridge deck stiffness. Figure 3-6 shows the load versus deflection behavior prediction for the bent with the addition of the bridge deck using the field-determined stiffness factor.

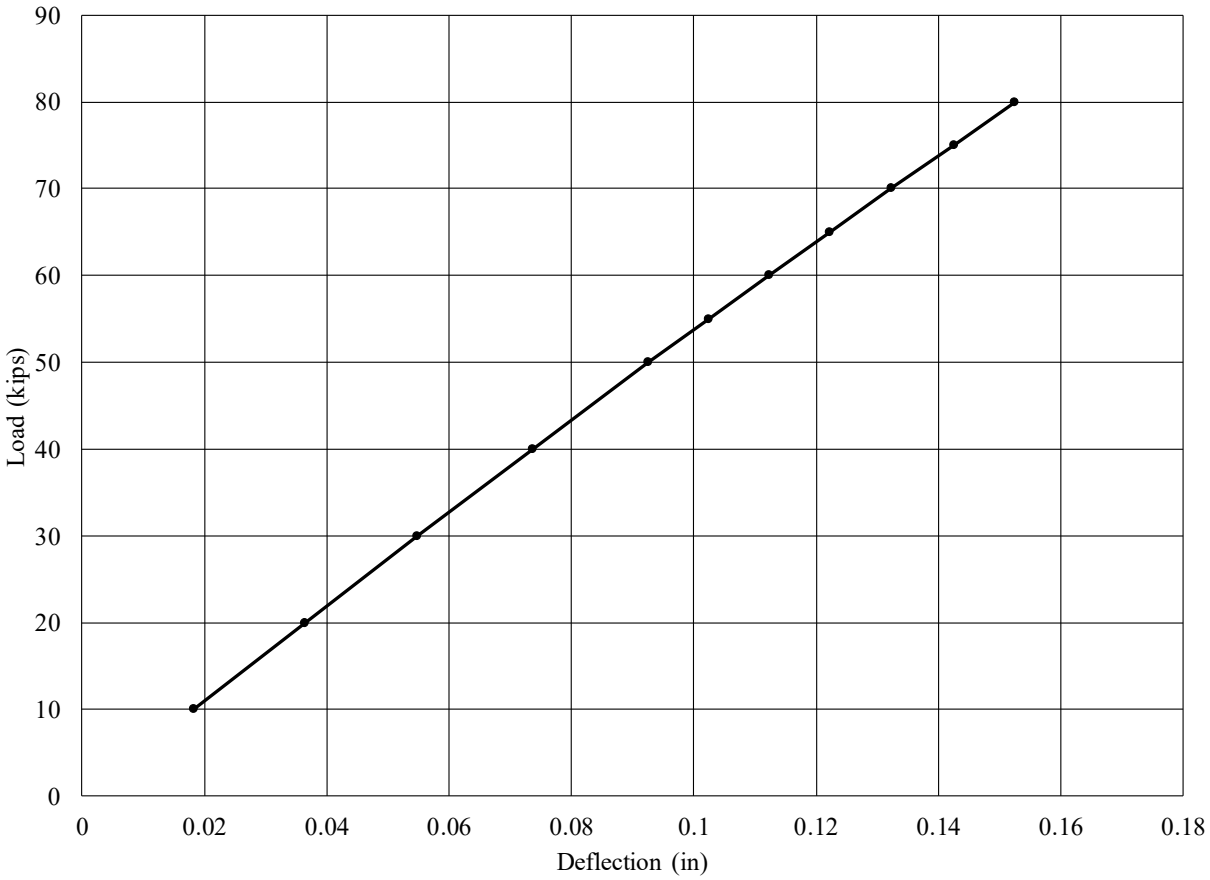

Figure 3-6 – Predicted Load versus Deflection Chart with Deck and No Load Truck

Figure 3-7 and Figure 3-8 show the pertinent results from model simulations. The figures show the theoretical distribution of axial load and bending moment with depth for each individual pile. Axial load profiles were used to analyze the effect of lateral load on the distribution of axial loads in the piles and bending moment profiles were used to verify the accuracy of model predictions. For clarity, only the 20k, 40k, 60k, and 80k load cases are shown. Induced moments in the pies were lesser than the moments induced in the bent piles without a bridge deck. This is likely due to additional weight and structural elements acting together to resist the lateral load. With the addition of a deck, the model results do not show the same increase in axial load for the central piles between the 60 and 80 kip loads.

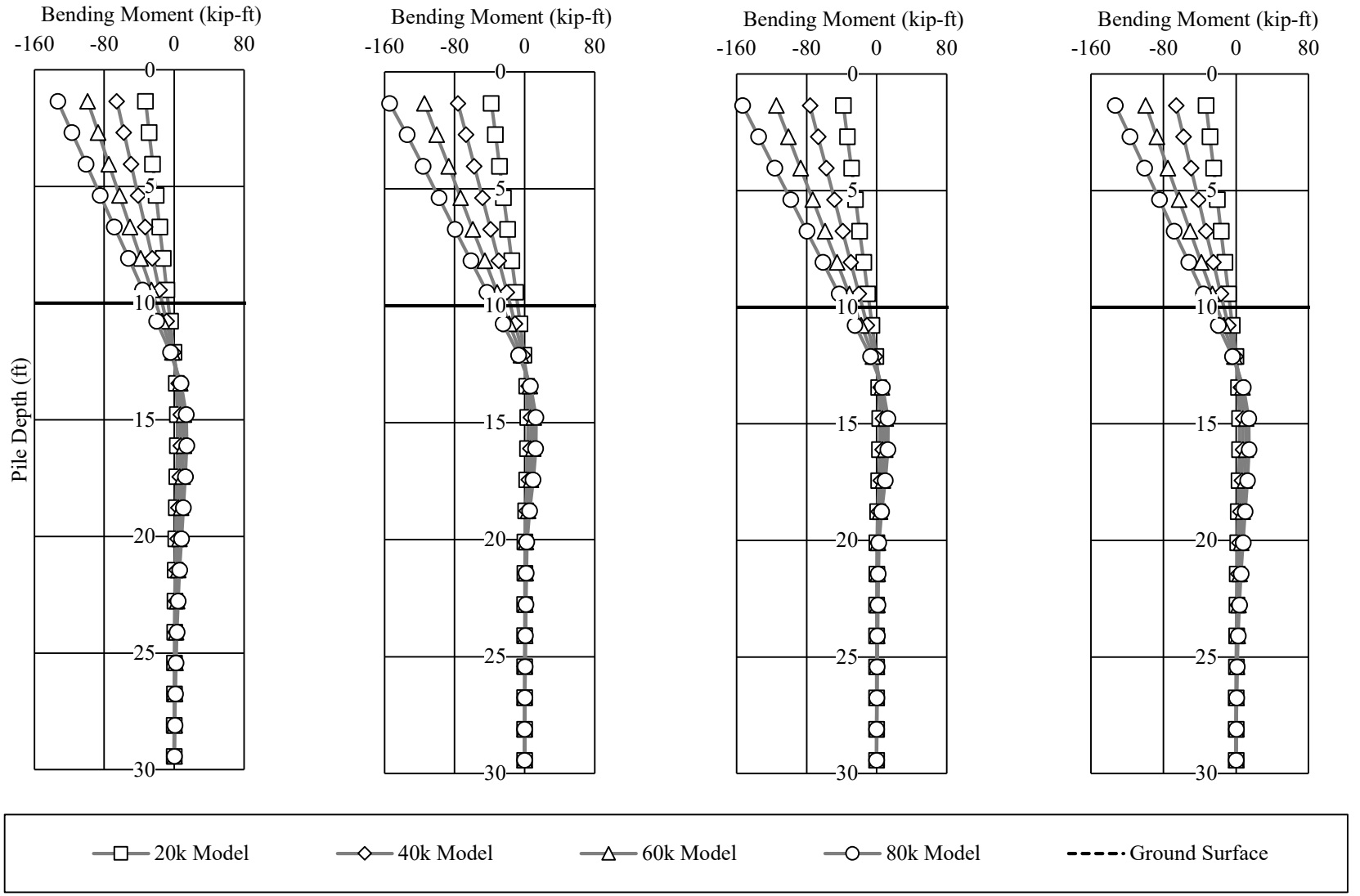

Figure 3-7 – Predicted Bending Moment Profiles with Deck and No Load Truck

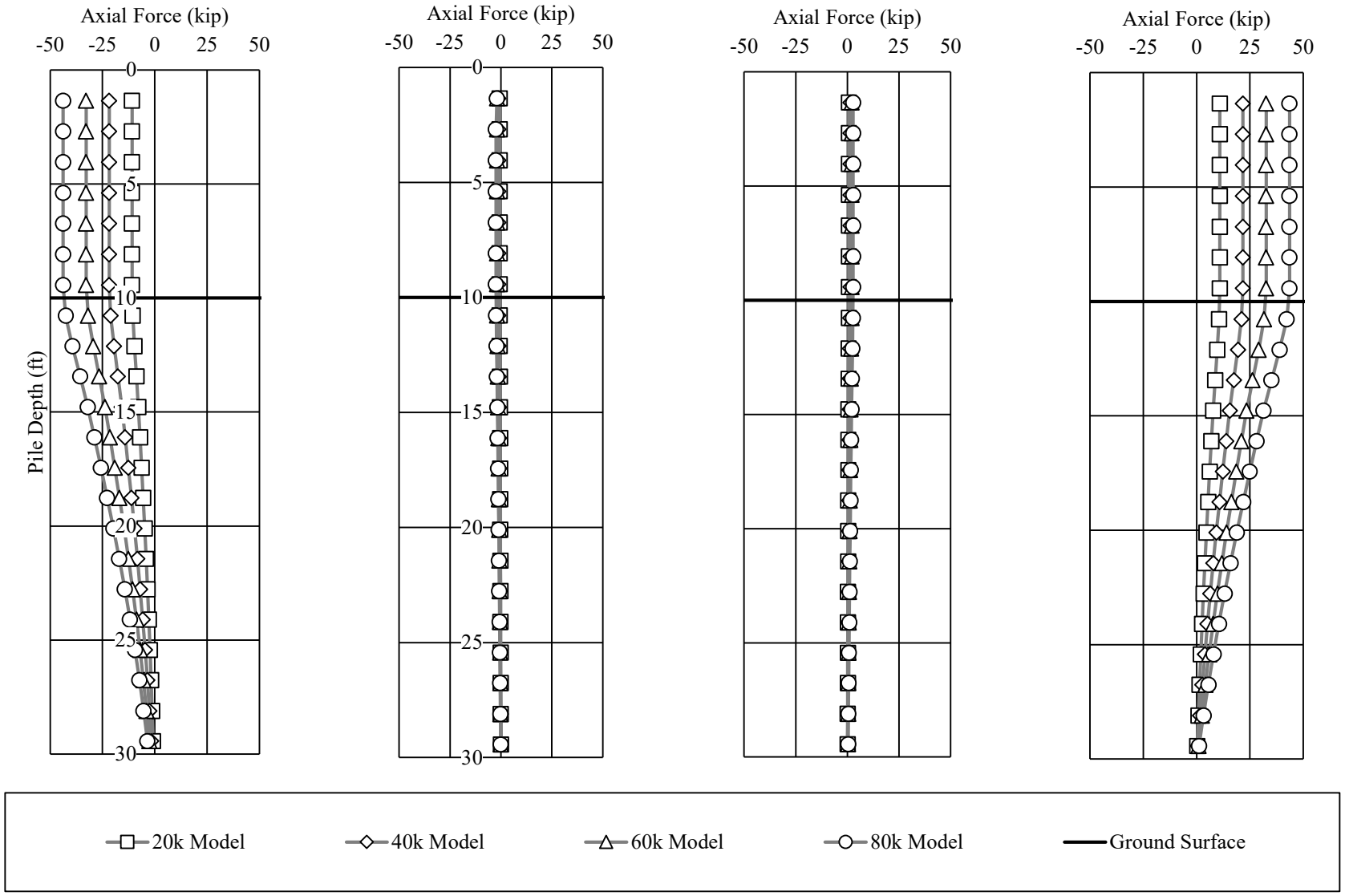

Figure 3-8 – Predicted Axial Load Profiles with Deck and No Load Truck

The third and fourth models of the Macon County Road 9 bent included the addition of axial load from an LC-5 Load truck. Figure 3-9 shows the layout wheel load magnitudes of the load truck.

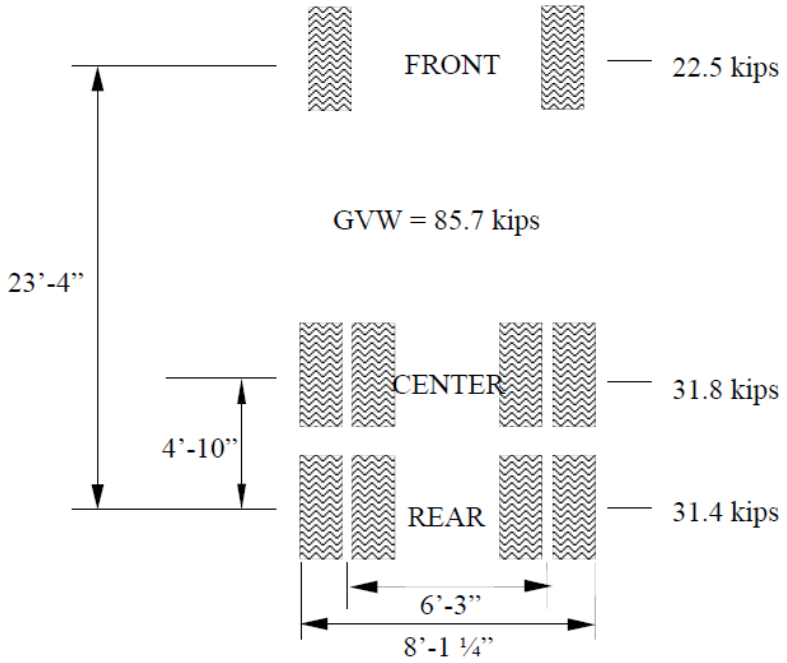

Figure 3-9 – Layout of LC-5 Load Truck (Miller, 2013)

The third model simulated the placement of the center of the center axle over the center of the roadway and bent. All axial loads were assumed to be applied at bearing locations above the tops of the piles. For the placement over the center of the roadway and bent, it was assumed that the bearings for the two center piles each carried half of the load truck weight. This equated to axial loads of 42.85 kips applied at the central bearing locations. The simulated load test was then conducted at the same ten loading increments as the simulations mentioned above. Figure 3-10 shows the load versus deflection behavior prediction of the bent with the bridge deck attached and the load truck centered over the roadway and bent.

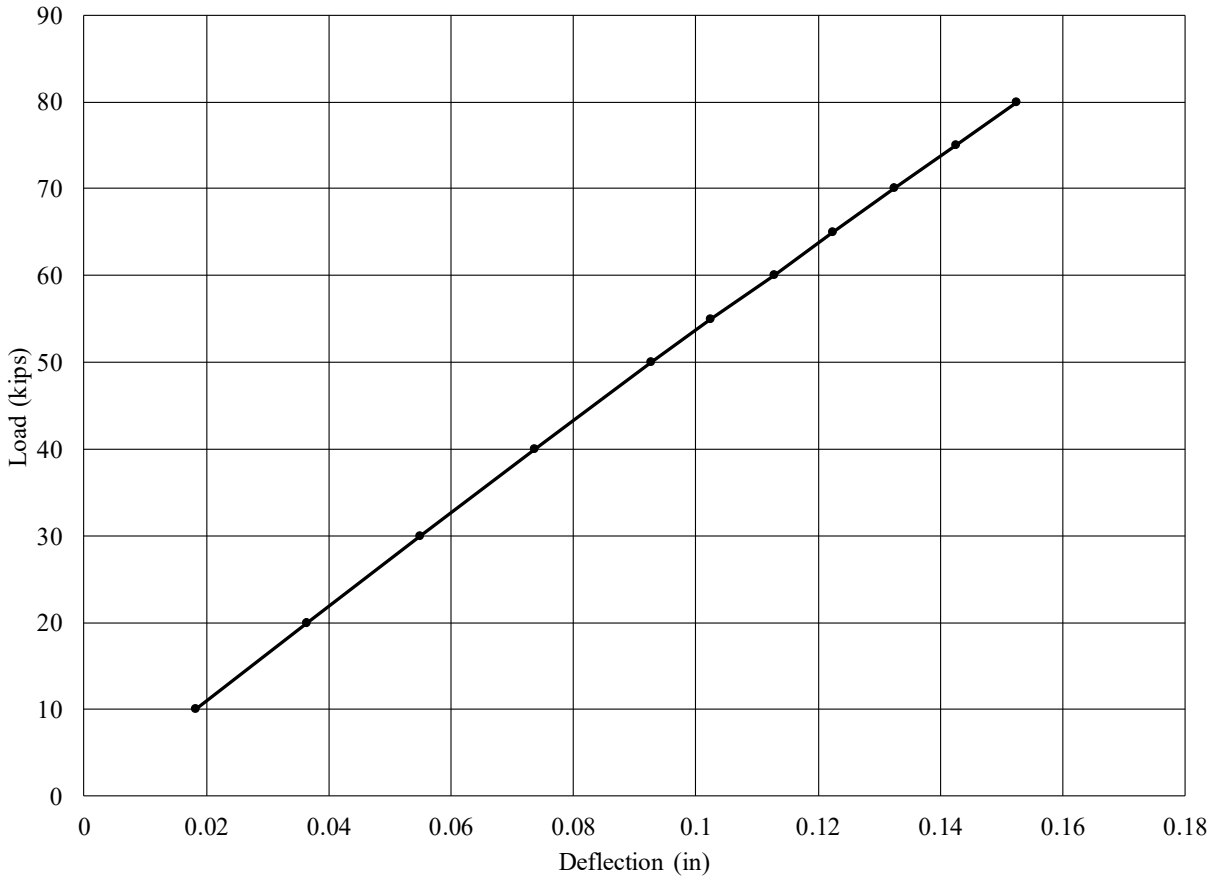

Figure 3-10 – Predicted Load versus Deflection Chart with Deck and Load Truck Centered over the Roadway

Figure 3-11 and Figure 3-12 show the pertinent results from model simulations. The figures show the theoretical distribution of axial load and bending moment with depth for each individual pile. Axial load profiles were used to analyze the effect of lateral load on the distribution of axial loads in the piles and bending moment profiles were used to verify the accuracy of model predictions. For clarity, only the 20k, 40k, 60k, and 80k load cases are shown.

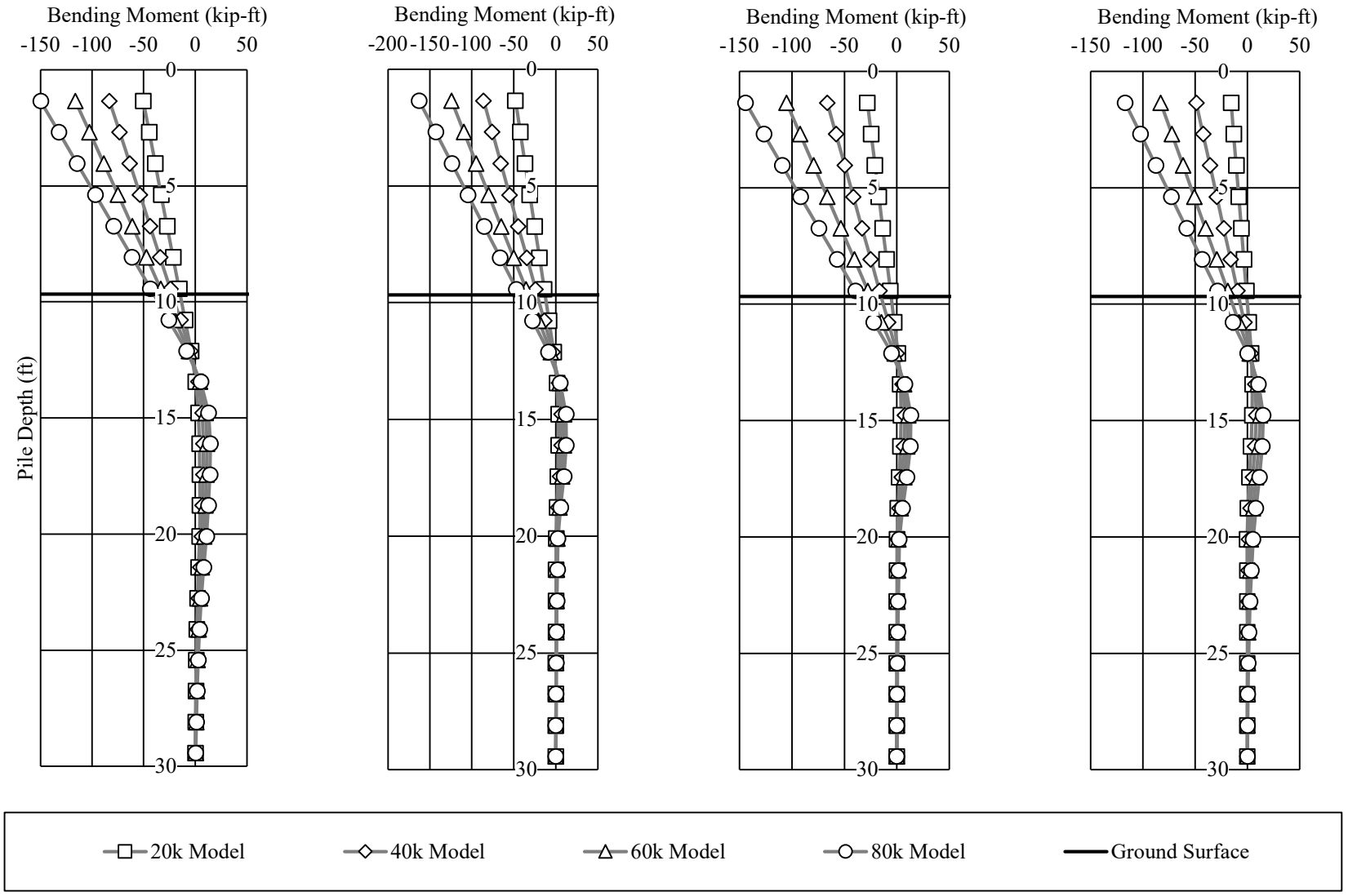

Figure 3-11 – Predicted Moment Profiles with Deck and Load Truck Centered over the Roadway

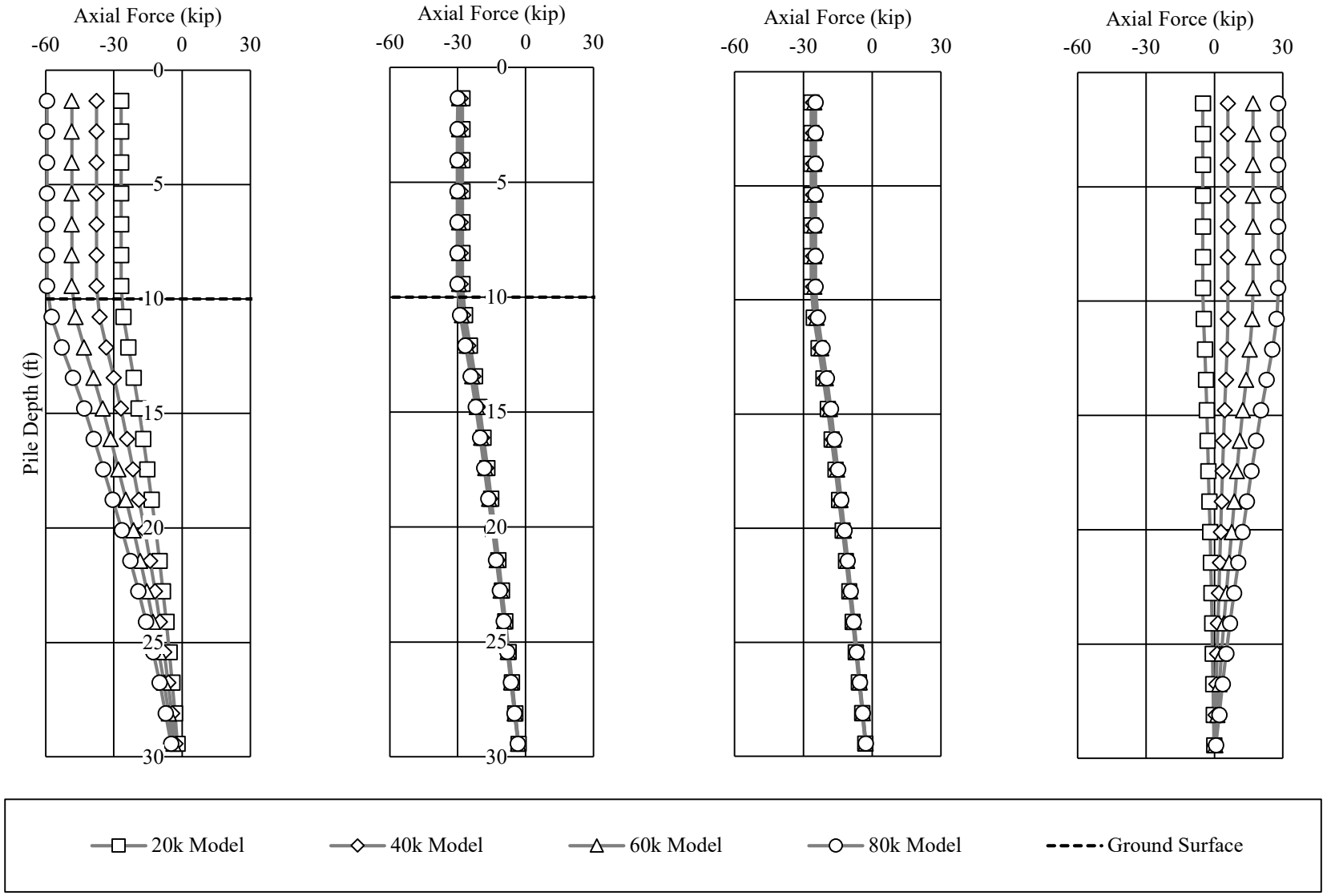

Figure 3-12 – Predicted Axial Load Profiles with Deck and Load Truck Centered over the Roadway

The fourth model simulated the placement of the load truck's exterior tire at the edge of the exterior girder opposite the applied load. It was assumed that the majority of the load was transferred to the exterior girder and into the bent through the bearing location below it. A portion of load was assumed to have been transferred into the bearing location below Pile 3 due to the location of the load truck tire. The axial load at the Pile 4 bearing location was 52.22 kips and the load at the Pile 3 bearing location was 33.48 kips. Figure 3-13 shows the prediction for the load versus deflection behavior of the bent with the load truck placed over the exterior girder.

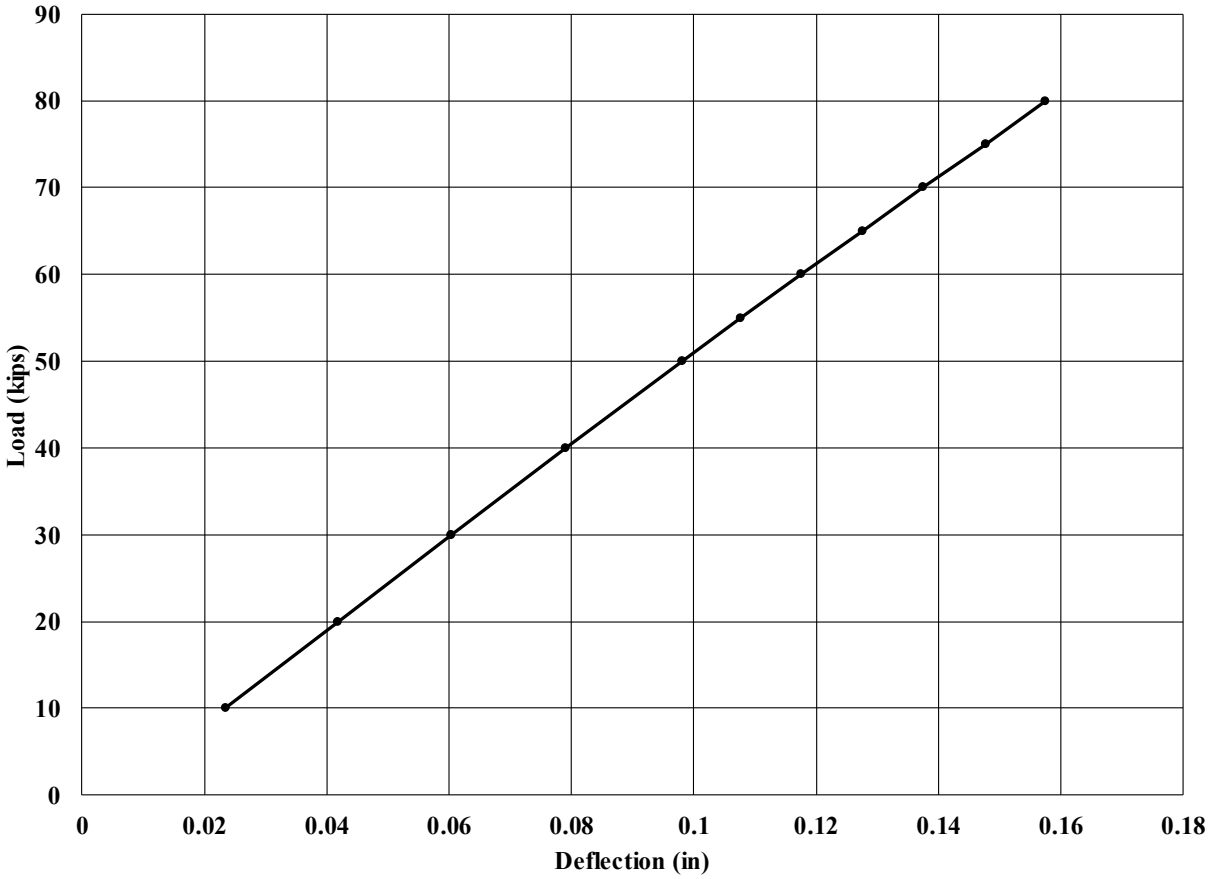

Figure 3-13 – Predicted Load versus Deflection Chart with Deck and Load Truck over the Exterior Girder

Figure 3-14 and Figure 3-15 show the pertinent results from model simulations. The figures show the theoretical distribution of axial load and bending moment with depth for each individual pile.

Axial load profiles were used to analyze the effect of lateral load on the distribution of axial loads in the piles and bending moment profiles were used to verify the accuracy of model predictions. For clarity, only the 20k, 40k, 60k, and 80k load cases are shown.

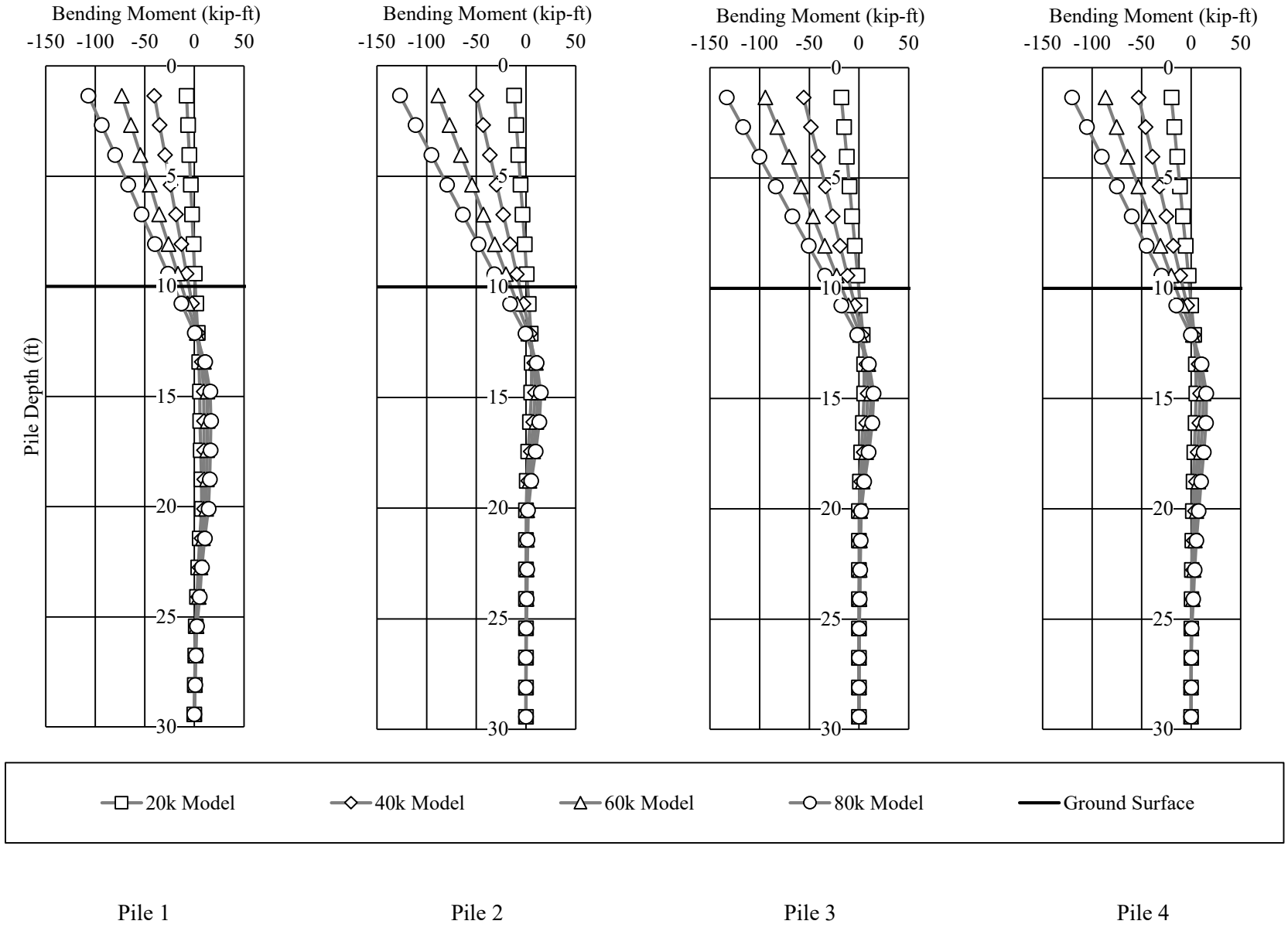

Figure 3-14 – Predicted Moment Profiles with Deck and Load Truck over the Exterior Girder

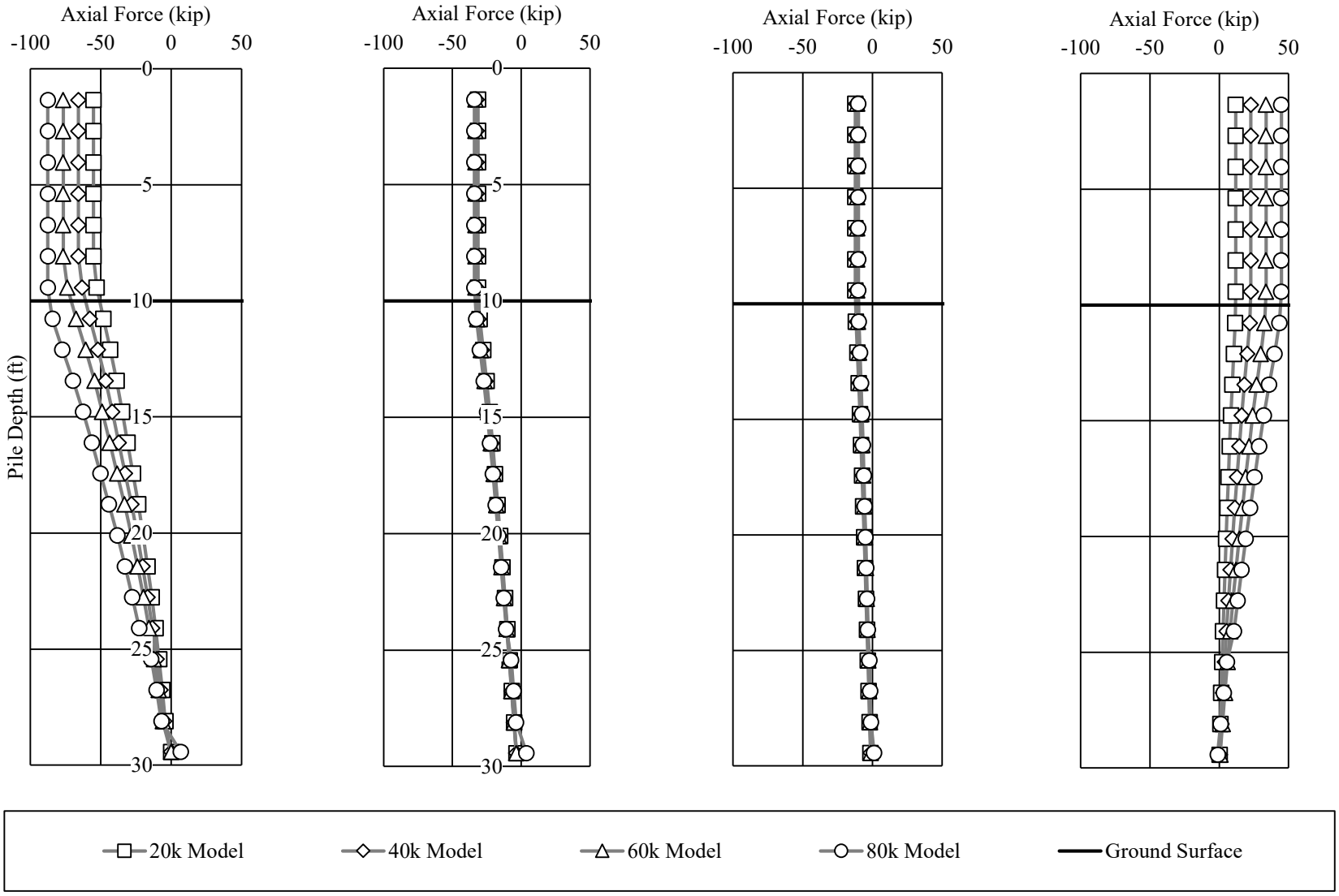

Figure 3-15 – Predicted Axial Load Profiles with Deck and Load Truck over Exterior Girder

The load versus deflection predictions for each of the simulated load tests were graphed together to compare the predicted behavior. Figure 3-16 shows the comparison of the predicted model load versus deflection curves.

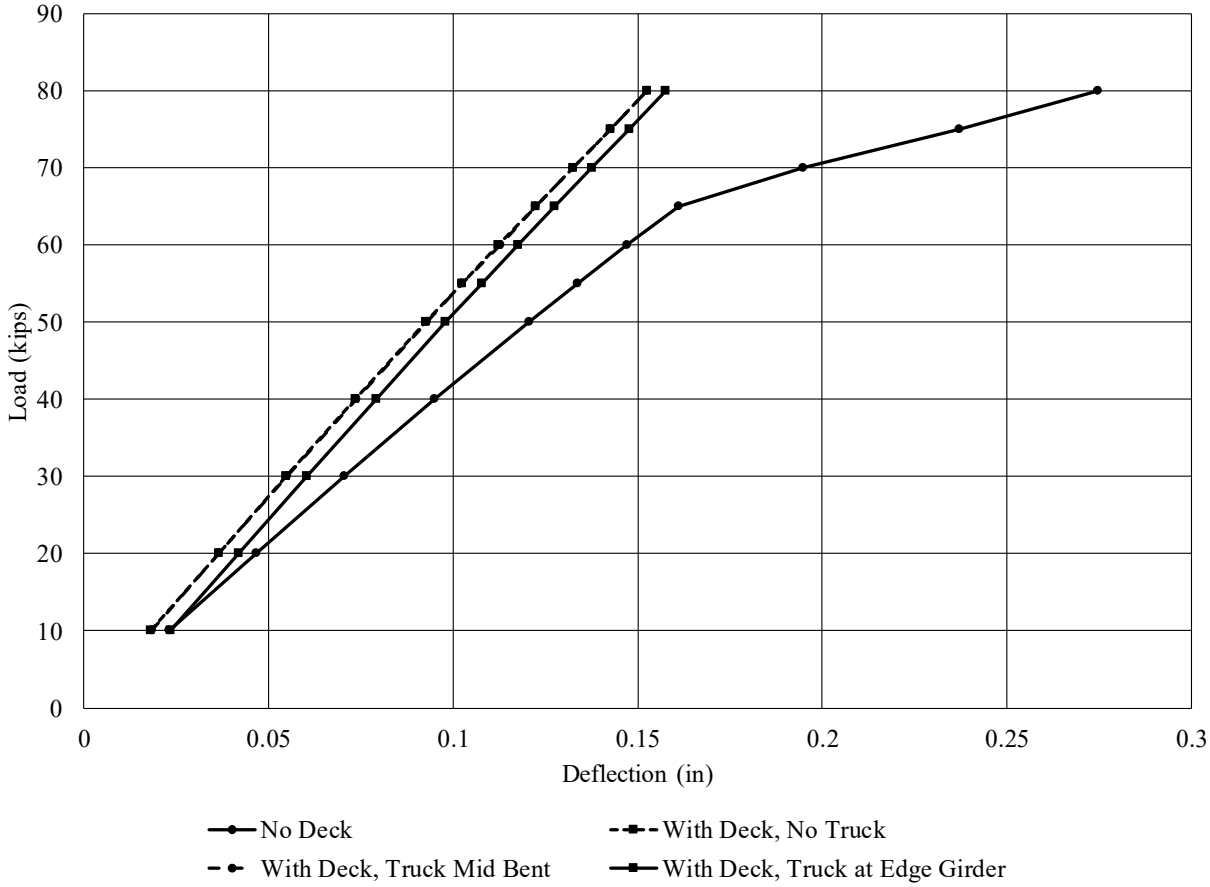

Figure 3-16 – Comparison of Predicted Load versus Deflection Curves from Model Simulations

The models predicted that the bent prior to the casting of the deck would experience the greatest deflection. Without the added stiffness of the bridge deck, the bent deflects more and seems to suggest a slight amount of yielding of the soil will occur as no structural elements reached stresses near yielding or failure according to the FB Multipier analysis. The models without the truck load and with the truck centered over the roadway and bent was expected to experience the least amount

of lateral deflection and experience nearly identical deflections. The curve with the truck over the exterior girder was predicted to deflect at the same rate as the other two models with the bridge deck, but the addition of the load at the edge of the deck seems to have induced an initial sway due to the unsymmetrical nature of the loading.

3.3.4 Reaction Bent

The Macon County Road 9 bent required a reaction bent to react against. The reaction bent was used to react the lateral loads in the bent during field load testing. The same soil profile used in the bent models was used to analyze the behavior of the reaction bent except the top clay layer was not replaced with rip-rap. The reaction bent featured two 35 feet long HP14x89 piles. The piles were oriented for weak axis bending in the direction of lateral loading. The two piles were driven in line with a 4 feet center to center spacing. The pile closest to the test bent was battered towards the second reaction pile with a 1.5/12 slope. A piece of pile cutoff was welded as a brace between the two reaction piles. Figure 3-17 shows the rendering of the FB Multipier model of the reaction bent.

Figure 3-17 – FB Multipier rendering of the Macon County Road 9 Bridge Reaction Bent

The reaction bent model was only analyzed at the maximum expected loading increment. The analysis was used to determine if the reaction bent had sufficient strength for the field lateral load tests, and to assure that the expected deflection did not exceed the stroke length of the jacks that were to be used to load the test bent.

3.4 U.S. Highway 331 Bridge

The second bridge bent modeled was a bridge on U.S. Highway 331 in southern Montgomery County, Alabama. The bridge featured 6 HP10x42 piles 28 feet long with 10 feet of clear height above ground. The piles were encased in 16 inch square concrete encasements. The exterior piles were battered at a 1.5/12 slope. The piles were oriented for weak axis bending in the direction of the lateral load. The piles and girders were spaced at 5 feet center to center. The pile cap was modeled as a 21 inch by 21 inch square cap to approximate the existing trapezoidal cap.

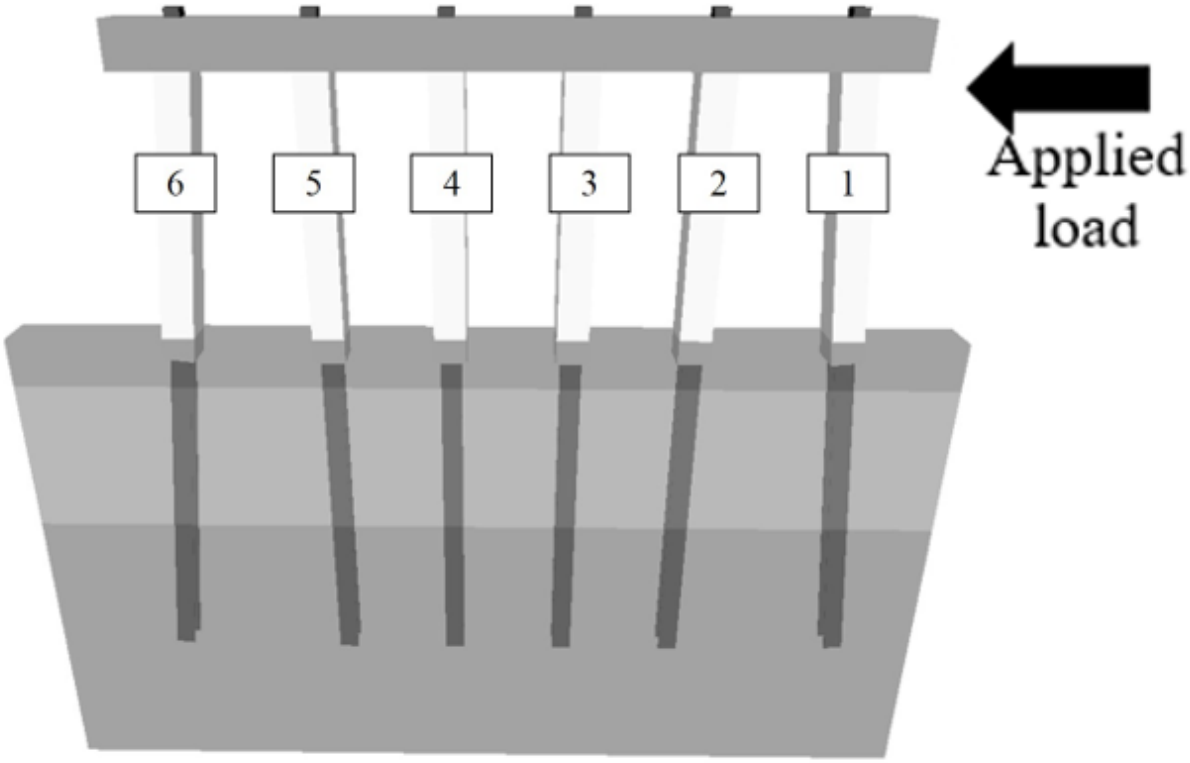

Figure 3-18 – FB Multipier Rendering of Highway 331 Bridge Bent

The model was created using construction documents provided by ALDOT. The geometric pile properties were taken from the AISC Steel Construction Manual (American Institute of Steel Construction, 2011). An initial estimate of 5,000 psi was used for the compressive strength of the concrete encasements. The steel piles were modeled using the FB Multipier default elastic modulus of 29,000 ksi and yield stress of 60 ksi. The p-y, q-z, and t-z curves for each soil layer were constructed from default FB Multipier options. The simulated load test featured ten load increments. The increments were as follows: 10 kips, 20 kips, 30 kips, 40 kips, 50 kips, 55 kips, 60 kips, 65 kips, 70 kips, and 75 kips. The axial load and bending moment predictions were compiled at node locations along the length of each pile for the distinct loading increments. The centerline deflection of the pile cap was also recorded at each loading increment. Two load tests

were simulated. The first test was a test of the bent alone. The second test included the weight of an LC-5 load truck placed over the exterior girder opposite the application of the load. Piles were named Pile 1, Pile 2, Pile 3, Pile 4, Pile 5, and Pile 6. Pile 6 was the leading pile, furthest away from the applied load and was battered. Pile 1, also battered, was the trailing pile closest to the load application point. Piles 2, 3, 4, and 5 were all vertical interior piles. This naming convention was used in every model simulation for the Highway 331 bent. The piles were spaced at 5 feet center to center spacing which was greater than five times the diameter of the pile. Therefore, p-multipliers to reduce the lateral capacities of the piles were not needed and were not included in any model simulations.

3.4.1 Soil Properties

The soil profile was compiled using SPT boring logs included in the construction documents. Three distinct soil layers were modeled. The pertinent soil properties used for the model analysis were determined using the SPT N-counts included with the boring logs. Figure 3-19 shows the soil profile used for model analysis and the pertinent soil properties for each soil layer.

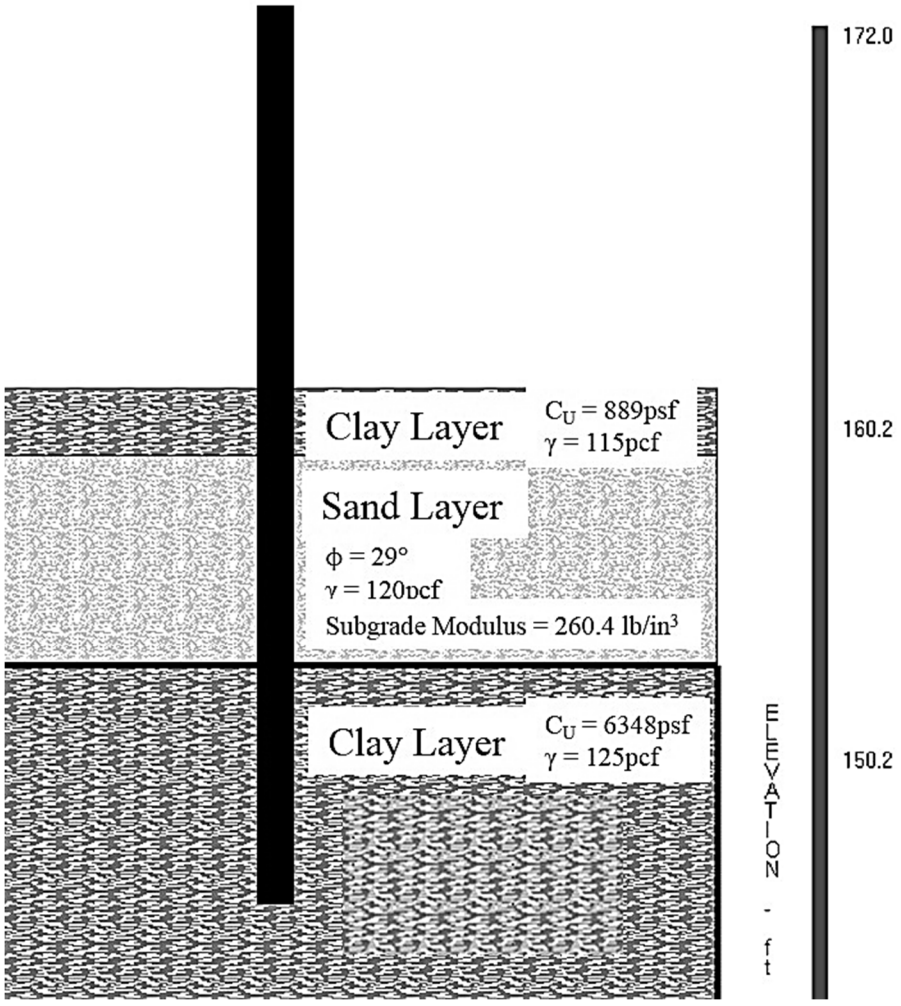

Figure 3-19 – Highway 331 Bridge Soil and Pile Profile (Adapted from FB Multipier)

The water table was not identified in the provided boring logs, so it was not included in the modeled soil profile.

3.4.2 Bent Model and Behavior Prediction

The initial model simulated the test bent with no additional load truck loading applied. The stiffness of the attached bridge deck was modeled as a spring attached to the center of the cap opposite the applied load. The spring stiffness used was the same as the spring stiffness used in

the Macon County Road 9 bent models. The stiffness value was calculated from observed differences in the load versus deflection behavior of the Macon County Road 9 bent field tests. Figure 3-20 shows the predicted load versus deflection behavior for the Highway 331 bridge bent without additional load truck axial load.

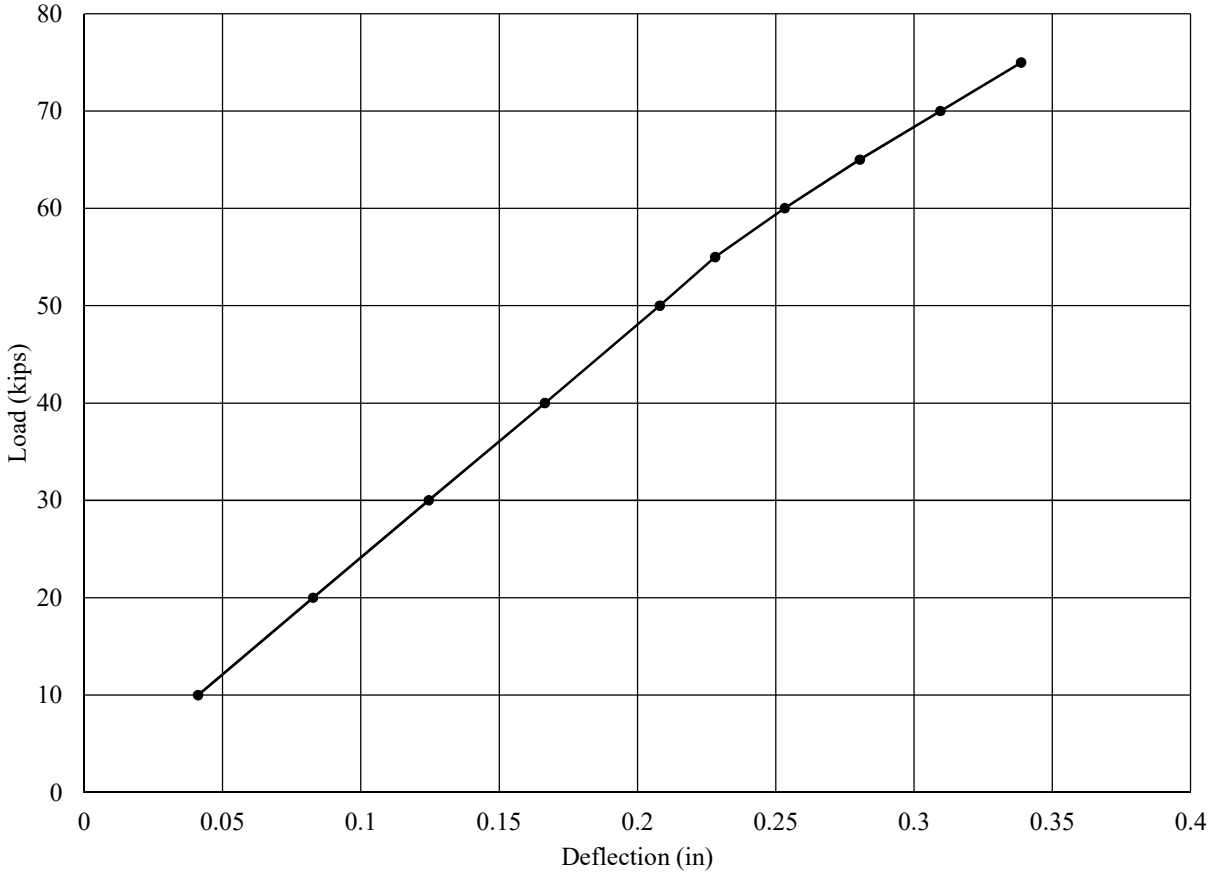

Figure 3-20 – Predicted Load versus Deflection Chart with no Load Truck

Figure 3-21, Figure 3-22, Figure 3-23, and Figure 3-24 show the pertinent results from model simulations. The figures show the theoretical distribution of axial load and bending moment with depth for each individual pile. Axial load profiles were used to analyze the effect of lateral load on the distribution of axial loads in the piles and bending moment profiles were used to verify the accuracy of model predictions. For clarity, 20k, 40k, 60k, and 75k load cases are the only cases shown.

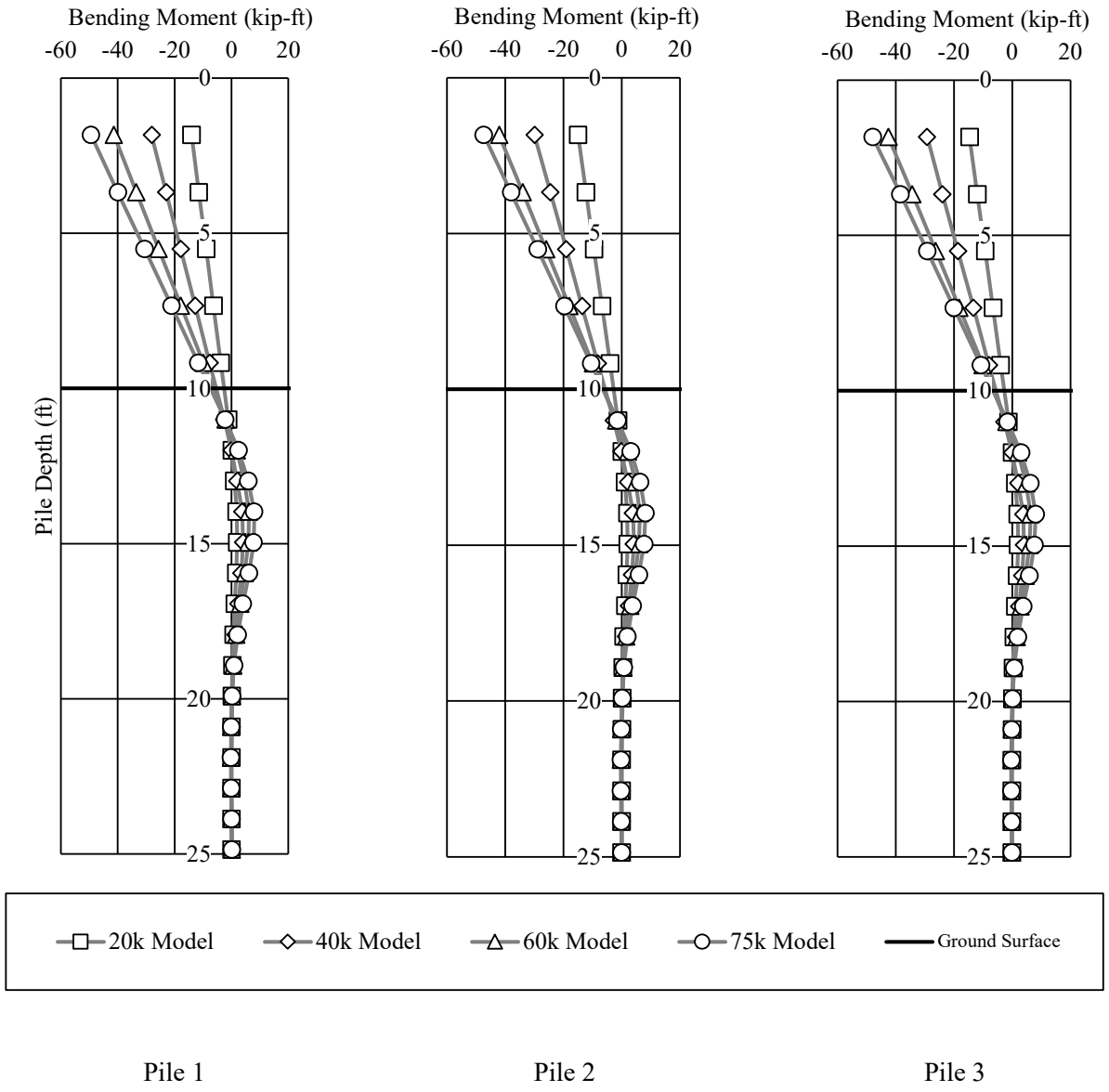

Figure 3-21 – Predicted Moment Profiles for Piles 1-3 with No Load Truck

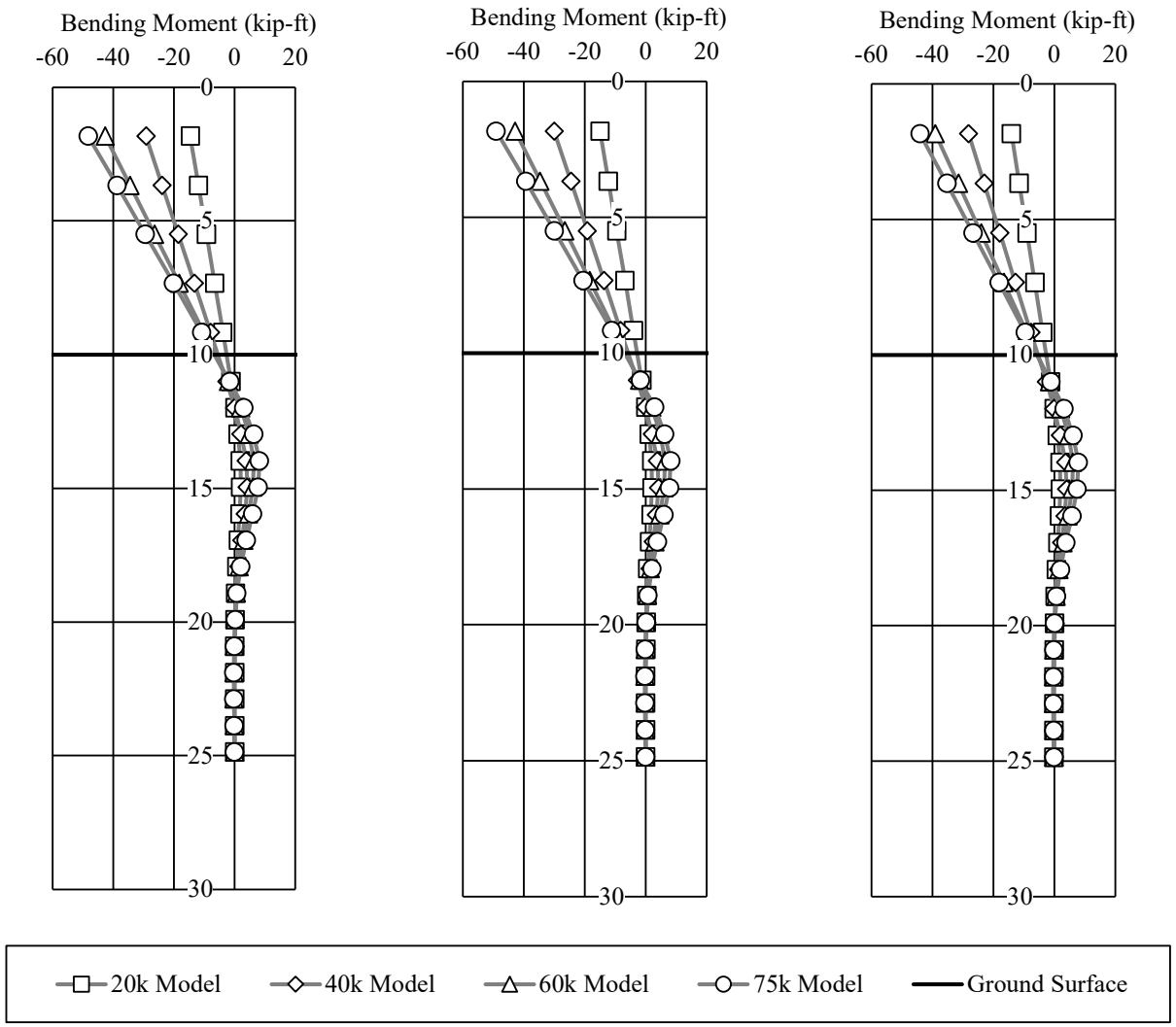

Figure 3-22 – Predicted Moment Profiles for Piles 4-6 with No Load Truck

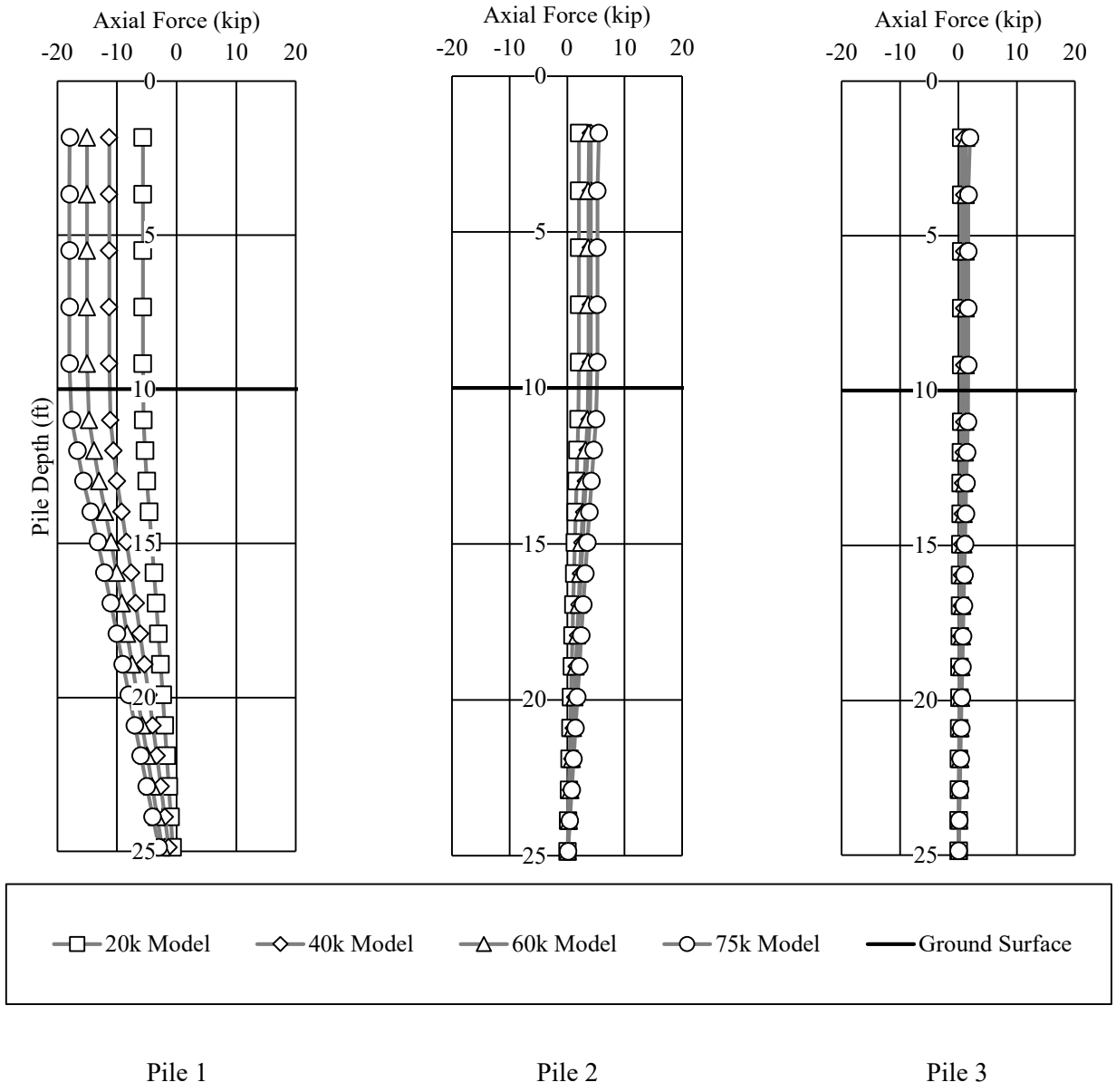

Figure 3-23 – Predicted Axial Load Profiles for Piles 1-3 with No Load Truck

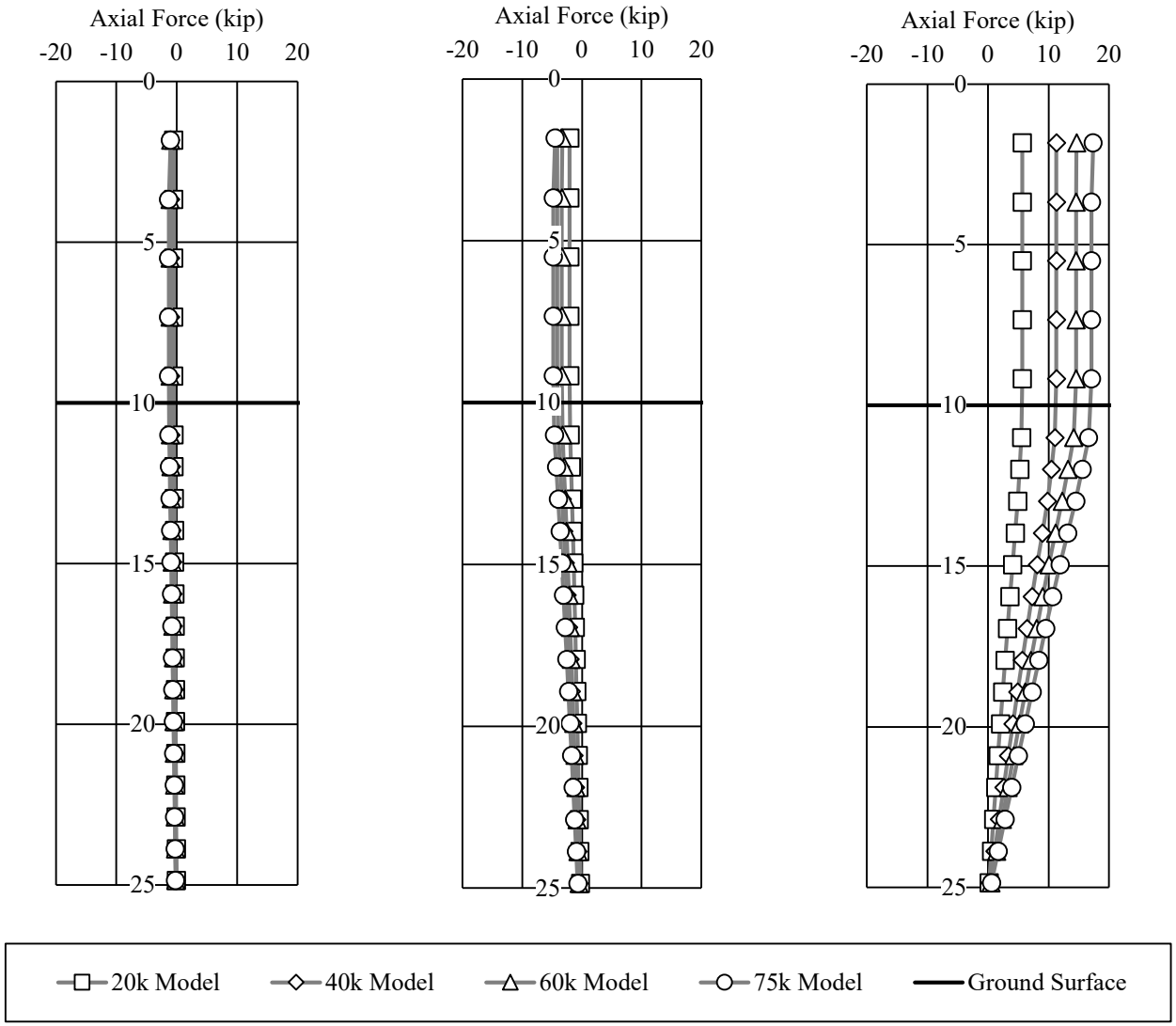

Figure 3-24 – Predicted Axial Load Profiles for Piles 4-6 with No Load Truck

The second model simulation for the Highway 331 bridge simulated the placement of an LC-5 load truck's exterior tire at the edge of the exterior girder opposite the load application point. It was assumed that the load from the load truck was carried only in the bearing locations beneath girders 5 and 6 (above piles 5 and 6). The weight of the truck was split evenly between these two locations at a magnitude of 42.85 kips at each bearing location. Figure 3-25 shows the predicted load versus deflection behavior of the bent with the addition of the load truck.

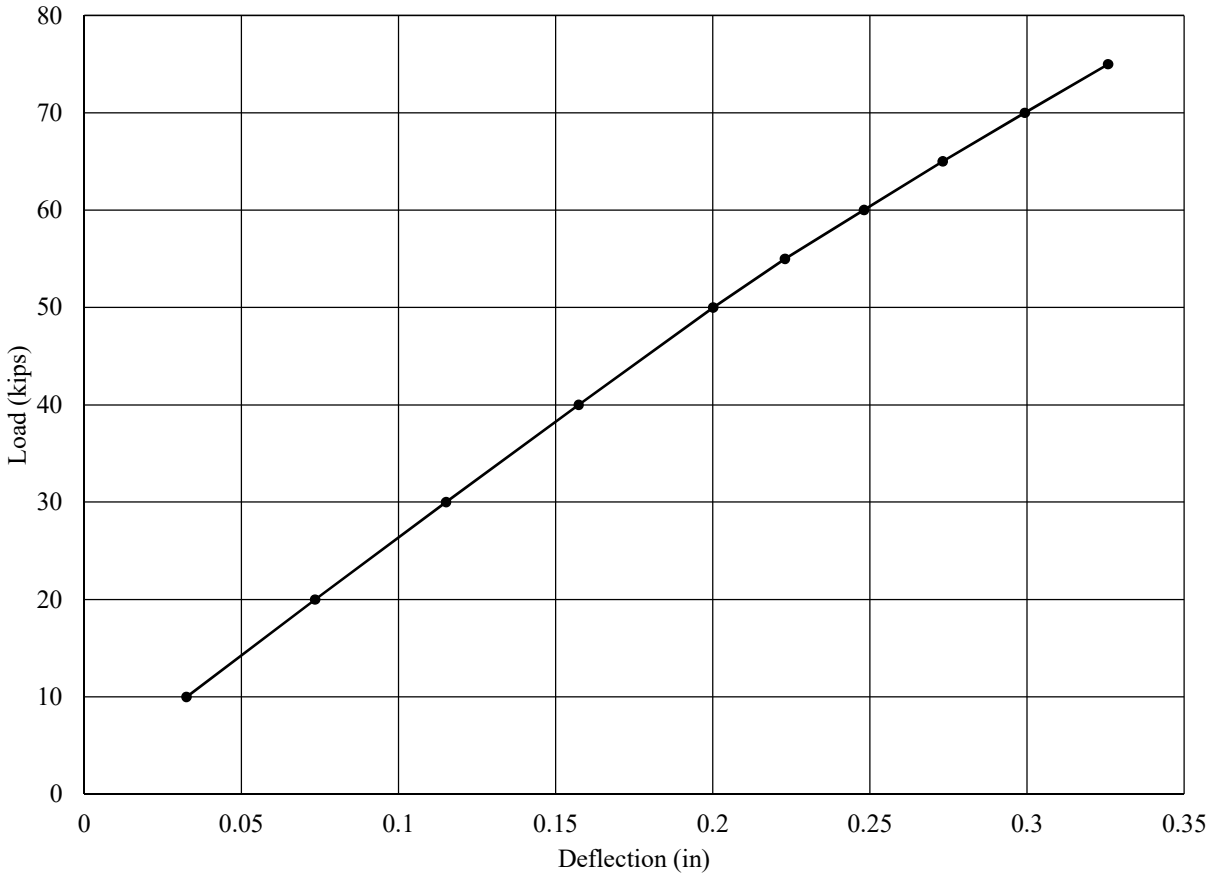

Figure 3-25 – Predicted Load versus Deflection Chart with Deck and Truck over the Exterior Girder

Figure 3-26, Figure 3-27, Figure 3-28, and Figure 3-29 show the pertinent results from model simulations. The figures show the theoretical distribution of axial load and bending moment with

depth for each individual pile. Axial load profiles were used to analyze the effect of lateral load on the distribution of axial loads in the piles and bending moment profiles were used to verify the accuracy of model predictions. For clarity, only the 20k, 40k, 60k, and 75k load cases are shown.

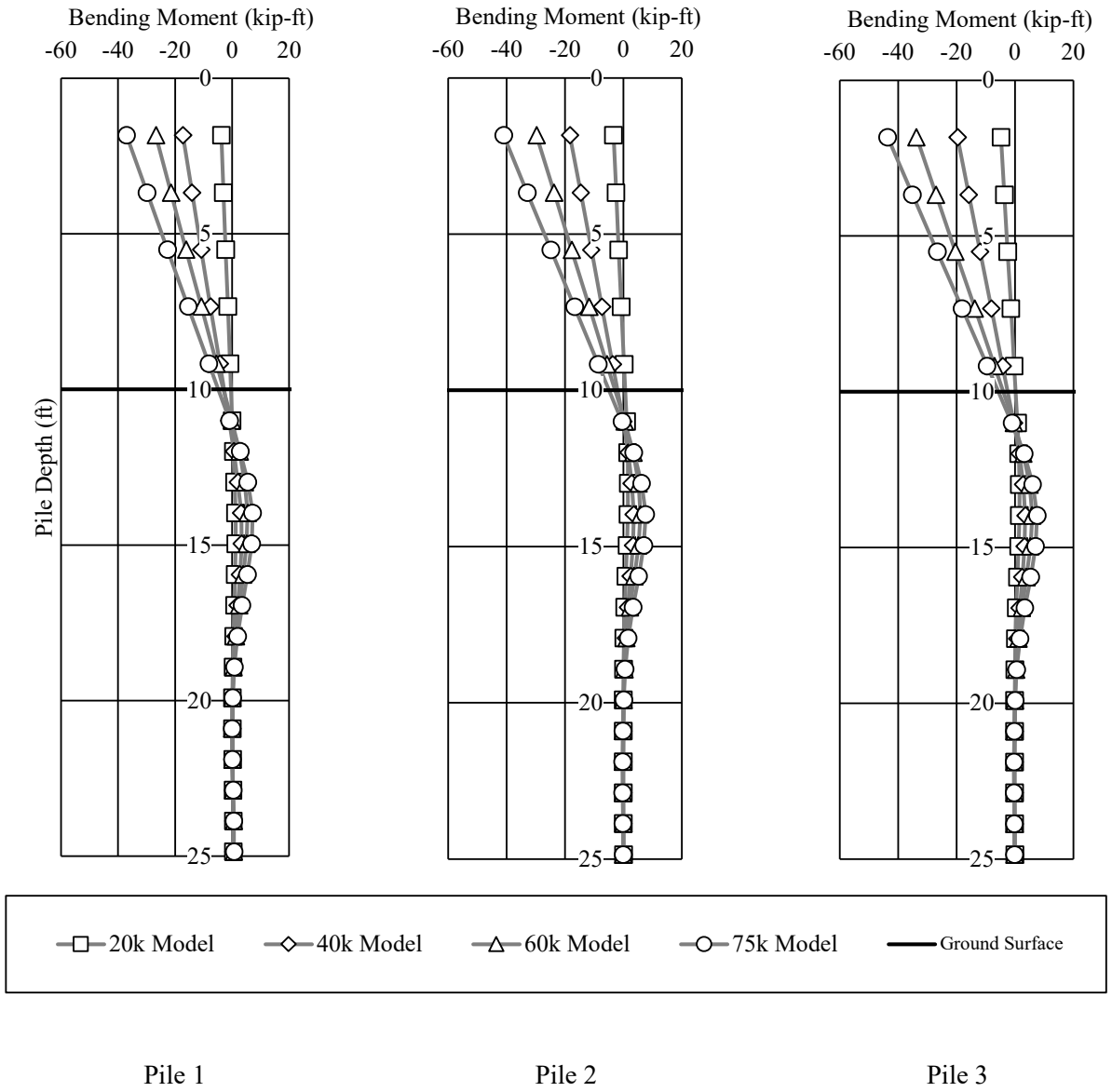

Figure 3-26 – Predicted Moment Profiles for Piles 1-3 with Load Truck over Exterior Girder

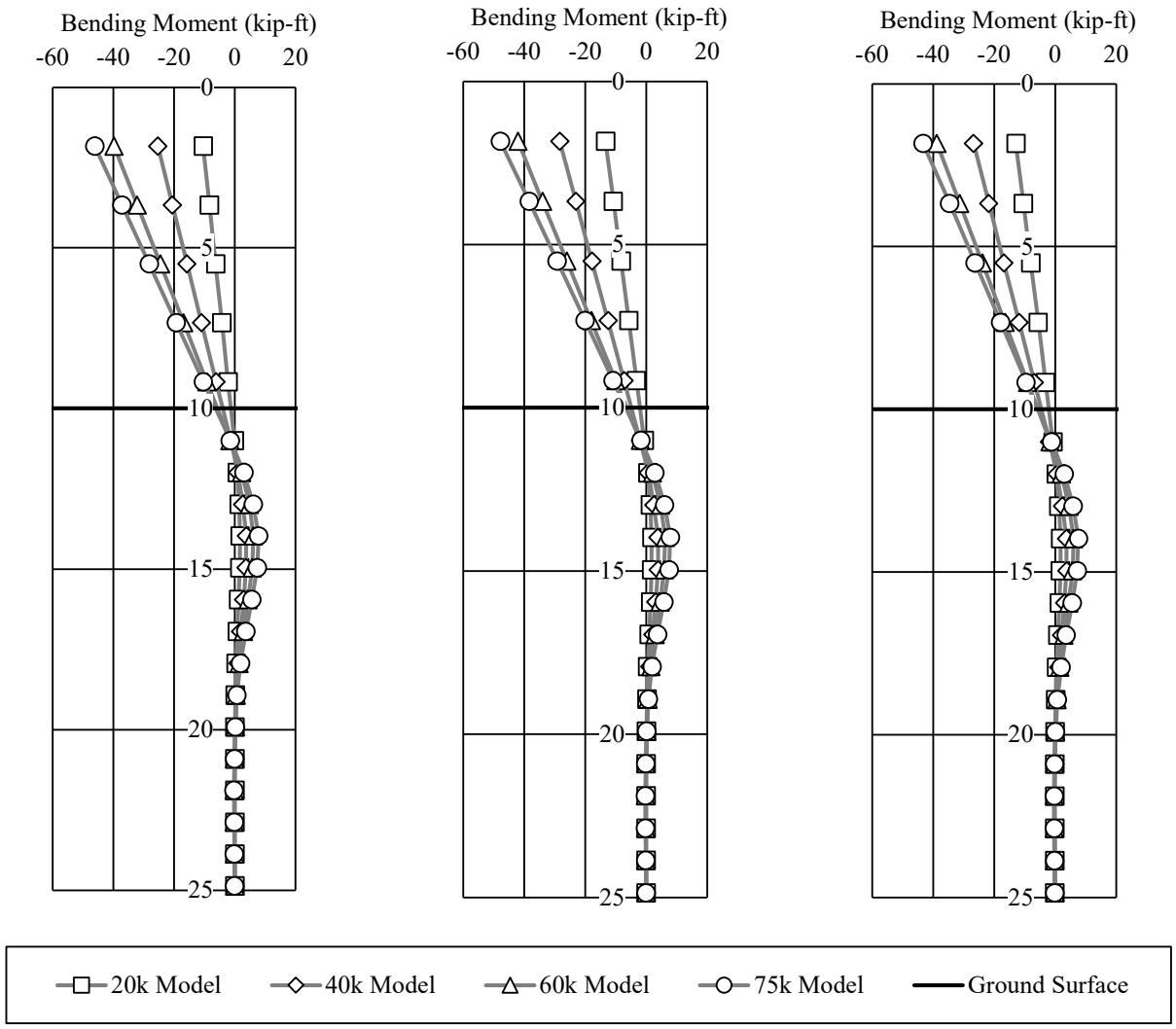

Figure 3-27 – Predicted Moment Profiles for Piles 4-6 with Load Truck over Exterior Girder

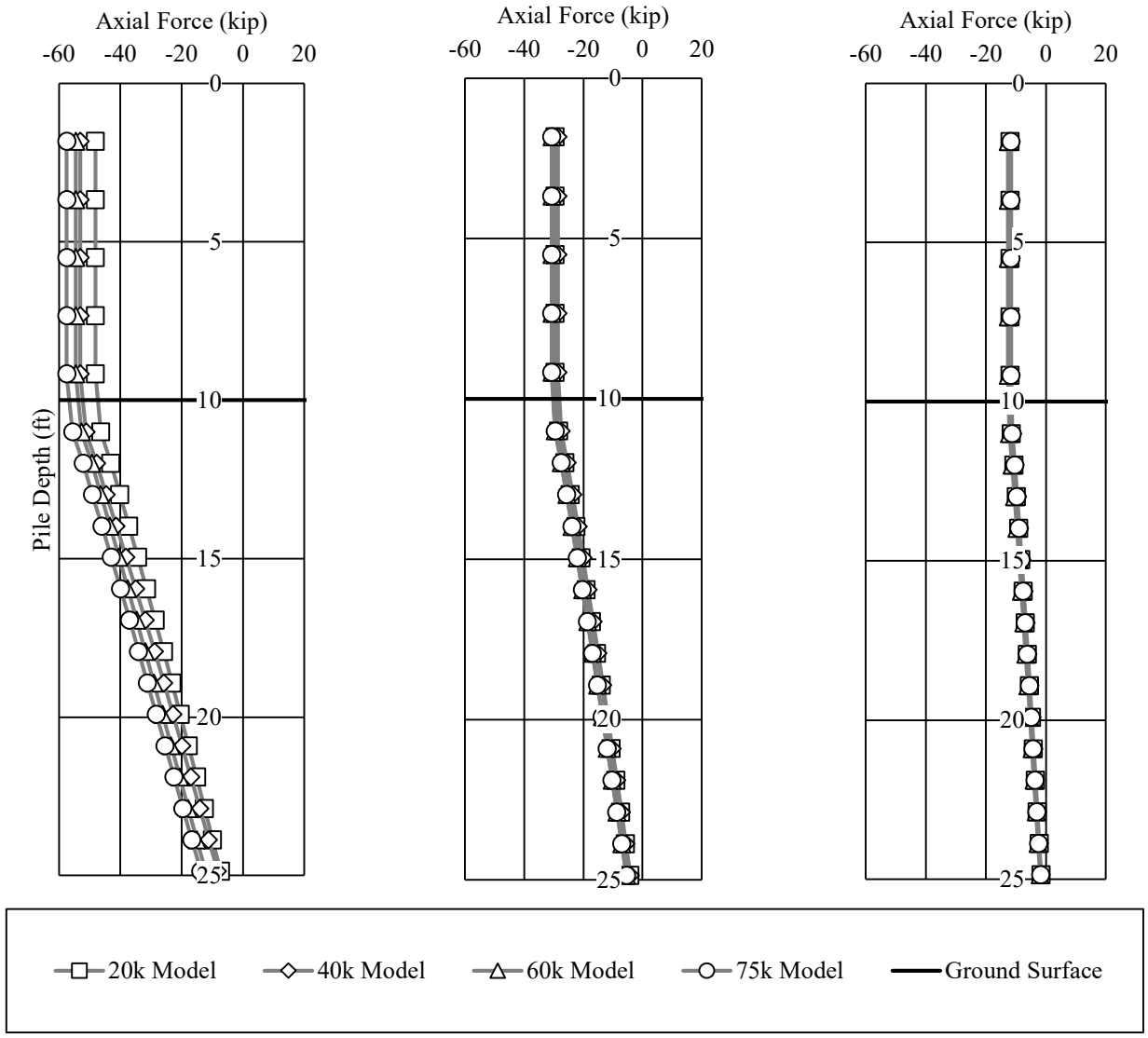

Figure 3-28 – Predicted Axial Load Profiles with Load Truck over Exterior Girder

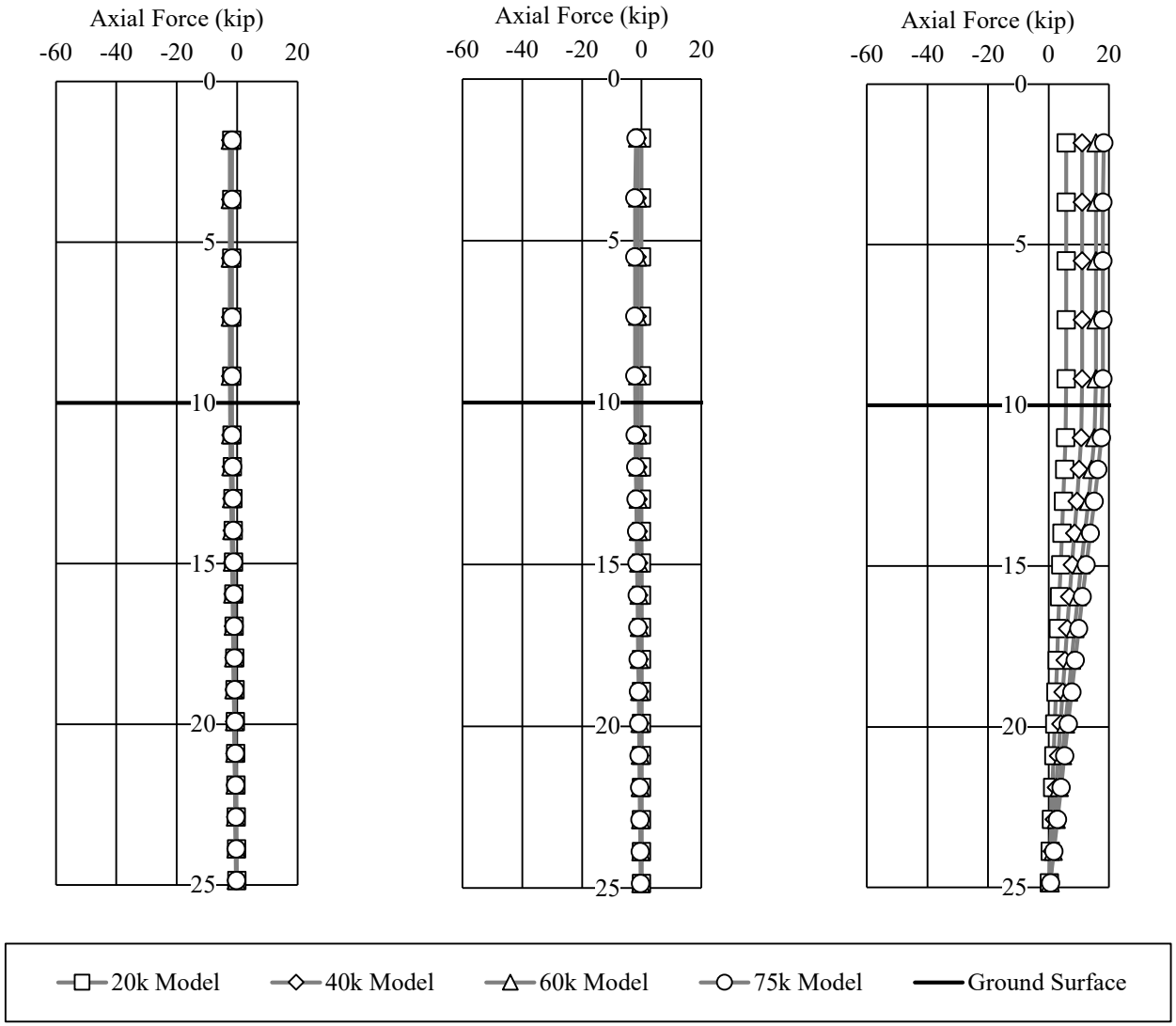

Figure 3-29 – Predicted Axial Load Profiles with Load Truck over Exterior Girder

The load versus deflection predictions for each of the simulated load tests were graphed together to compare the predicted behavior. Figure 3-30 shows the comparison of the predicted model load versus deflection curves.

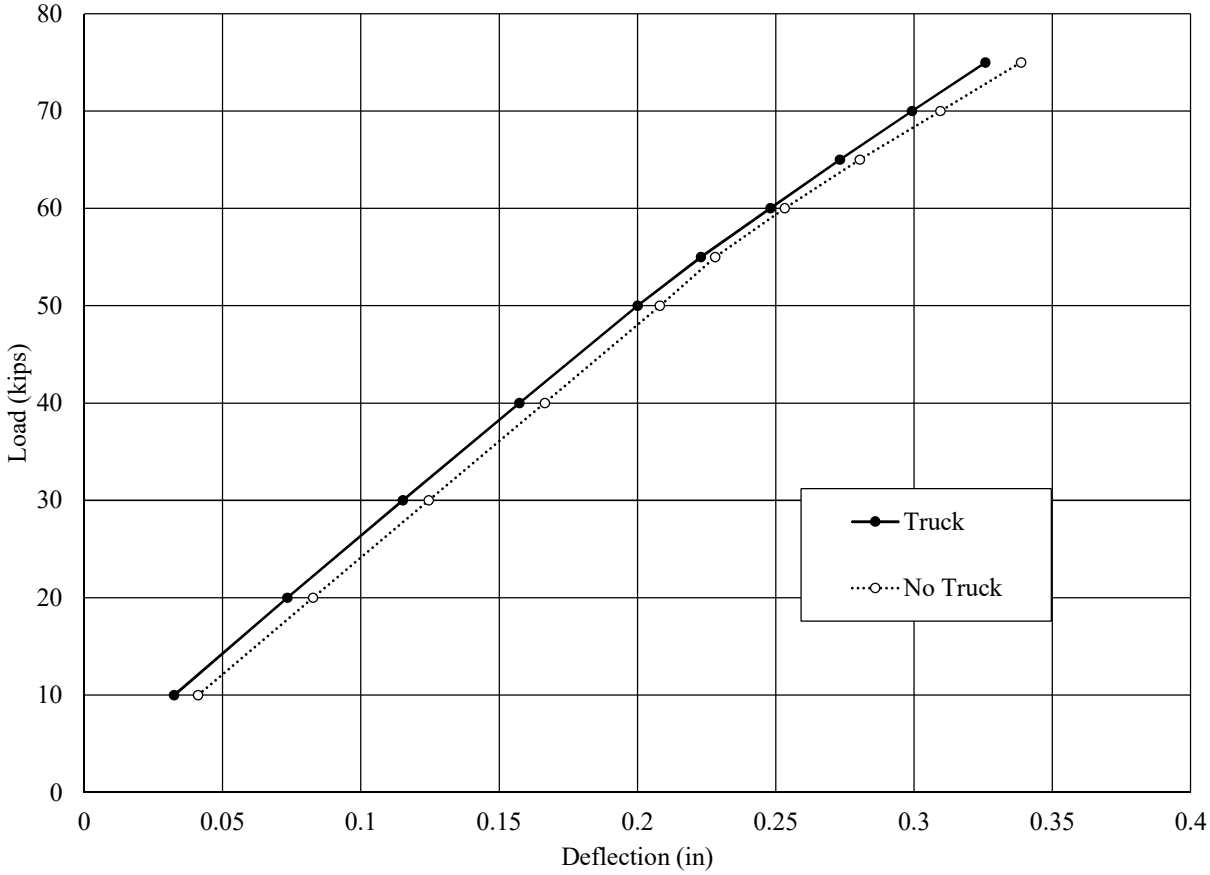

Figure 3-30 – Comparison of Predicted Load versus Deflection Curves from Model Simulations

The simulations predicted the bent with no truck would deflect more than the bent with additional load truck, but the difference is likely due to an initial sway due to the presence of the load truck.

3.5 AUNGES Test Bents

The final phase of modeling simulated the bents constructed at the AUNGES located at the NCAT test track facility in Opelika, Alabama. The models simulated four load tests on two separate stand-

alone bents. Initial models were developed to design the two test bents. Parametric model analysis of the two proposed bent types was conducted to aid in the selection of pile length and to assure the proposed bent designs could feasibly be tested to failure with the available hydraulic jacks. The first modeled bent featured four 35 feet long HP12x53 piles with 10 feet of clear height between the ground surface and the bottom of the pile cap. The exterior piles were battered with a 1.5/12 slope and the two interior pile were vertical. The piles were oriented for weak axis bending in the direction of lateral load. The piles were spaced 8 feet center to center. The second bent was identical to the first bent except that no piles were battered. The pile cap for the battered pile bent model was modeled as 54 inches wide and 24 inches tall to model the 12 inch embedment of the actual piles. The pile cap for the vertical pile bent was modeled as a 36 inch by 36 inch square cap.

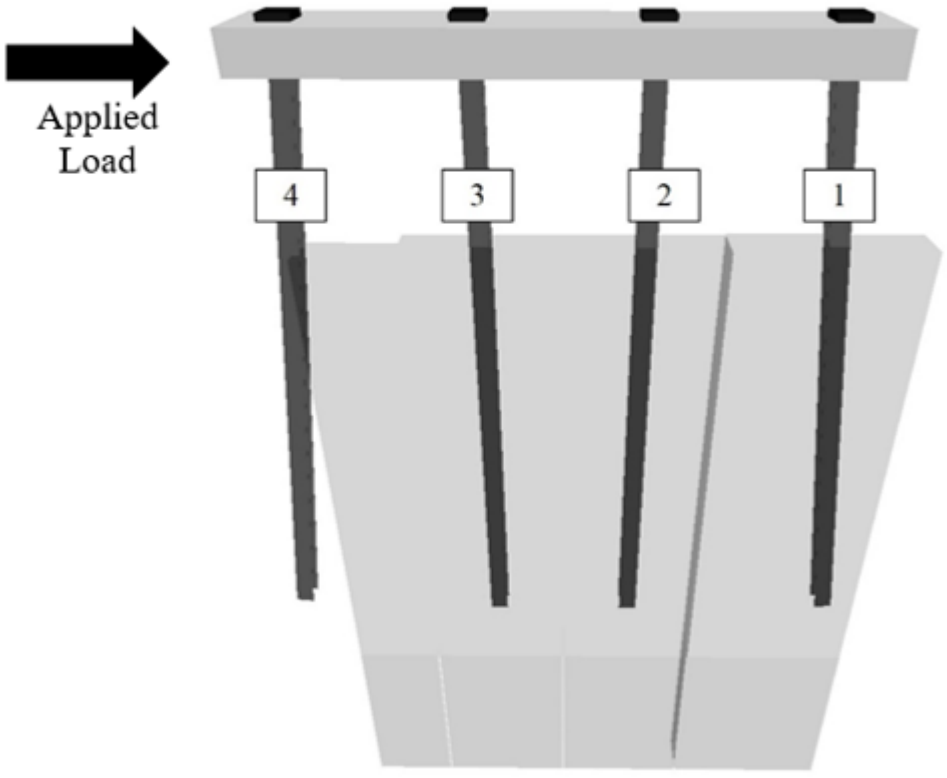

Figure 3-31 – FB Multipier Rendering of the Battered Pile Test Bent

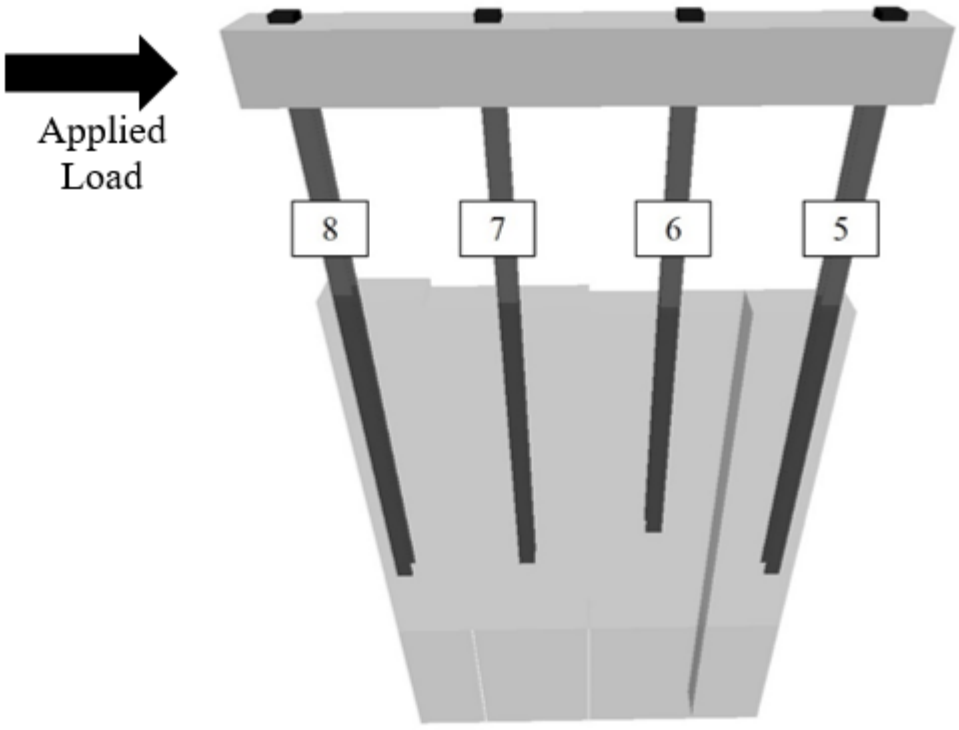

Figure 3-32 – FB Multipier Rendering of the Vertical Pile Test Bent

The models were created to resemble standard ALDOT bridge configurations. The geometric pile properties were taken from the AISC Steel Construction Manual (American Institute of Steel Construction, 2011). An initial estimate of 5,000 psi was used for the compressive strength of the concrete encasements. The steel piles were modeled using the FB Multipier default elastic modulus of 29,000 ksi and yield stress of 58 ksi according to coupon tests conducted on the piles. The q-z and t-z curves for each soil layer were constructed from default FB Multipier options. The p-y curves were developed from dilatometer testing conducted on site. The initial simulations (bent dead load only) for each model simulated a load test with twelve loading increments. The increments were as follows: 10 kips, 20 kips, 30 kips, 40 kips, 50 kips, 60 kips, 70 kips, 80 kips, 90 kips, 100 kips, 110 kips, and 120 kips. The two bent models were also analyzed using a pushover analysis to determine the force required to fail the bents. This analysis was used to

develop a loading schedule for the full-scale load tests. The axial load and bending moment predictions were compiled at node locations along the length of each pile for the distinct loading increments. The centerline deflection of the pile cap was also recorded at each loading increment. Another model was created to simulate the reaction bent needed to field test the bent. The reaction model was subjected to the expected maximum magnitude of loading to ensure the design had sufficient strength and did not experience excessive deflection. Piles were named Pile 1, Pile 2, Pile 3, and Pile 4 on the battered pile bent and Pile 5, Pile 6, Pile 7, and Pile 8 on the vertical pile bent. Pile 1 and Pile 5 were the leading piles, furthest away from the applied load. The piles were spaced at 8 feet center to center spacing which was greater than five times the diameter of the pile. Therefore, p-multipliers to reduce the lateral capacities of the piles were not needed and were not included in any model simulations.

3.5.1 Soil Properties

The soil profile used in the AUNGES bent models was created from dilatometer and SPT data collected on May 28, 2015. The drill rig used to push the dilatometer was operated by an ALDOT drilling team. The dilatometer was operated by Dr. Anderson. Readings were taken every 20 centimeters until the drill rig could no longer push the dilatometer. The SPT was conducted by the same ALDOT drilling crew. The SPT was terminated at a depth of 50 feet with N-counts recorded every 5 feet. The SPT data was used to determine the soil type, and the dilatometer data was used to calculate unit weight, undrained shear strength, and to determine the p-y curves to be used in the analysis of the test bents.

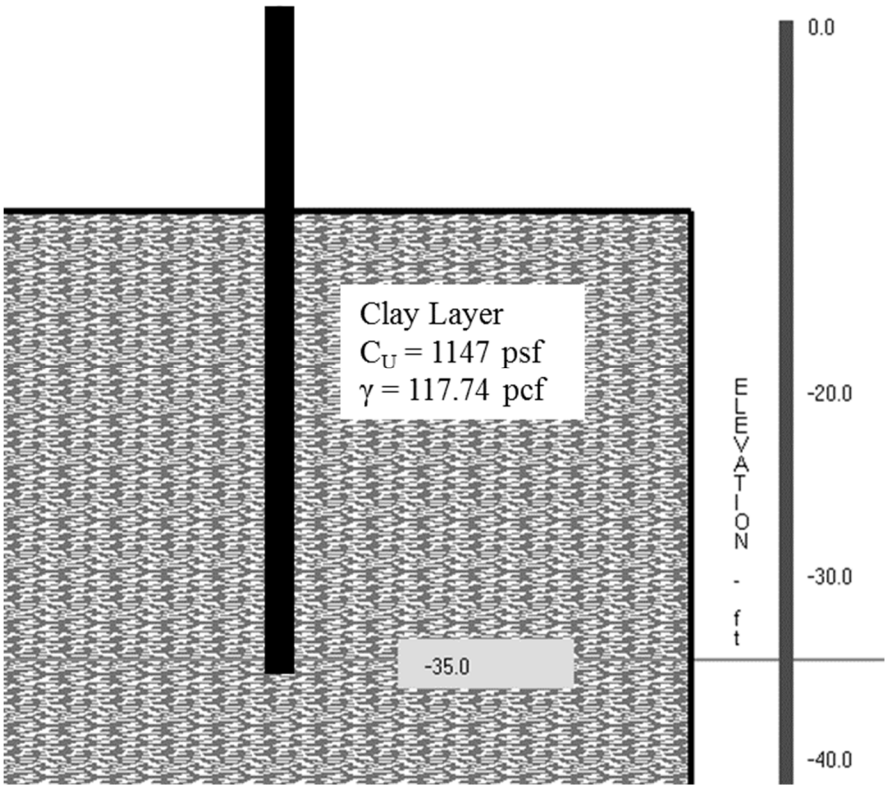

Figure 3-33 – AUNGES Soil and Pile Profile (Adapted from FB Multipier)

Table 3.1 – p-y Values Determined from Dilatometer Data

y (in)	p (lb)
0	0
0.2	6141
0.4	7719
0.6	8825
0.8	9703
1	10445
1.2	11093
1.4	11672
1.6	12197
2	13129

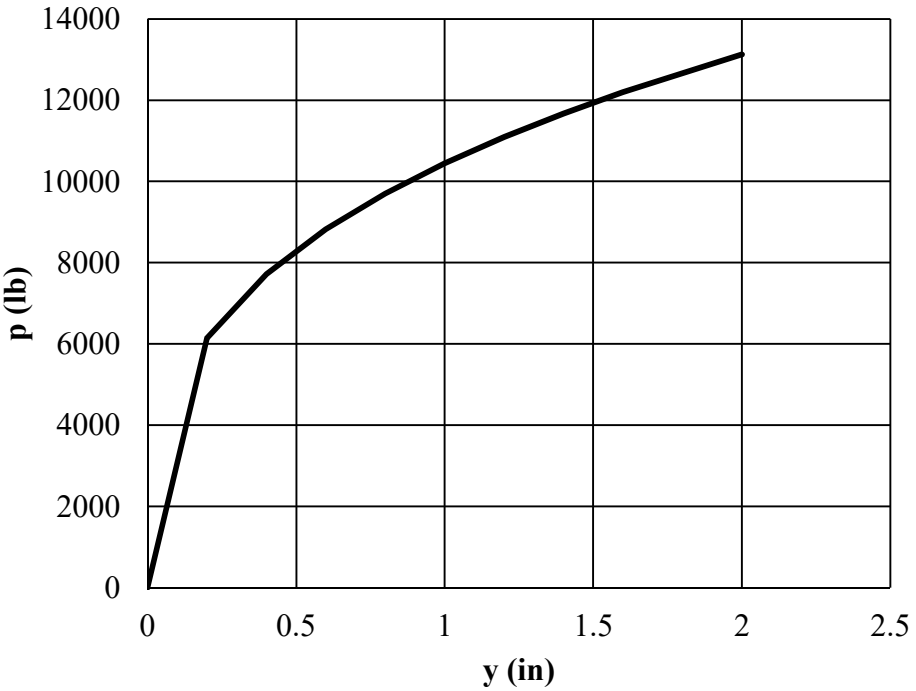

Figure 3-34 – p-y curve Developed from Dilatometer Test

3.5.2 Battered Pile Test Bent Model and Behavior Prediction

The initial model on the battered pile bent was a full pushover analysis. The result was a target load to fail the bent as well as a schedule target when field testing the actual bent. The pushover analysis began at 70 kips and increased in 5 kip increments until an element experienced failure and the model analysis failed to converge on a single solution. The target failure load for the Battered pile bent was 140 kips.

The second model was subjected to the bent dead loads and increasing amounts of lateral load at the same schedule created from the pushover analysis starting at 10 kips and increasing in 10 kip increments until reaching the predicted failure load. Figure 3-35, Figure 3-36, Figure 3-37, and Figure 3-38 show the pertinent results from model simulations. For clarity, only the 20k, 40k, 60k, and 80k load cases are shown. The figures show the theoretical distribution of bending moment with depth for each individual pile. Bending moment profiles were used to verify the accuracy of model predictions. The models also predicted the load versus deflection behavior to

be compared with the wire pot data and produced deflected shapes at the loads where inclinometer tests were scheduled to be conducted on piles 2 and 3. These predictions were used to assess the accuracy of the model predictions, and to verify calibrated models accurately predicted the observed behavior.

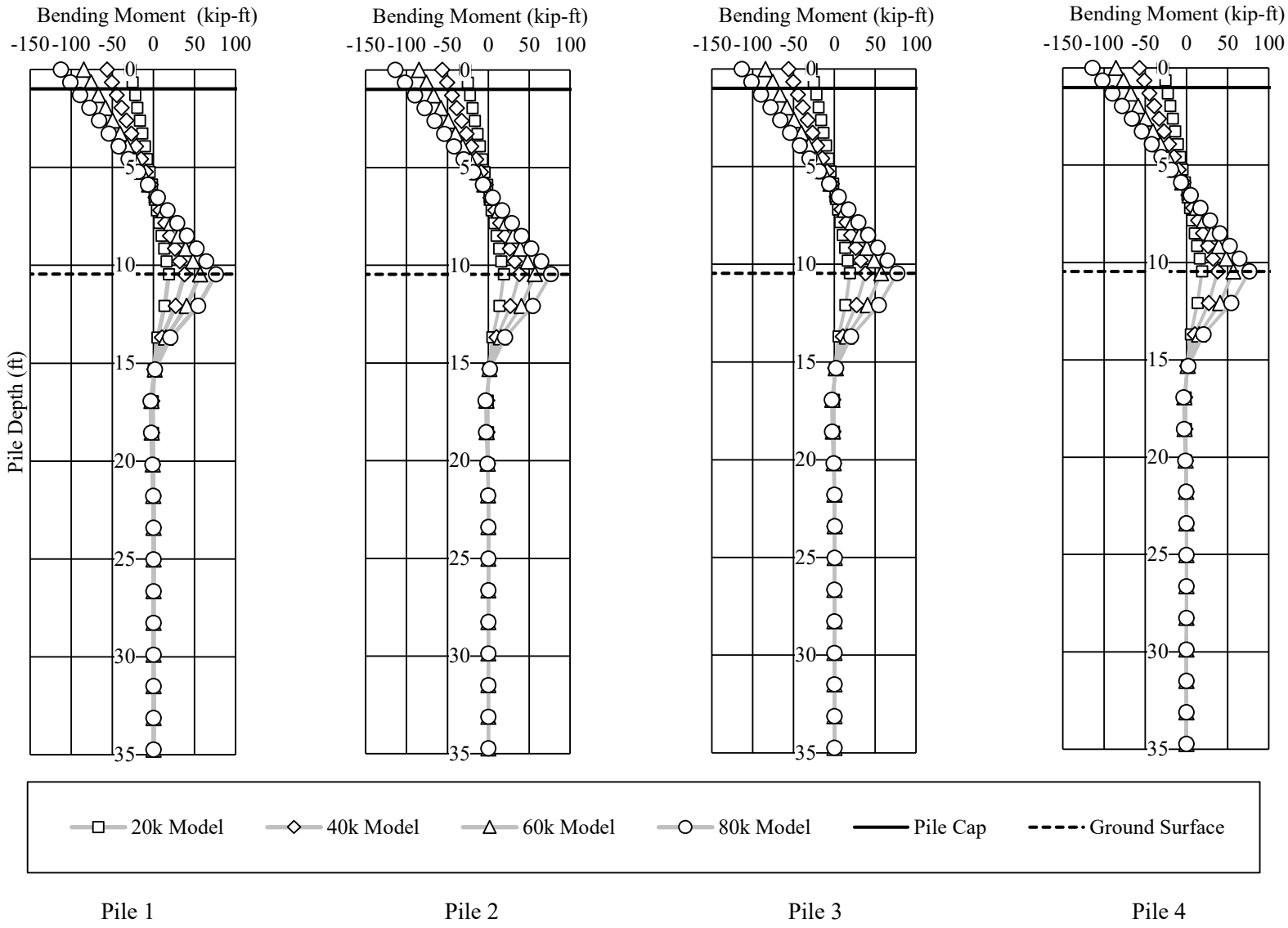

Figure 3-35 – Predicted Moment Profiles for the AUNGES Battered Pile Bent

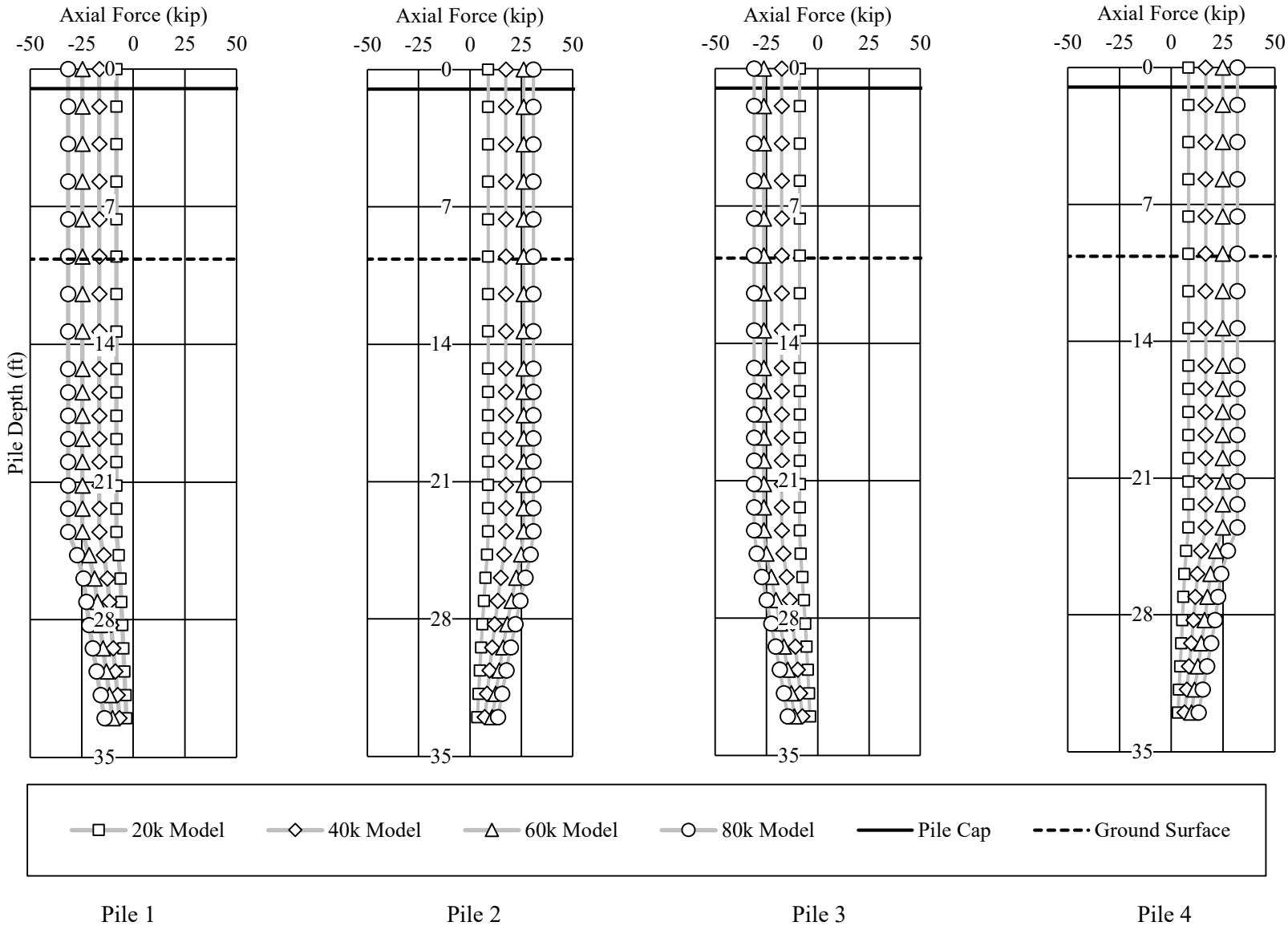

Figure 3-36 – Predicted Axial Load Profiles for the AUNGES Battered Pile Bent

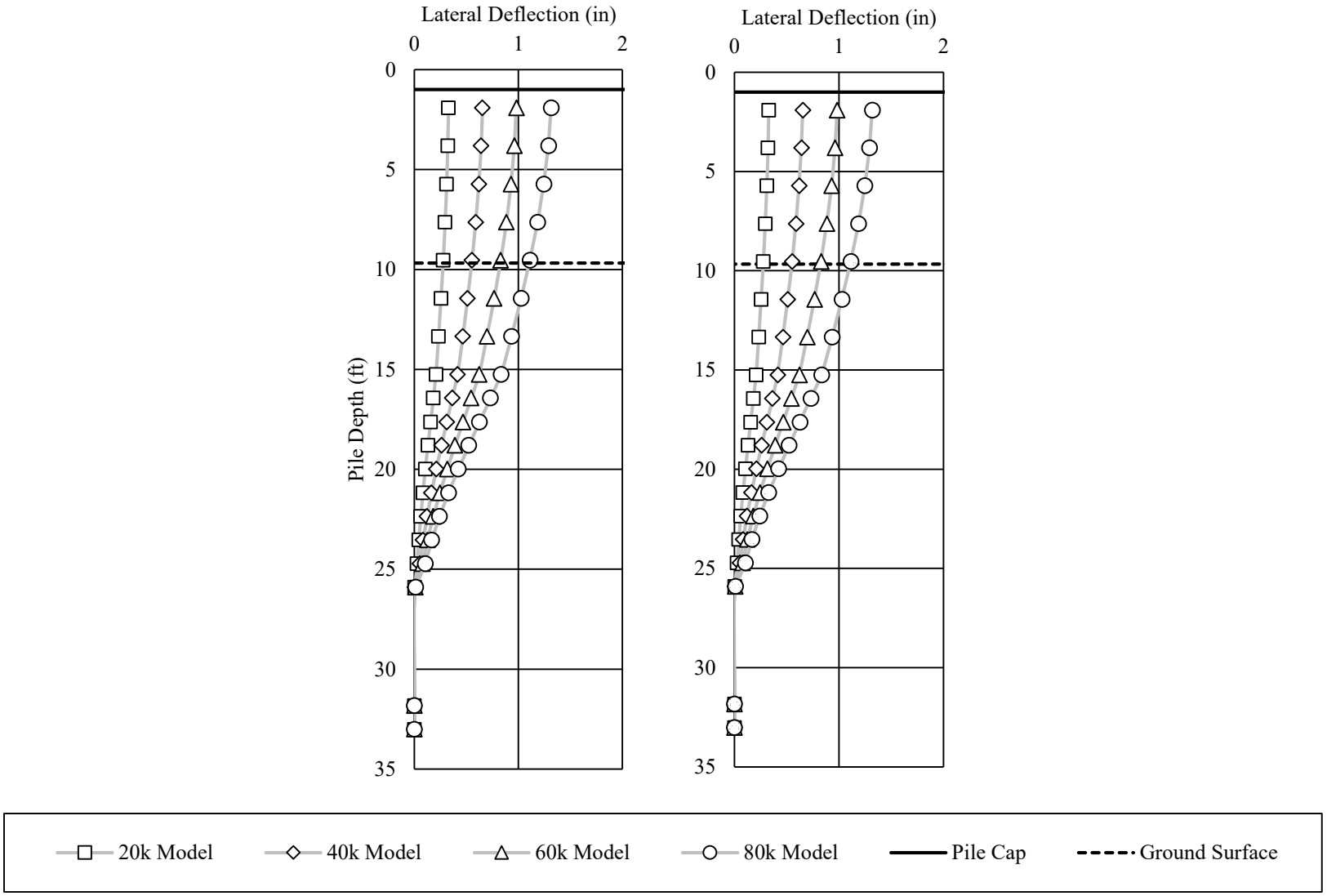

Figure 3-37 – Predicted Lateral Deflection Profiles for the AUNGES Battered Pile Bent

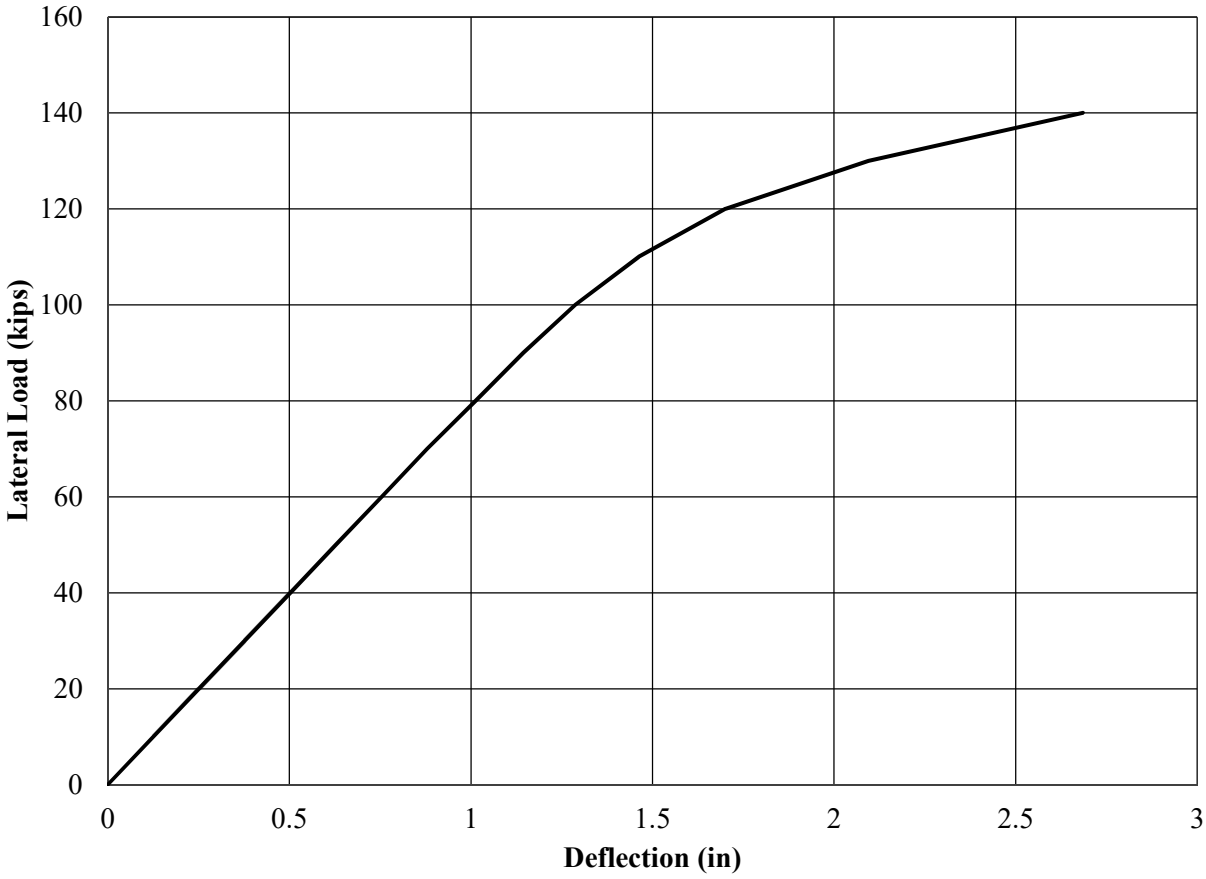

Figure 3-38 – Predicted Load versus Deflection Behavior for the AUNGES Battered Pile Bent

3.5.3 Vertical Pile Test Bent Model and Behavior Prediction

The initial model on the battered pile bent was a full pushover analysis. The result was a target load to fail the bent, as well as a target schedule for field testing the actual bent. The pushover analysis began at 70 kips and increased in 5 kip increments until an element experienced failure and the model analysis failed to converge on a single solution. The target failure load for the Vertical pile bent was 120 kips.

The second model was subjected to the bent dead loads and increasing amounts of lateral load at the same schedule created from the pushover analysis starting at 10 kips and increasing in

10 kip increments until reaching the predicted failure load. Figure 3-39, Figure 3-40, Figure 3-41, and Figure 3-42 show the pertinent results from model simulations. For clarity, only the 20k, 40k, 60k, and 80k load cases are shown. The figures show the theoretical distribution of bending moment with depth for each individual pile. Bending moment profiles were used to verify the accuracy of model predictions. The models also predicted the load versus deflection behavior to be compared with the wire pot data and produced deflected shapes at the loads where inclinometer tests were scheduled to be conducted on piles 5 and 7. These predictions were used to assess the accuracy of the model predictions, and to verify calibrated models accurately predicted the observed behavior.

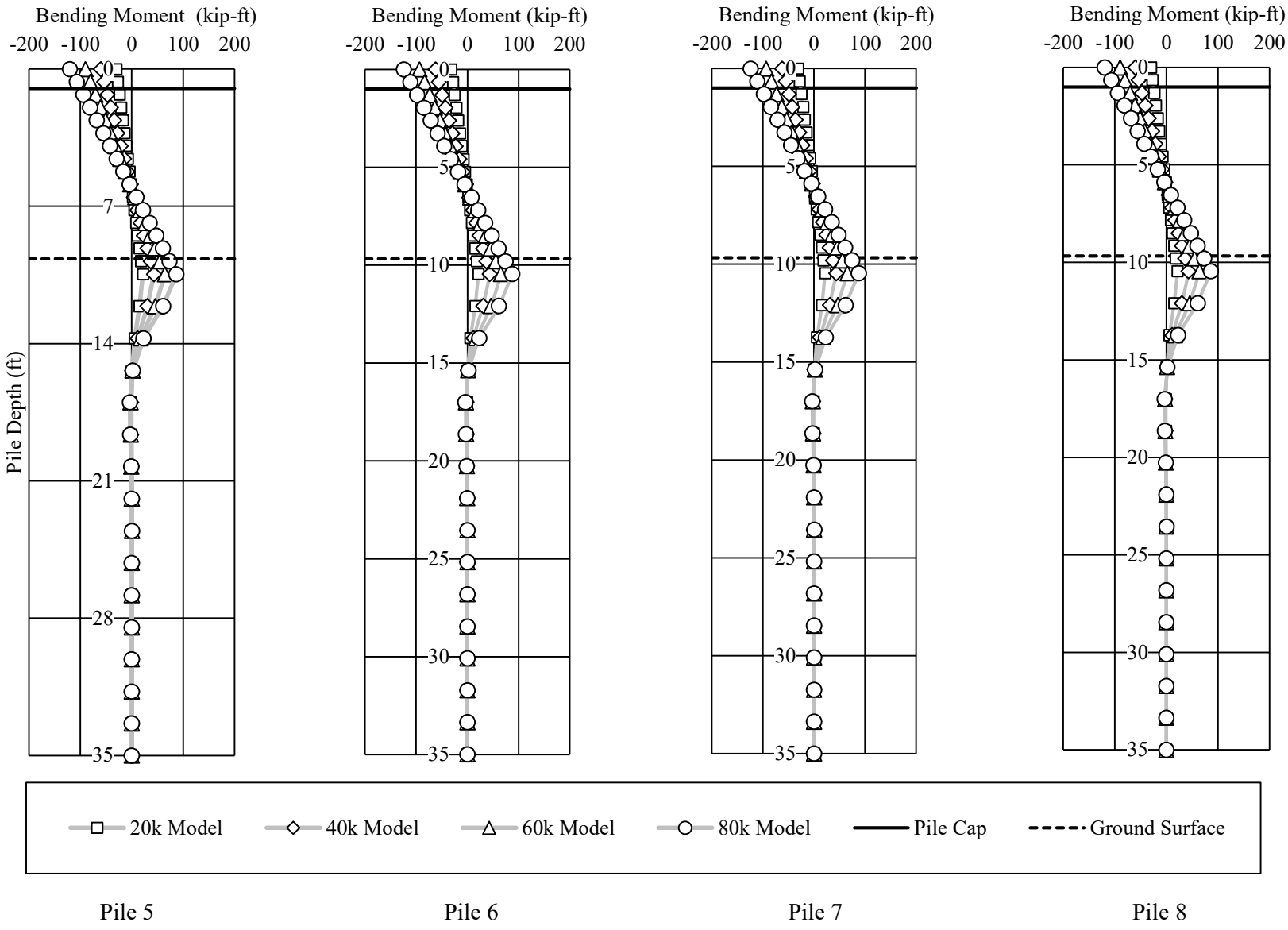

Figure 3-39 – Predicted Moment Profiles for the AUNGES Vertical Pile Bent

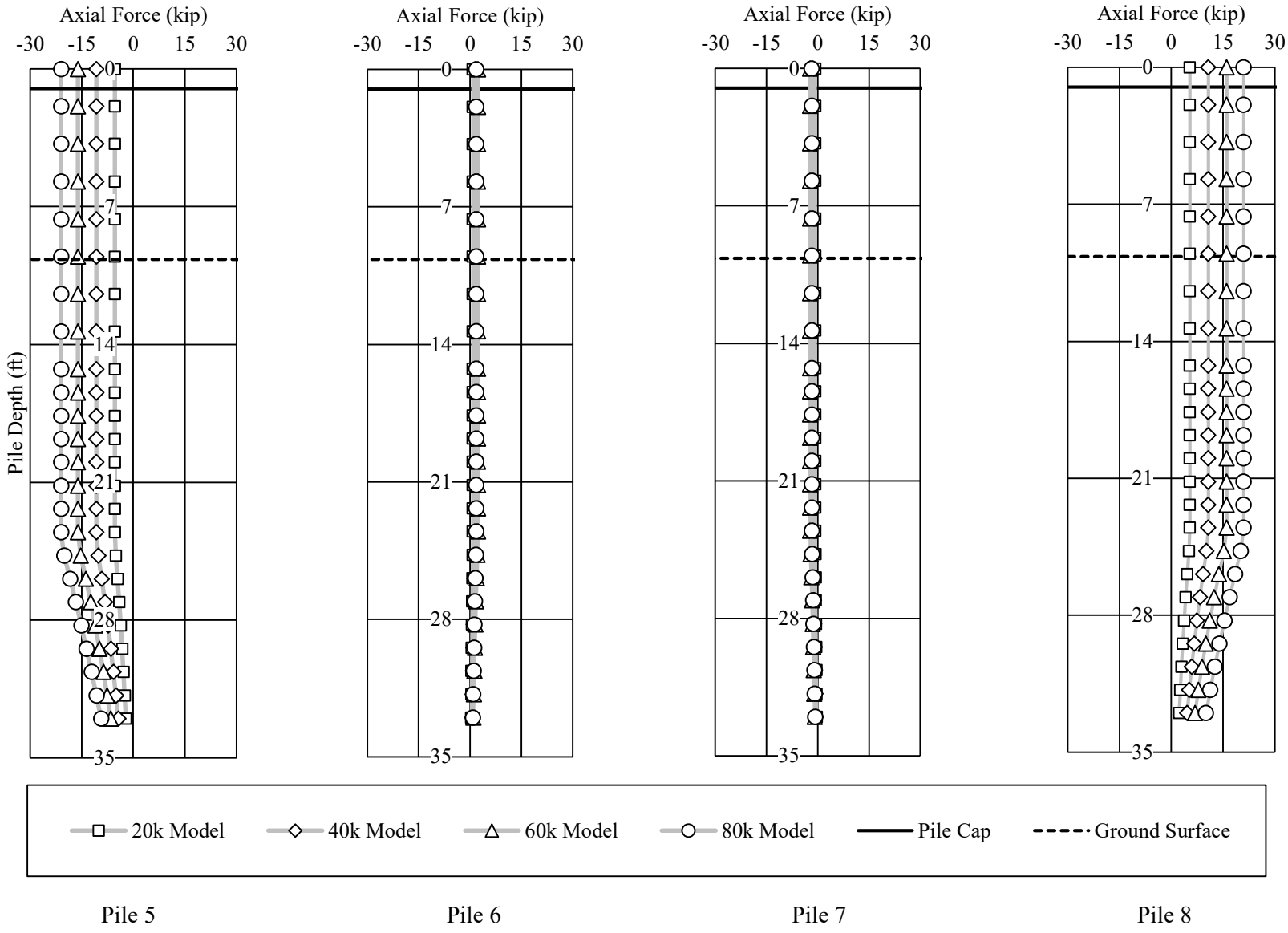

Figure 3-40 – Predicted Axial Load Profiles for the AUNGES Vertical Pile Bent

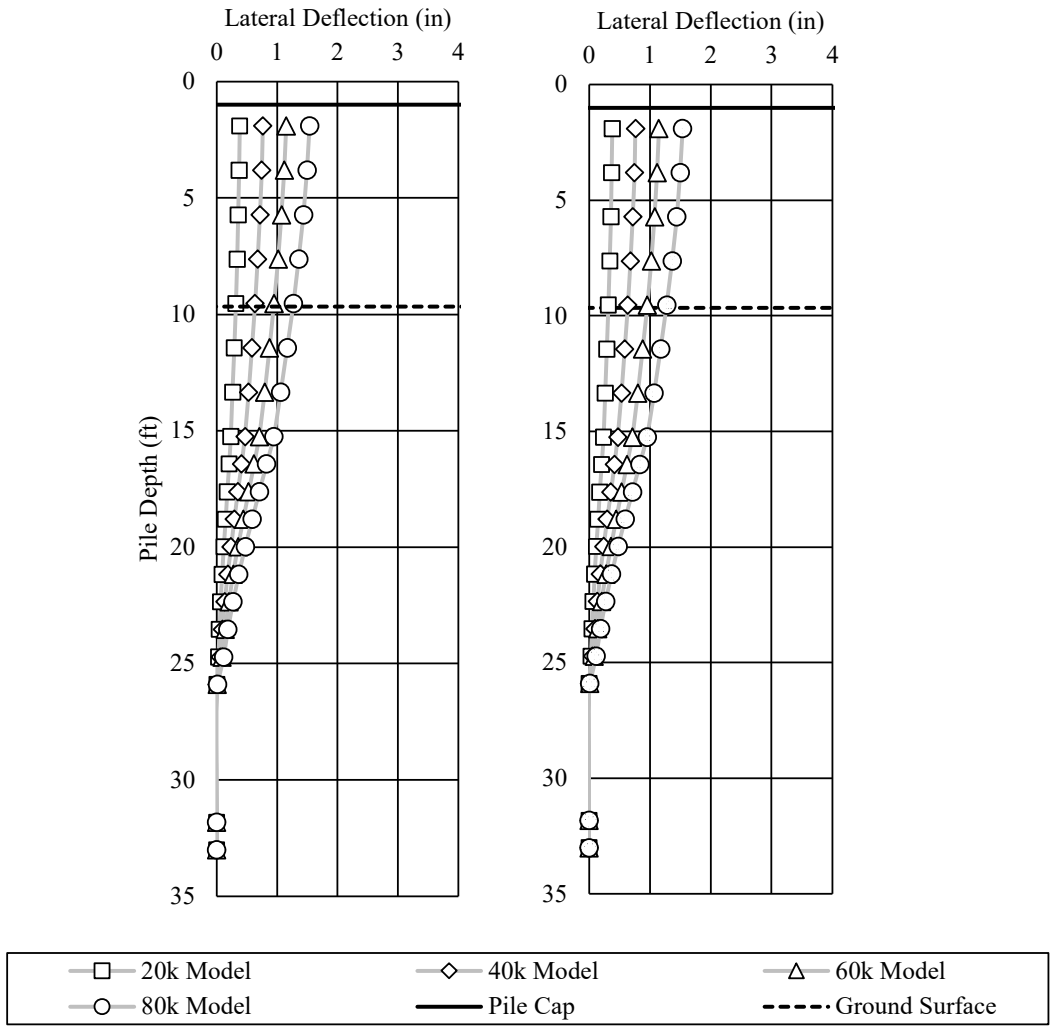

Figure 3-41 – Predicted Lateral Deflection Profiles for the AUNGES Vertical Pile Bent

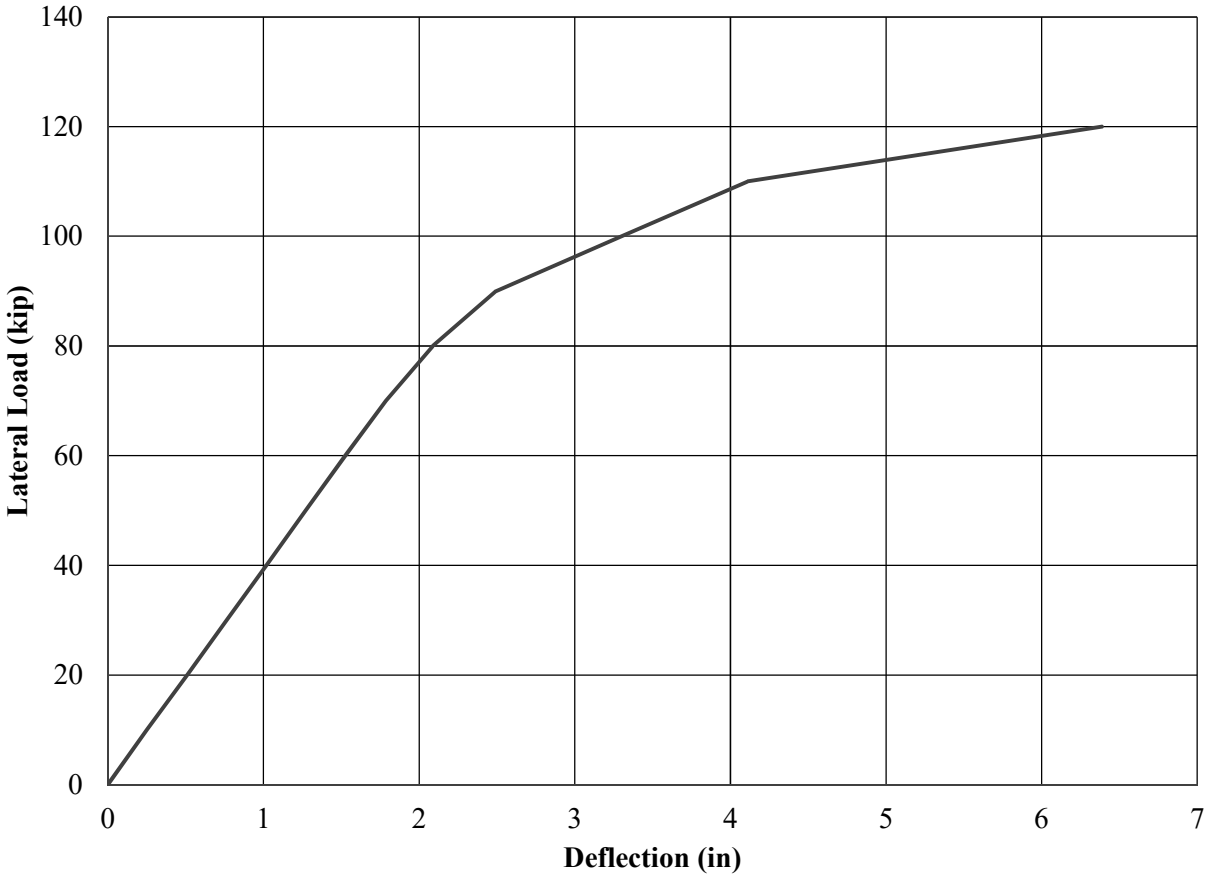

Figure 3-42 – Predicted Load versus Deflection Behavior for the AUNGES Vertical Pile Bent

3.5.4 Pipe Pile Reaction Bent

The reaction bent for the AUNGES bents was a 9 pile bent cap consisting of a 3x3 grid of steel pipe piles. The pipe piles were 41 feet long with an outer diameter of 10.75 inches. The piles were assumed to have an elastic modulus of 29,000 ksi and a yield stress of 43 ksi. The pile cap was 10 feet by 10 feet wide and 33 inches deep. The concrete of the pile cap was assumed to have a compressive strength of 5,000 psi. The soil profile used for the reaction model was the same soil profile used in the test bent models. The model was run to determine if the pile group would be

able to provide the required reaction to sufficiently load the test bents without experiencing excessive deflections. The pipe piles extended out of the concrete cap. The loading plan for the field load tests involved loading the pile cap by the using two steel reaction beams to bear against these pile extensions. FB Multipier was used to analyze the free lengths of the piles to ensure they were structurally sound for the intended application. All models verified that the pile group was sufficient to provide the required reaction forces for the field load tests without causing failures in the free length of the piles.

Chapter 4 Full-Scale Lateral Load Testing of Bridge Bents

4.1 Purpose

Field load tests were conducted to gather data on the behavior of bridge bents subjected to lateral loads. Data was collected to better understand the load path under axial loads and how the addition of lateral loads affects the magnitude of axial force in each pile in a bent. This data was gathered so that it could be compared to theoretical models to assess the accuracy of model predictions. Observed axial load and moment profiles were produced using data collected in a series of tests designed to simulate standard ALDOT designs.

4.2 Overview

Full-scale lateral load tests were conducted at three locations on a total of four bridge bents. The first bent tested was located on Macon County Road 9 in Shorter, Alabama. The bent was subjected to four load tests in 2014. The second bent was located in an existing bridge on U.S. Highway 331 in southern Montgomery County, Alabama. The bent was subjected to three load tests in November 2014. The final two bents were located at the AUNGES at the NCAT test track facility in Opelika, Alabama. Two load tests on each bent were conducted in 2015.

4.3 Instrumentation and Equipment

Several types of instrumentation and equipment were used to execute and monitor the field load tests. Strain gages were attached to steel piles and concrete encasements to monitor the behavior of the piles under lateral load for all tested bridge bents. Instrumented sister bars were placed in the cap to measure strains during the Macon County Road 9 and AUNGES load tests. Instrumented steel threaded rods were used to measure the lateral force applied to the bent for all load tests. Wire pots measured the displacement of the bent caps during every field load test. Two different sets of hydraulic jacks were utilized to apply the needed lateral force for the load tests. Inclinometer

testing was also used to measure the deflected shapes of piles during load testing for the AUNGES test bents. Detailed descriptions of the instrumentation and equipment is presented in the following sections.

4.3.1 Steel Strain Gages

Electrical resistance strain gages were applied directly to the steel piles for the Macon County Road 9 bridge and AUNGES test bents. The application process was conducted in accordance with the gage manufacturer's provided application procedure guide. The first step for steel strain gage application was to remove the oxidized scale on the outer surface of the pile. Dremel tools were used to remove the scale from the piles. Once the scale was removed, the site was degreased to remove any substance that would hinder the adhesive used to bond the gage to the pile. An acidic compound was used to ensure the application site was completely clean. The site was then wet sanded with a fine grit sand paper and a neutralizing agent. Once the application site was clean, epoxy was applied to the pile.

Figure 4-1 – Application of Epoxy to Prepared Strain Gage Location

The stain gage was removed from the package and covered with a piece of clear scotch tape. The back of the gage, the side that would be bonded to the pile, was coated with epoxy and placed onto the prepared site.

Figure 4-2 – Process of Adhering Strain Gage to the Steel Pile

Mastic tape was place underneath the lead wires attached to the strain gage. The mastic tape prevented the lead wires from touching the pile or each other and shorting out the gage. The lead wires were then wrapped around tinned wires and soldered together to create a secure connection. Two wires were soldered to one lead wire so that one would serve as the ground wire and one would serve as reading wire. The other lead wire was soldered to one single wire to complete the circuit required to read the gages. Mastic tape was the place over the exposed wires to separate and protect the connections.

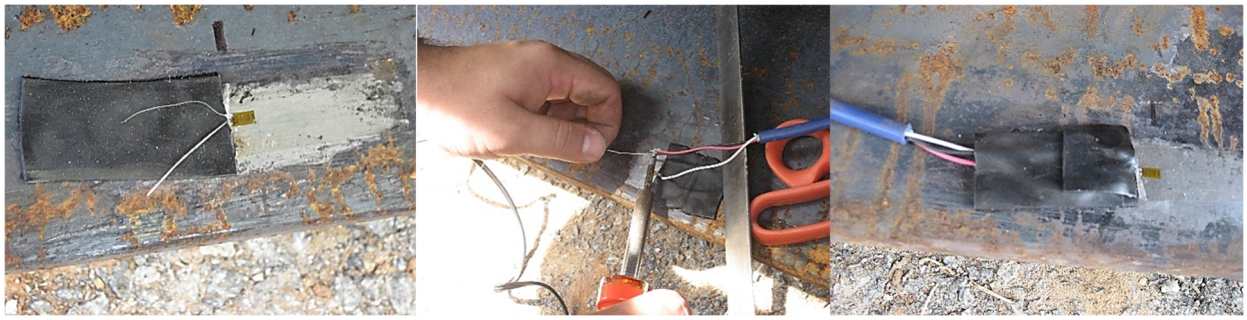

Figure 4-3 – Process of Wiring and Protecting Applied Stain Gage

Once the wires were connected, gages were covered with a waterproofing agent to protect the gages from any water exposure. Strain relief was provided by securing the wires to the piles at locations far enough from the gages to prevent the gages from being ripped from the piles.

Gages were also installed at locations on the piles that would be below the ground surface. Steel angle was welded to the piles to protect the gages from the soil during the driving process. Steel angle was modified to add a driving head so that it would better penetrate the soil.

Figure 4-4 – Subsurface Strain Gage Protection

4.3.2 Concrete Strain Gages

Strain gages were applied to the exterior of the concrete encasements at both the Macon County Road 9 bridge bent and the U.S. Highway 331 bridge bent. The gages used for these locations were

resistance gages. The gages were installed according to the manufacturer's suggested methods. The process began with using Dremel tools to sand the rough concrete surface. The sections were then wet sanded with a slightly acidic solution to clean the exposed surface. The surface was then neutralized with a basic solution and allowed to dry. Epoxy was place on the surface to fill any exposed voids in the concrete. Epoxy was also applied to the back of the gage. The gage was then applied to the surface and the epoxy was allowed to harden. The gages were covered with electrical tape and a waterproofing substance to protect the gages from moisture damage.

Figure 4-5 – Concrete Strain Gage and Initial Layer of Protection

The gages featured attached lead wires. These wires were soldered to longer wires so that the gages could be connected to the data logger.

4.3.3 Data Logger

A Campbell Scientific data logger was used to collect strain data during each field load test conducted. The wires connected to the strain gages were wired into quarter bridge circuit completion units.

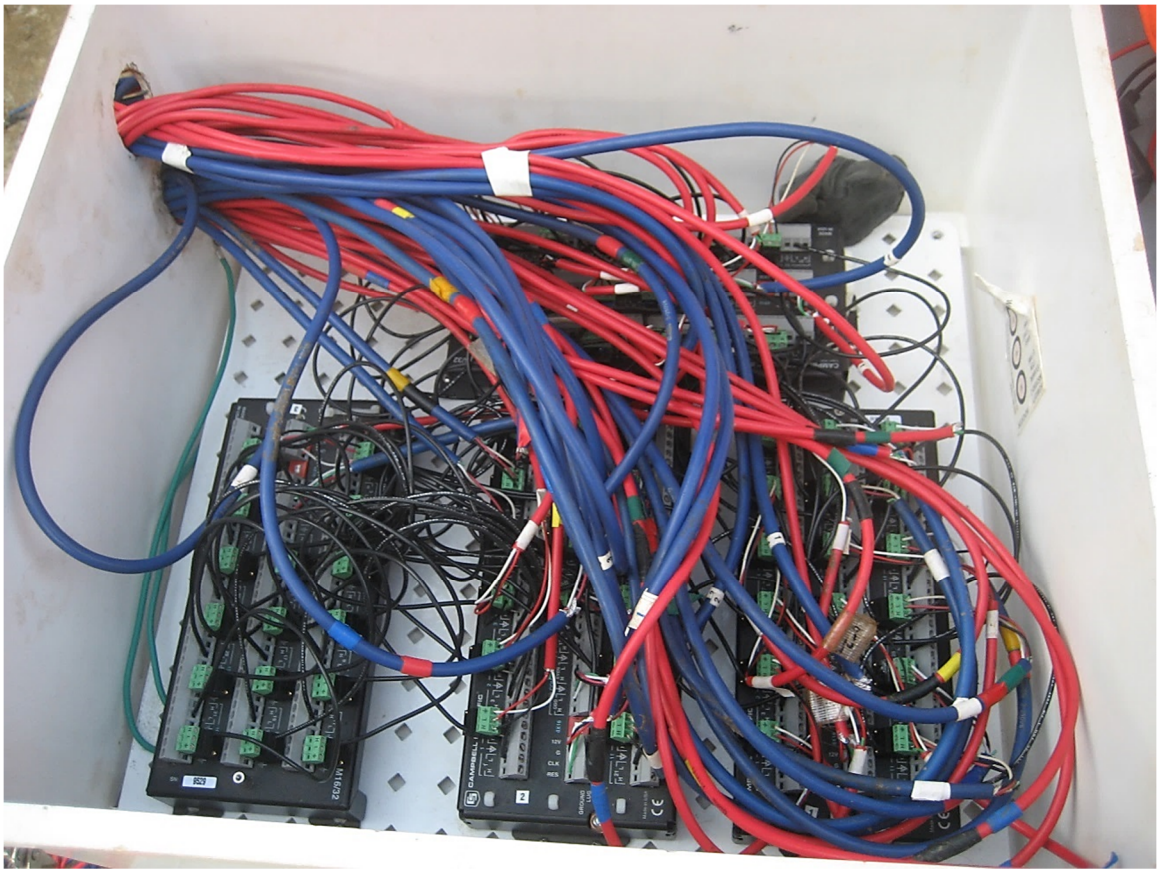

Figure 4-6 – Data Logger during Field Load Test

Campbell software was used to read the voltage readings from the strain gages to determine the amount of strain each gage was measuring. This was accomplished by a program written to automate the reading of the gages and the conversion of the voltage readings to strain values. The data logger was program to read and record the data coming into each channel every 15 seconds. This increment was chosen to provide a sufficient amount of data points without recording an overwhelming amount of redundant data points.

The data collector was also used to monitor the behavior of the bent during the load test. Instrumented threaded rods and load cells were connected to the data acquisition system and used to monitor the magnitude of lateral force applied to the bent. Wire pots were also connected to the data acquisition system. These instruments measured the deflection of the bent under lateral load. The following sections discuss these instruments in greater detail.

4.3.4 Instrumented Threaded Rods

High strength threaded rods were used to apply lateral load to the test bents. Two small sections of threaded rod were instrumented with strain gages at two locations at the center of the segments. These two strain gages were used to measure the tension in the rods during testing. Each rod corresponded to the force supplied by one of the hydraulic jacks used to load the test bents. The rods were monitored during the tests to ensure that both jacks were supplying similar amounts of lateral load and that the loading condition remained symmetric. The rods were also used to calculate the amount of lateral force the bents were exposed to and to monitor the target loading schedule. The instrumented threaded rod segments were used for all the load tests conducted on the Macon County Road 9 Bent, the U.S. Highway 331 Bent, and the AUNGES test bents. Prior to use in load tests, the threaded rods were calibrated in the lab. Correction factors were used during testing for accurate load readings.

Figure 4-7 – Instrumented Threaded Rods prior to Load Testing

4.3.5 Wire Pots

Wire pots were used during load test to measure the magnitude of deflection the bent caps experienced due to the application of lateral load. The wire pots utilize wire wound inside an instrumented housing. Hooks were anchored to the bent caps using drilled holes filled with epoxy. The wire pot housings were attached to a lumber frame that was anchored a short distance from the bent. The frame was rigid and anchored to the ground so that the wire pot housings remain fixed in place. The wire in the wire pots was extended and connected to the epoxied hooks. This initial distance served as the baseline measurement. As lateral load was applied to the bent, the wire would extend or retract. The data acquisition system recorded each measurement, and deflections were calculated based on changes from this initial measurement.

Figure 4-8 – Wire Pot Deflection Measurement Devices prior to Load Testing

The deflection measurements for the Macon County Road 9 bent and U.S. Highway 331 bent were used to ensure the bents did not experience excessive deflections that would result in permanent damage to the bents. The deflection measurements for each load test conducted were coupled with the load data from the instrumented threaded rods and load cells to create load versus deflection curves. The load versus deflection curves were compared to model predictions to assess the accuracy of preliminary models and to accurately calibrate the final models.

4.3.6 Hydraulic Jacks

Two sets of dual hydraulic jacks were used to conduct the lateral load tests. The Macon County Road 9 and U.S. Highway 331 bent tests were conducted on bridges that could not suffer permanent damage since they were part of bridges that were, or soon to be, in service. These bents

were tested using two RRH3010 Enerpac hydraulic jacks. The jacks were capable of applying a combined 60 ton (120 kip) load to the bent cap. This load capacity and jack stroke length was sufficient for the Shorter and Highway 331 bents since they were not pushed to failure.

Figure 4-9 – Enerpac RRH3010 Hydraulic Jacks

The AUNGES bents were designed to be tested to failure. Therefore, higher capacity jacks with greater stroke length were required to provide the necessary lateral load. Two Beerman PTRH6010 hydraulic jacks were used to load the test bents at the AUNGES. These jacks were both 60 ton jacks capable of applying 120 tons (240 kips) of lateral load. These jacks were chosen so that there would be sufficient capacity to induce failure in the piles.

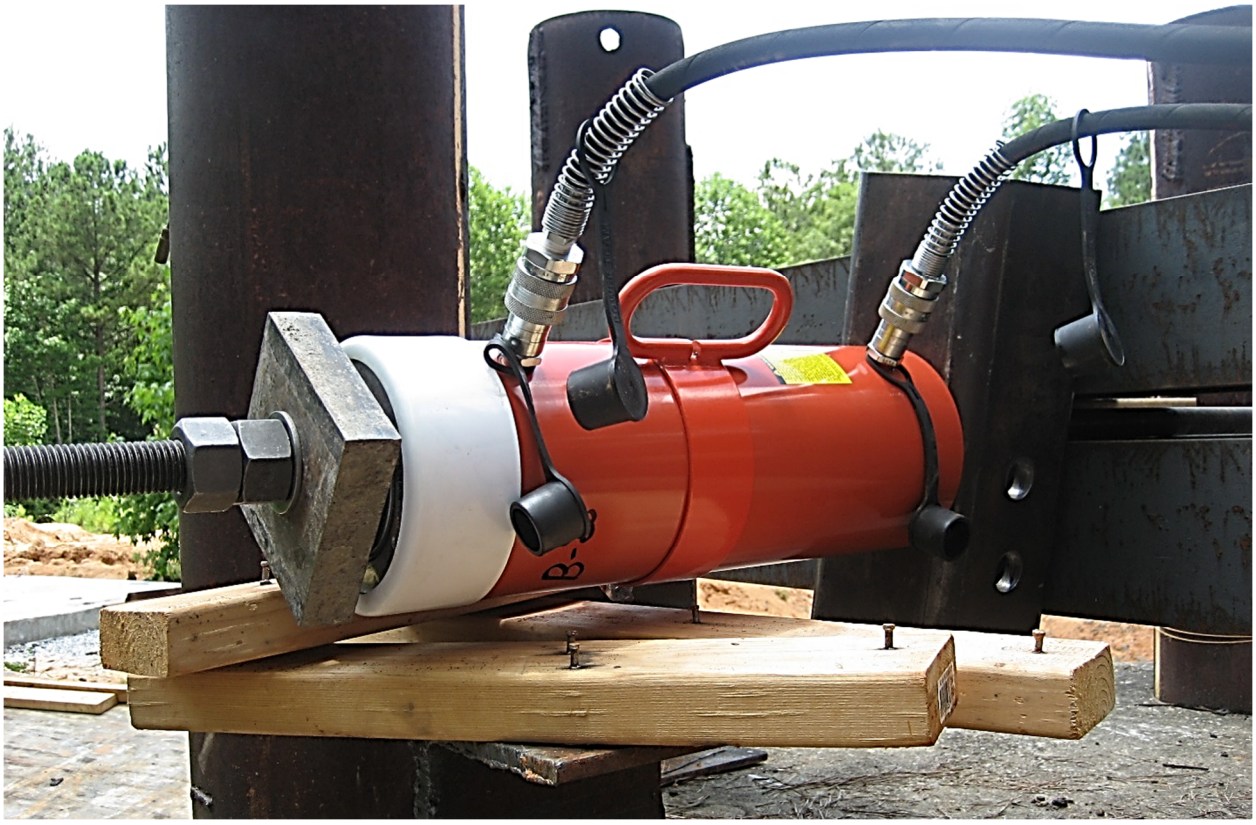

Figure 4-10 – Beerman PTRH6010 Hydraulic Jack

4.3.7 Inclinometer

The inclinometer is a probe equipped with accelerometers used to measure the deflected shape of geotechnical structural elements. Figure 4-11 shows the inclinometer used during the load tests of the AUNGES test bents.

Figure 4-11 – Geokon Inclinometer

The wheels on the probe are designed to travel down tracks in a casing sleeve that is securely connected to the test element. For the AUNGES tests, 2.5 inch square steel tubing was welded to the web of two piles for each test bent to serve as the inclinometer casing. Figure 4-12 shows the inclinometer casing extending out of the cap.

Figure 4-12 – Inclinometer Casing with Inclinometer Downhole

The inclinometer probe was lowered to the bottom of the casing. Before the first inclinometer test, the probe was left at the bottom of the casing for approximately 10 minutes to allow the probe to reach the same temperature as the bottom of the casing. This was done to eliminate any errors in the calculated deflected shape profile due to a variance in temperature. The probe was then pulled back to the top of the casing, pausing every 2 feet for readings. Tape marks every 2 feet along the length of the cable denoted when data points were to be collected. The bottom of the tape was held at the same corner of the inclinometer casing for each data point. Once the inclinometer was pulled out of the casing, it was rotated 180 degrees and lowered back to the bottom of the casing. The probe was then pulled back up to the top of the casing with data points collected every 2 feet as before. The profiles captured from each time the inclinometer was pulled up and out of the casing were used to close the measurement loop and eliminate any error in the deflected shape profile.

4.4 Macon County Road 9 Bent Tests

The first bent tested was located in Shorter, Alabama on Macon County Road 9. The bridge was under construction when this research project began. The test bent was selected after a review of the design drawings and a site visit. The bent was chosen because it was the easiest to instrument and test. The selected bent location had sufficient space for the construction of the required reaction bent and was out of the contractor's critical path so research would not delay the ongoing construction. The bent featured four 31.5 feet long HP14x89 piles with 5 feet of clear height above ground. The exterior piles were battered at 1.5/12 slope. All piles were encased with 30 inch diameter concrete encasements from the bottom of the pile cap to 5 feet below the expected ground surface. The piles were oriented for weak axis bending in the direction of lateral loading. The cap was a standard ALDOT trapezoidal cap 3.5 feet wide at the top, 2.5 feet wide at the bottom, and 2 feet deep. Figure 4-13 shows the planned dimensions of the test bent.

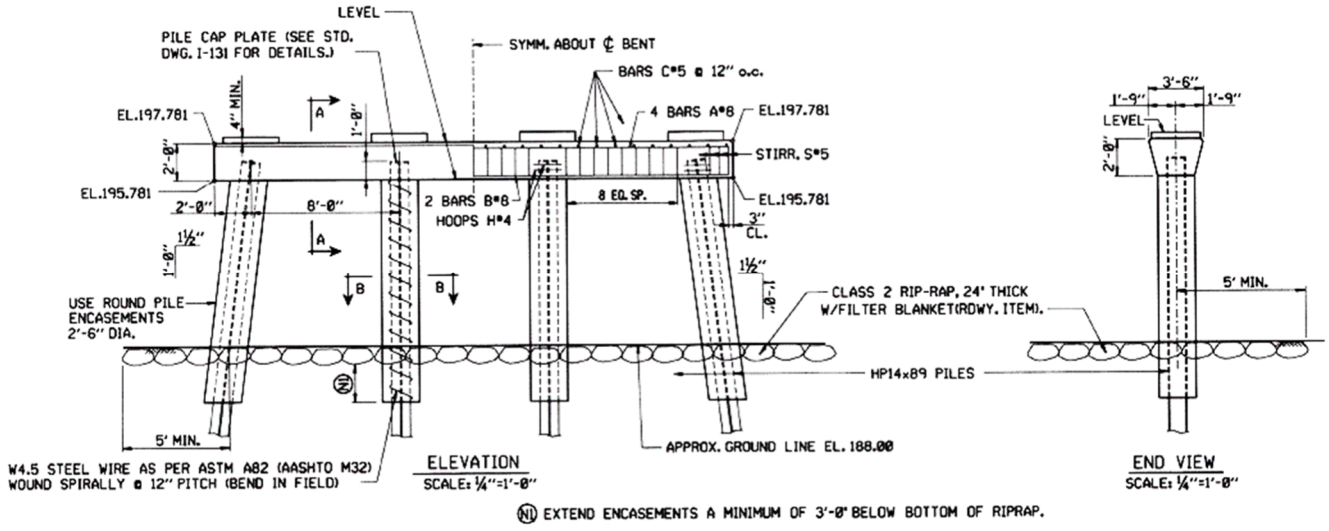

Figure 4-13 – Construction Drawings of Macon County Road 9 Test Bent

Four load tests were conducted on the selected bent. The first test occurred prior to the casting of the bridge deck and was purely a lateral test. The remaining three tests were conducted after the bridge deck was cast. The first test was purely a lateral test to analyze the difference in the behavior

of the bent with and without the deck under lateral loads. The final two tests involved the specific placement of an ALDOT LC-5 load truck. One test featured the load truck centered over the roadway and the bent. The final load test featured the load truck positioned so that the outer edge of the rear tire was aligned with the exterior edge of the exterior girder. The following sections will provide in depth details of the instrumentation locations, the loading apparatus, and the results of the field load tests.

Figure 4-14 – Macon County Road 9 Bridge Test Bent prior to the Casting of the Bridge Deck

4.4.1 Test Overview

The piles in the test bent were instrumented four cross-sections on each pile and at two to three locations at each cross-section. Cross-section locations were chosen based off the theoretical

model predictions of the moment profile. In cases where the instrumented pile section was covered by an encasement, strain gages were also placed at the same cross-section on the concrete encasements to capture a complete strain profile. Figure 4-15 and Figure 4-16 Show the location of each cross-section instrumented for the series of load tests. The color code shown in Figure 4-15 denotes the location of the cross-section so that the wires could be identified after the casting of the bent cap. Gages below ground were connected with blue wire and gages above ground were connected with red wire. Black denotes the upper gage and red denoted the lower gage whether above or below the ground. The final color denotes where on the cross-section the gage was located.

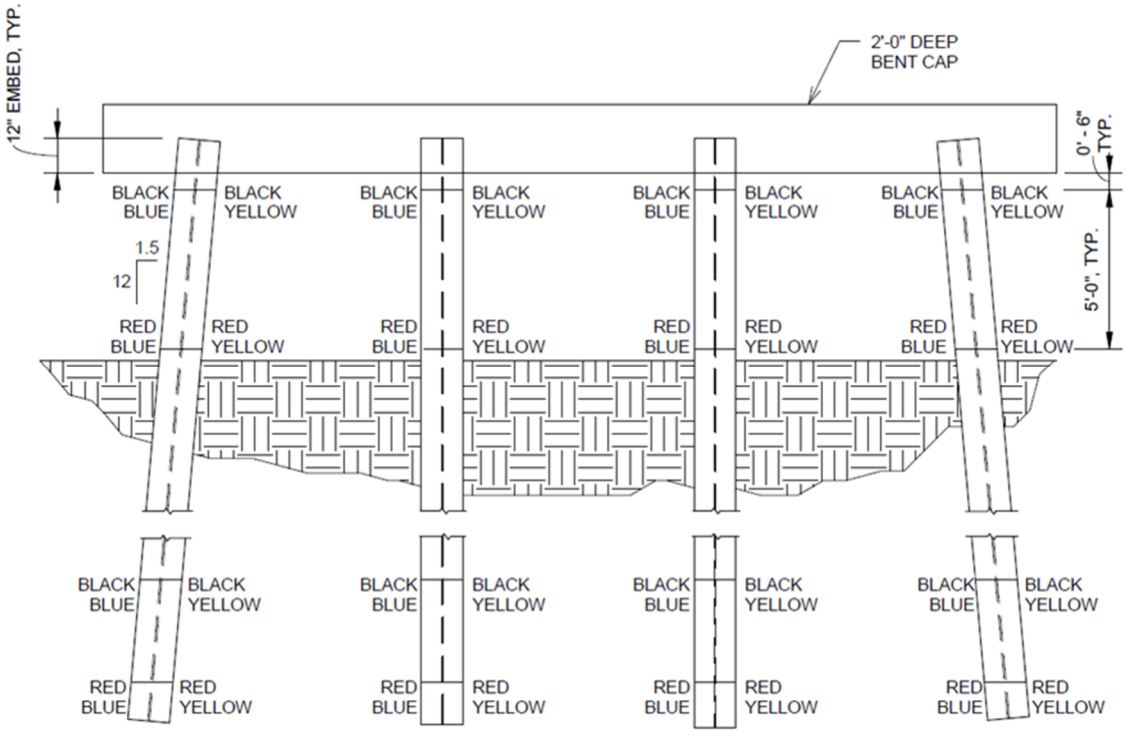

Figure 4-15 – Instrumented Cross-sections on the Steel Piles (Courtesy of Campbell 2015)

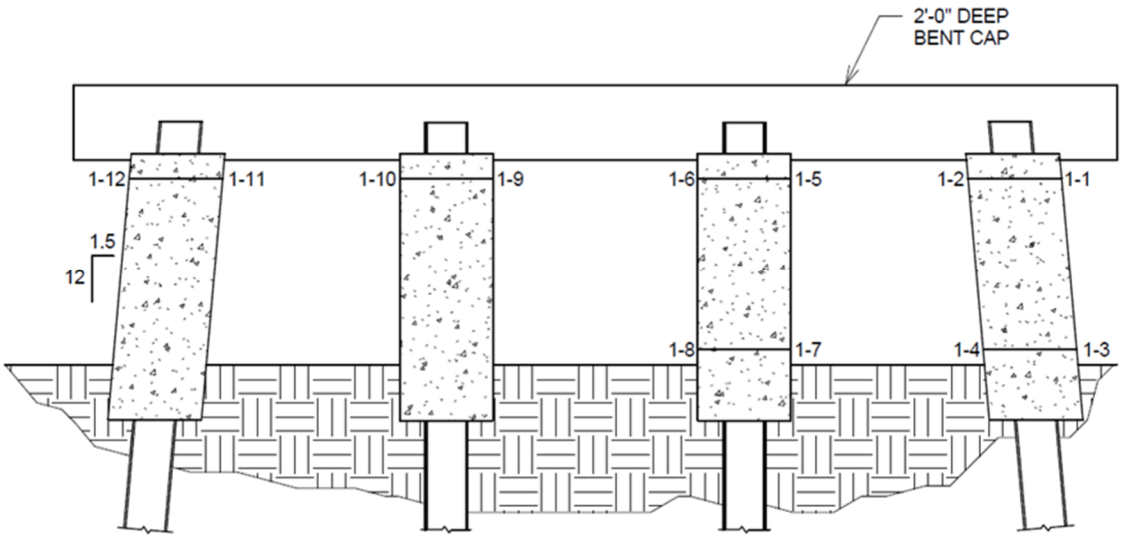

Figure 4-16 – Instrumented Cross-sections on the Concrete Encasements (Courtesy of Campbell 2015)

The locations were meant to capture important points in the moment profile so that the observed moment profile could be compared to the theoretical model profile. This comparison would serve as a barometer of the accuracy of the model predictions. Each cross-section was instrumented with at least two stain gages to capture a complete strain profile across the cross-section. The gages were distinguished using the color coding shown in Figure 4-17 shown below.

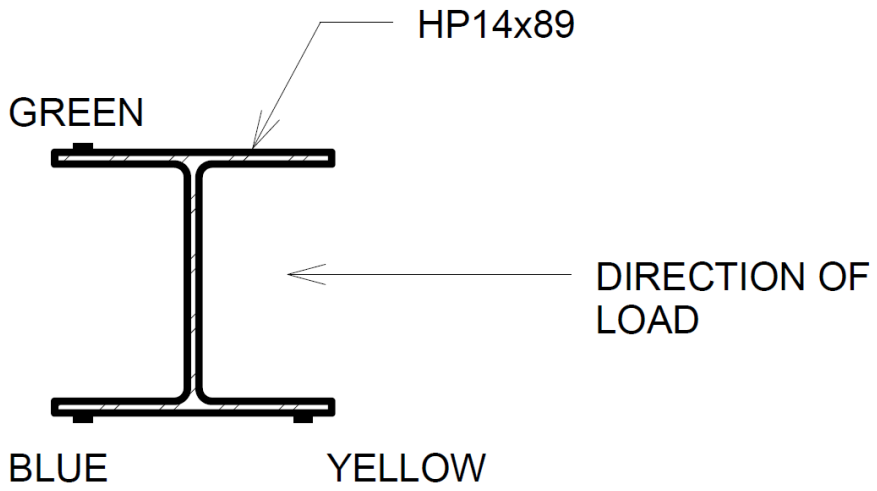

Figure 4-17 – Location of Strain Gages at Each Cross-section (Courtesy of Campbell 2015)

The gages that were below ground were the first gages installed. Prior to the driving process the gages were attached and steel angle was welded to the pile to protect the gages during driving. The wires were fixed to nuts welded on the piles to prevent the wires from being ripped from the gages. Once the piles were driven, the above ground sections were instrumented. All the wires for each pile were then bundled on top of the piles and placed in heavy-duty plastic bags to protect from moisture damage. The bent cap was then formed around the top of the piles. The wires from the first two piles and second two piles were bundled together, protected by a PVC sheathing, and run out of the top of the bent cap formwork. After the encasements were cast, concrete strain gages were applied to the outer surface of the encasements. The wires for the concrete gages were added to the bundle of steel gage wires and protected with heavy-duty plastic bags.

The piles for the reaction bent were driven at the same time as the piles for the test bent. This featured two piles driven with a slight batter 11 feet away from the test bent. Pile cut-off was welded between the two piles to serve as a brace when subjected to lateral loads. Pile cut-off was also welded to the sides of the reaction piles so that the reaction bent could be loaded. The threaded rod was passed through the cut-off sections and hollow tube steel with predrilled holes were placed onto the threaded rods. Nuts were used to hold the tubes in place. Figure 4-18 shows the completed reaction bent. Figure 4-19 shows the steel tube bearing against the pile cut-off welded to the sides of the reaction piles.

Figure 4-18 – Reaction Piles

Figure 4-19 – Hollow Steel Tube Sections Bearing Against the Reaction Bent

The threaded rod passed through the steel tube, through PVC sheathing cast into the bent cap, and out to the opposite side of the cap. An elastomeric bearing pad and a steel plate were placed onto the ends of the rods. These were included to evenly distribute the load from the jacks into the cap and to prevent localized failures such as crushing of the concrete. The jacks were then placed onto the ends of the rods and nuts were used to securely fix the jacks to the steel bearing plate.

Figure 4-20 – Threaded Rods Passing through PVC Sheathing in the Bent Cap

Figure 4-21 – Hydraulic Jacks Bearing Against Steel and Elastomeric Bearing Pads on the Bent Cap

4.4.2 Load Test without Deck

The first load test was conducted prior to the casting of the bridge deck. This test was conducted to measure the bent's response to lateral load without the additional stiffness provided by the bridge deck. The test was conducted on June 27, 2014. The girders for the bridge were already in place. The load schedule was determined using the preliminary models discussed in Chapter 3. It was determined that each loading increment would be held for ten minutes to allow for the data acquisition system to record a sufficient amount of data. This time increment was less than the suggested hold time in ASTM D 3966, but was selected to speed up the load test so as not to overly inconvenience the contractor. The targeted load schedule is shown in Table 4.1 below.

Table 4.1 – Load Schedule for Load Test without the Bridge Deck Cast

Increment Number	Load Amount (kips)	Target Time Hold (min)
1	10	10
2	20	10
3	30	10
4	40	10
5	50	10
6	60	10
7	50	5
8	40	5
9	65	5
10	70	10
11	75	5

The unload portions of the load test were held for shorter increments since the data points were only intended to monitor the behavior of the loading apparatus and ensure it was functioning properly.

4.4.3 Load Test with Deck and No Load Truck

The second load test was conducted after the casting of the bridge deck. This test was conducted to measure the bent's response to lateral load with the additional stiffness provided by the bridge deck. The test was conducted on September 18, 2014. The load schedule was determined using the preliminary models discussed in Chapter 3. It was determined that each loading increment would be held for ten minutes to allow for the data acquisition system to record a sufficient amount of data. This time increment was less than the suggested hold time in ASTM D3966, but was selected to speed up the load test so as not to overly inconvenience the contractor. The targeted load schedule is shown in Table 4.2.

Table 4.2 – Load Schedule for Load Test with Deck and No Load Truck

Increment Number	Load Amount (kips)	Duration (min)
1	10	10
2	20	10
3	30	10
4	40	10
5	50	10
6	60	10
7	70	10

4.4.4 Load Test with Deck and Load Truck Centered over the Bent and Roadway

The third load test was conducted after the casting of the bridge deck. This test was conducted to measure the bent's response to lateral load with the additional stiffness provided by the bridge deck and additional dead load induced by placing a load truck on the bridge. For this test, the load truck was centered over the roadway and the bent. Figure 4-22 shows the placement of the load truck on the bridge.

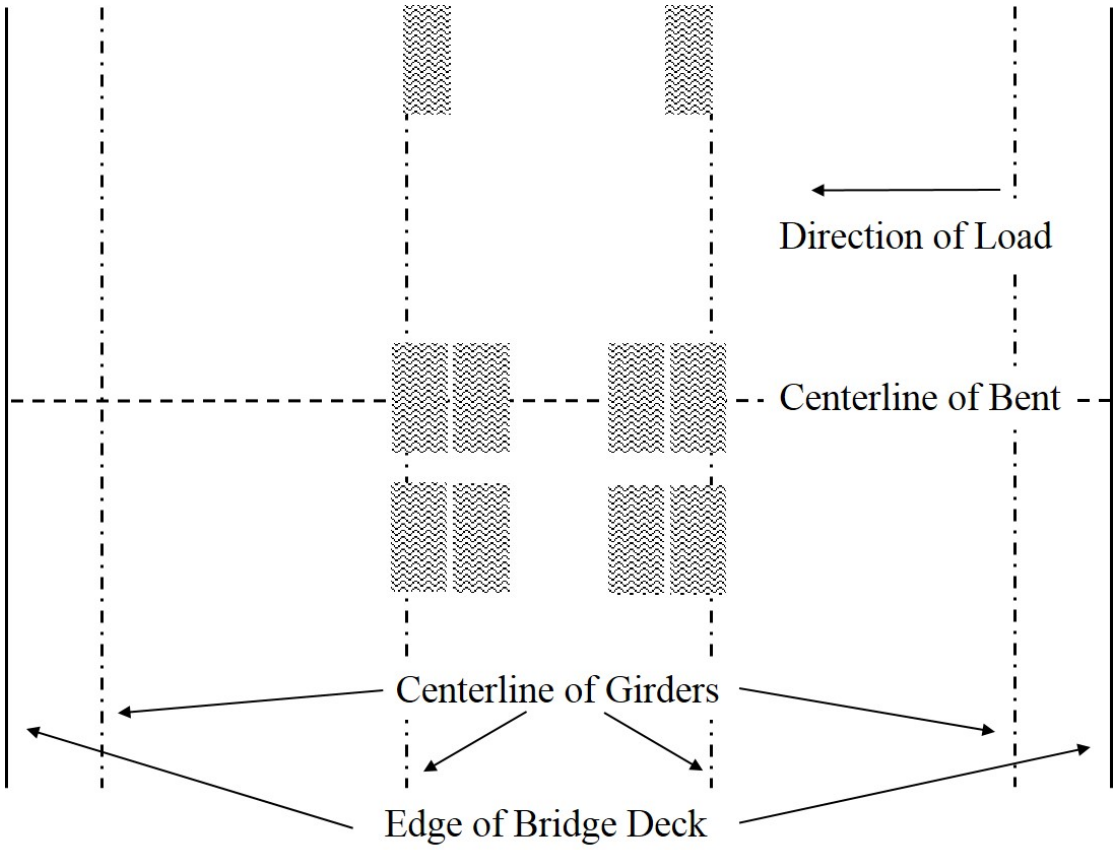

Figure 4-22 – Placement of Load Truck during the Third Macon County Road 9 Load Test

The test was conducted on September 18, 2014. The load schedule was determined using the preliminary models discussed in Chapter 3. It was determined that each loading increment would be held for ten minutes to allow for the data acquisition system to record a sufficient amount of data. This time increment was less than the suggested hold time in ASTM D3966, but was selected to speed up the load test so as not to overly inconvenience the contractor. The targeted load schedule is shown in Table 4.3.

Table 4.3 – Load Schedule for Load Test with Deck and Truck Centered on the Deck

Increment Number	Load Amount (kips)	Duration (min)
1	10	10
2	20	10
3	30	10
4	40	10
5	50	10
6	60	10
7	70	10

4.4.5 Load Test with Deck and Load Truck over the Exterior Girder

The fourth load test was conducted after the casting of the bridge deck. This test was conducted to measure the bent's response to lateral load with the additional stiffness provided by the bridge deck and additional dead load induced by placing a load truck on the bridge. For this test, the load truck was centered over the roadway and the bent. Figure 4-23 shows the placement of the load truck on the bridge.

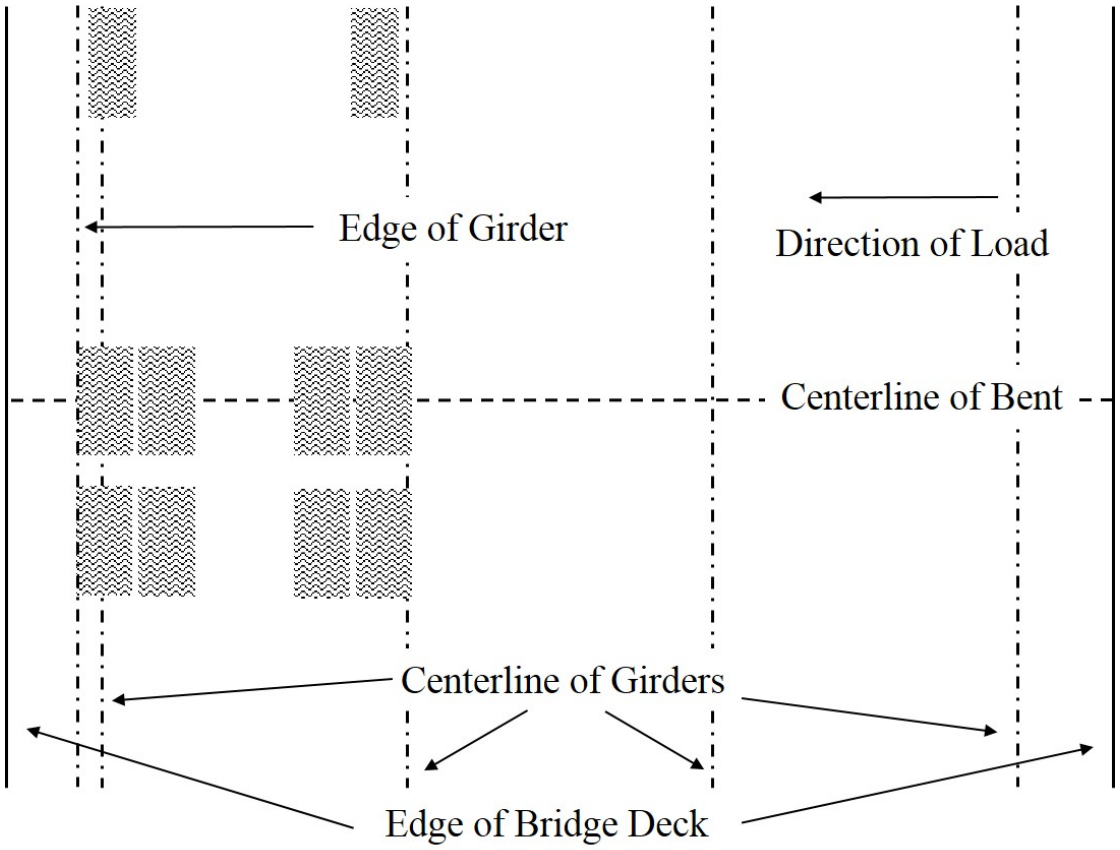

Figure 4-23 – Placement of Load Truck during the Fourth Macon County Road 9 Bent Load Test

The test was conducted on September 18, 2014. The load schedule was determined using the preliminary models discussed in Chapter 3. It was determined that each loading increment would be held for ten minutes to allow for the data acquisition system to record a sufficient amount of data. This time increment was less than the suggested hold time in ASTM D 3966, but was selected to speed up the load test so as not to overly inconvenience the contractor. The targeted load schedule is shown in Table 4.4. Figure 4-24 shows the load truck positioned over the edge girder.

Table 4.4 – Load Schedule for the Load Test with Deck and Truck over the Edge Girder

Increment Number	Load Amount (kips)	Duration (min)
1	10	10
2	20	10
3	30	10
4	40	10
5	50	10
6	60	10
7	70	10

Figure 4-24 – Placement of Load Truck over the Edge Girder

4.5 U.S. Highway 331 Bent Test

The second bent tested was located in Montgomery County, Alabama on U.S. Highway 331. Two in service sister bridges were chosen so that one of the bridges could serve as a reaction bent and the other could serve as the instrumented test bent. The test bent was selected after a review of the design drawings and a site visit as because the bent featured smaller piles and greater free length above the ground than the Macon County Road 9 bridge bent. The chosen test bent featured 6 HP10x42 piles 28 feet long with 10 feet of clear height above ground. The piles were encased in 16 inch square concrete encasements. The exterior piles were battered at a 1.5/12 slope. The piles

were oriented for weak axis bending in the direction of the lateral load. The piles and girders were spaced at 5 feet center to center. The trapezoidal pile cap was 3.5 feet wide at the top, 2.5 feet wide at the bottom, and 2 feet deep. Two load tests were conducted on the selected bent. The first test was purely a lateral test. The remaining test was conducted with the addition of dead weight from an ALODT LC-5 load truck. The load test featured the load truck positioned so that the outer edge of the rear tire was aligned with the exterior edge of the exterior girder. The following sections will provide in depth details of the instrumentation locations, the loading apparatus, and the results of the field load tests.

Figure 4-25 – Selected U.S. Highway 331 Test Bent

4.5.1 Test Overview

The piles in the test bent were instrumented at three cross-sections on each pile and at two locations at each cross-section. Three piles in the reaction bent were also instrumented at two locations.

Cross-section locations were chosen based off the theoretical model predictions of the moment profile. All gages for these tests were located on the concrete encasements as there was no access to the steel piles. Figure 4-26 and Figure 4-27 show the location and name of each gage for the series of load tests. Gages were named using two numbers. The first number was the number of the pile on which the gage was located. The second number referred to the cross-section on the pile where the gage was located.

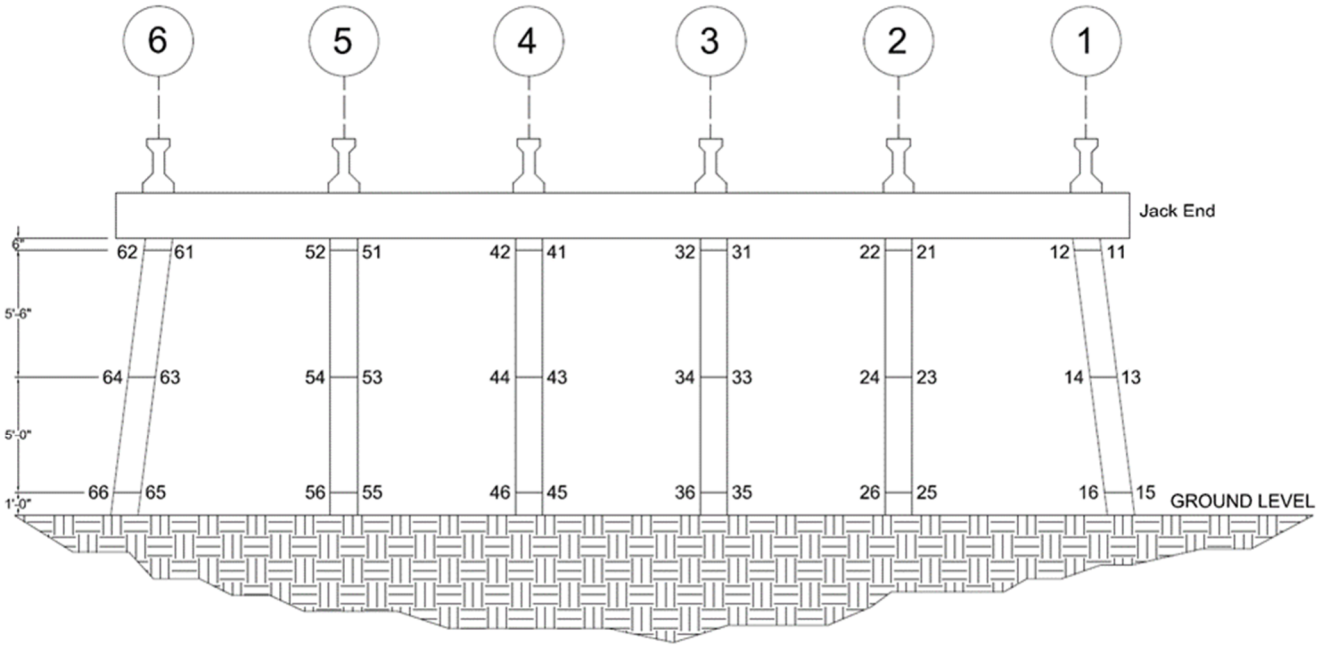

Figure 4-26 – U.S. Highway 331 Test Bent Gage Names and Locations (Campbell, 2015)

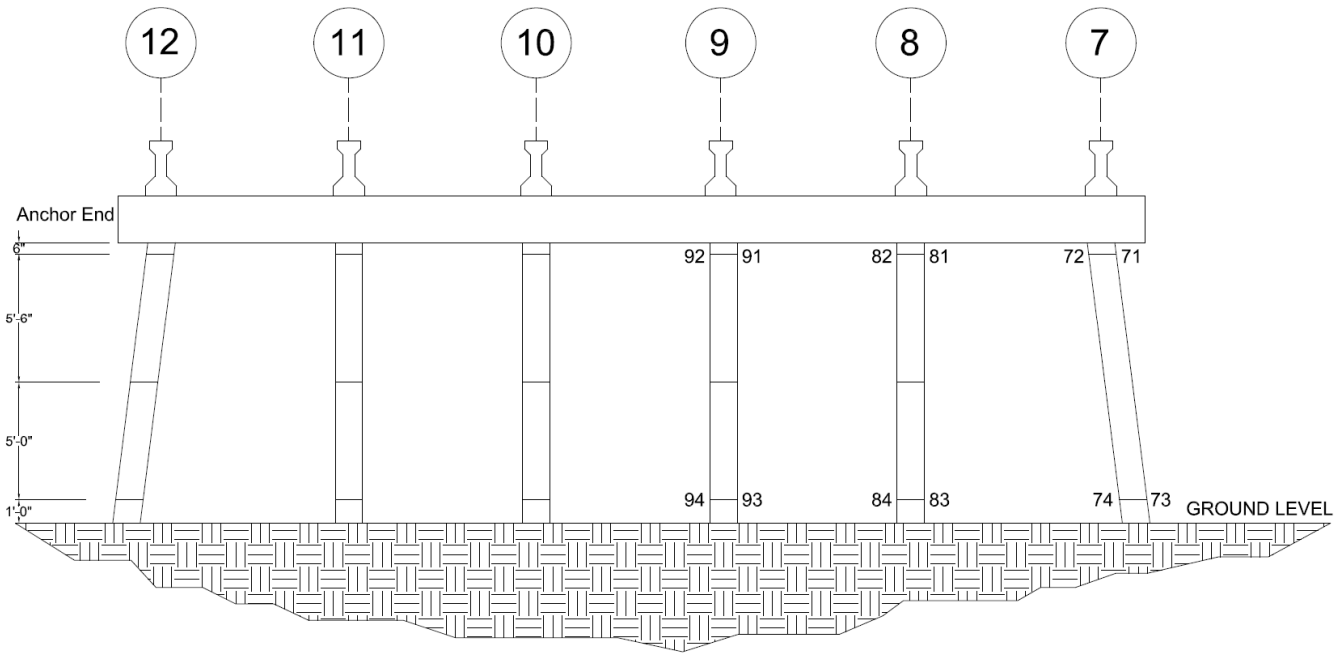

Figure 4-27 – U.S. Highway 331 Reaction Bent Gage Names and Locations (Campbell, 2015)

The gages were installed on the day before the load test was conducted. The bridge deck was counted on for protection from the moisture so gages were only covered in mastic tape and secured to the pile for the night before testing.

The bent was loaded by running a series of joined threaded rods from the jack end of the test bent to the anchor end on the reaction bent. The rods were suspended from hooks placed on top of the bent caps to remove as much sag as possible from the length of coupled rods. 32 inch long hollow steel tube sections were hoisted into place on the exterior cap faces with elastomeric bearing pads placed between the tube and the cap. The threaded rods ran through predrilled holes. The tube at the anchor end was secured to the cap face using nuts. The jacks were placed onto the rods and allowed to bear directly on the steel tube. The jacks were then secured in place with nuts.

4.5.2 Load Test with No Load Truck

The first load test was conducted without additional load due to a load truck. The test was conducted on November 18, 2014. The load schedule and predicted behavior was determined using

the preliminary models discussed in Chapter 3. It was determined that each loading increment would be held for ten minutes to allow for the data acquisition system to record a sufficient amount of data. This time increment was less than the suggested hold time in ASTM D3966, but was selected to speed up the load test so as not to overly inconvenience the local traffic which was stopped during testing. The targeted load schedule is shown in Table 4.5.

Table 4.5 – Load Schedule for the Load test with No Load Truck

Increment Number	Load Amount (kips)	Duration (min)
1	10	10
2	20	10
3	30	10
4	40	10
5	50	10
6	60	10
7	70	10
8	80	10
9	90	10

The maximum load applied to the bent was restricted to prevent permanent damage to the structure. At 90 kips of lateral load, there was little visual evidence of strain on the structure. Measured deflections were less than one inch and no cracking was observed on the pile encasements.

4.5.3 Load Test with Load Truck Centered over the Exterior Girder

The second load test was conducted with additional axial load due to the addition of a load truck. The test was conducted on November 18, 2014. The load schedule and predicted behavior was determined using the preliminary models discussed in Chapter 3. It was determined that each loading increment would be held for ten minutes to allow for the data acquisition system to record a sufficient amount of data. This time increment was less than the suggested hold time in ASTM D 3966, but was selected to speed up the load test so as not to overly inconvenience the local traffic which was stopped during testing. The targeted load schedule is shown in Table 4.6.

Table 4.6 – Load Schedule for the Load test with Load Truck over the Edge Girder

Increment Number	Load Amount (kips)	Duration (min)
1	10	10
2	20	10
3	30	10
4	40	10
5	50	10
6	60	10
7	70	10
8	80	10
9	90	10

Figure 4-28 shows the plan view location of the load truck on the deck, and Figure 4-29 shows the load truck on the deck during the load test.

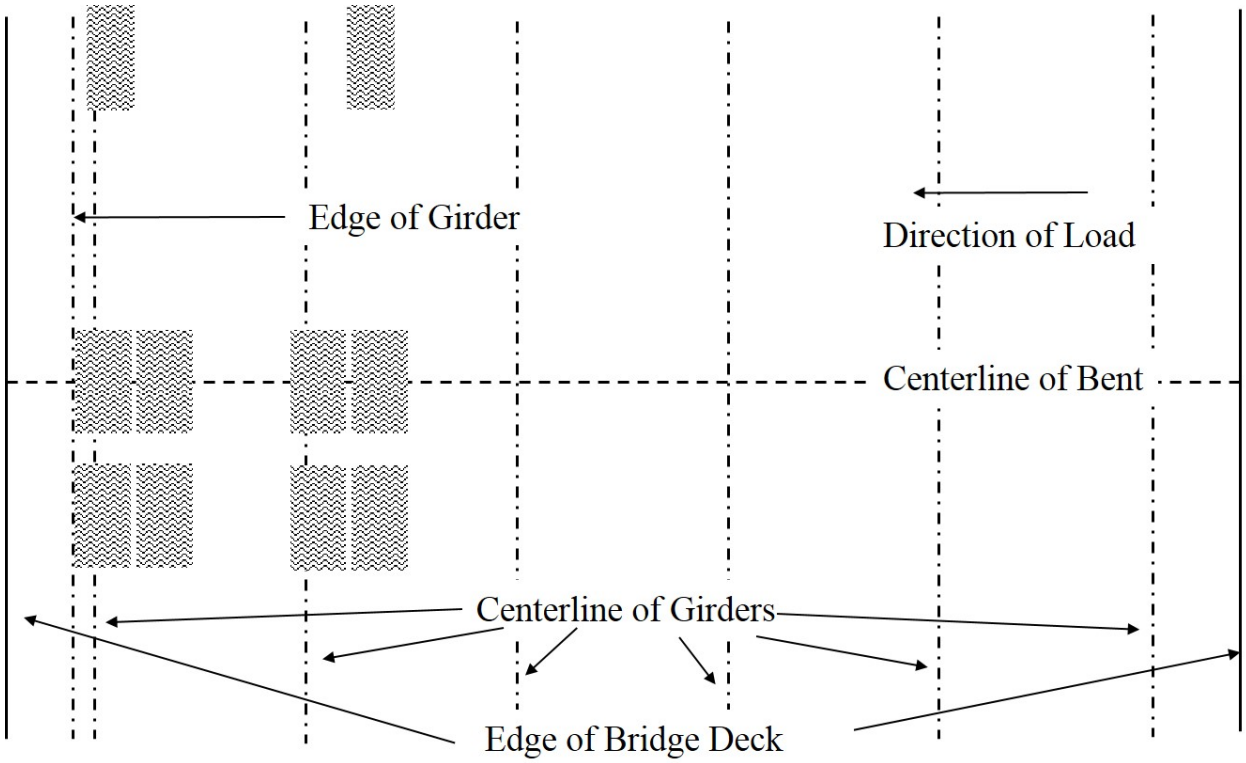

Figure 4-28 – Placement of Load Truck on U.S. Highway 331 Bridge Deck

Figure 4-29 – Load Truck on Highway 331 Test Bent

The maximum load applied to the bent was restricted to prevent permanent damage to the structure. At 90 kips of lateral load, there was little visual evidence of strain on the structure. Measured deflections were less than one inch and no cracking was observed on the pile encasements.

4.6 AUNGES Bent Tests

The last bents tested were located in Lee County, Alabama at the Auburn University National Geotechnical Experimentation Site located at the National Center for Asphalt Technology Test Track Facility. Two bents were constructed by Scott Bridge, LLC for the sole purpose of testing the bents to failure. The test bents featured 4 HP12x42 piles 35 feet long. The piles were driven

using a vibratory hammer, and each pile achieved at least 20 feet of embedment into the ground. Once the piles were driven, the tops were cut off so that there would be uniform embedment in the pile cap. The bents were designed to have 9 feet of clear pile length above the ground surface. The first bent tested was an experimental design of all vertical piles embedded 18 inches into the pile cap. The second bent was constructed according to standard ALDOT design practice with two vertical piles and two battered piles embedded 12 inches into the pile cap. The exterior piles were battered at a 1.5/12 slope. Two piles on each bent were fitted with a steel tube. The tube was used to run inclinometer tests during the load tests. The piles in both test bents were oriented for weak axis bending in the direction of the lateral load. The pile caps were 3 feet by 3 feet by 28 feet long. The concrete in the bent caps was a 3,000 psi mix design. During construction, 6 inch by 12 inch test cylinders were made to gauge the strength of the concrete at the time of the load tests. The strength tests were used to assure that the concrete would not be a limiting factor during the tests. Cylinders were broken at 7 days, 28 days, and on the day of the load tests. Concrete strength recorded on the day of the load tests was used in model calibration to more accurately simulate the behavior of the bents during the load tests. Figure 4-30, Figure 4-31, Figure 4-32, Figure 4-33, and Figure 4-34 detail the construction phases of the AUNGES test bents.

Figure 4-30 – AUNGES Piles Prior to Cut off and Cap Construction

Figure 4-31 – AUNGES Pile Cap Construction

Figure 4-32 – AUNGES Pile Cap before the Addition of the Reinforcing Steel

Figure 4-33 – AUNGES Pile Cap Reinforcement Cage

Figure 4-34 – Completed AUNGES Test Bent

Two load tests were conducted on each test bent. The first test was a lateral test to ensure the hydraulic jacks and loading apparatus was functioning properly. The second test was a lateral test until an observable failure occurred, or the jacks reached full load or extension capacity. The following sections provide in depth details of the instrumentation locations, the loading apparatus, and load schedules for the field load tests.

4.6.1 Battered Bent

Two load tests on the battered pile bent were conducted on July 17, 2015. Figure 4-35 shows the battered pile bent constructed for this research prior to the lateral load test.

Figure 4-35 – AUNGES Battered Pile Test Bent

The piles were named Pile 1, Pile 2, Pile 3, and Pile 4. Pile 1, the leading pile, and Pile 4, the trailing pile, were battered at a 1.5/12 slope. The piles were instrumented at three cross sections along the depth of the piles. The first location was 6 inches from the bottom of the bent cap, the second gage location was 42 inches from the bottom of the bent cap, and the lowest gage location was 84 inches from the bottom of the bent cap. Each instrumented location featured two gages on the exterior of the flanges to measure strain during weak axis bending. The two center piles, Pile 2 and Pile 3, were also instrumented with a third gage at the lowest instrumented cross section so that any strong axis rotation could be observed. Figure 4-36 shows the instrumented cross-sections for the battered pile test bent and their designated names. Figure 4-37 shows the locations of the gages for a typical pile cross-section.

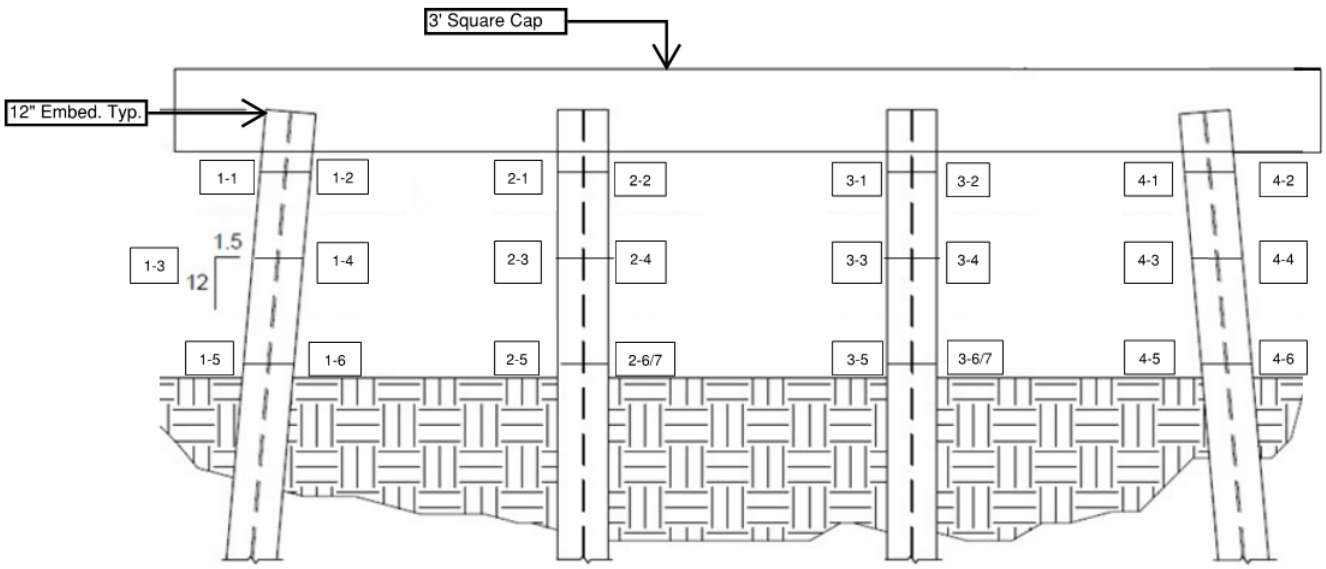

Figure 4-36 – AUNGES Battered Pile Test Bent Gage Locations

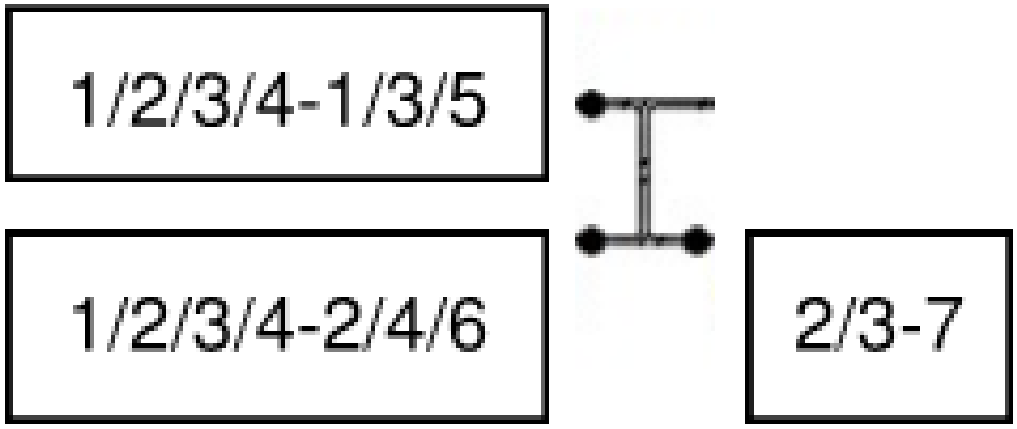

Figure 4-37 – AUNGES Battered Pile Test Bent Cross-section Gage Locations

Pile 2 and Pile 3 were also fitted with 2.5 inch hollow tube steel to serve as tracks for inclinometer testing. Figure 4-38 shows the inclinometer casing at Pile 2 with inclinometer downhole.

Figure 4-38 – Inclinometer Downhole at Pile 2

A baseline shape was found by conducting an inclinometer test on each pile while the bent was without lateral load. During the load tests, the inclinometer was conducted at every 20 kip loading increment until 80 kips, when the inclinometer tests were conducted at every subsequent load increment. The bending in the piles however prevented inclinometer tests from being conducted at higher load increments and on the unload portion of the test. This was due to a weld joint present in the area of maximum bending moment. Permanent deflection in the piles caused the joint at the weld to become misaligned, which prevented the inclinometer from traveling down the corners of the tube. The inclinometer tests for the 140 kip load increment and all of the unload increments were unable to be performed.

The lateral load in the test bent was induced by running high strength threaded rods around the bent cap. A bearing tube was placed on one end of the bent cap. The threaded rods passed

through predrilled holes in the tube and was used to pull the bent cap towards the reaction pile group.

The reaction pile group was an existing 9 pipe pile group. The steel pipe pile had an outside diameter of 10.75 inches and were used in previous load testing at the site (Brown, O'Neill, McVay, El Naggar, & Chakraborty, 2001). Two W10x23 were used to engage the reaction pile group. The two beams were stacked on top of each other with spacers in place to allow the threaded rod to pass between the two beams. The threaded rod then passed through slotted holes in tube sections and through the hydraulic jacks. The tube steel bore on the two beams which bore on the pipe piles that projected out of the 9 pile cap.

Figure 4-39 – Reaction Pile Group (Brown, O'Neill, McVay, El Naggar, & Chakraborty, 2001)

The initial test was conducted to ensure the jack system and loading apparatus were functioning properly. The test bent was loaded at 10 kip increments to approximately 40kips. At each loading increment, once the target load was achieved, the load was held for 10 minutes or

until the inclinometer tests were completed. Inclinometer tests were conducted at the initial, 20 kip, and 40 kip loading increments.

The full load test was conducted on July 17, 2015. The vertical pile test bent was loaded until the stroke capacity of the jacks was exceeded. The lateral load on the piles was increased by 10 kips for each load increment. Inclinometer profiles were captured at every 20 kip increment until the 80 kip increment. After reaching 80 kips an inclinometer profile was captured for each subsequent load increment. Table 4.8 shows the target load schedule for the load test to failure.

Table 4.7 – Target Load Schedule for the AUNGES Battered Pile Test Bent

Target Load (kip)	Hold Time (min)	Inclinometer Test
0	-----	Yes
10	10	No
20	10	Yes
30	10	No
40	10	Yes
50	10	No
60	10	Yes
70	10	No
80	10	Yes
90	10	Yes
100	10	Yes
110	10	Yes
120	10	Yes
130	10	Yes
140	10	Yes
100	10	Yes
50	10	Yes
20	10	Yes
0	-----	Yes

The first significant development during the load test occurred at 100 kips of applied lateral load. The bent cap began to crack linearly along the location of the rebar above Pile 2 and extending toward Pile 1. This crack was likely due to large tension forces being induced at the connection location as the cap tried to rotate and Pile 2 began to get pulled out of the bent cap. As further load was applied, the bent significantly deflected and the linear crack widened. At 110 kips, mill scale

began to flake off the pile as the flanges at the pile cap began to yield. At 130 kips, the flanges at Piles 1 and 3 began to experience significant buckling in the region 5-7 inches below the bottom of the bent cap. At 140 kips, the cracks became significantly larger and the drift of the bent increased drastically, shedding the energy from the jacks through deflection. At the 140 kip load case, the stroke capacity of the jacks was exceeded, and the primary loading was completed. The deflection of the bent was significant enough to prevent any further inclinometer testing due to damage to the welded connections of the inclinometer tubing. Wire pots determined the maximum deflection to be approximately 6 ¾ inches with a residual drift of 4 ½ inches. The figures below show pictures of the bent and piles at failure.

Figure 4-40 – Bent Cracking

Figure 4-41 – Cracking below the Bent Cap

Figure 4-42 – Flange Buckling at Pile 3

Figure 4-43 – Residual Drift due to Lateral Load Test

4.6.2 Vertical Bent

The two load tests on the vertical pile test bent were conducted on Thursday June 18, 2015 and Friday June 19, 2015. Figure 4-44 shows the vertical pile test bent constructed for this research prior to the lateral load test.

Figure 4-44 – AUNGES Vertical Pile Bent

The piles were named Pile 5, Pile 6, Pile 7, and Pile 8. Pile 5 was the leading pile and Pile 8 was the trailing pile. The piles were instrumented at three cross sections along the depth of the piles. The first location was 6 inches from the bottom of the bent cap, the second gage location was 44 inches from the bottom of the bent cap, and the lowest gage location was 82 inches from the bottom of the bent cap. Figure 4-45 shows the instrumented locations along each pile for the test bent. Each instrumented location featured two gages on the exterior of the flanges to measure strain during weak axis bending. The two center piles, Pile 6 and Pile 7, were also instrumented with a third gage at the lowest instrumented cross section so that any strong axis rotation could be

observed. Figure 4-46 shows the gage locations for the instrumented cross sections and the strong axis gage present at the bottom gage locations of the two center piles. The bent cap was also instrumented with two sister bars at Pile 6. Each sister bar was instrumented with 4 strain gages meant to capture the strain in the bent cap in the zone around the embedded pile.

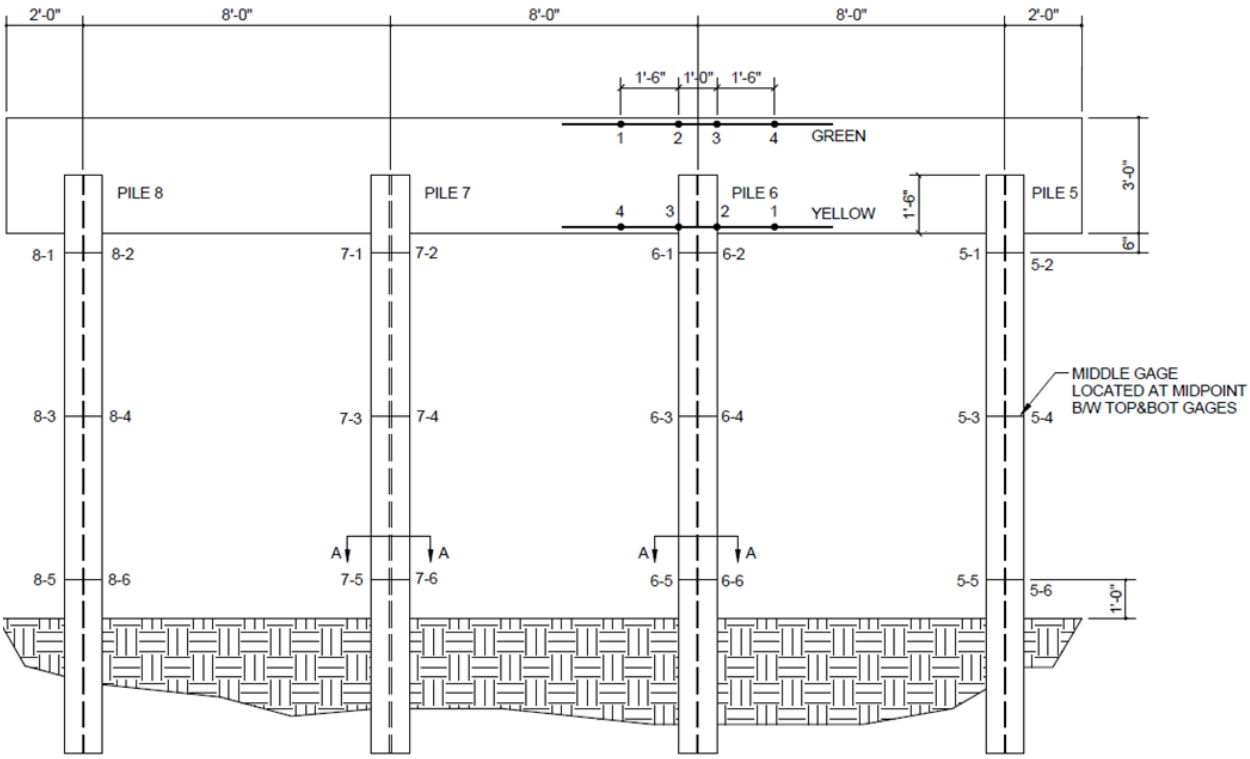

Figure 4-45 – Gage Positions for Vertical Pile Bent Load Test

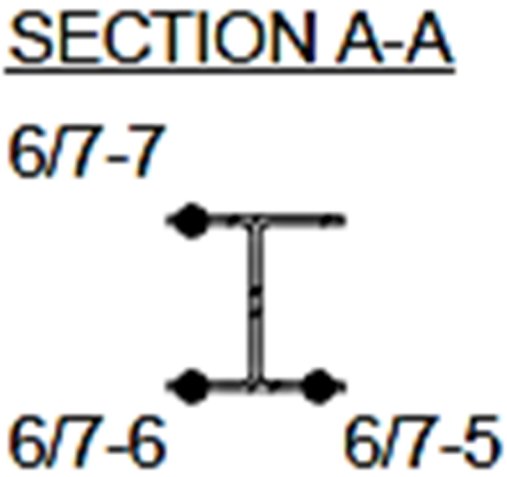

Figure 4-46 – Instrumentation Locations at Gaged Cross Section

Pile 5 and Pile 7 were also fitted with 2.5 inch hollow tube steel to serve as tracks for inclinometer testing. Figure 4-47 shows the inclinometer casing attached to Pile 5. A baseline shape was determined by conducting an inclinometer test on each pile while the bent was without lateral load. During the load tests, the inclinometer was conducted at every 20 kip loading increment until reaching loading increments close to the predicted failure load. Inclinometer tests were also conducted at each unload increment and in the final unloaded case to observe any residual deflections due to the applied lateral load.

Figure 4-47 – Inclinometer Casing on Pile 5

The lateral load in the test bent was induced by running high strength threaded rods around the bent cap. A bearing tube was placed on one end of the bent cap. The threaded rods passed through predrilled holes in the tube and was used to pull the bent cap towards the reaction pile group.

Figure 4-48 – High Strength Threaded Rod and HSS Bearing Tube

The The reaction pile group was an existing 9 pipe pile group. The steel pipe pile had an outside diameter of 10.75 inches and were used in previous load testing at the site (Brown, O'Neill, McVay, El Naggar, & Chakraborty, 2001). Two W10x23 were used to engage the reaction pile group. The two beams were stacked on top of each other with spacers in place to allow the threaded rod to pass between the two beams. The threaded rod then passed through slotted holes in tube sections and through the hydraulic jacks. The tube steel bore on the two beams which bore on the pipe piles that projected out of the 9 pile cap. Figure 4-49 shows the reaction pile group and the W-sections used to spread the load from the two threaded rods to the reaction pile group.

Figure 4-49 – Reaction Pile Group with W10x23 Load Beams (Brown, O'Neill, McVay, El Naggar, & Chakraborty, 2001)

The initial test was conducted to ensure the jack system and loading apparatus was functioning properly. The test bent was loaded at 10 kip increments to approximately 50% of the predicted failure load. At each loading increment, once the target load was achieved the load was held for 10 minutes or until the inclinometer tests were completed.

The second load test was conducted on June 19, 2015. The vertical pile test bent was loaded until a structural failure occurred or the capacity of the jacks was exceeded. The lateral load on the piles was increased by 10 kips for each load increment. Inclinometer profiles were captured every 20 kip increment until the 80 kip increment. After reaching 80 kips an inclinometer profile was

captured for each load increment. Table 4.8 shows the target load schedule for the load test to failure.

Table 4.8 – Load Schedule for the AUNGES Vertical Pile Test Bent

Target Load (kip)	Hold Time (min)	Inclinometer Test
0	-----	Yes
10	10	No
20	10	Yes
30	10	No
40	10	Yes
50	10	No
60	10	Yes
70	10	No
80	10	Yes
90	10	Yes
100	10	Yes
110	10	Yes
120	10	Yes
130	10	Yes
140	10	Yes
100	10	Yes
80	10	Yes
40	10	Yes
0	-----	Yes

The maximum load applied to the test bent was 140 kips. At this point, the piles were experiencing localized yielding in the pile flanges. The bent cap deflection began to increase nonlinearly once the yielding occurred. Yielding was observed on the trailing flanges of each pile to a depth of 5 to 7 inches below the bent cap. Strain gages in this area experienced excessive strain and failed at the higher load increments. Pile 5, the leading pile, was the best visual example of the deflection the bent cap experienced with respect to the ground surface. Unlike the battered pile bent, there was little evidence of cracking in the bent cap. This is likely due to the vertical pile bent deflecting laterally without rotation induced by a battered leading pile. This in tur, did not induce the large tensile forces causing pull out at the pile to cap connection. Figure 4-50 shows the drift of the bent at Pile 5. Figure 4-51 and Figure 4-52 show the localized buckling in the trailing pile

flanges. The lateral force induced in the pile bent was distributed into the surrounding soil structure. Evidence of large amounts of energy imparted into the soil is evident in ground cracks opening around the test bent. Figure 4-53 shows one of the ground cracks caused by the lateral load test. The test resulted in residual drift of the pile bent. Figure 4-54 shows the residual drift in the vertical pile test bent. Detailed results from lateral load test data reduction is presented in Section 5.4.2 of this thesis.

Figure 4-50 – Lateral Deflection Induced in Pile 5 during Field Load Testing

Figure 4-51 – Pile 5 Vertical Flange Buckling

Figure 4-52 – Pile 7 Vertical Flange Buckling

Figure 4-53 – Ground Crack Due to Lateral Load

Figure 4-54 – Lateral Displacement of Test Pile

Chapter 5 Lateral Load Test Results

5.1 Introduction

The various instrumentation devices used to monitor the bents during field load tests recorded important data on the behavior of piles subjected to lateral loading. The data came in many forms, from applied load, deflection magnitude, and resulting strain values. The recorded data was reduced to produce meaningful visual representations of pile and bent behavior under applied lateral load. The scope of this thesis includes only the data reduction for the AUNGES test bents. The data reduction for the Macon County Road 9 and US Highway 331 bridges was conducted in the companion thesis produced by Jonathon Campbell (Campbell, 2015). The data results for the Macon County Road 9 and Highway 331 bridges are presented below. The AUNGES section of this chapter explains in greater detail the types of data recorded and presents the results in graphical form.

5.2 Macon County Road 9

The Macon County Road 9 test bent was tested with four different load tests to capture behavioral changes from a standalone bent to a bent fully connected in a bridge system. The bent was instrumented during the construction phase and all load tests were conducted prior to the bridge opening for full-time service. The tests were designed to induce minor deflections to avoid permanent deflections or damages that would need repairs. The data used to produce the results presented in this chapter was gathered from resistance stain gages applied directly to the steel piles as well as resistance gages mounted to the surface of the concrete encasements. Deflection measurements were recorded from wire pots attached to a stationary reference frame. The following sections present the load test results for the Macon County Road 9 load tests.

5.2.1 Pre-Deck

The first load test on the Macon County Road 9 test bent was conducted on June 27, 2014 prior to the casting of the bridge deck. All data reduction in Section 5.2.1 was conducted by and used with the permission of Jonathon Campbell from his thesis published in 2015. The results from this load test are presented in the figures below. All axial and moment profiles were computed from field strain measurements. Strain profiles between the gages were used to calculate axial and moment values at each instrumented cross section.

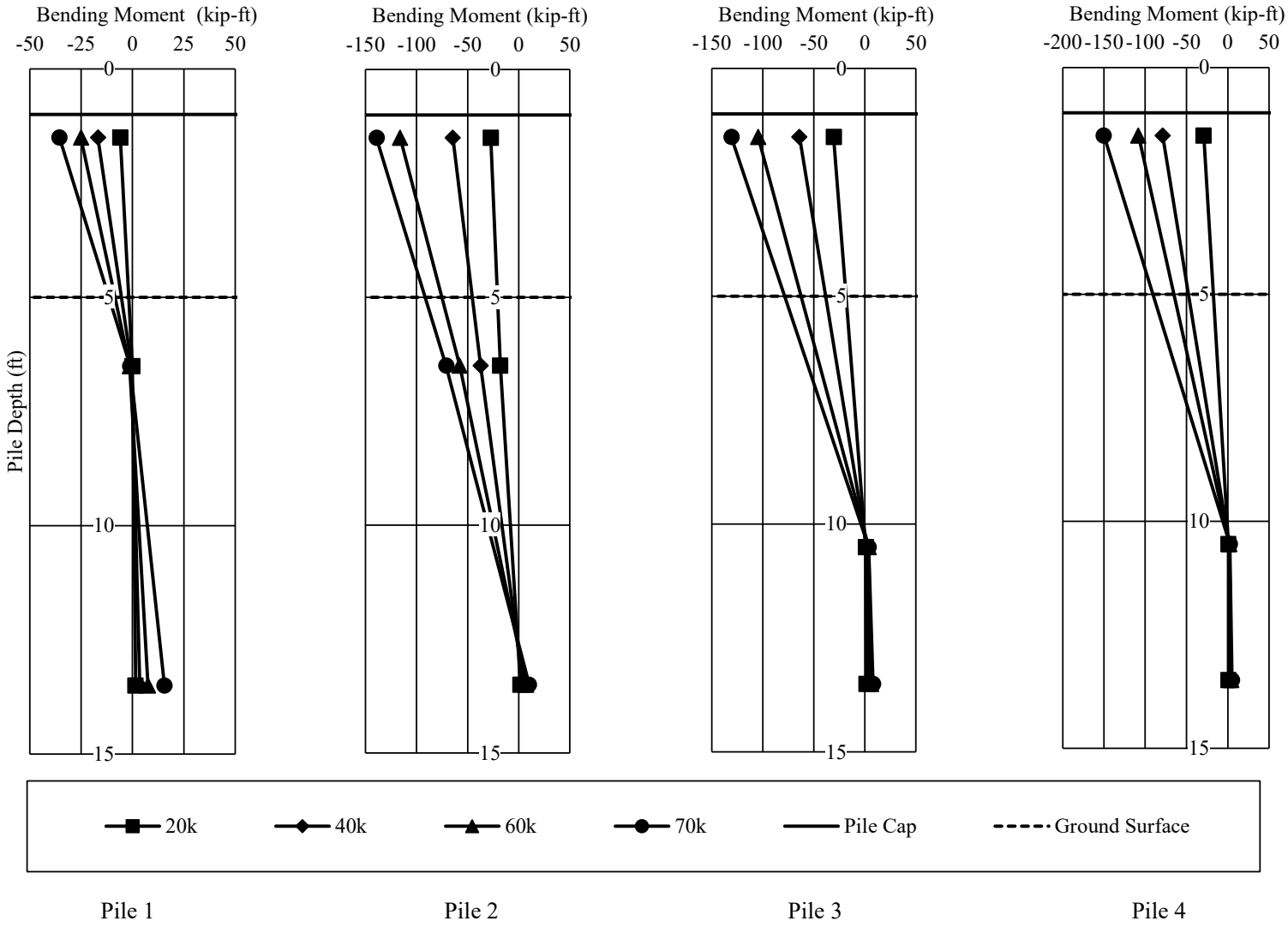

Figure 5-1 – Macon County Road 9 No Deck Moment Profiles

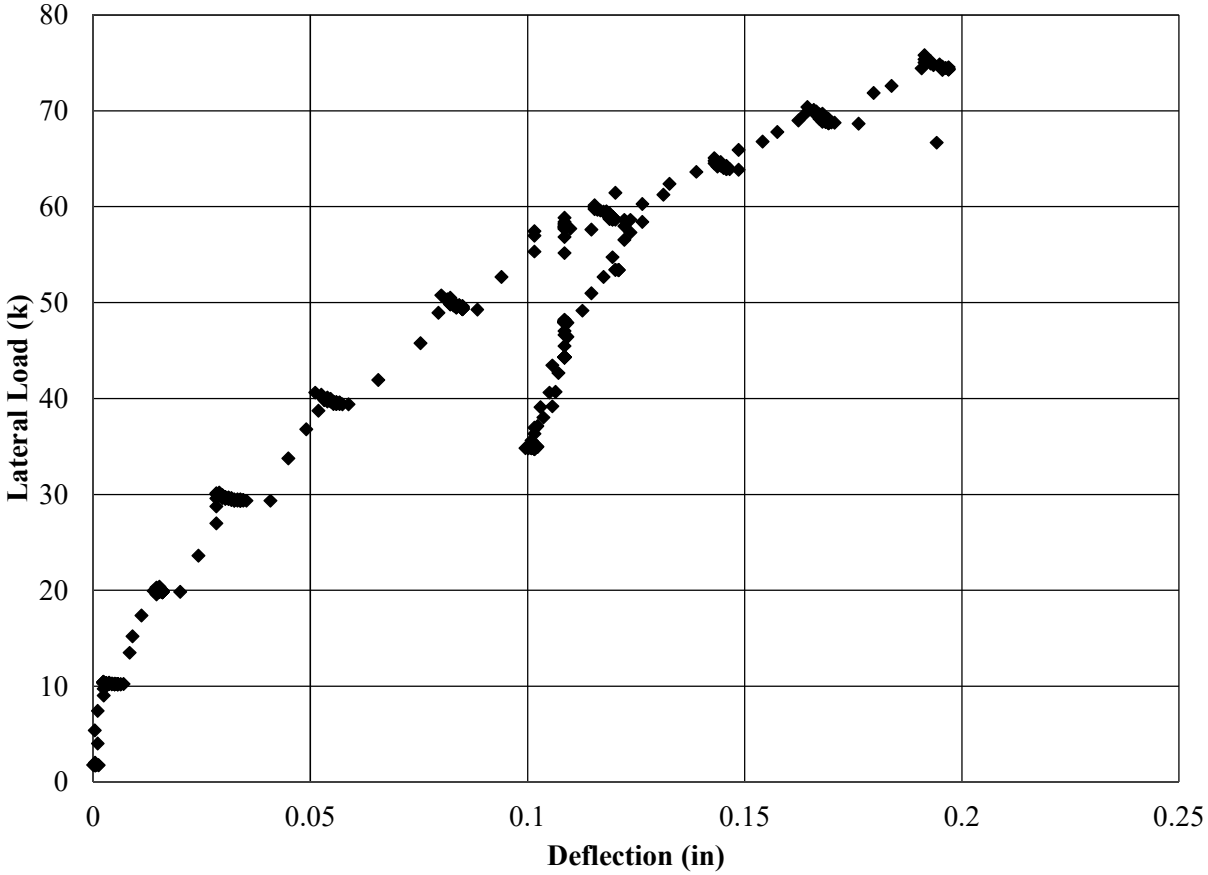

Figure 5-2 – Macon County Road 9 No Deck Lateral Load vs. Deflection Behavior

5.2.2 Post Deck No Load Truck

The second load test on the Macon County Road 9 test bent after the casting of the bridge deck and without a load truck was conducted on September 18, 2014. All data reduction in Section 5.2.2 was conducted by and used with the permission of Jonathon Campbell from his thesis published in 2015. Results from pile 1 were not included in this section due to gage malfunction or damage incurred between the initial and second load tests. The results from this load test are presented in the figures below.

All axial and moment profiles were computed from field strain measurements. Strain profiles between the gages were used to calculate axial and moment values at each instrumented cross section.

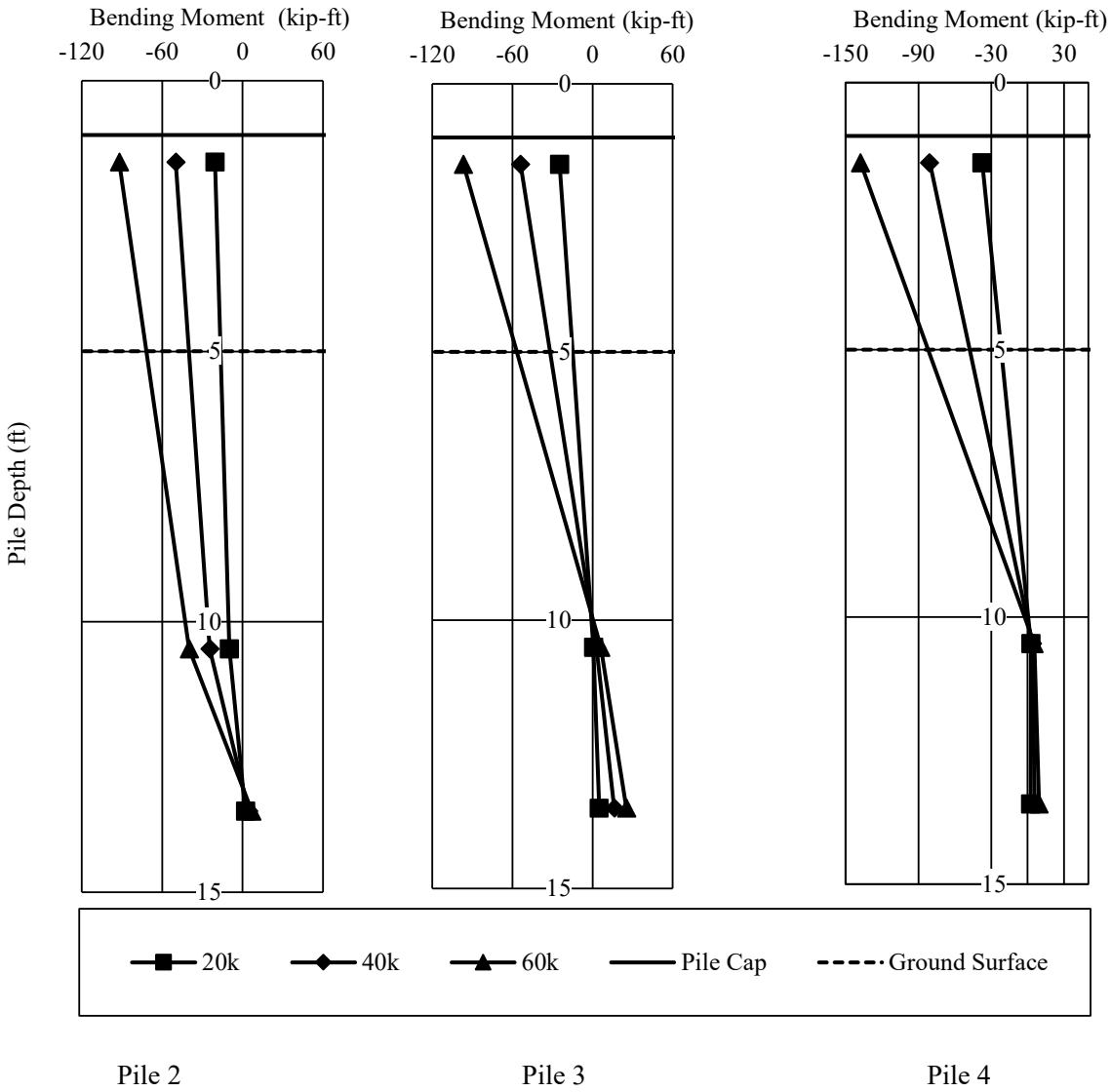

Figure 5-3 – Macon County Road 9 Post Deck No Load Moment Profiles

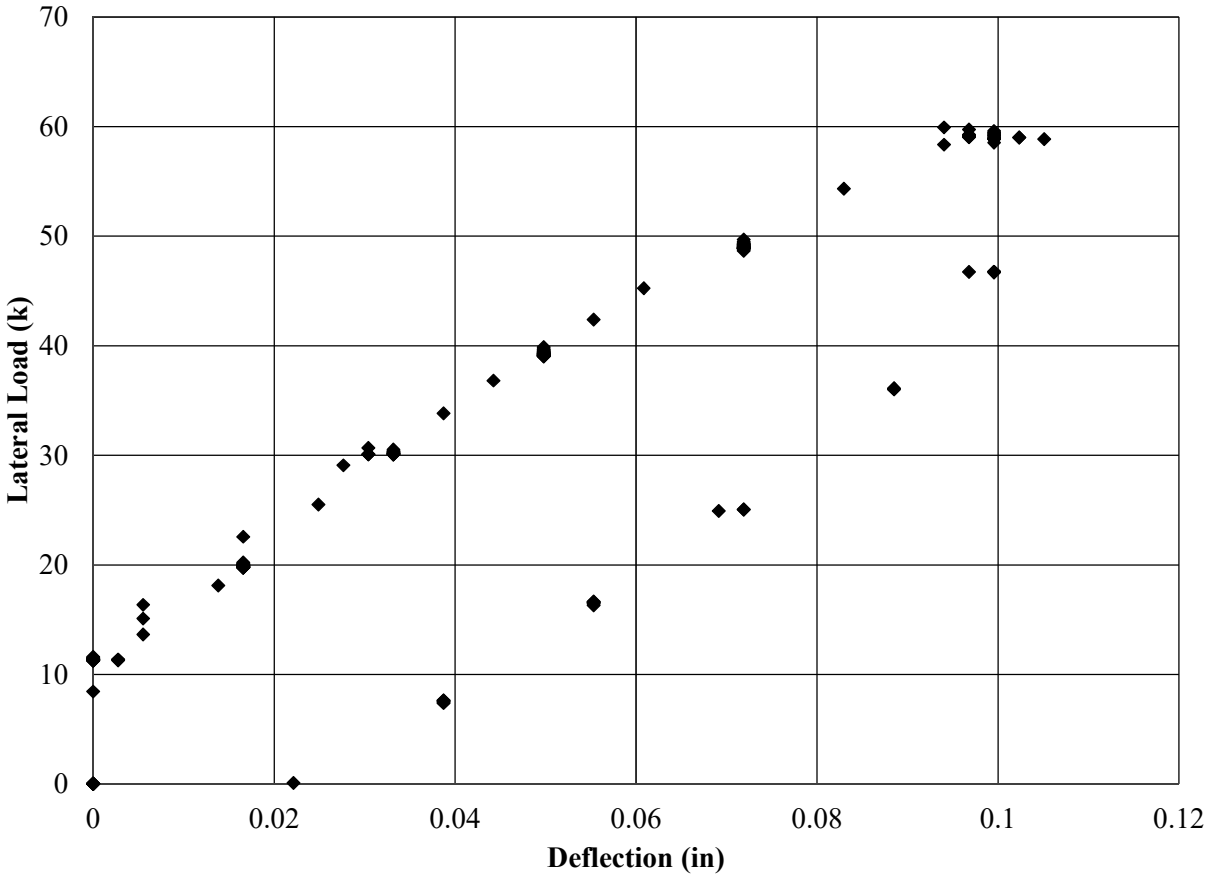

Figure 5-4 – Macon County Road 9 Post Deck No Load Truck Lateral Load vs. Deflection Behavior

5.2.3 Post Deck Load Truck Centered over the Roadway

The third load test on the Macon County Road 9 test bent after the casting of the bridge deck and with a load truck centered over the roadway was conducted on September 18, 2014. All data reduction in Section 5.2.3 was conducted by and used with the permission of Jonathon Campbell from his thesis published in 2015. Results from pile 1 were not included in this section due to gage malfunction or damage incurred between the initial and second load tests. The results from this load test are presented in the figures below.

All axial and moment profiles were computed from field strain measurements. Strain profiles between the gages were used to calculate axial and moment values at each instrumented cross section.

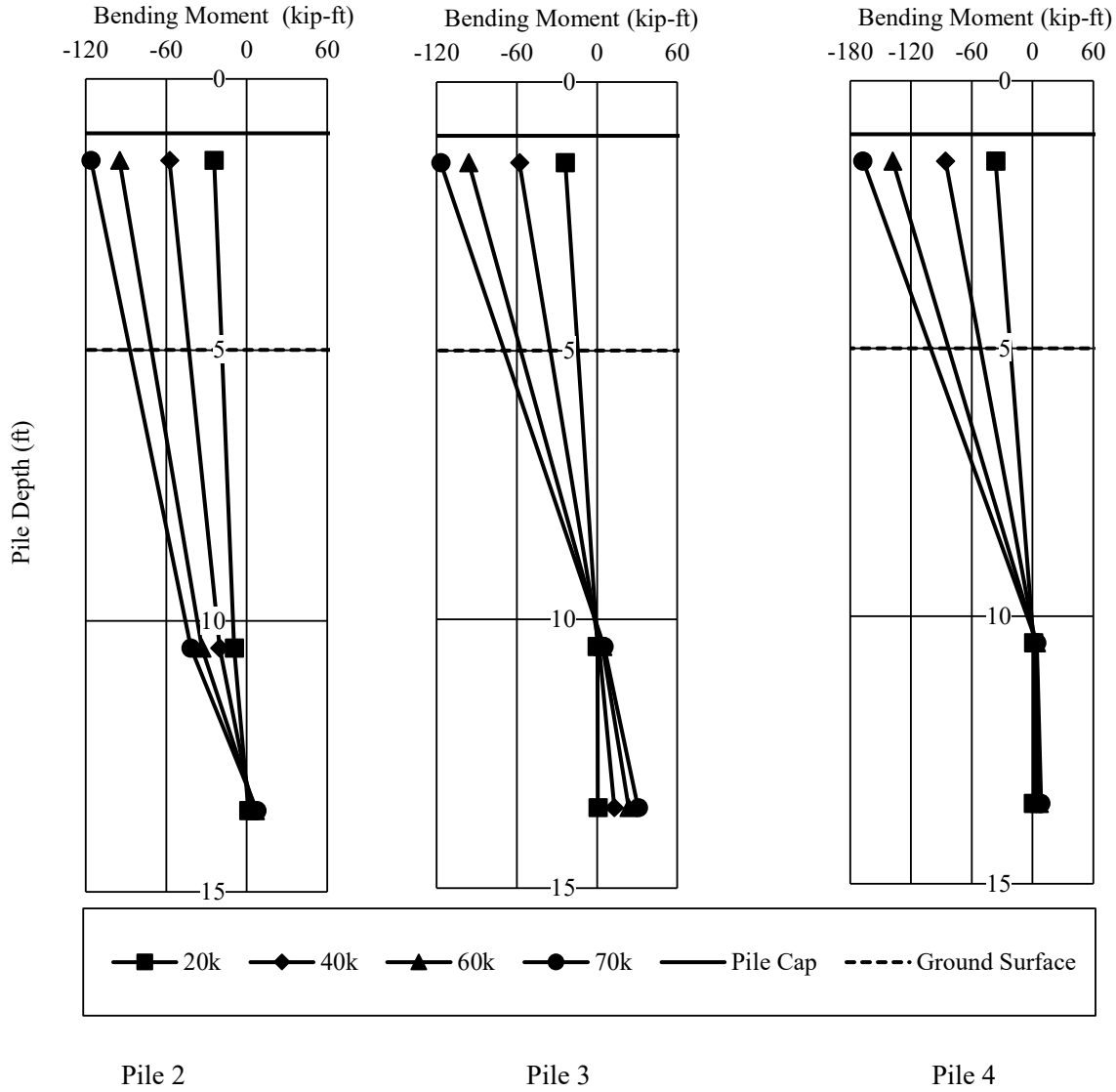

Figure 5-5 – Macon County Road 9 Post Deck Centered Load Truck Moment Profiles

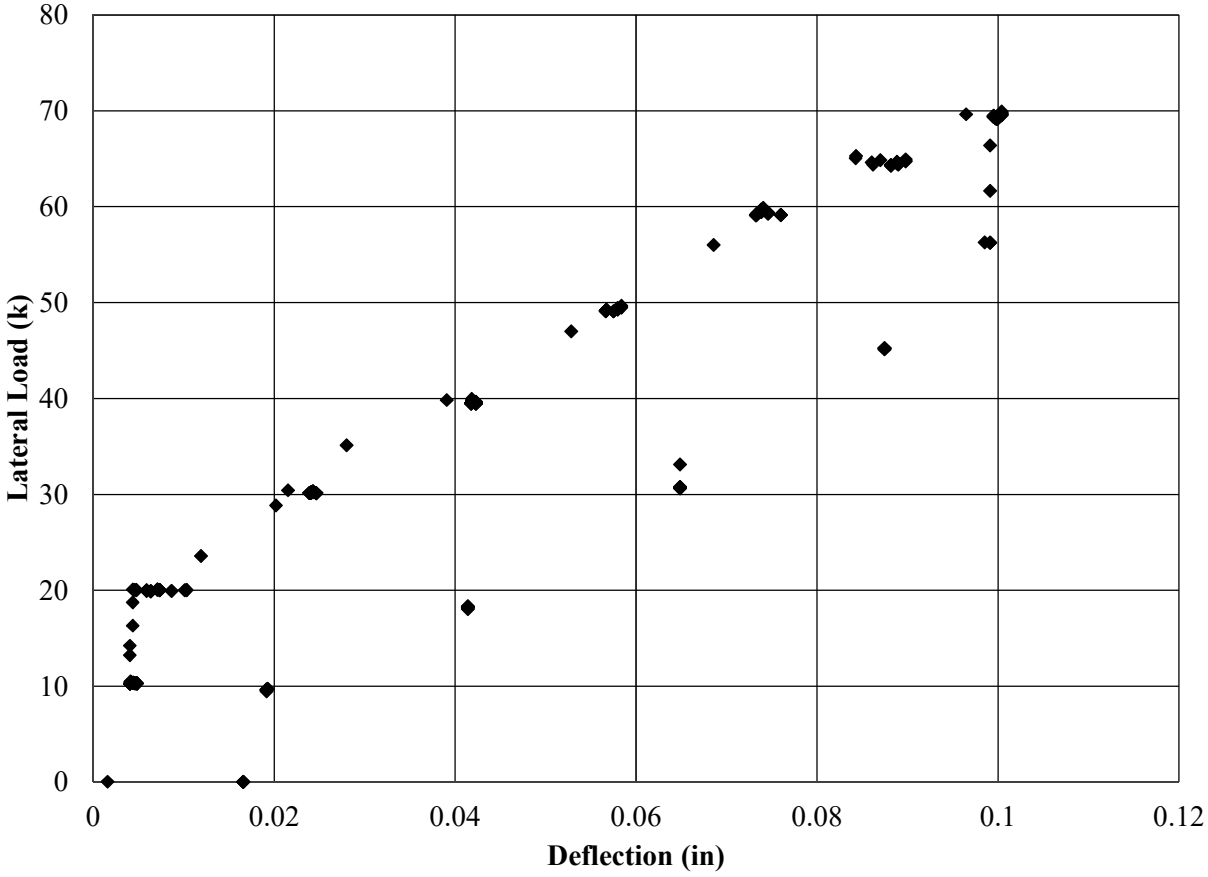

Figure 5-6 – Macon County Road 9 Post Deck Centered Load Truck Lateral Load vs. Deflection Behavior

5.2.4 Post Deck Load Truck over Edge Girders

The final test on the Macon County Road 9 test bent after the casting of the bridge deck and with a load truck over the edge girders was conducted on September 18, 2014. All data reduction in Section 5.2.4 was conducted by and used with the permission of Jonathon Campbell from his thesis published in 2015. Results from pile 1 were not included in this section due to gage malfunction or damage incurred between the initial and second load tests. The results from this load test are presented in the figures below.

All axial and moment profiles were computed from field strain measurements. Strain profiles between the gages were used to calculate axial and moment values at each instrumented cross section.

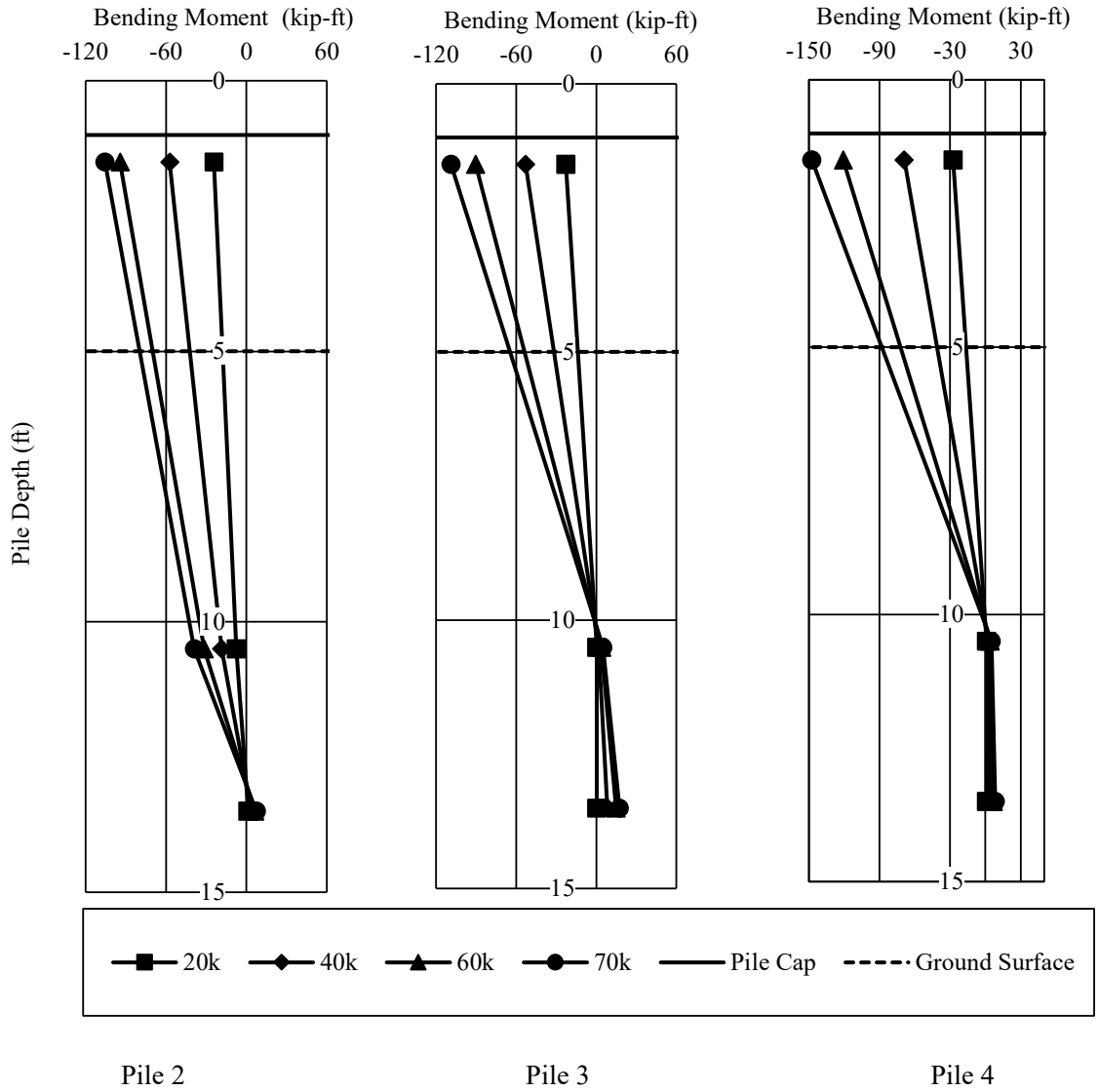

Figure 5-7 – Macon County Road 9 Post Deck Load Truck at Edge Moment Profiles

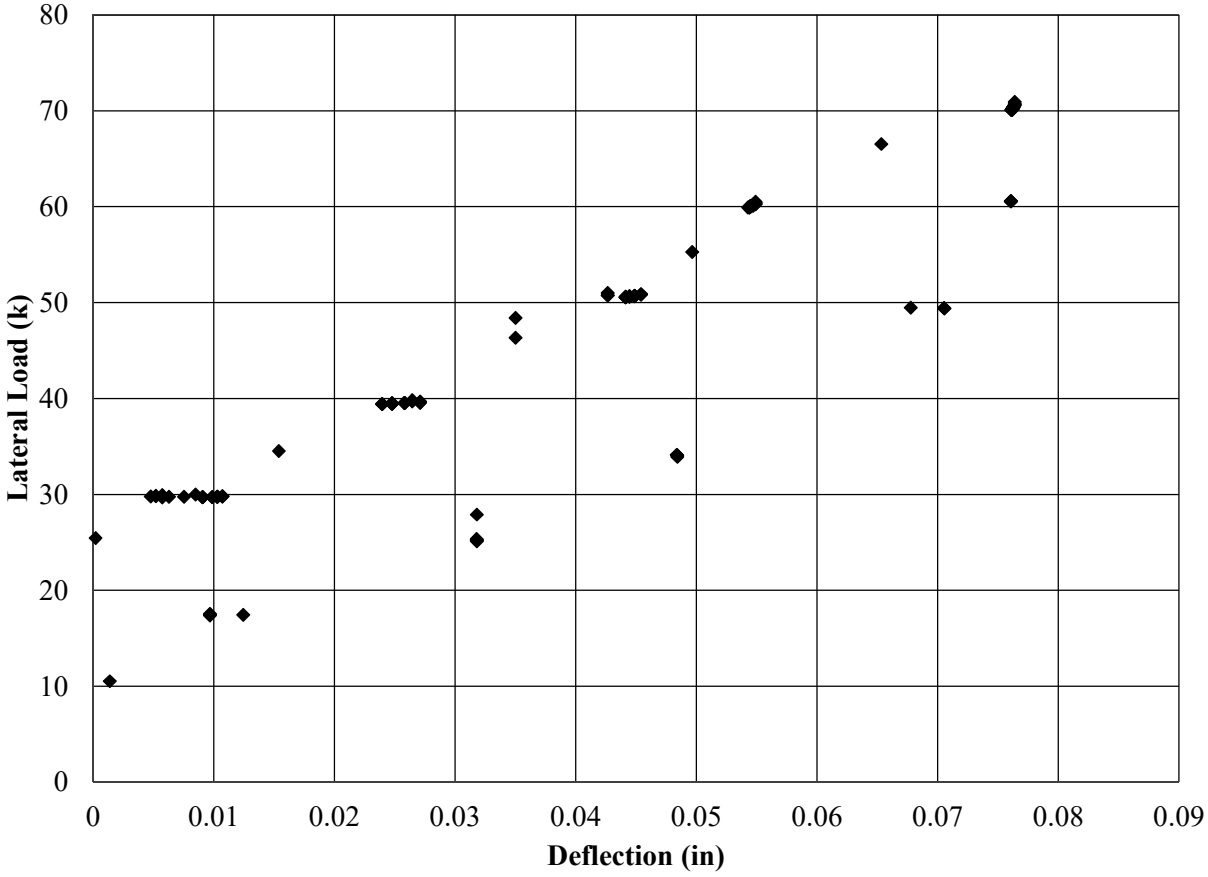

Figure 5-8 – Macon County Road 9 Post Deck Load Truck at Edge Lateral Load vs. Deflection Behavior

5.3 US Highway 331

The US Highway 331 bent was chosen to be tested because it featured a large free distance from the ground surface to the bottom of the bent cap. The bridge was an in-service bridge, and could not be shut down for testing. The tests were designed to induce minor deflections to avoid permanent deflections or damages that would need repairs and to reduce the amount of time traffic would need to be halted during testing. The data used to produce the results presented in this chapter was gathered from resistance stain gages applied to the surface of the concrete

encasements. Deflection measurements were recorded from wire pots attached to a stationary reference frame. The following sections present the load test results for the Macon County Road 9 load tests.

5.3.1 No Load Truck

The first load test on the US Highway 331 test bent was conducted without a load truck on the deck on November 18, 2014. All data reduction in Section 5.2.4 was conducted by and used with the permission of Jonathon Campbell from his thesis published in 2015. The results from this load test are presented in the figures below. All axial and moment profiles were computed from field strain measurements. Strain profiles between the gages were used to calculate axial and moment values at each instrumented cross section.

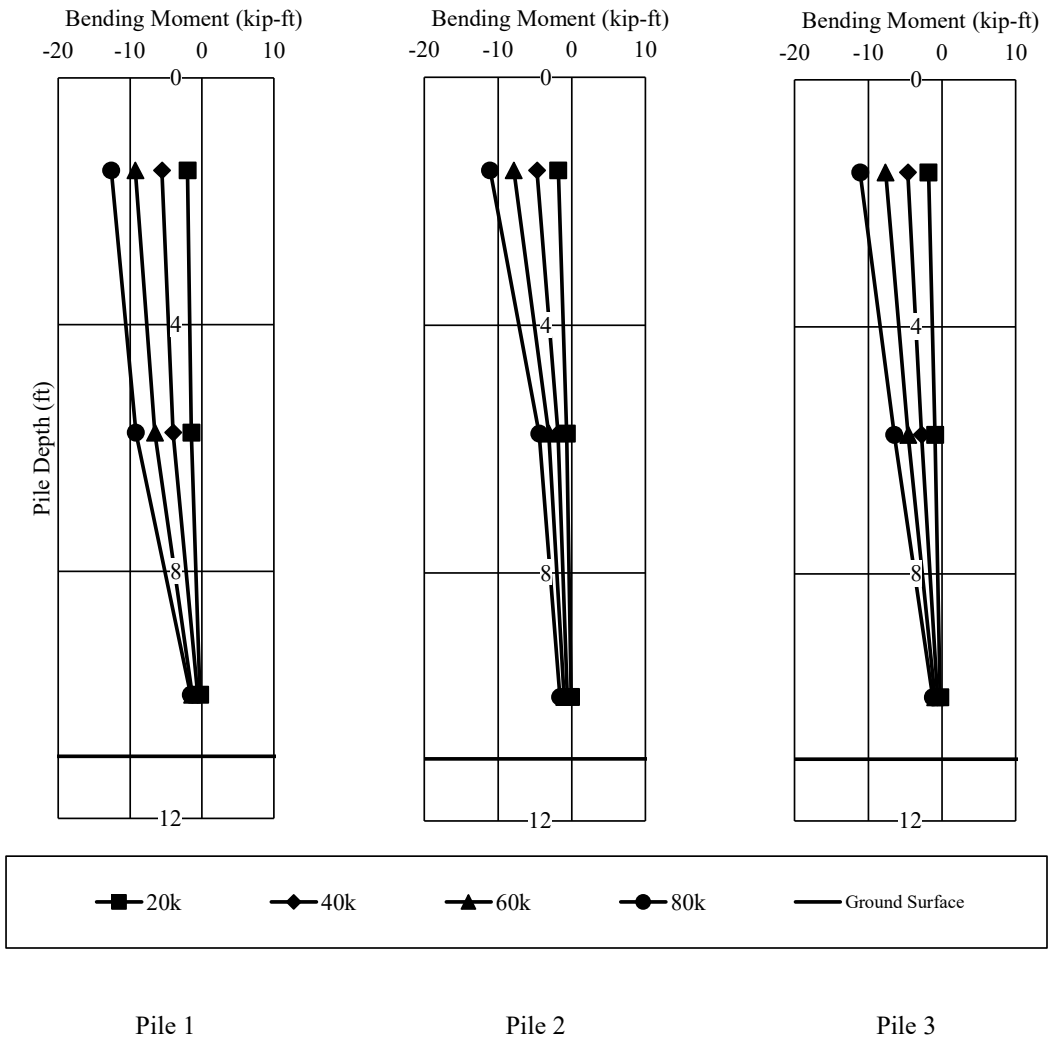

Figure 5-9 – Moment Profiles for Pile 1-3 of US 331 Bent with No Load Truck

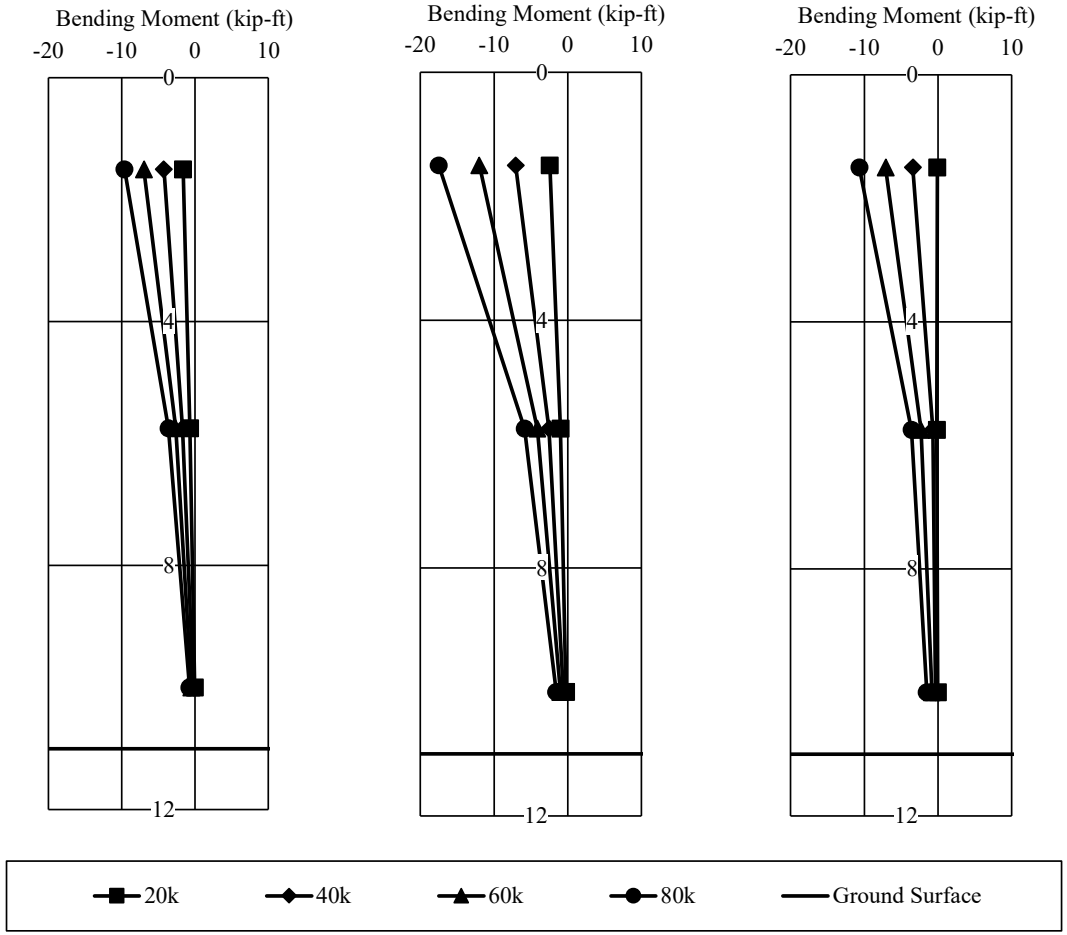

Figure 5-10 – Moment Profiles for Pile 4-6 of US 331 Bent with No Load Truck

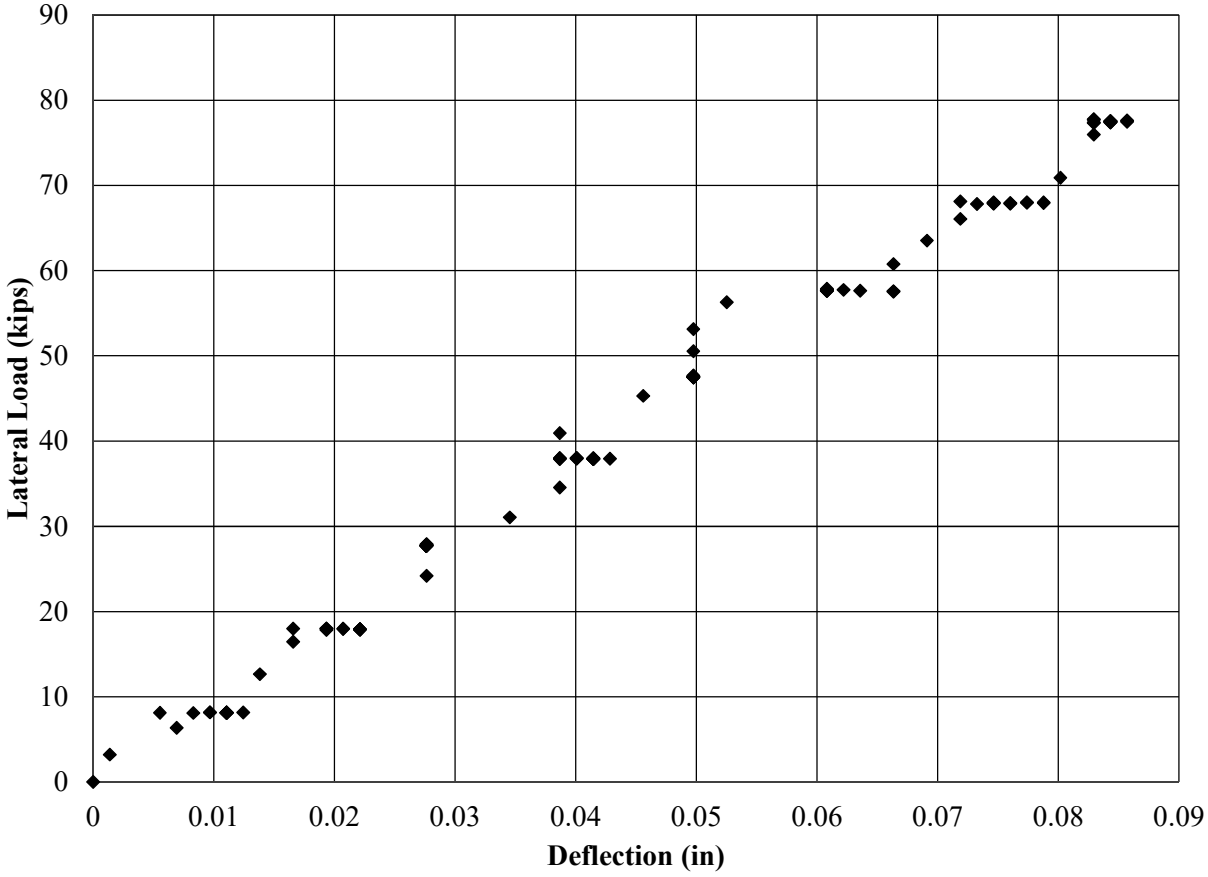

Figure 5-11 – Load Deflection Behavior of US 331 Bent with No Load Truck

5.3.2 Load Truck over Edge Girders

The second load test on the US Highway 331 test bent was conducted without a load truck on the deck on November 18, 2014. All data reduction in Section 5.2.4 was conducted by and used with the permission of Jonathon Campbell from his thesis published in 2015. The results from this load test are presented in the figures below. All axial and moment profiles were computed from field strain measurements. Strain profiles between the gages were used to calculate axial and moment values at each instrumented cross section.

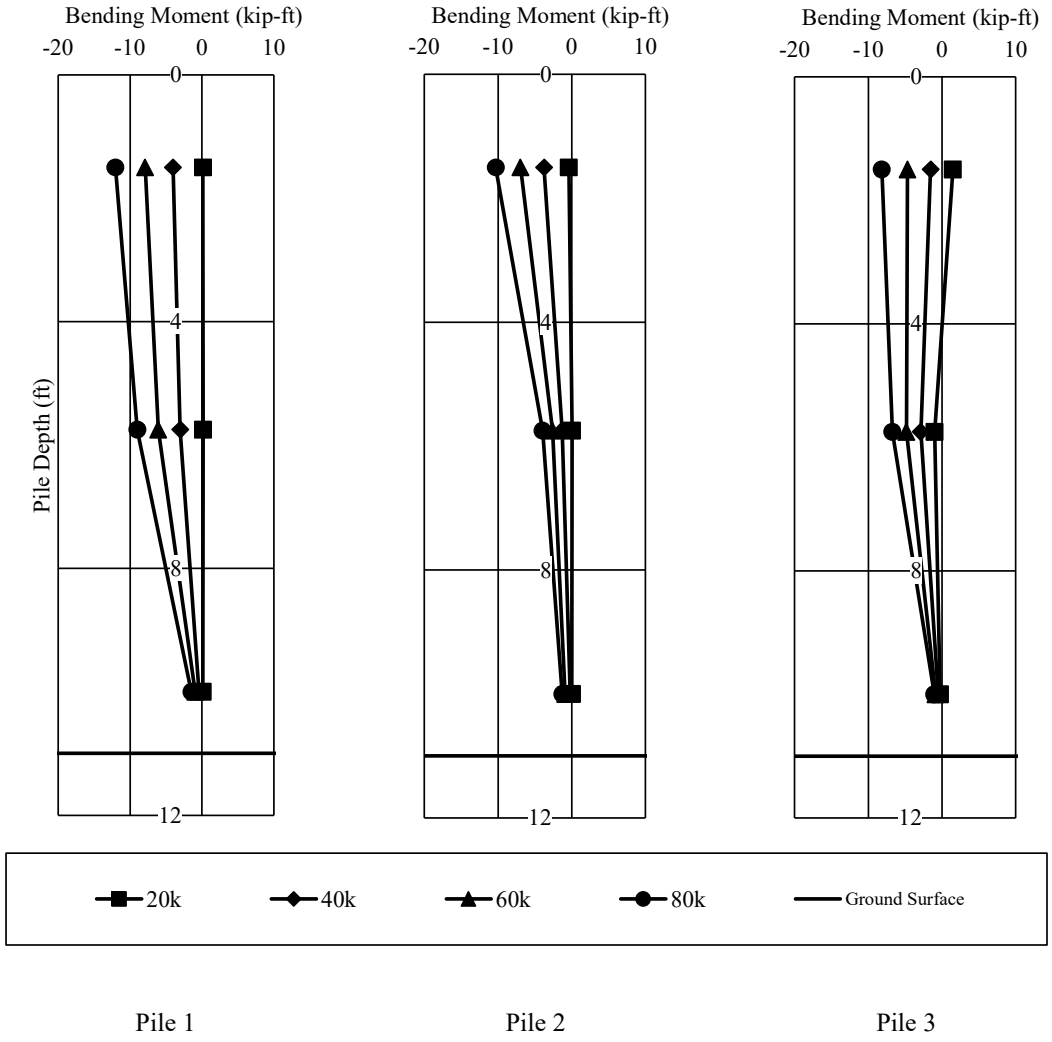

Figure 5-12 – Moment Profiles for Pile 1-3 of US 331 Bent with Load Truck at Edge Girder

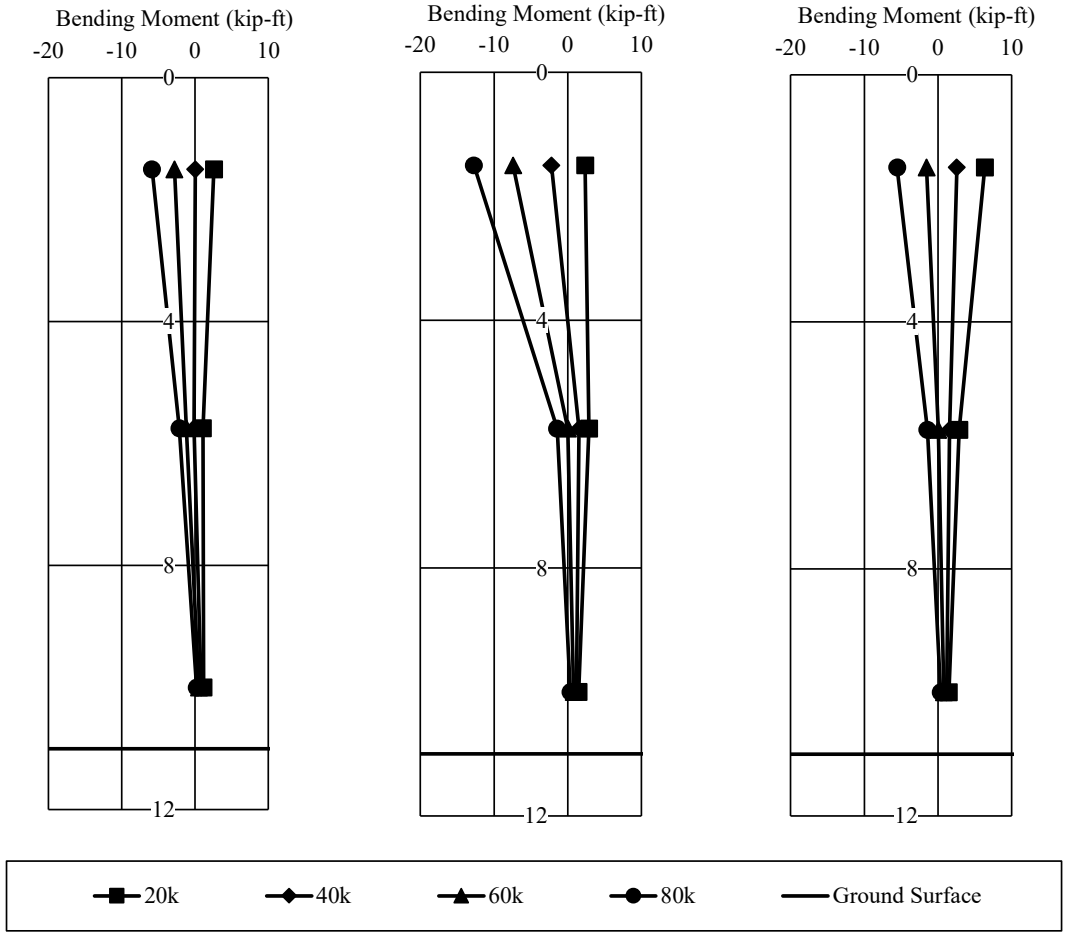

Figure 5-13 – Moment Profiles for Pile 4-6 of US 331 Bent with Load Truck at Edge Girder

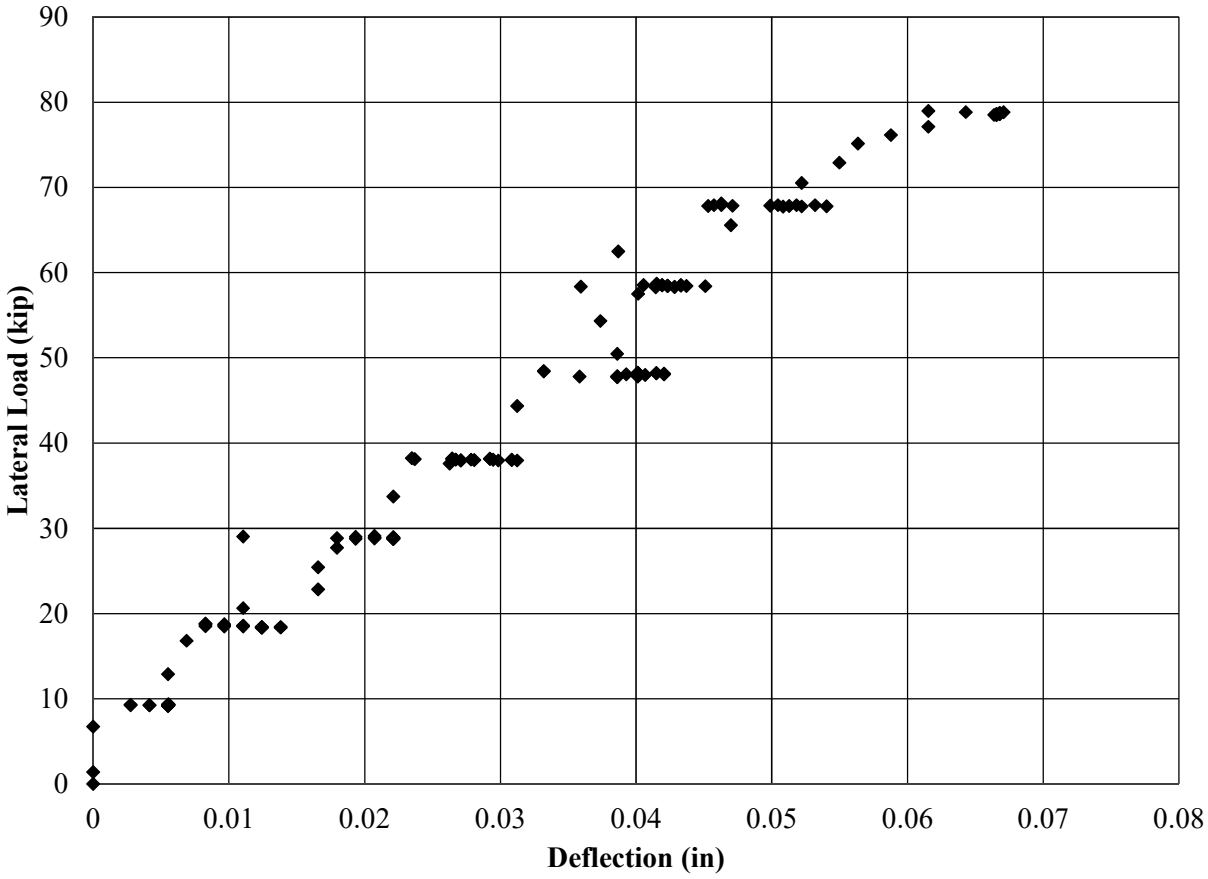

Figure 5-14 – Load Deflection Behavior of US 331 Bent with Load Truck at Edge Girder

5.4 AUNGES

The two AUNGES test bents were loaded to failure. Strain gages captured strain data during the load tests. The data was used to calculate the moment at each cross-section that was instrumented for each loading increment. Data readings were recorded every 15 seconds during testing. Detailed notes were taken to determine the time frame in which the target load was applied at each target increment. The strain values collected in each increment on each flange were adjusted to consider the strain over the entire pile cross-section. The values were then averaged together over the hold

period to calculate a composite average strain due to the target lateral load at each flange. The composite strain values were then used to calculate the curvature of the section. Using the curvature and the material properties of the piles, the composite bending moment on the cross section was calculated. Coupon tests determined that the yield stress of the piles was 58 ksi. When composite strain values produced stresses exceeding this value, the stress was capped at 58 ksi for moment calculations. In the sections below, the composite moment values were graphed against the depth of the piles to produce moment profile for each pile in the test bents.

Inclinometer data was also recorded during these two load tests. Inclinometer tests were conducted at every other loading increment until the higher load levels were reached at which point they were conducted for each increment unless the bending of the piles prevented the probe from reaching the pile bottom. The data recorded from the inclinometer tests was used to graph the deflected shape of the piles with depth. The deflected shape profiles produced during each test are presented in the sections below.

The wire pots connected to the pile caps of the test bents recorded the deflection of the pile caps during the load tests. The deflection of the pile cap versus the applied lateral load for each test bent is presented in the sections below.

5.4.1 Battered Pile Test Bent

The battered pile test bent was conducted on July 17, 2015. The test bent was loaded until the hydraulic jacks used to load the test bent reached maximum stroke. The yield stress of the piles was determined from steel coupon tests. The yield stress was 58 ksi. During data reduction, this value was used to cap the stress in the piles. When calculating moments, if the strain differential produced a stress higher than 58 ksi, then the stress used for calculating the bending moment on the section was 58 ksi. This limit only came into effect at the top gages where yielding occurred in the pile flanges. The results for the inclinometer tests on Piles 2 and 3 are presented in Figure

5-15. The calculated moment profiles for the battered pile bent tests are presented in Figure 5-16. Figure 5-17 shows the observed axial load profiles. The load deflection behavior captured from the wire pots is presented in Figure 5-18. For calibration and clarity in the figures presented, the maximum load case shown for the axial profile, moment profile, and inclinometer deflected shape was the 80 kip load just prior to the beginning of yielding behavior in the piles.

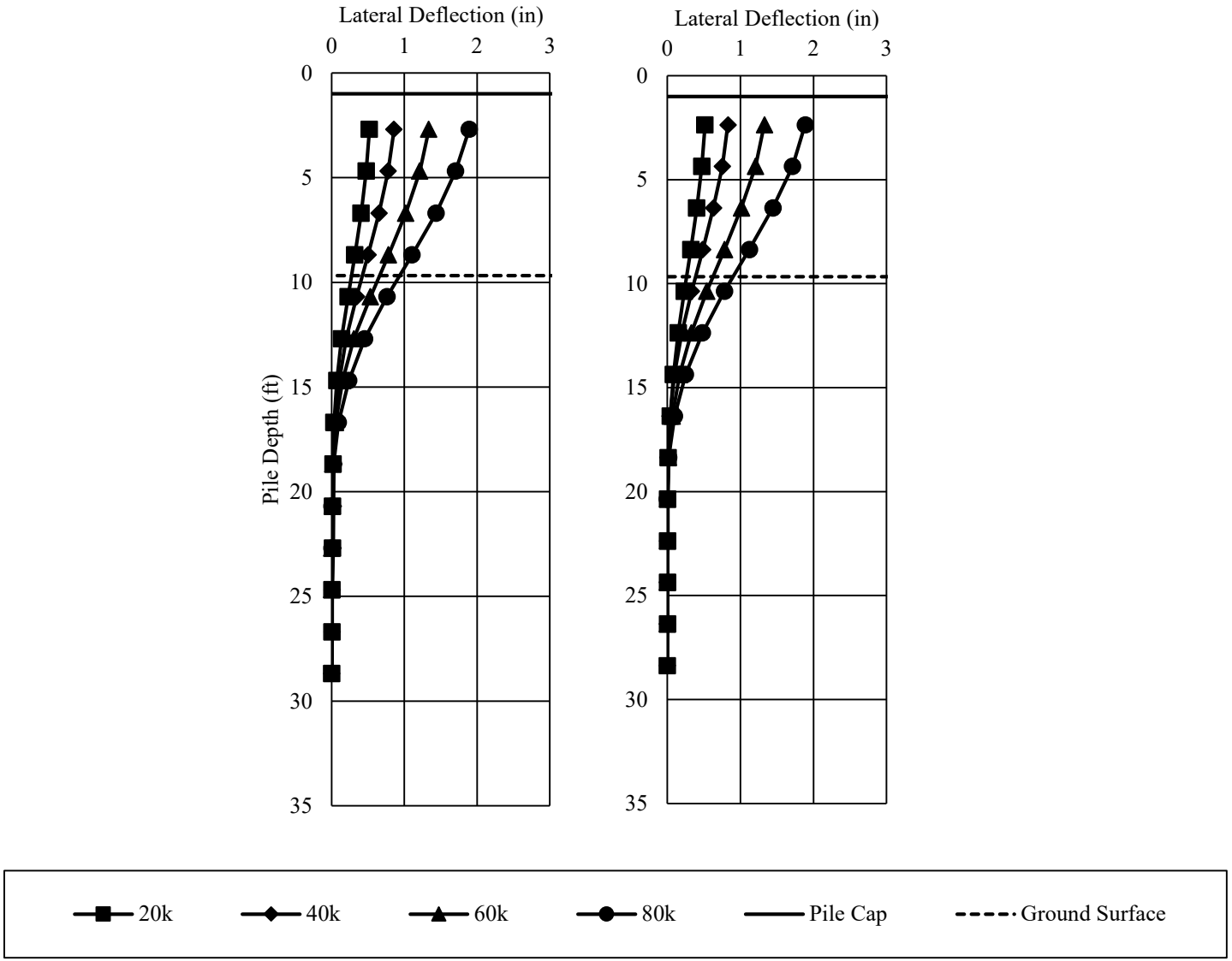

Figure 5-15 – Observed Inclinometer Profiles for the AUNGES Battered Pile Bent

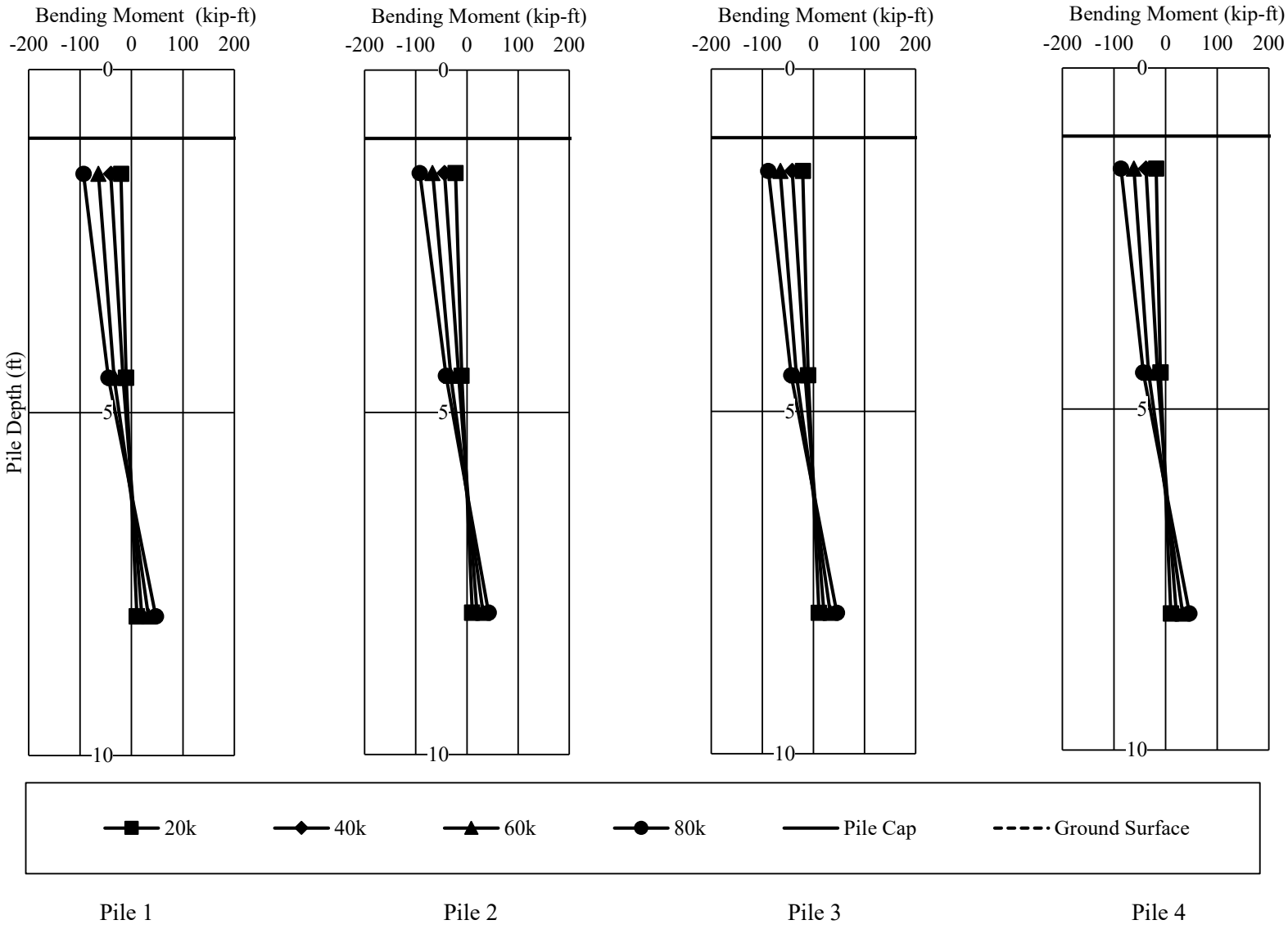

Figure 5-16 – Observed Moment Profiles for the AUNGES Battered Pile Bent

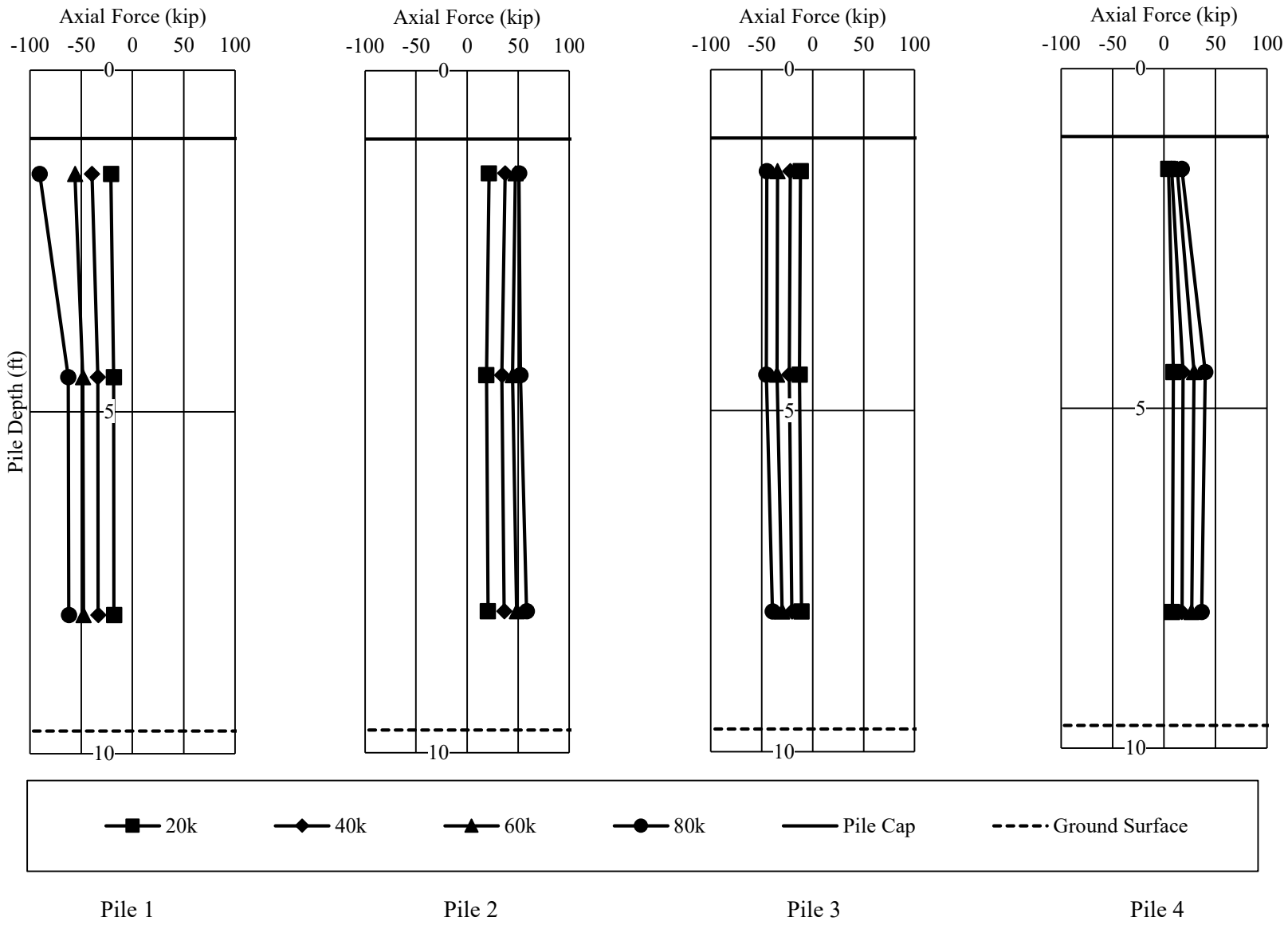

Figure 5-17 – Observed Axial Load Profiles for the AUNGES Battered Pile Bent

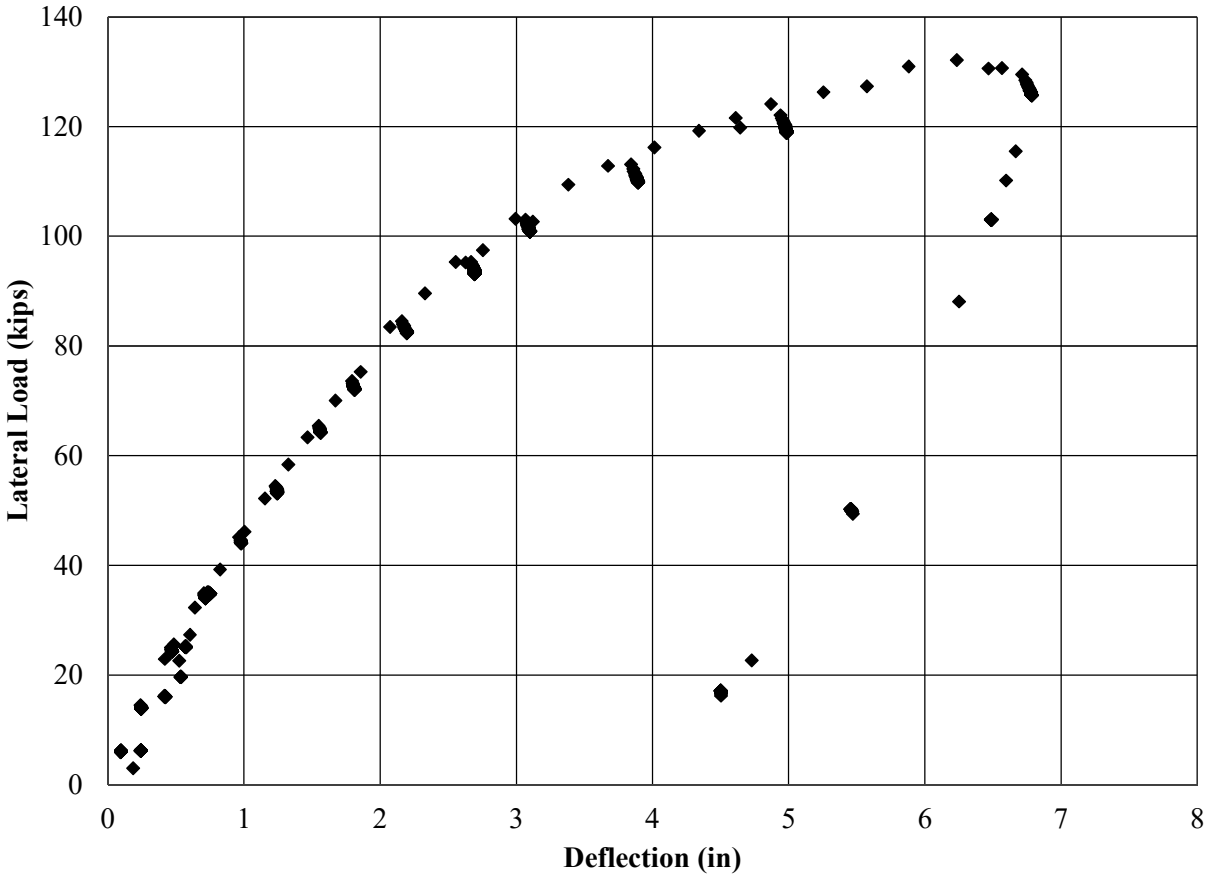

Figure 5-18 – Observed AUNGES Battered Pile Bent Wire Pot Load Deflection Behavior

Data gathered during the load test produced viable profiles for the deflected shape, moment, and axial load. All gages functioned properly at lower level load cases. As the bents approached failure, the upper gages on the pile began to fail because of buckling in the pile flanges. Load cases 20k, 40k, 60k, and 80k were the only load cases presented so that comparisons between the initial and calibrated models would be consistent.

5.4.2 Vertical Pile Test Bent

The vertical pile test bent was conducted on June 18, 2015. The test bent was loaded until the hydraulic jacks used to load the test bent reached maximum stroke. The yield stress of the piles

was determined from steel coupon tests. The yield stress was 58 ksi. During data reduction, this value was used to cap the stress in the piles. When calculating moments, if the strain differential produced a stress higher than 58 ksi, then the stress used for calculating the bending moment on the section was 58 ksi. This limit only came into effect at the top gages where yielding occurred in the pile flanges. The results for the inclinometer tests on Piles 5 and 7 are presented in Figure 5-19. The calculated moment profiles for the vertical pile bent tests are presented in Figure 5-20. Observed axial load profiles are shown in Figure 5-21. The load deflection behavior captured from the wire pots is presented in Figure 5-22. For calibration and clarity in the figures presented, the maximum load case shown for the axial profile, moment profile, and inclinometer deflected shape was the 80 kip load just prior to the beginning of yielding behavior in the piles.

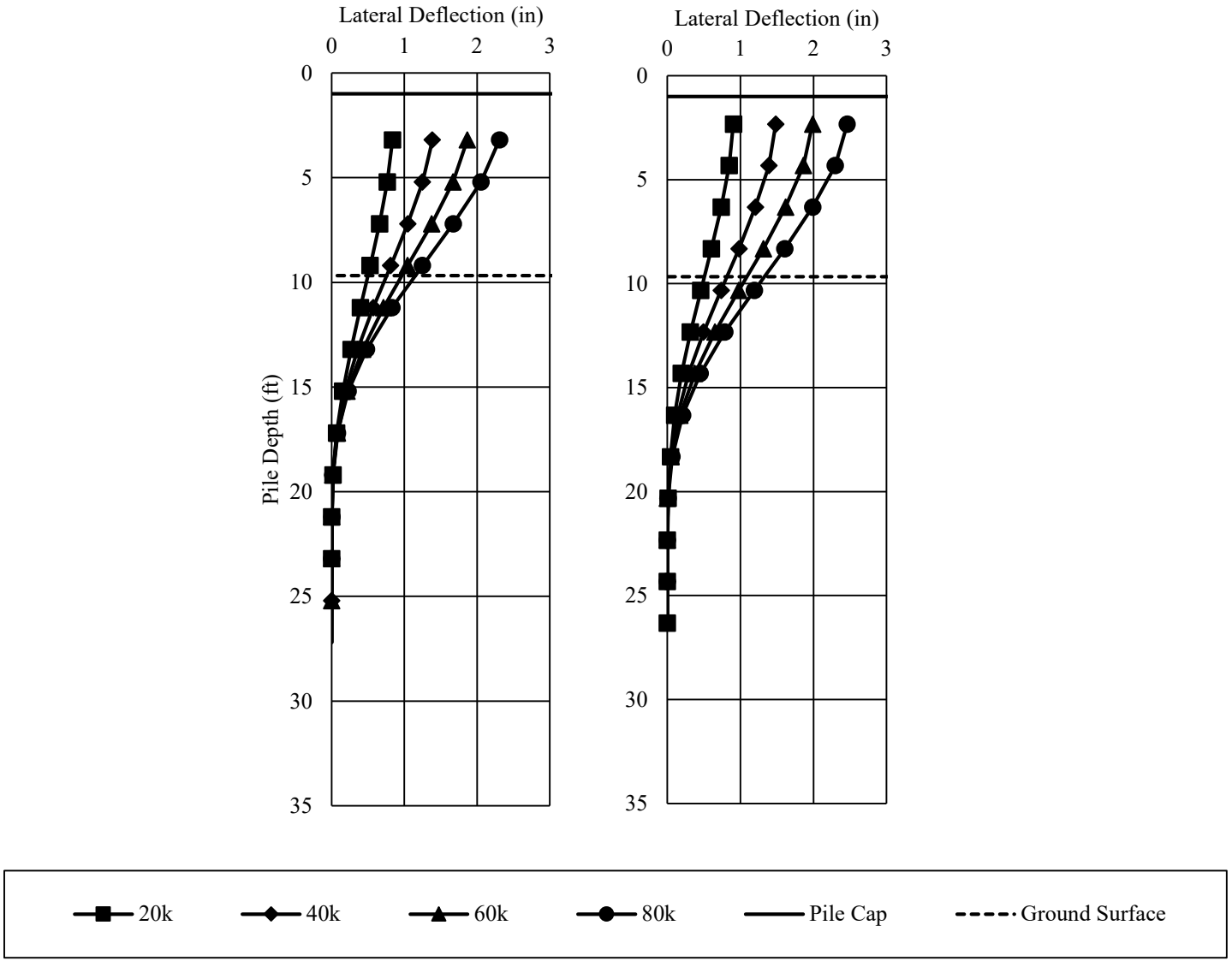

Figure 5-19 – Observed Inclinometer Profiles for the AUNGES Vertical Pile Bent

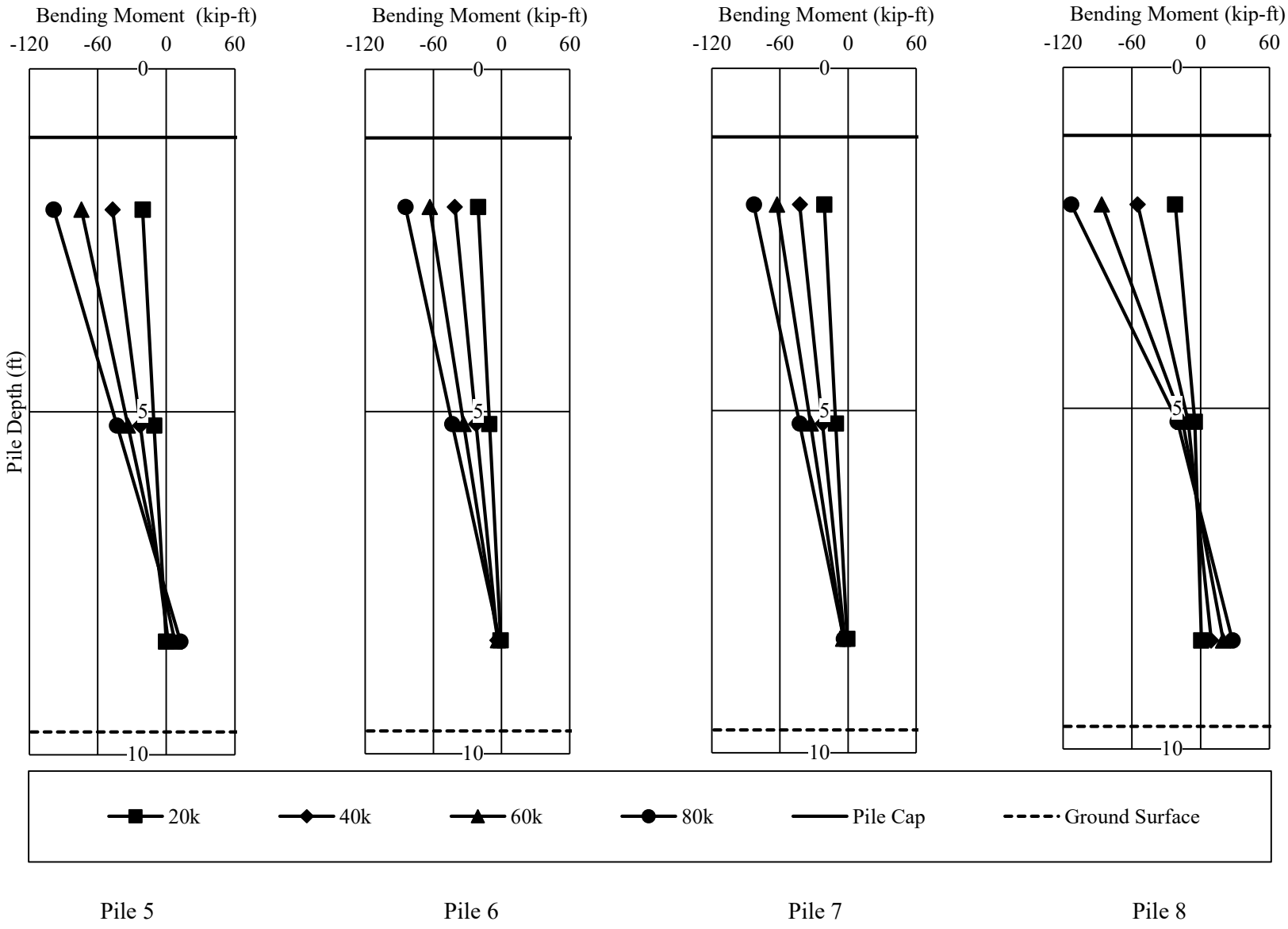

Figure 5-20 – Observed Moment Profiles for the AUNGES Vertical Pile Bent

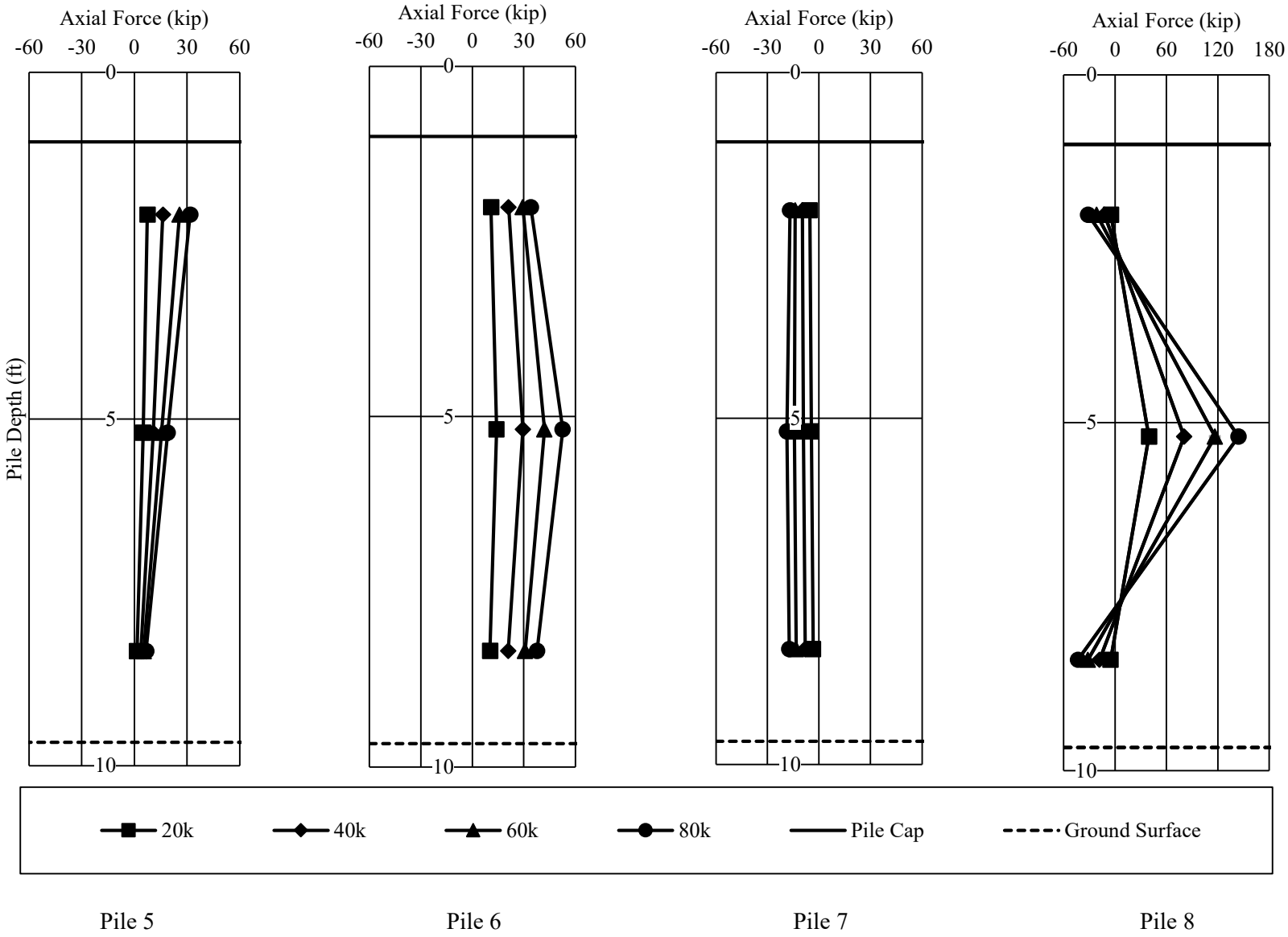

Figure 5-21 – Observed Axial Load Profiles for the AUNGES Vertical Pile Bent

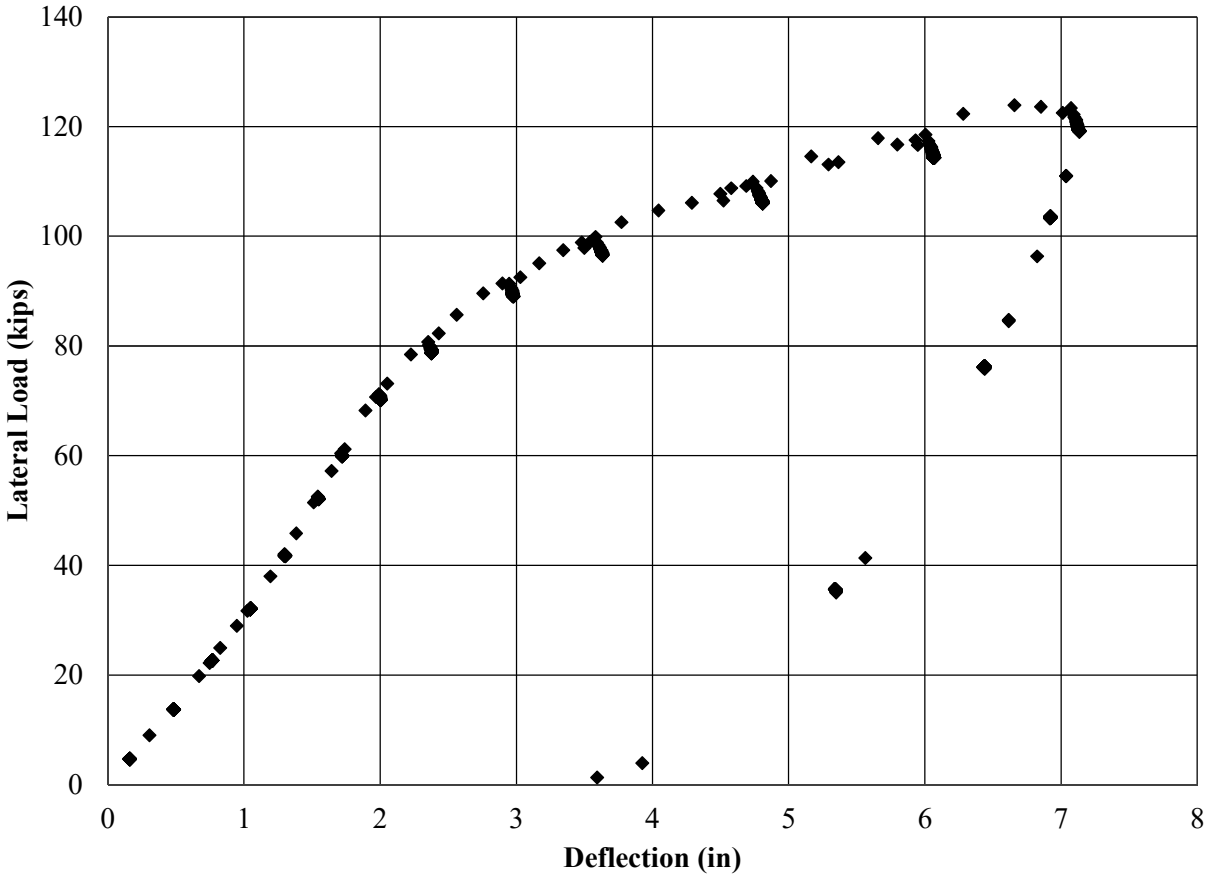

Figure 5-22 – Observed AUNGES Vertical Pile Bent Wire Pot Load Deflection Behavior

Data gathered during the load test produced viable profiles for the deflected shape, moment, and axial load. Most gages functioned properly at lower level load cases. The results show that the middle gage on pile 8 likely malfunctioned. Gage data for the upper and lower gages seemed to be viable and was included in the results profiles. As the bents approached failure, the upper gages on the pile began to fail because of buckling in the pile flanges. Load cases 20k, 40k, 60k, and 80k were the only load cases presented so that comparisons between the initial and calibrated models would be consistent.

The load test results show that the vertical pile bent performed well in resisting lateral load though it was less stiff than the battered pile bent. The vertical pile bent featured more embedment than the battered pile bent. This created a more fixed connection that allowed for more moment development. This transferred more lateral load into the pile through induced moment than through additional axial load. All vertical pile bents are more constructable than battered pile bents. Results of the load tests show that the utilization of all vertical pile bents could provide ALDOT with bridges comparable performance to the current design while delivering them more quickly. The vertical pile bent may be less stiff than the battered pile bent, but the vertical piles are not subjected to the same tensile pull out failure as the battered pile bent. This provides a more ductile system that deforms more under lateral loads that could provide better behavior under extreme loading scenarios. Additional research into this bent design and the embedment depth of piles into the pile cap would be beneficial to confirming that this design is a viable option for future ALDOT bridges.

Chapter 6 Comparison of Model and Lateral Load Test Results

6.1 Introduction

This chapter presents the results of the field load tests superimposed on the initial model predictions used to design the field tests. Model data is presented in a series of moment versus depth curves for each pile at the discrete loading increments of the field load tests. Load test data is plotted as discrete points from each target load at the depth of the installed gage. This creates a visual comparison for the accuracy of the predicted curves and the observed field data.

6.2 AUNGES

The models for the AUNGES piles were accurate in matching moment profiles but were not close matches to the observed deflected shapes from inclinometer tests. The models consistently predicted the observed moments. Observed moment profiles lined up with the preliminary models. The inclinometer behavior for the battered pile and vertical pile bents was under predicted by the models. The observed inclinometer data also suggested that the piles were less stiff than the coupon tests suggested. The piles showed more deflection below the ground surface than the models suggested. The load deflection behavior calculated from the wire pots was not accurately predicted by the models for the battered pile bent, but the vertical pile bent and model were in strong agreement. The battered pile bent model predicted the bent was stiffer than the observed data suggested. Axial comparisons between observed data and preliminary models did not show strong agreement. The observed axial forces were higher than predicted by the preliminary models. Graphical comparisons between model predictions and observed data are presented in section 6.2.1 for the battered pile bent and section 6.2.2 for the vertical pile bent.

6.2.1 Battered Pile Bent

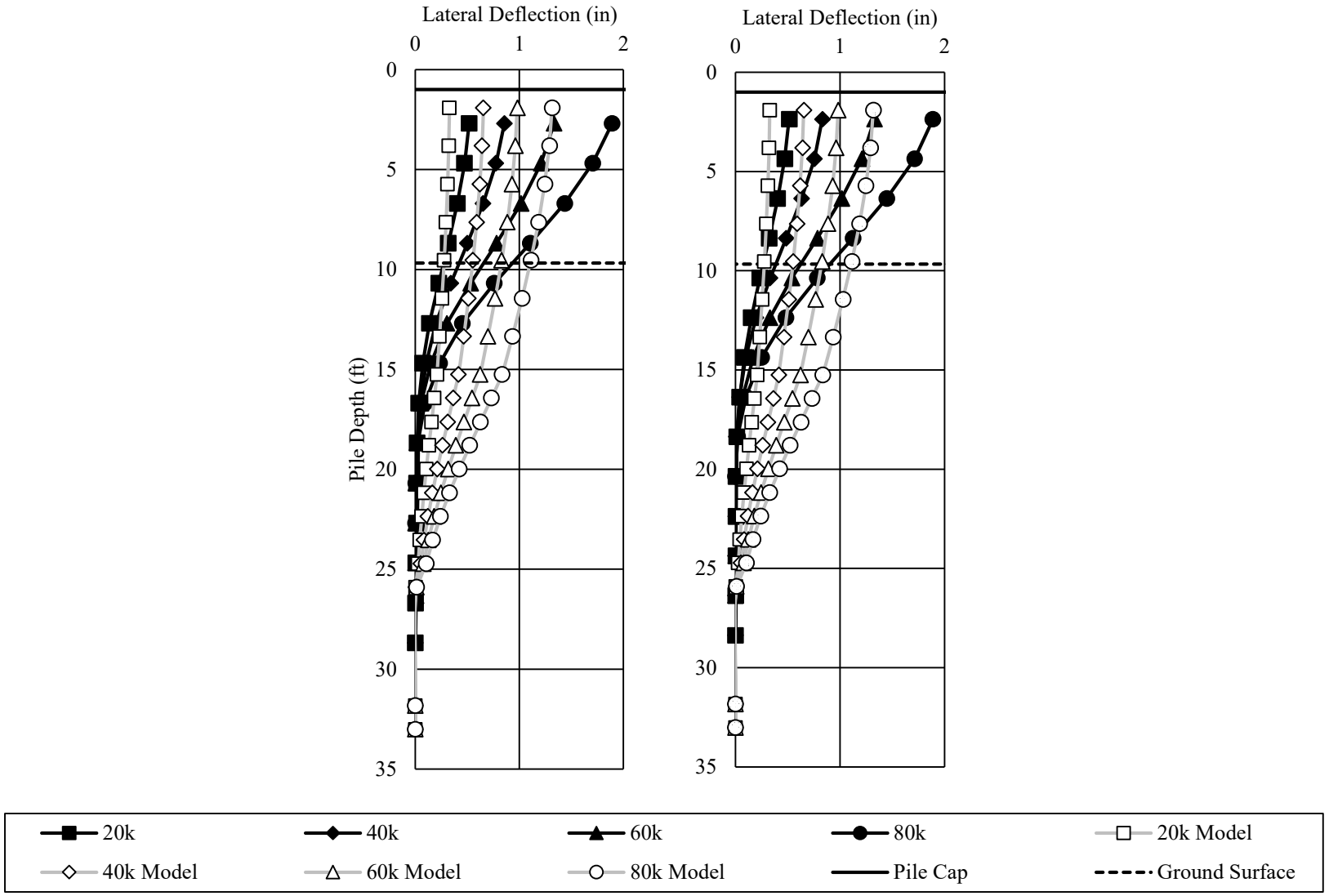

Figure 6-1 – Preliminary Model and Observed Inclinometer Profiles Comparison for the AUNGES Battered Pile Bent

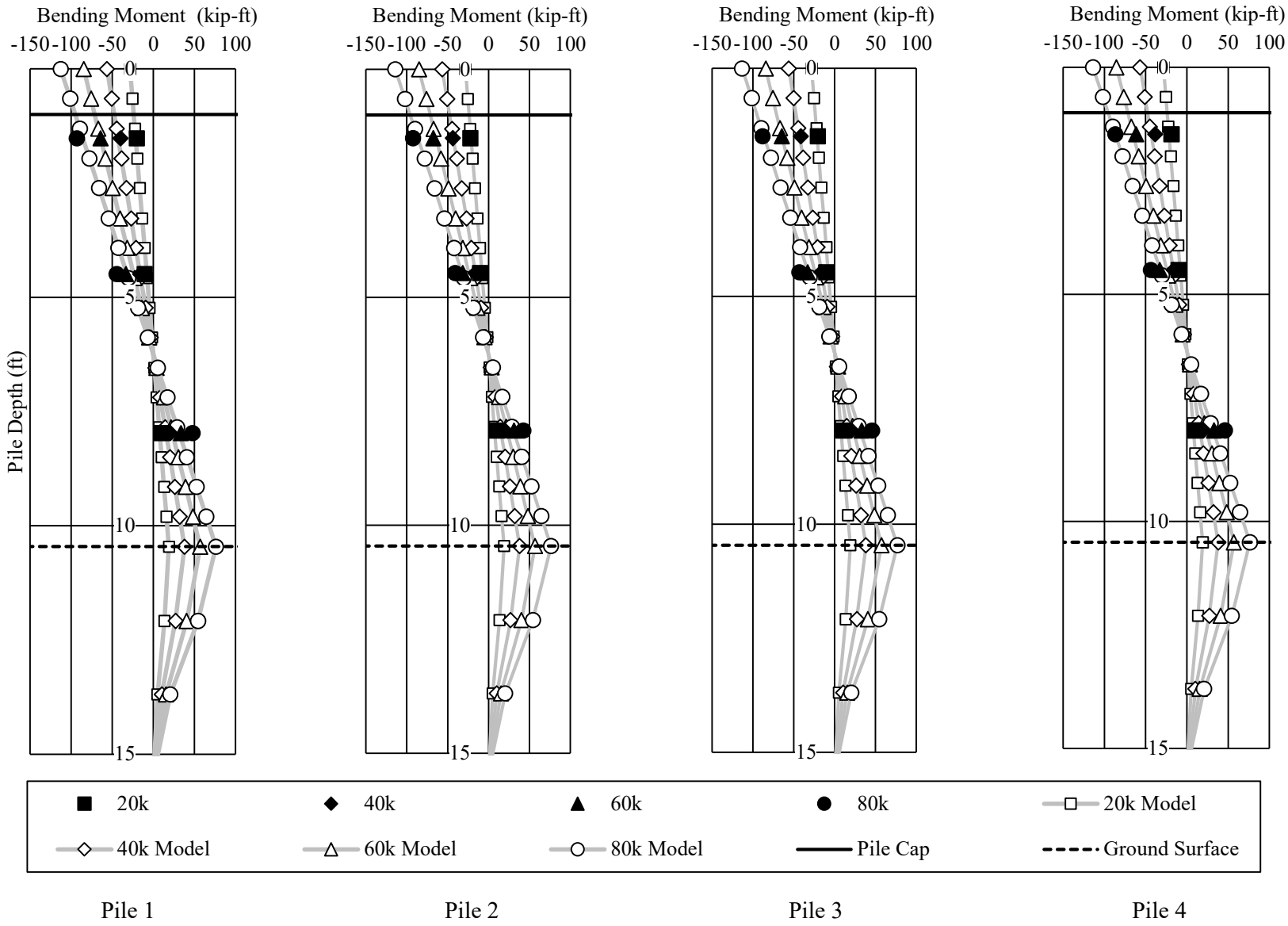

Figure 6-2 – Preliminary Model and Observed Moment Profiles Comparison for the AUNGES Battered Pile Bent

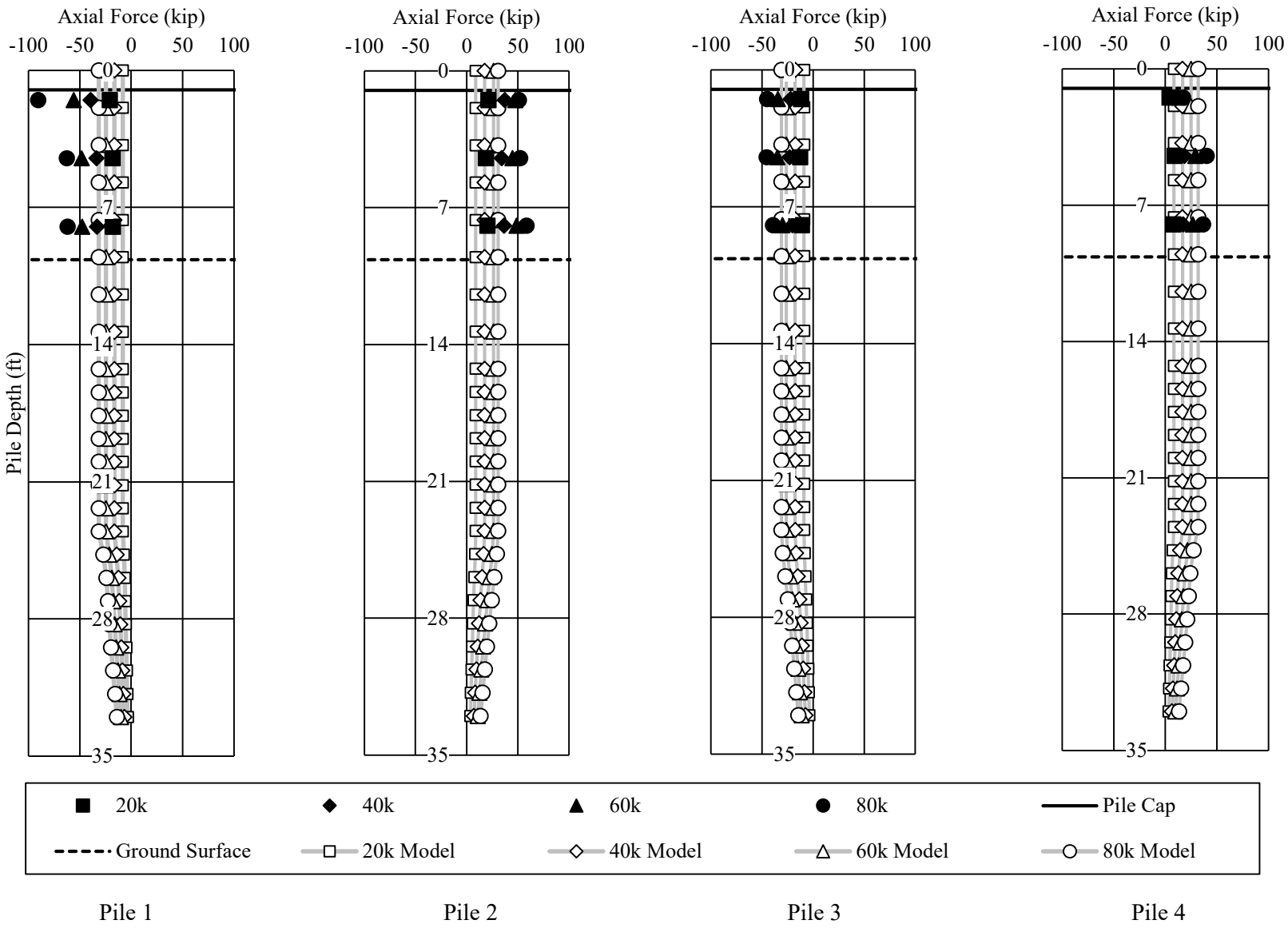

Figure 6-3 – Preliminary Model and Observed Axial Load Profiles Comparison for the AUNGES Battered Pile Bent

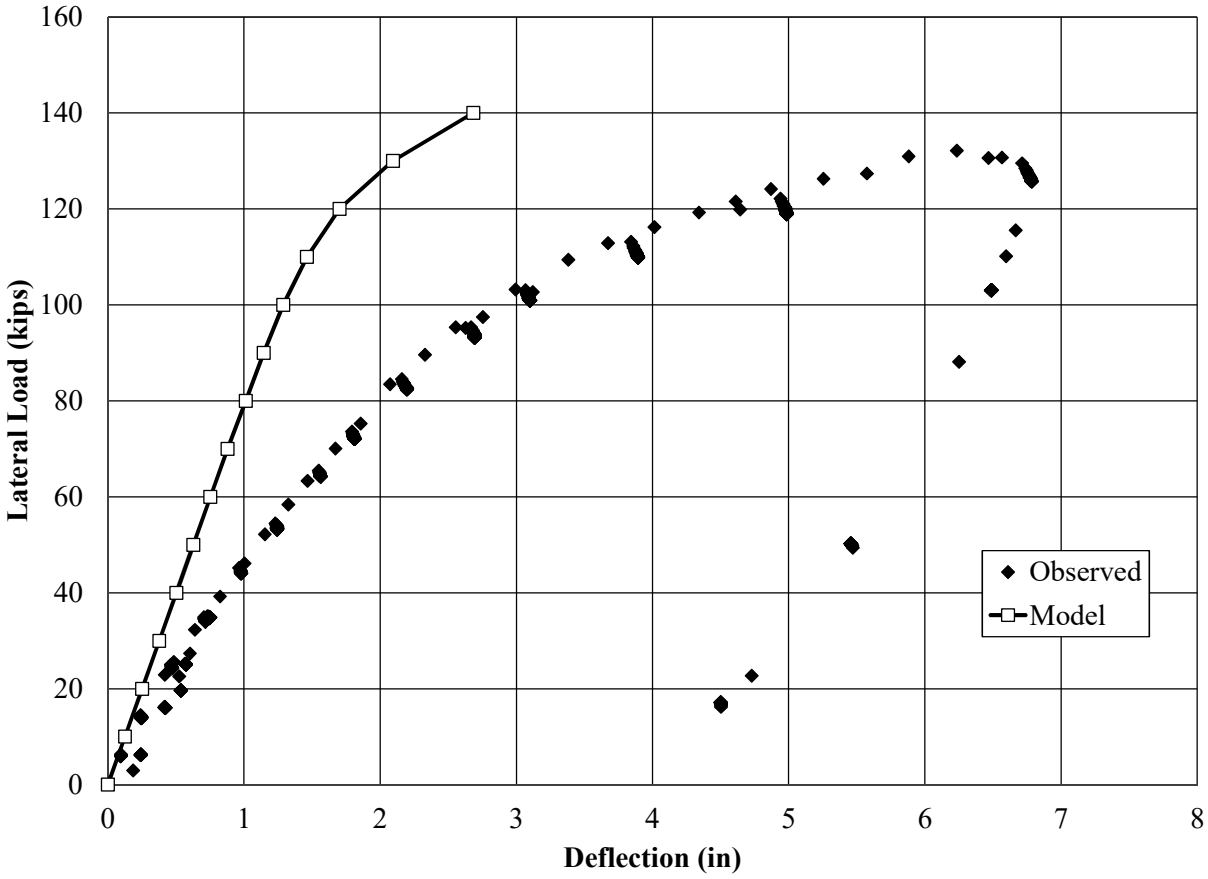

Figure 6-4 – Battered Pile Bent Comparison of Model and Observed Load Deflection Behavior

Preliminary models did not accurately match the observed inclinometer test data. Models predicted stiffer pile behavior and a higher point of inflection than observed in the load tests. The comparison chart also suggested the soil itself may not have provided the resistance predicted by the initial soil profiles. Calibration of the models to the load test results sought to match the deflection profiles to the observed inclinometer profiles. Initial moment profiles accurately predicted the observed moment profiles. The comparison showed that the models accurately reflected the flexural properties of the piles and bent cap. The axial models predicted much less axial load transference into the piles. Observed axial load profiles were greater than the model predictions. This likely

indicates that the lateral load is being transferred into the piles as axial load. The load deflection comparison also shows that observed bent behavior was less stiff than the model predicted. This indicates that disregarding p-y multipliers overpredicted the stiffness behavior of the bent and was not a valid modelling choice for the battered pile bent.

6.2.2 Vertical Pile Bent

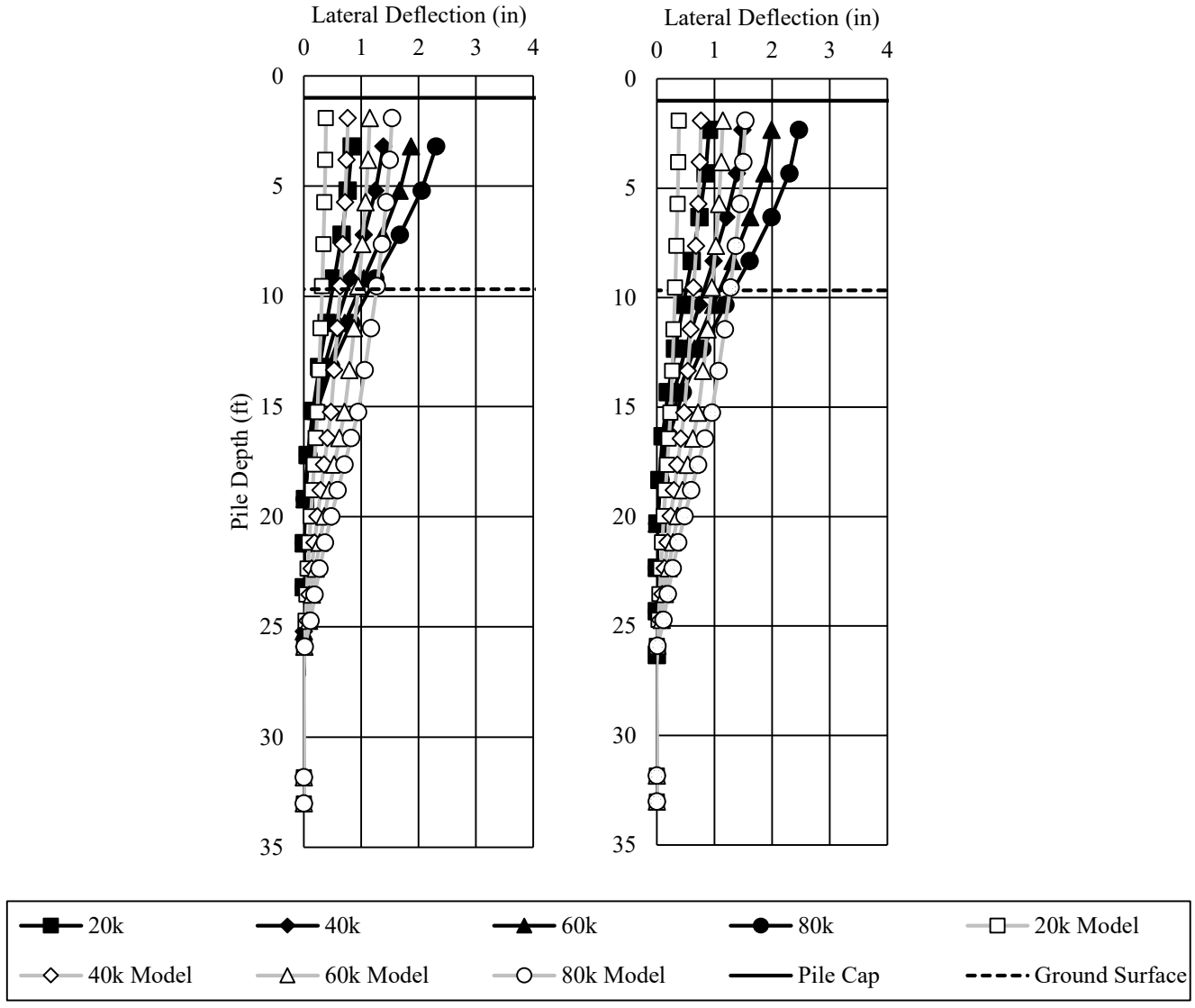

Pile 5 Pile 7

Figure 6-5 – Preliminary Model and Observed Inclinometer Profiles Comparison for the AUNGES Vertical Pile Bent

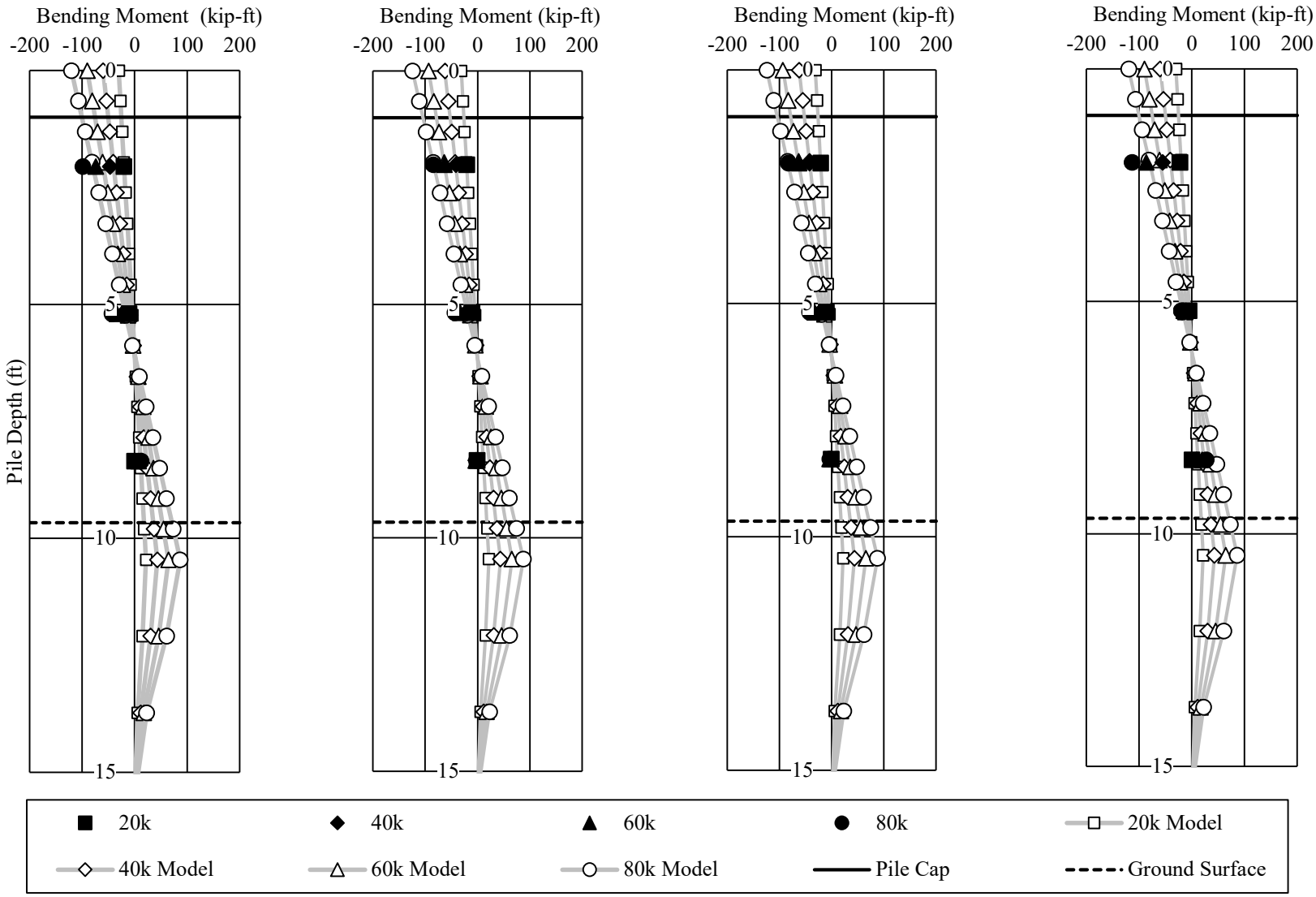

Figure 6-6 – Preliminary Model and Observed Moment Profiles Comparison for the AUNGES Vertical Pile Bent

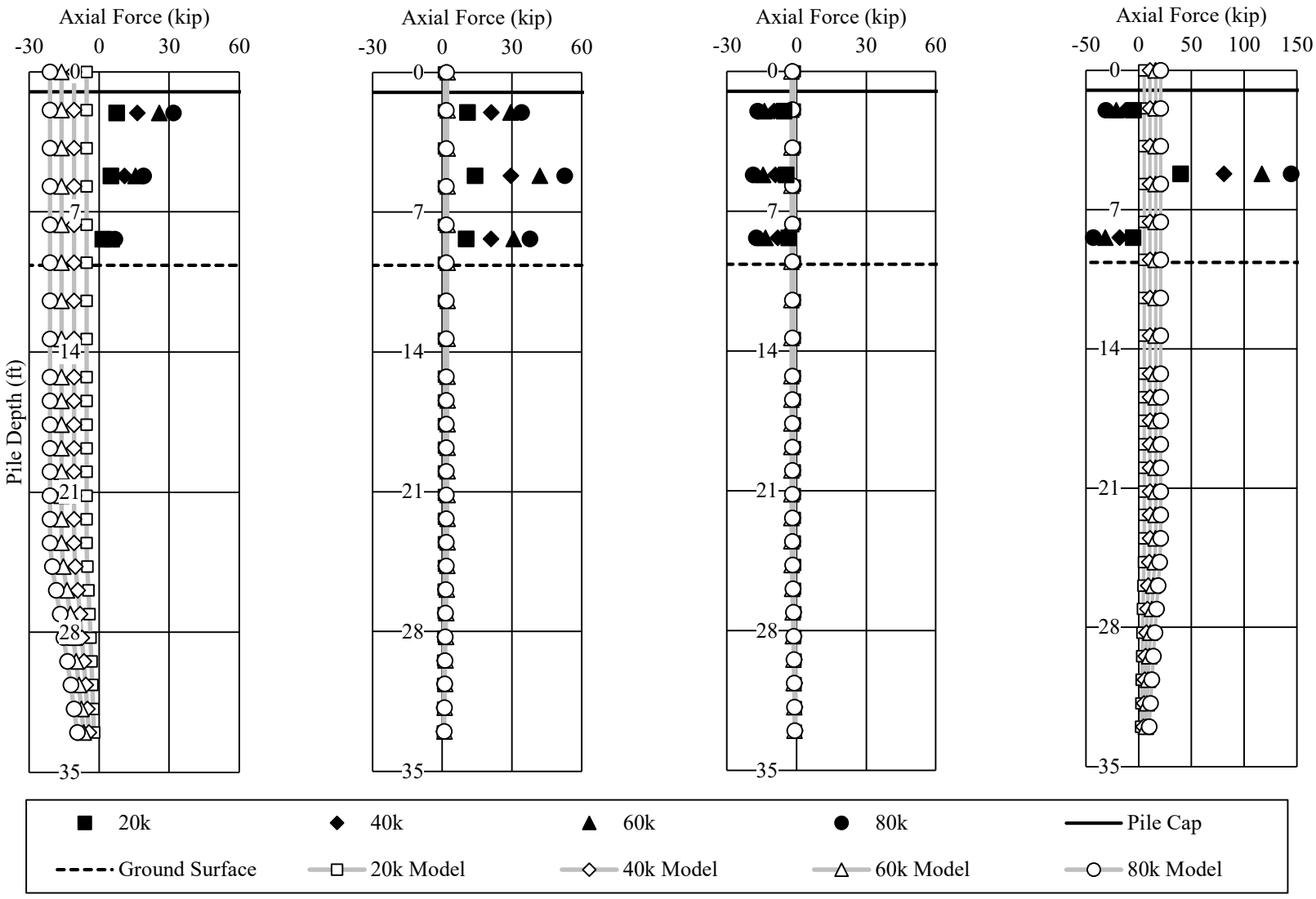

Figure 6-7 – Preliminary Model and Observed Axial Load Profiles Comparison for the AUNGES Vertical Pile Bent

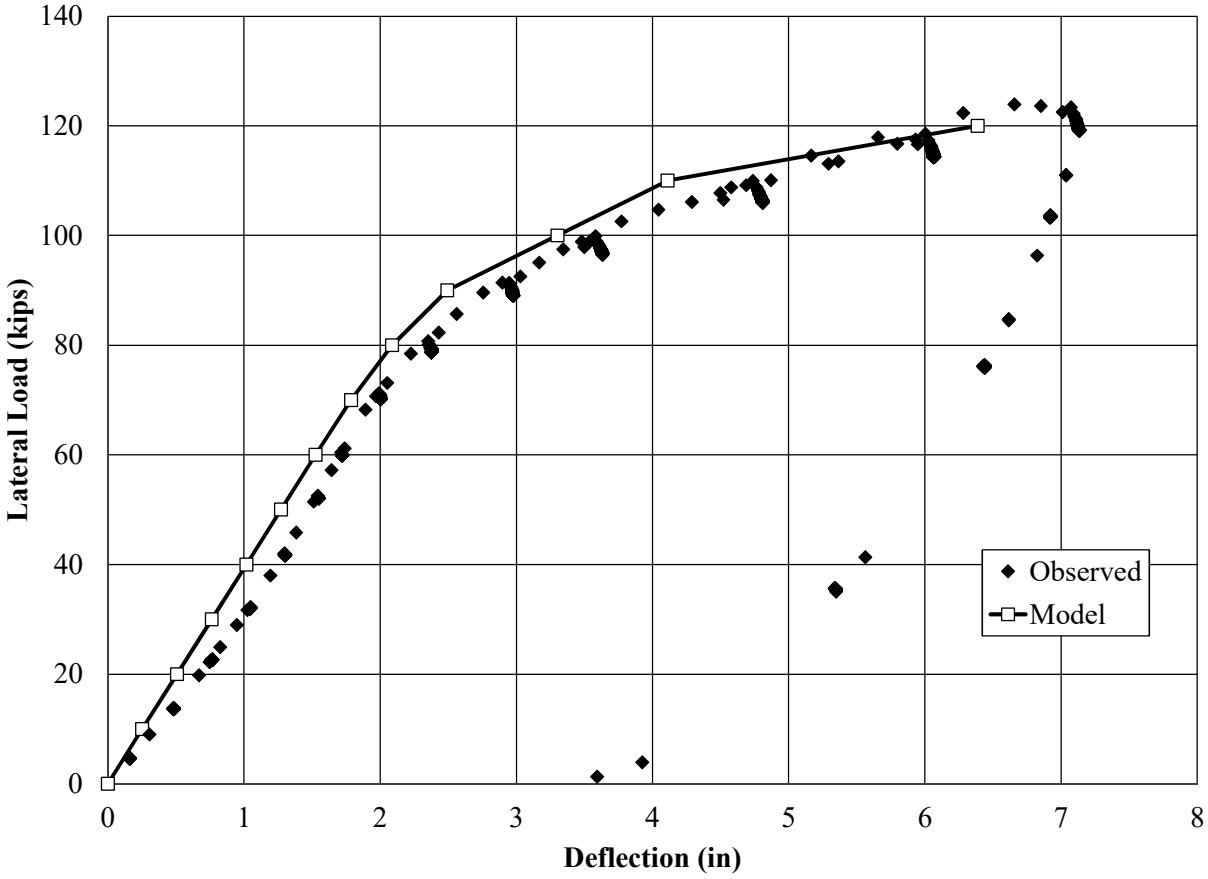

Figure 6-8 – Vertical Pile Bent Comparison of Model and Observed Load Deflection Behavior

Preliminary models did not accurately match the observed inclinometer test data. Models predicted stiffer pile behavior and a higher point of inflection than observed in the load tests. The comparison chart also suggested the soil itself may not have provided the resistance predicted by the initial soil profiles. Calibration of the models to the load test results sought to match the deflection profiles to the observed inclinometer profiles. Initial moment profiles accurately predicted the observed moment profiles at the upper gage locations. Lower gages indicated that the observed moment approached zero while the model profiles predicted slightly higher magnitudes of moment than observed. The comparison showed that the models accurately reflected the flexural properties of

the piles and bent cap, but likely overpredicted the stiffness of the soil. The axial models predicted much less axial load transference into the piles. Observed axial load profiles were greater than the model predictions. Models predicted that little to no load would be transferred into the middle two piles, but observed data indicates that the middle two piles carried similar amounts of lateral load as the outer two piles. The load deflection comparison also shows that observed bent behavior was slightly less stiff than the model predicted. The model was a close match to the observed profile. This indicates that disregarding p-y multipliers for the vertical pile bent was a valid modelling assumption.

Chapter 7 Calibration of Theoretical Models

7.1 Introduction

The results from the full-scale field lateral load tests were used to calibrate and refine the initial models. The only model calibration conducted for this research involved the AUNGES test bents. Model calibration for the Macon County Road 9 and US Highway 331 bridge bents was detailed in the companion thesis written by Jonathon Campbell. Calibration was conducted to determine what modeling assumptions should be made to produce more accurate models that better predict the behavior of bridge bents when they are subjected to lateral loads. Calibration was conducted by iterating soil profiles to match the observed Inclinometer data. The sections below show comparisons between the field load test results and refined models. The changes made to the initial models to produce the final models are detailed along with the comparisons below.

7.2 AUNGES

Initial models for the AUNGES bents were built using data collected during the construction process. Soil properties such as unit weight, p-y behavior, and undrained shear strength, were estimated from dilatometer testing. The yield stress of the steel was determined from coupon testing conducted by the steel pile supplier. Concrete compressive strength and elastic modulus were determined from cylinder testing conducted in the Auburn University structures lab. Several strategies were used to attempt to match the models to the observed data. One strategy that was attempted and discarded was to model the pile cap as a pinned connection. Models run with pinned connections departed greatly from the observed data on moment capacity, moment profile shape, and deflection behavior. This suggests the pile to cap connection is primarily a fixed connection even when the pile flanges at the pile to cap connection begin to yield. The models were calibrated by trying to match the observed deflection behavior from the field load tests. The comparisons between the calibrated models and the observed data are shown in the sections below.

7.3 Battered Pile Bent

The initial change to the Battered Pile bent model was to add p-y multipliers to account for group behavior of the piles. The default setting was chosen in FB Multipier. This applied a reduction factor of 0.8 to the leading pile, 0.4 to the pile behind the leading pile, and 0.3 to the last two piles. This change affected the deflection behavior of the bent model. The magnitude of the deflection was very close to the observed deflection behavior at the top of the piles, but the behavior of the piles instrumented with inclinometers could not be matched. The models also over predicted the stiffness of the soil, so the p-y curve of the soil was reduced to try and match the observed shape of the load deflection curve. The upper soil layer was lowered to allow more deflection and to lower the inflection point observed in the inclinometer data. The models also over predicted the moment in the piles after the piles began to yield. The compressive strength and elastic modulus of the concrete in the cap was changed to reflect the values calculated in cylinder testing. The values were computed from cylinders tested on the same day as the load test to provide the most accurate representation of the in place concrete strength. Figure 7-1, Figure 7-2, Figure 7-3, Figure 7-4, Figure 7-5, Figure 7-6, Figure 7-7, and Figure 7-8 Show the calibrated model profiles and comparisons of the calibrated models to the observed field load test results.

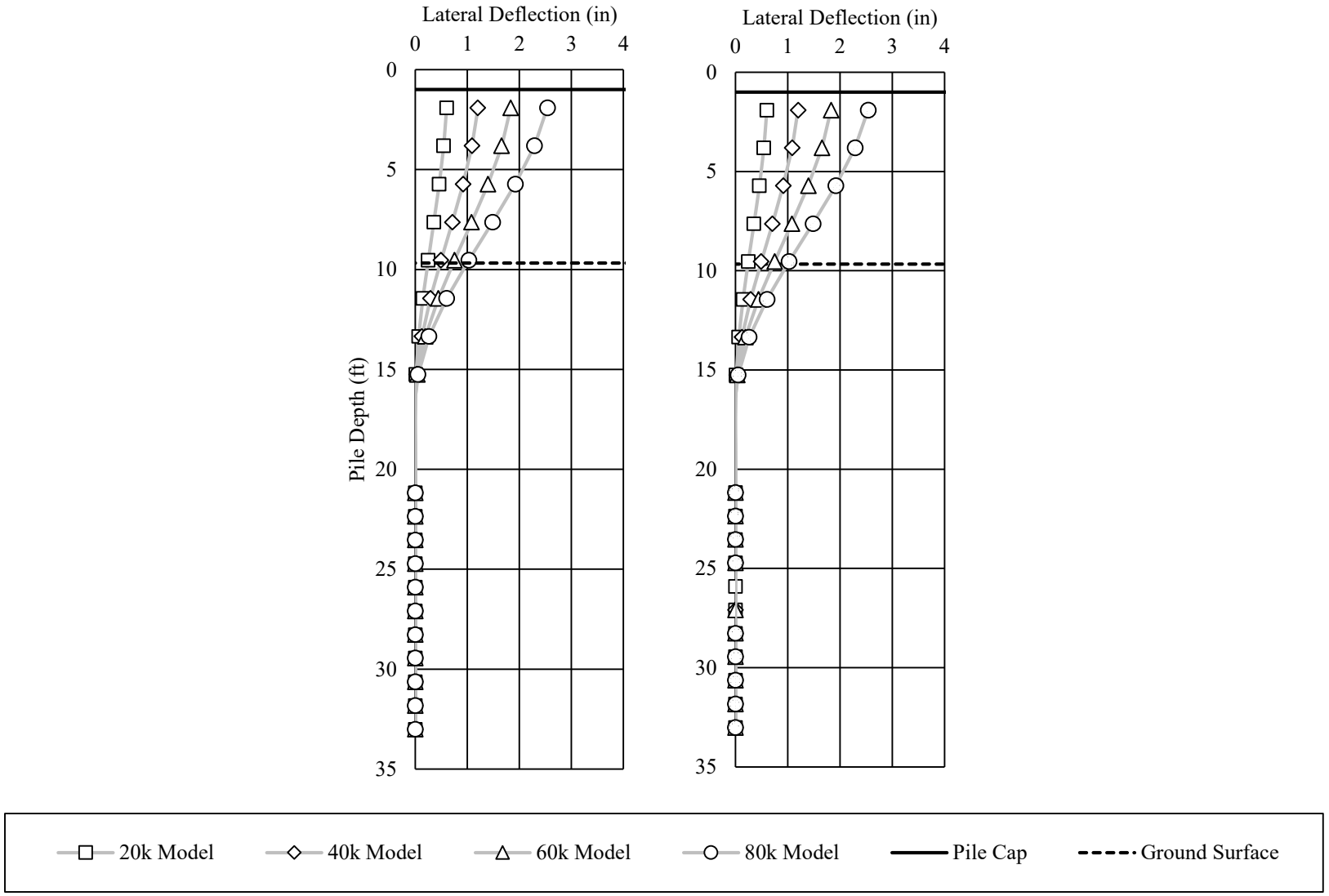

Figure 7-1 – AUNGES Battered Pile Bent Calibrated Model Inclinometer Profiles

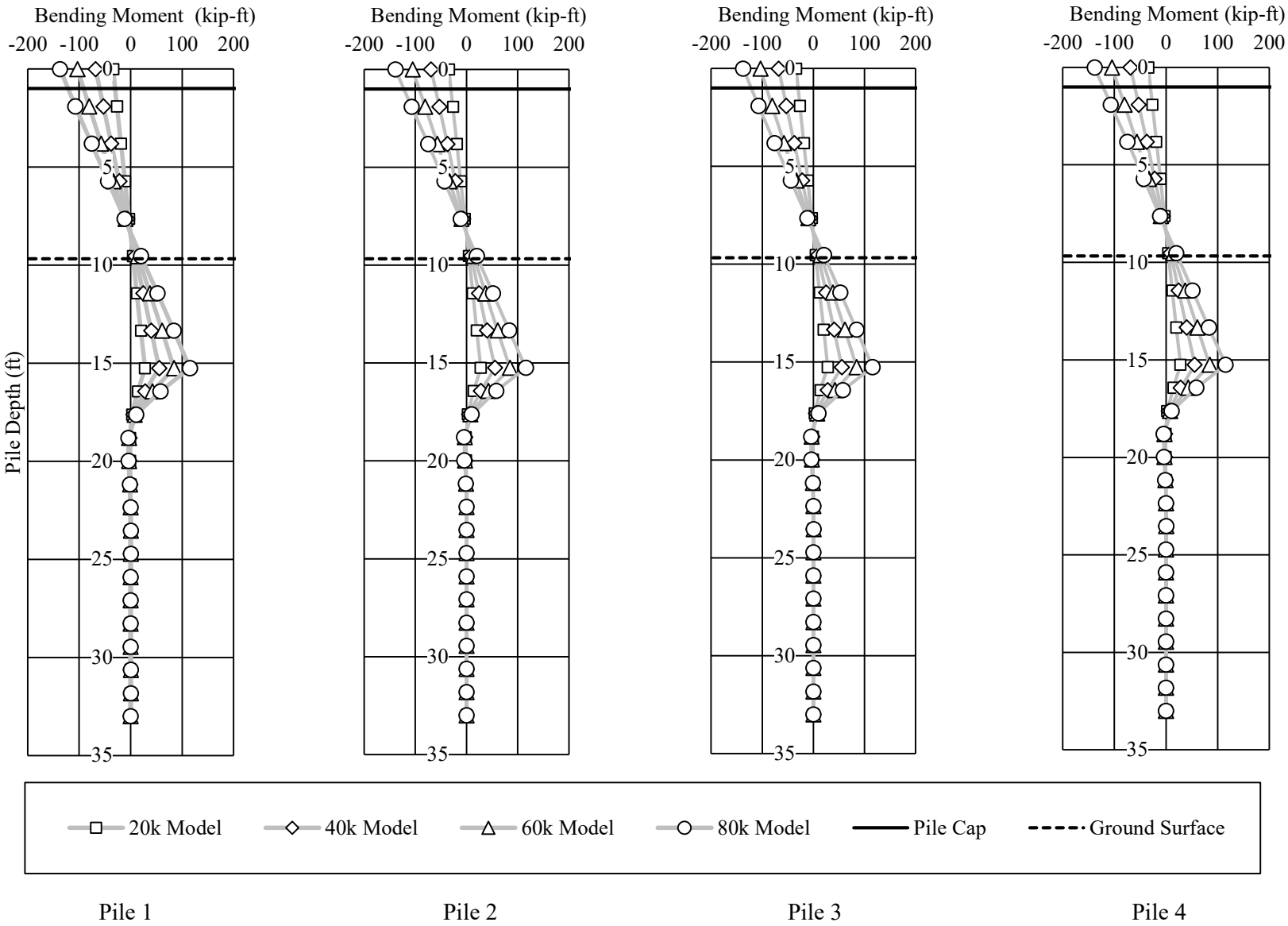

Figure 7-2 – AUNGES Battered Pile Bent Calibrated Model Moment Profiles

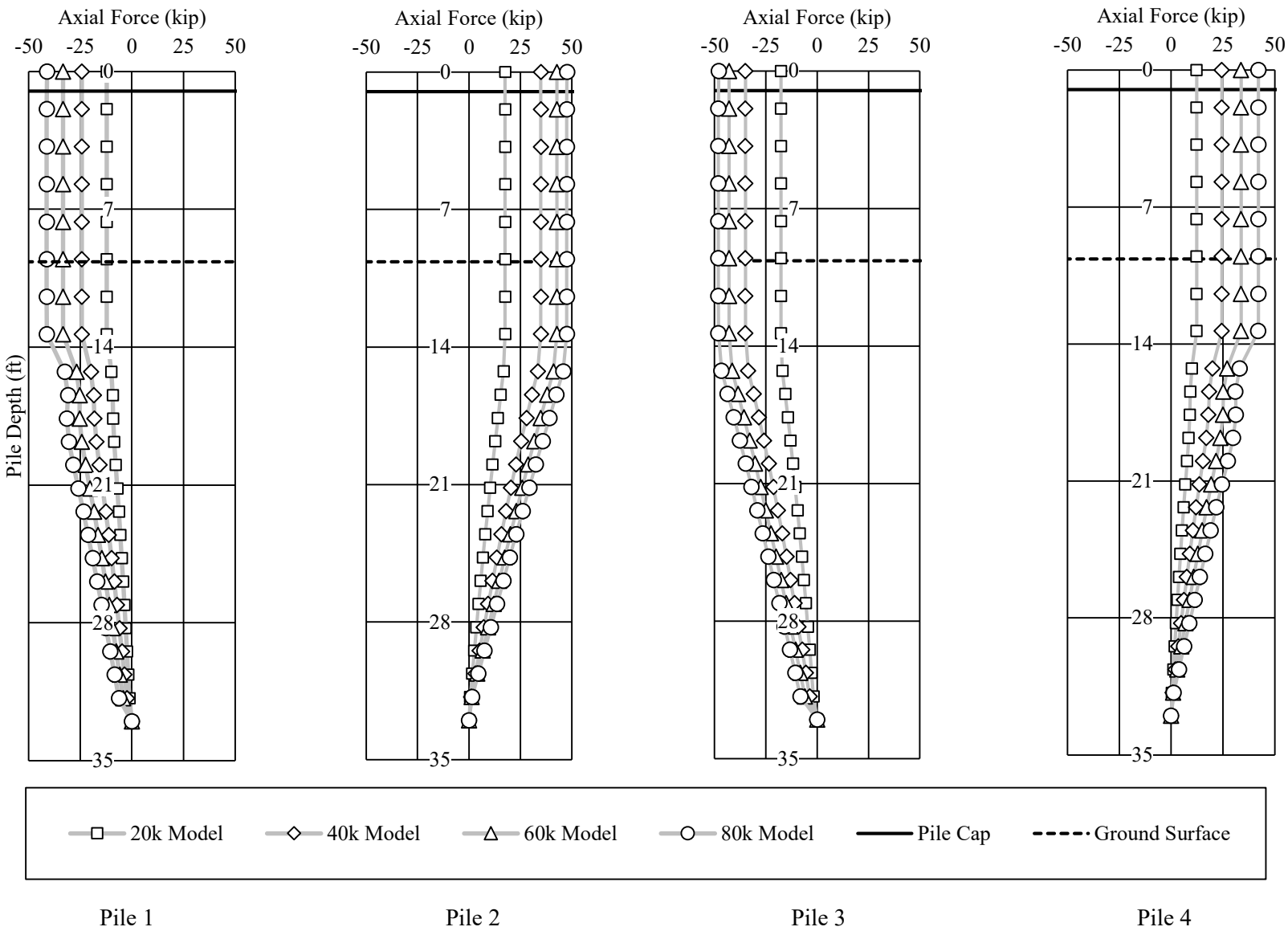

Figure 7-3 – AUNGES Battered Pile Bent Calibrated Model Axial Load Profiles

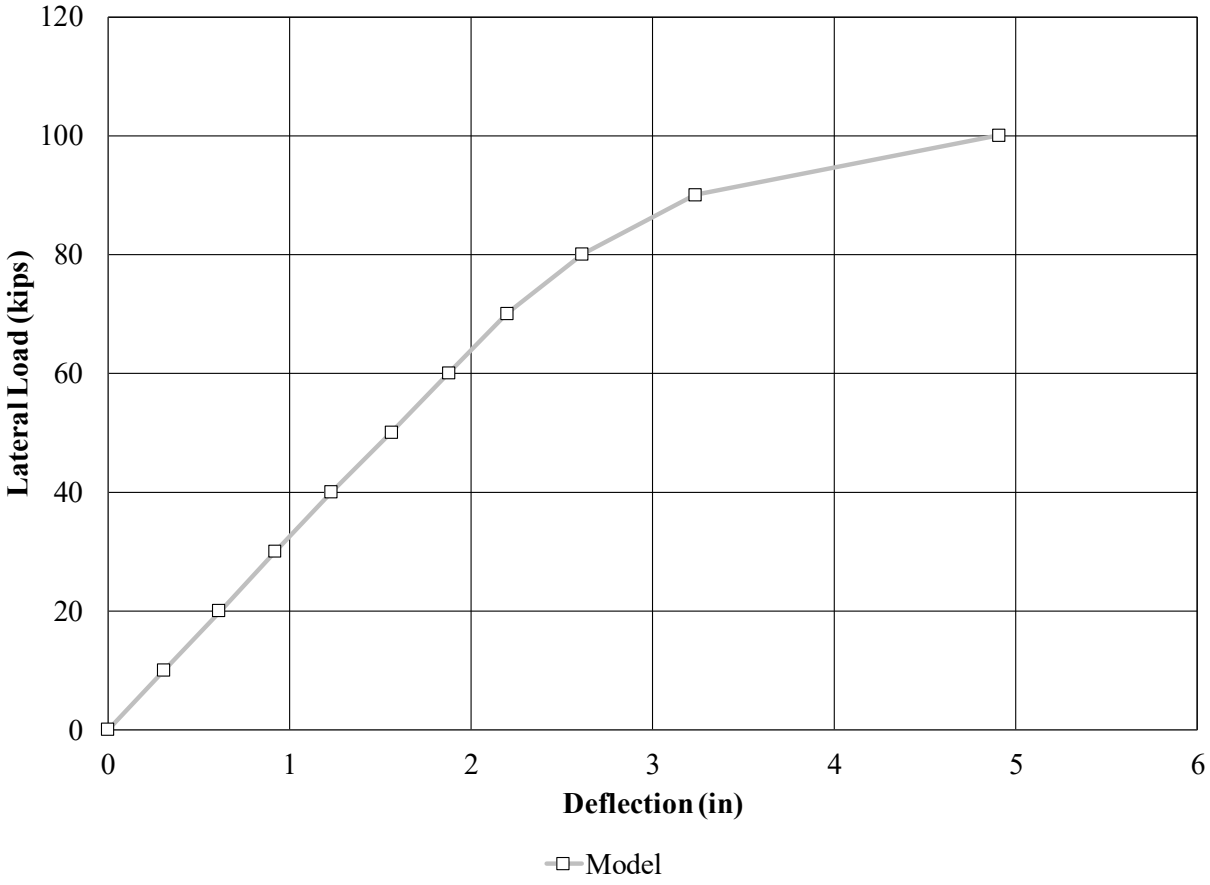

Figure 7-4 – Calibrated Model Load versus Deflection Profile for the AUNGES Battered Pile Bent

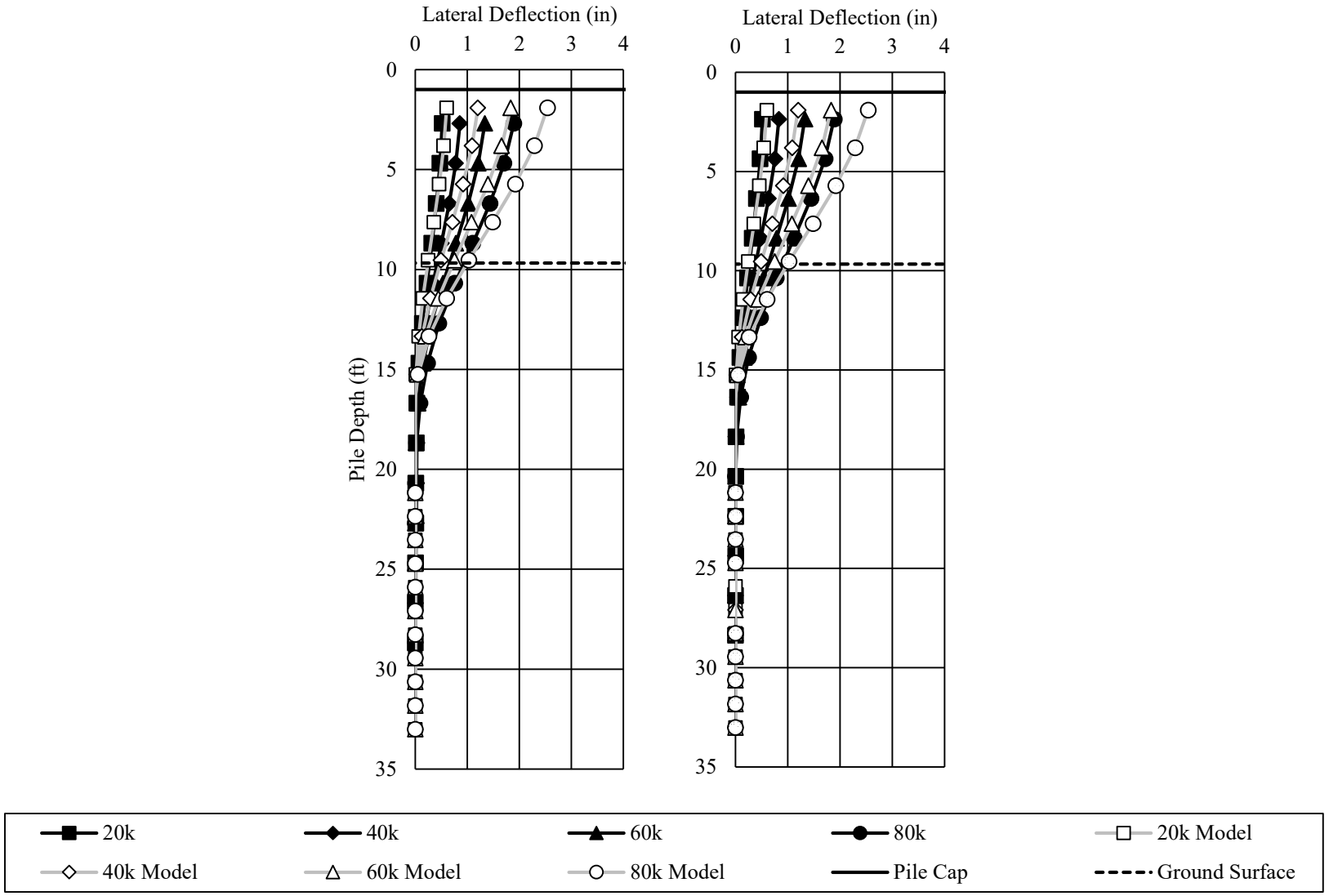

Figure 7-5 – AUNGES Battered Pile Bent Calibrated Model Inclinometer Profiles Comparison

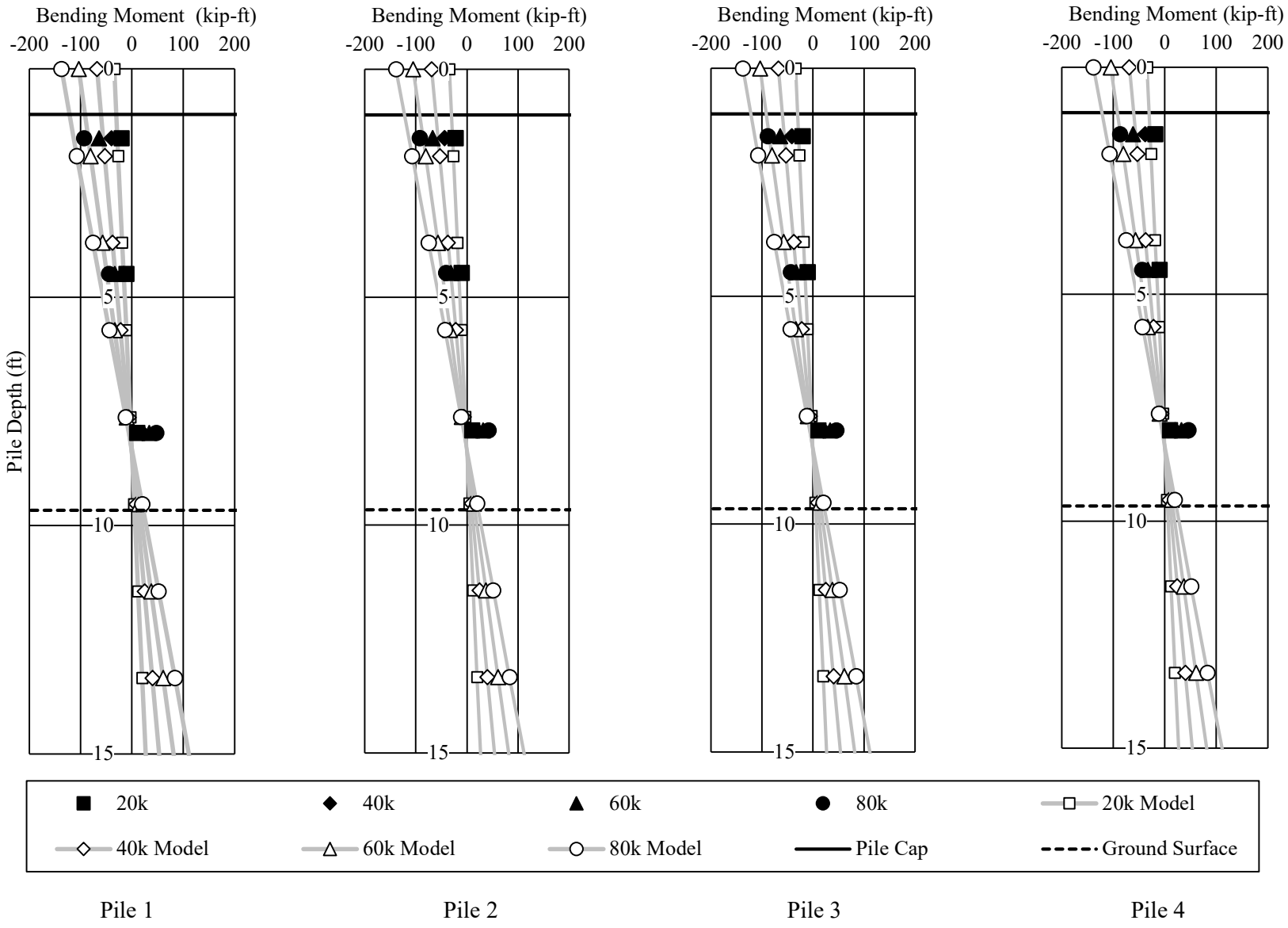

Figure 7-6 – AUNGES Battered Pile Bent Calibrated Model Moment Profiles Comparison

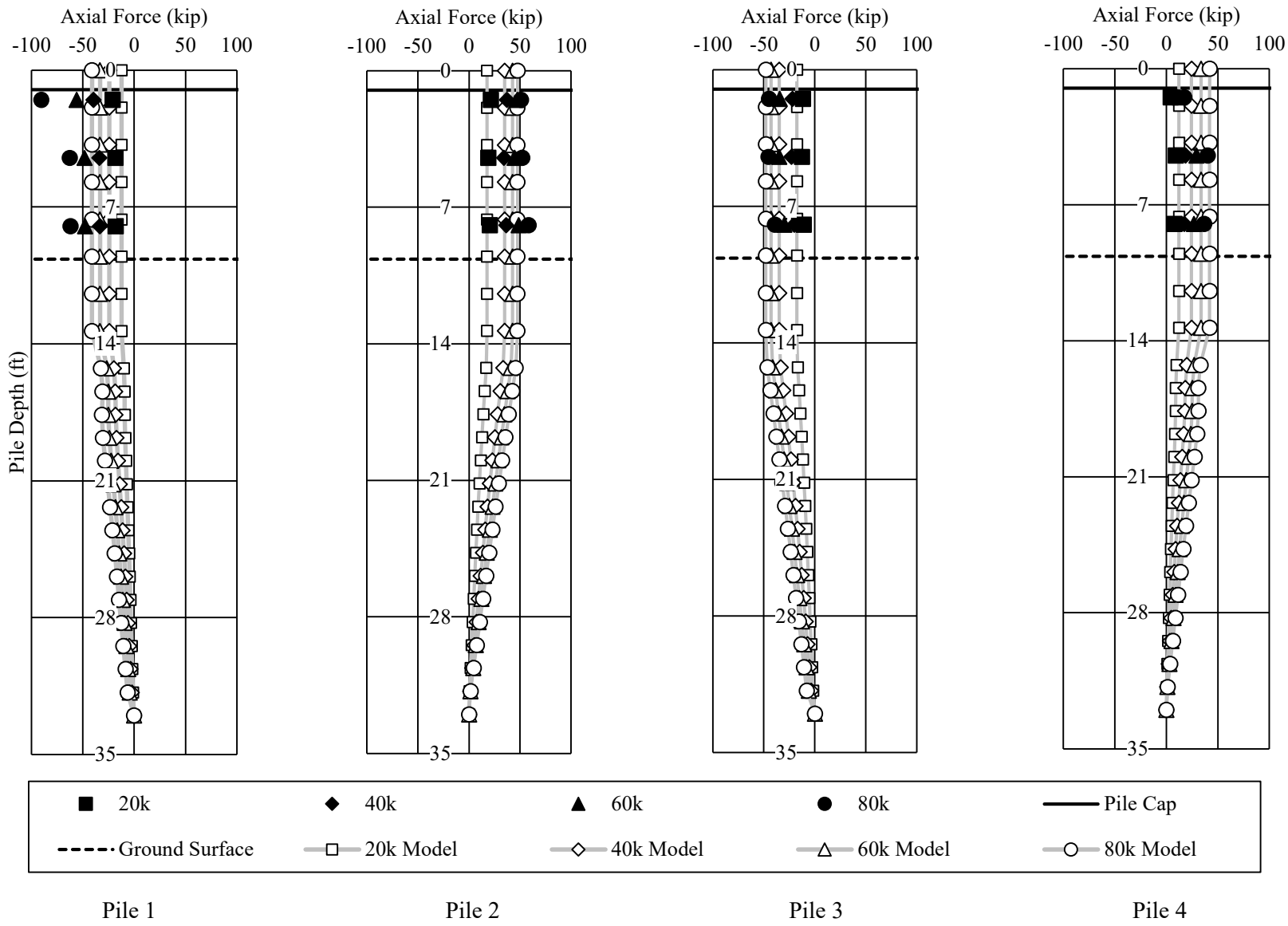

Figure 7-7 – AUNGES Battered Pile Bent Calibrated Model Axial Load Profiles Comparison

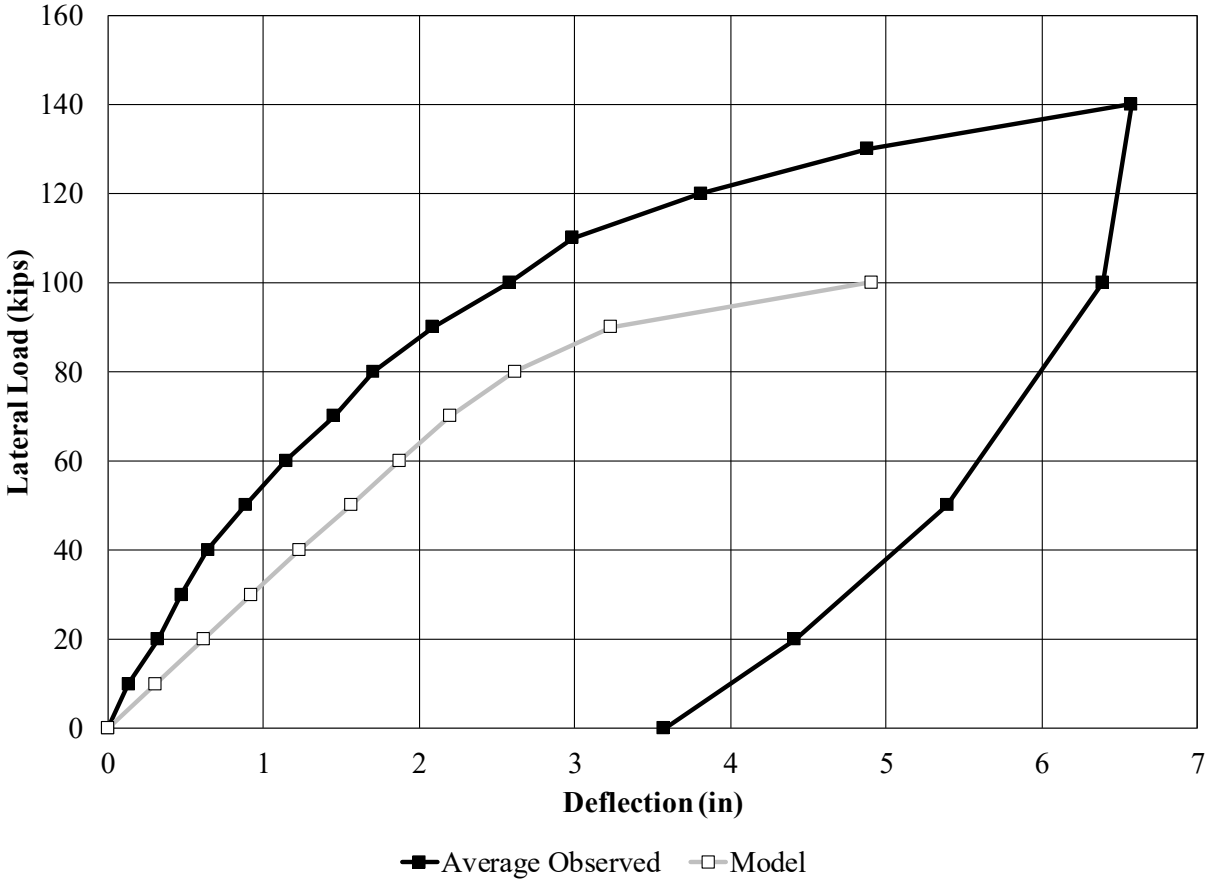

Figure 7-8 – AUNGES Battered Pile Bent Calibrated Model Load versus Deflection Comparison

The calibrated models accurately matched the inclinometer profiles. The point of inflection was matched by lowering the soil profile around the piles. The soil initial soil parameter models included soil profiles developed from in-situ testing. For calibration, the profiles were modeled using standard models in FB-Multipier. Soil properties were altered to create accurate matches. The calibrated models negatively affected the match seen in the comparison between the initial models and observed data. Calibrated models overpredicted the magnitude of moment in the piles. Axial matches were stronger than seen in the initial model comparisons. The load deflection chart showed that the calibrated model charts predicted less stiff bent behavior than the observed results.

Results of the calibration suggest that accurately predicting the lateral deflection of the piles produces a better prediction of the axial load induced by laterally loading the bent. This is accomplished by incorporating p-y modifiers to models of battered pile bents. Models show that the upper few feet of soil surrounding the pile provides little resistance to the lateral load. When modelling lateral load tests, it is suggested to disregard the upper two feet of soil.

7.4 Vertical Pile Bent

Similarly, to the battered pile bent, the initial change to the Vertical Pile bent model was to add p-y multipliers to account for group behavior of the piles. The default setting was chosen in FB Multipier. This applied a reduction factor of 0.8 to the leading pile, 0.4 to the pile behind the leading pile, and 0.3 to the last two piles. This change affected the deflection behavior of the bent model. This was chosen even though the preliminary model showed strong agreement with the observed load data to better match the inclinometer profiles. The magnitude of the deflection was very close to the observed deflection behavior at the top of the piles, but the behavior of the piles instrumented with inclinometers could not be matched directly through these methods alone. The initial models slightly over predicted the stiffness of the soil, so the p-y curve of the soil was reduced to try and match the observed shape of the load deflection curve. The models also over predicted the moment in the piles after the piles began to yield. The compressive strength and elastic modulus of the concrete in the cap was changed to reflect the values calculated in cylinder testing. The values were computed from cylinders tested on the same day as the load test to provide the most accurate representation of the in place concrete strength. Figure 7-9, Figure 7-10, Figure 7-11, Figure 7-12, Figure 7-13, Figure 7-14, Figure 7-15, and Figure 7-16 show the calibrated model profiles and the comparison between the calibrated model and the results from field load tests.

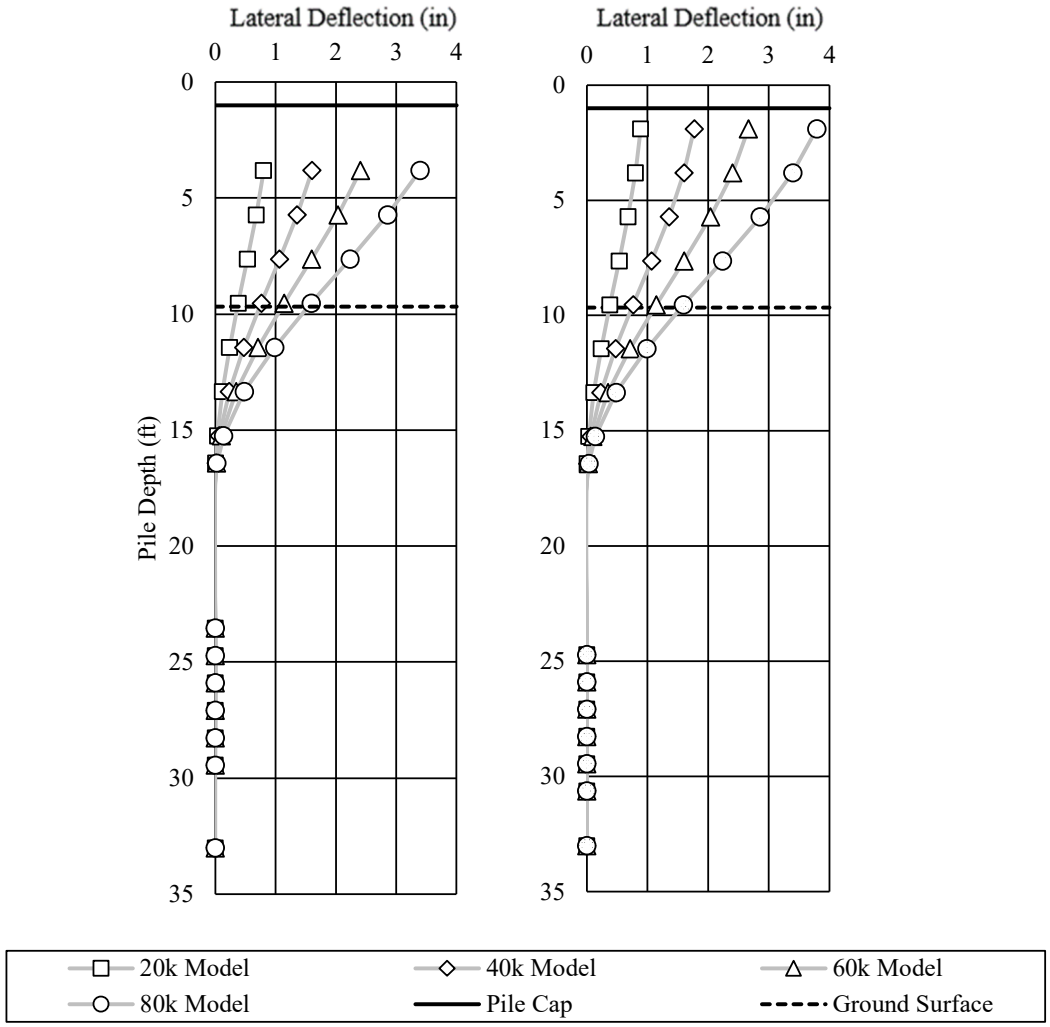

Pile 5 Pile 7

Figure 7-9 – AUNGES Vertical Pile Bent Calibrated Model Inclinometer Profiles

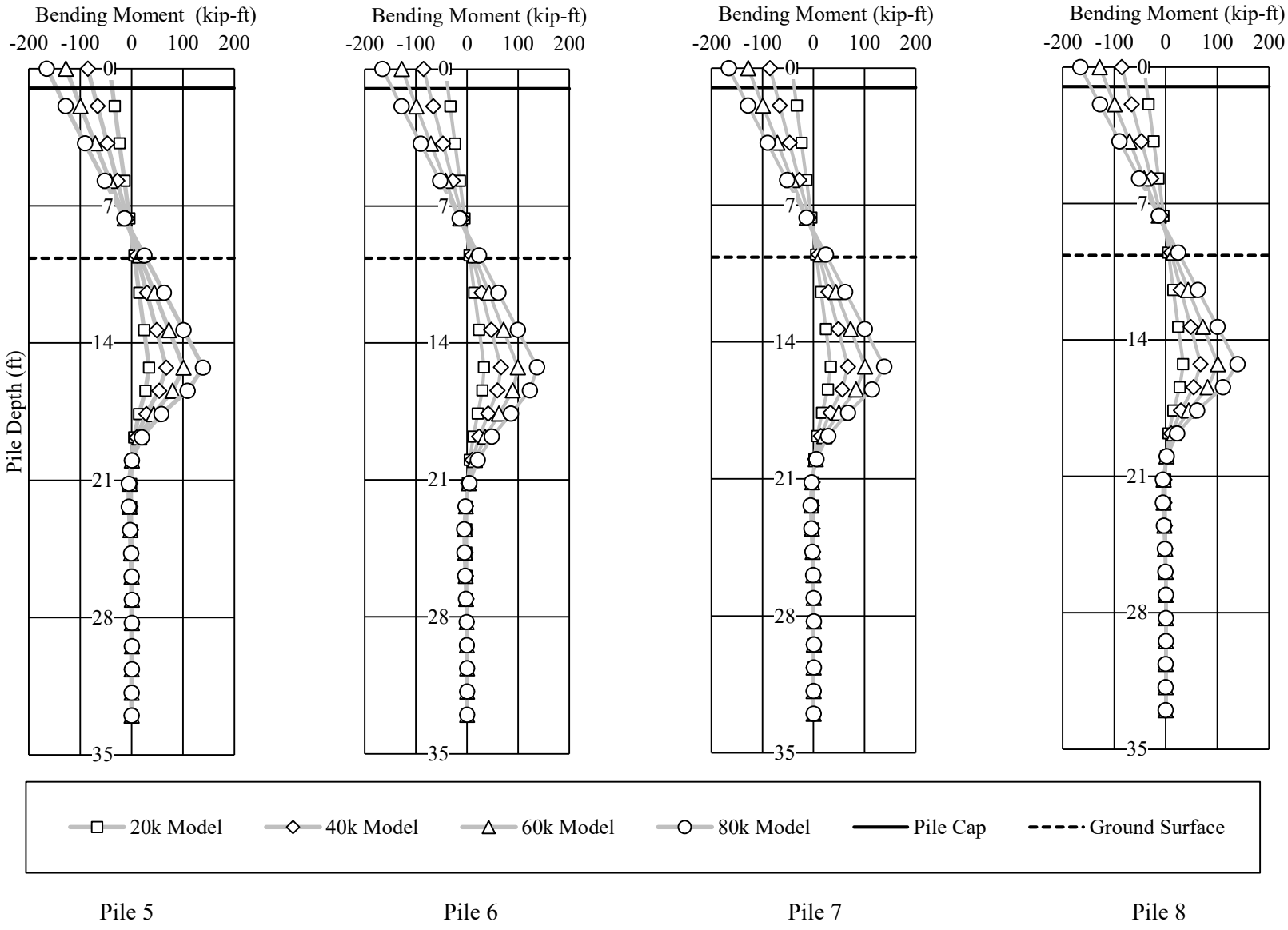

Figure 7-10 – AUNGES Vertical Pile Bent Calibrated Model Moment Profiles

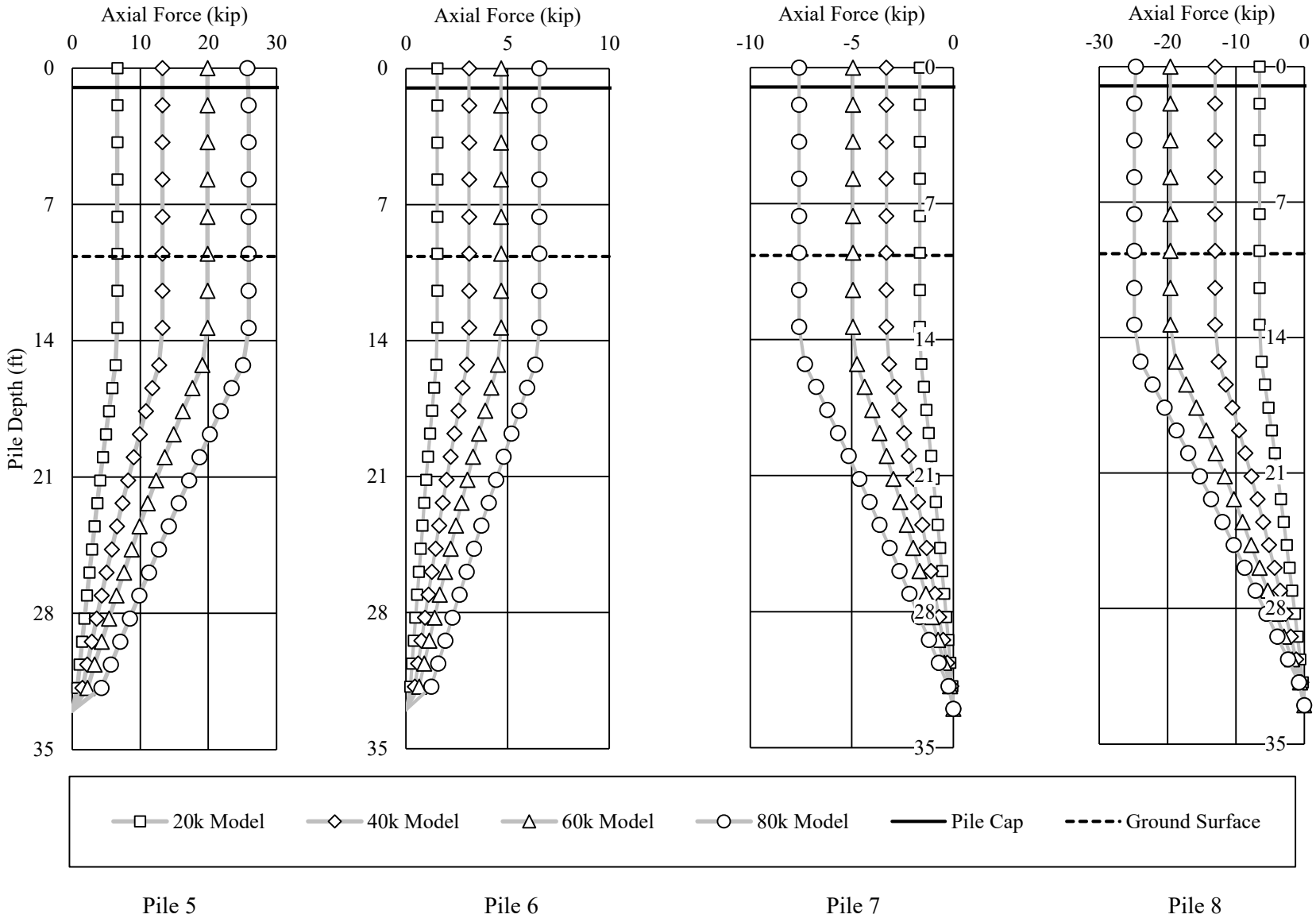

Figure 7-11 – AUNGES Vertical Pile Bent Calibrated Model Axial Load Profiles

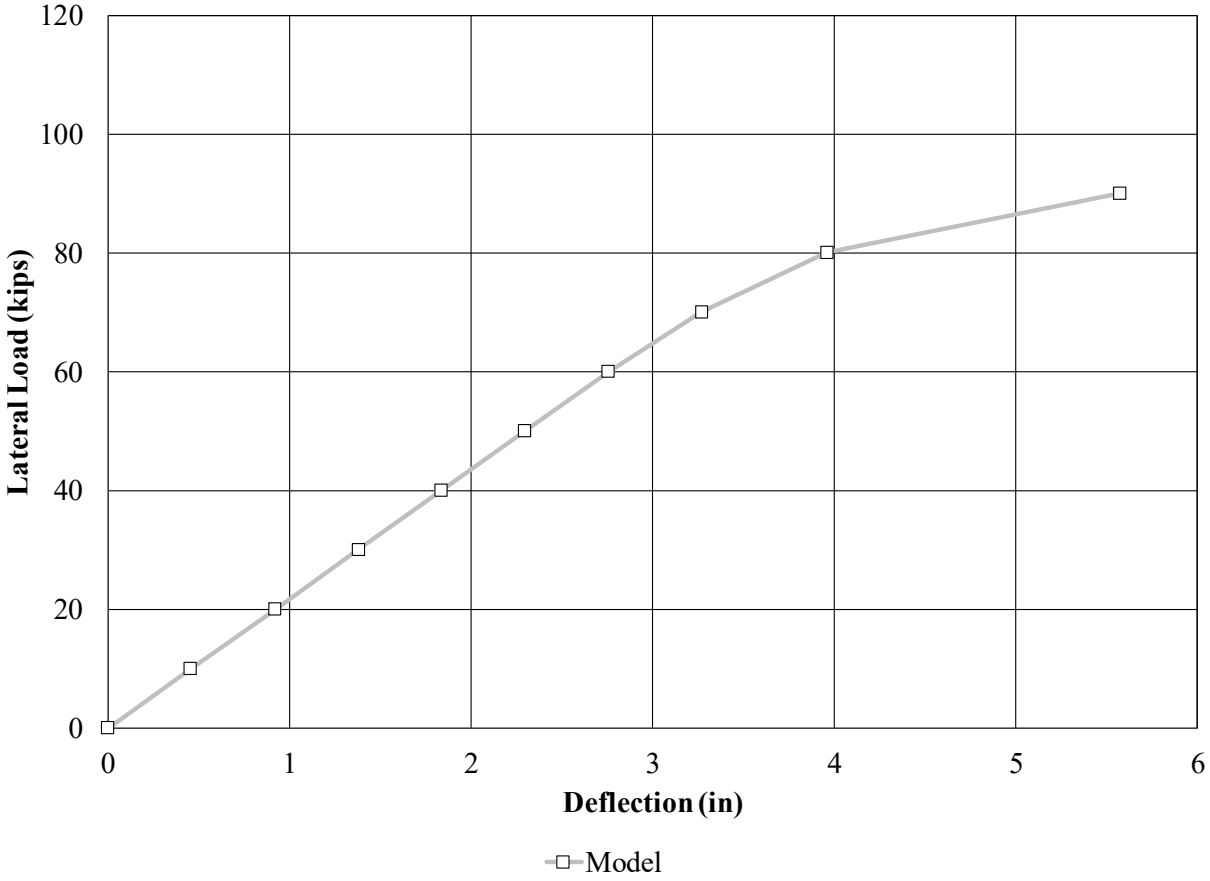

Figure 7-12 – AUNGES Vertical Pile Bent Calibrated Model Load versus Deflection

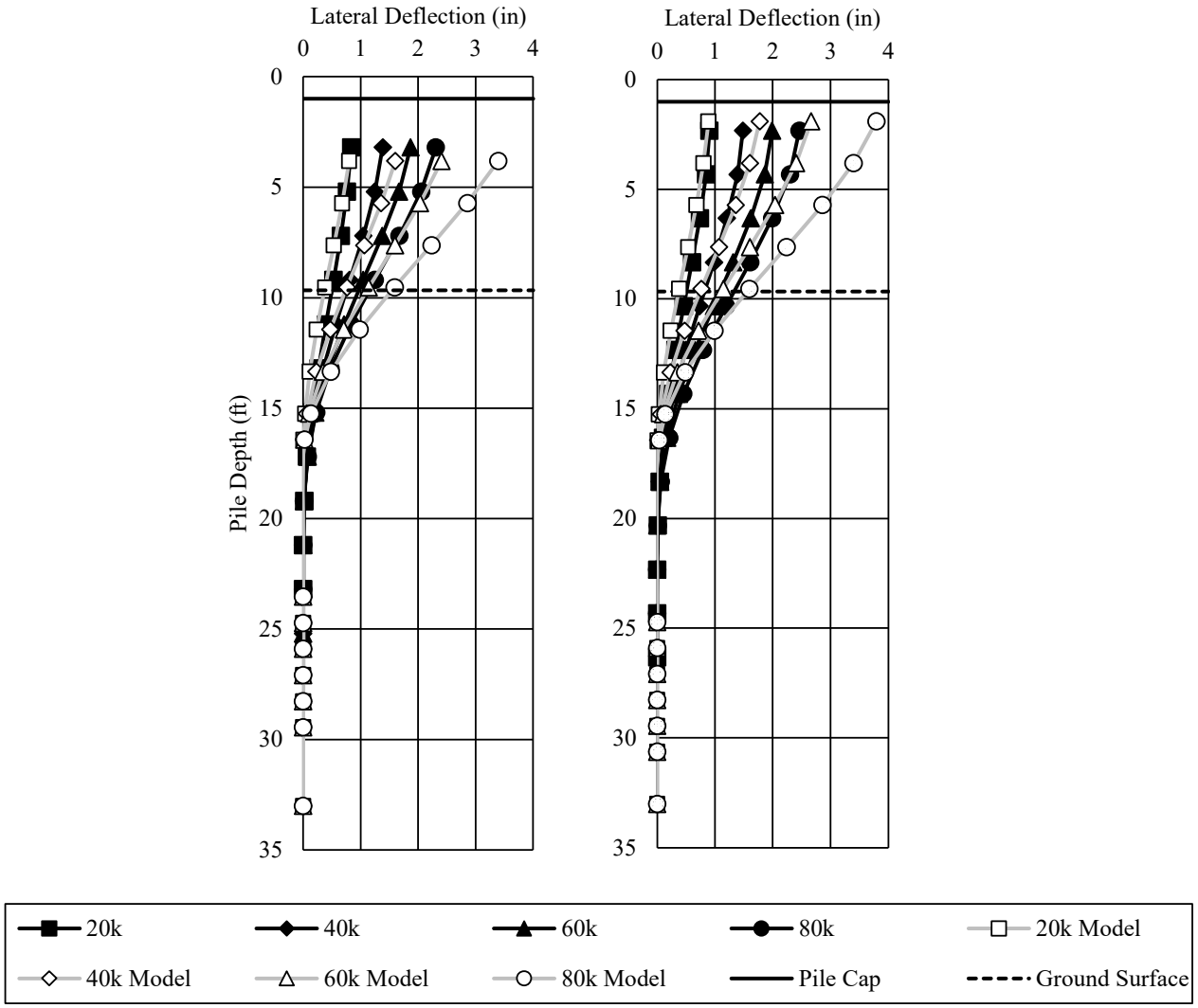

Figure 7-13 – AUNGES Vertical Pile Bent Calibrated Model Inclinometer Profiles Comparison

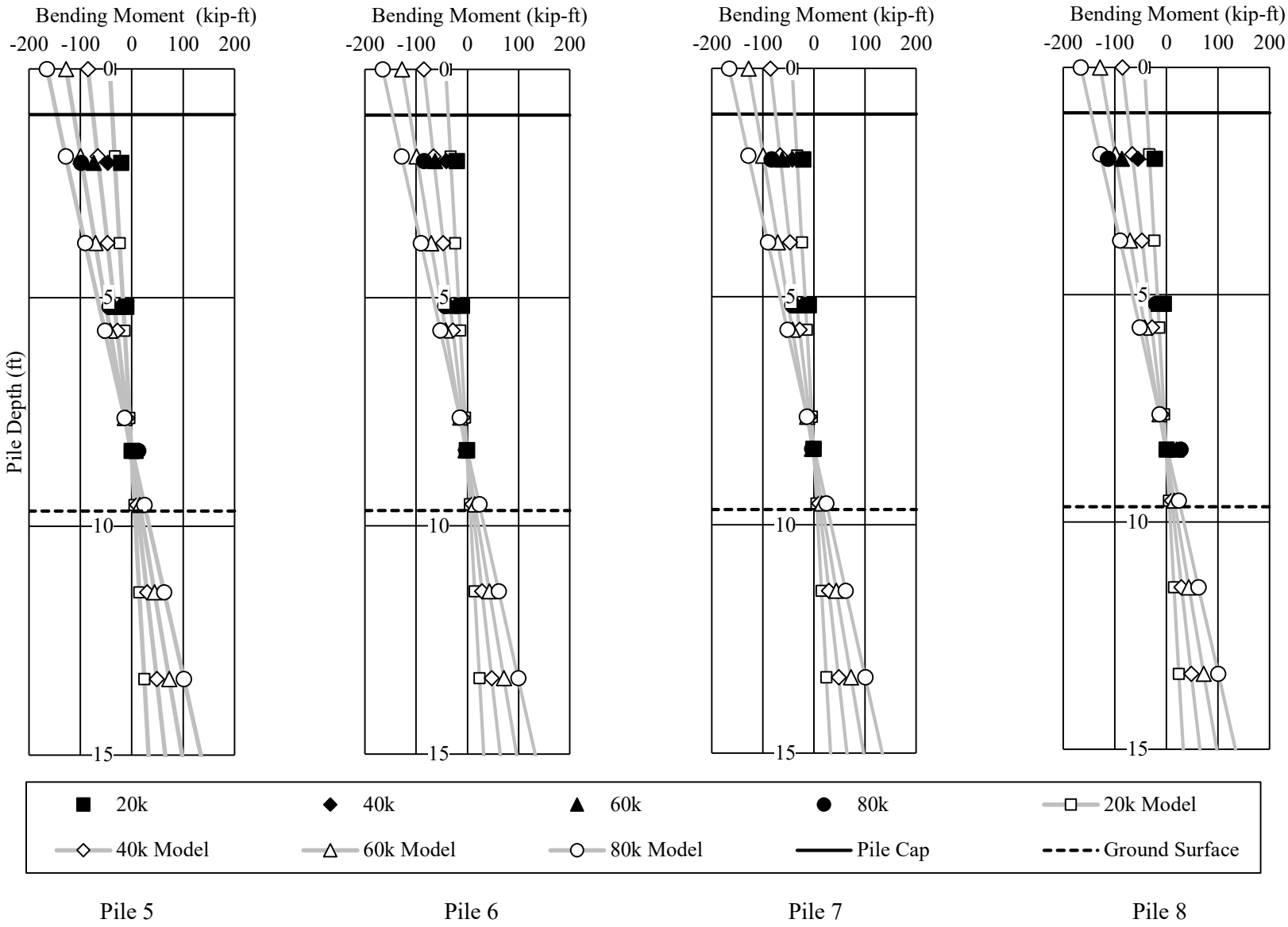

Figure 7-14 – AUNGES Vertical Pile Bent Calibrated Model Moment Profiles Comparison

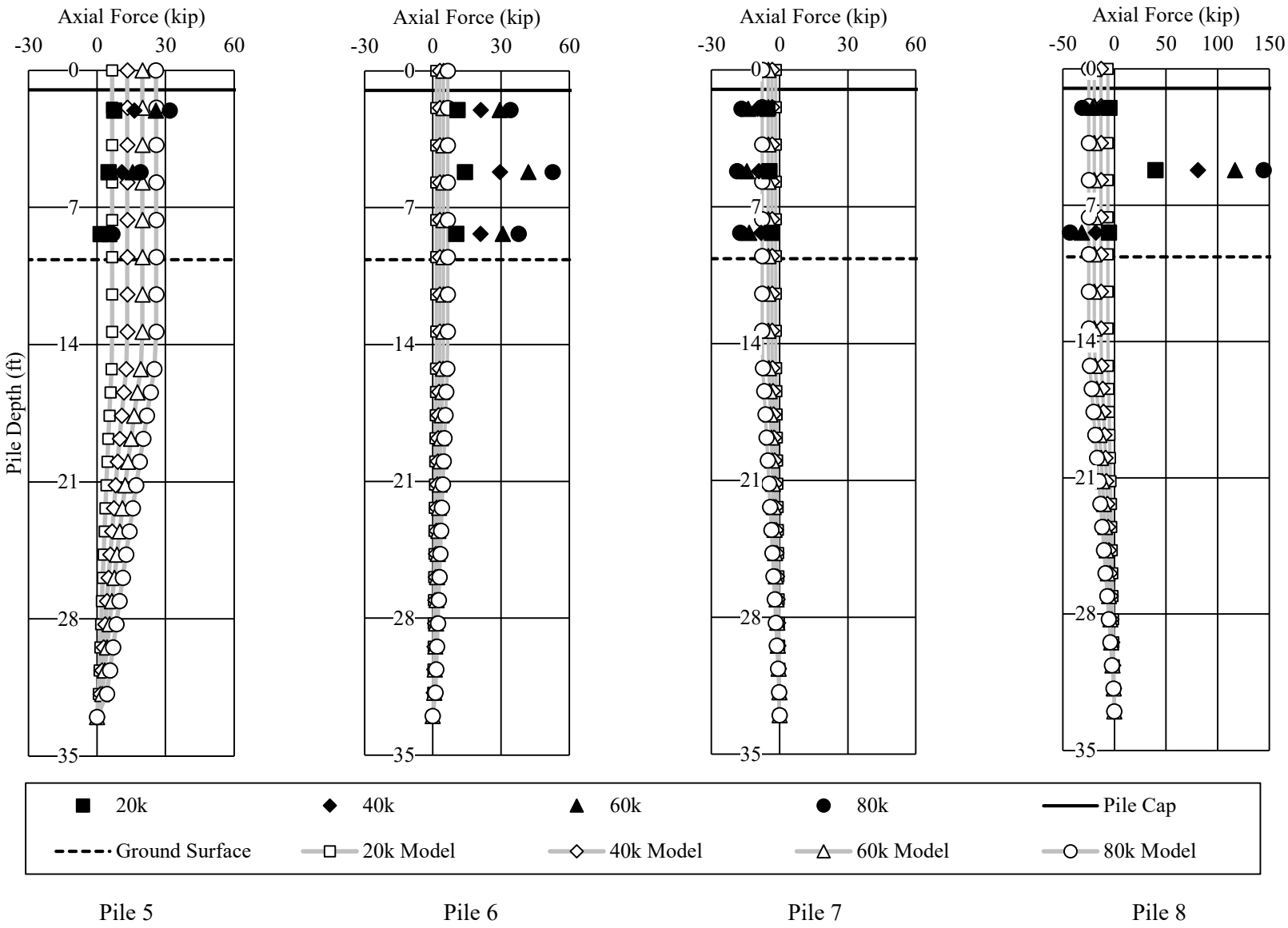

Figure 7-15 – AUNGES Vertical Pile Bent Calibrated Model Axial Load Profiles Comparison

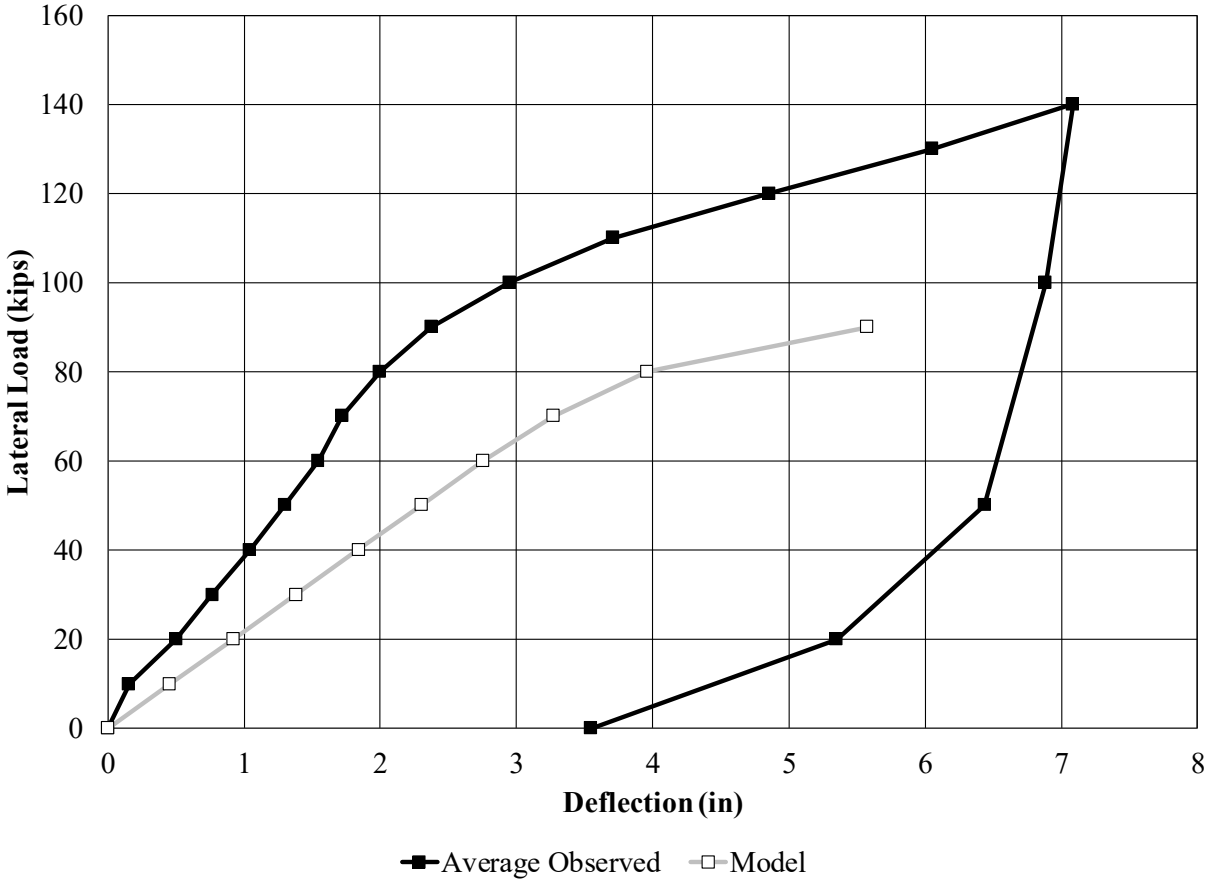

Figure 7-16 – AUNGES Vertical Pile Bent Calibrated Model Load versus Deflection Comparison

The calibrated models accurately matched the inclinometer profiles. The point of inflection was matched by lowering the soil profile around the piles. The soil initial soil parameter models included soil profiles developed from in-situ testing. For calibration, the profiles were modeled using standard models in FB-Multipier. Soil properties were altered to create accurate matches. The calibrated models negatively affected the match seen in the comparison between the initial models and observed data. Calibrated models overpredicted the magnitude of moment in the piles. Axial matches were stronger than seen in the initial model comparisons, but were still not strong matches to the field results. The load deflection chart

showed that the calibrated model charts predicted less stiff bent behavior than the observed results.

Results of the calibration suggest that accurately predicting the lateral deflection of the piles produces a better prediction of the axial load induced by laterally loading the bent. This is accomplished by incorporating p-y modifiers to models of battered pile bents. Models show that the upper few feet of soil surrounding the pile provides little resistance to the lateral load. When modelling lateral load tests, it is suggested to disregard the upper two feet of soil.

Chapter 8 Conclusions and Recommendations for Future Work

8.1 Summary

Bridges with multiple standalone bents are commonly used by ALDOT for the support of bridges statewide. This thesis investigated the load path of lateral load into typical ALDOT bridge bents. The research was initiated when assumptions used in bridge design caused large variations in the expected axial loads for bent piles. Research was conducted on four full scale test bents. One bent was a new construction, the second bent was an in service bent, and the last two were standalone bents. Test bents were modeled and full scale load tests were schedule. Each bent was subjected to lateral load test in accordance with the schedule determined from initial modeling. Data collected during the load tests was reduced and axial versus depth, moment versus depth, and load versus deflection plots were created. These results were compared to initial models. Initial models were then calibrated to try and match the observed bent behavior to produce recommendations on design assumptions.

Results and calibrated models from the AUNGES standalone test bents provided insight into the transfer of lateral load from the pile cap to the piles, the differences in the behavior of piles in battered and vertical pile bents, and the failure mechanisms of pile bents at high lateral loads. Lateral load was seen to be transferred into the piles through induced moments. The magnitude and effectiveness of the moment development was affected by the depth of the pile embedment into the pile cap. Load tests results showed that increasing lateral loads induces different behavior in battered pile and vertical pile bents specifically in the amount of axial load transferred to interior

piles. For vertical pile bents, lateral loads induce horizontal sway without rotation. This leads to increased amounts of deflection and higher moment transfer. There is also less axial load transferred to the piles than in the battered pile bent under the same loads. Battered pile bents also experience rotation when lateral load is applied. This induces large axial forces in the interior piles. The difference in behavior also provides insight into the predicted failure mode. In battered pile bents, the failure was seen when interior piles tried to pull out of the cap. In vertical pile bents, failure was more evident in the yielding of the pile flanges. The load test and modeled information was used to determine the conclusions and recommendations presented in the following sections.

8.2 Conclusions

- The research objective of modeling all test bents to develop full scale load test schedules was accomplished.
- Four separate test bents were instrumented and full scale load tests were completed.
- Preliminary models were successfully calibrated to represent the observed load test results for the two AUNGES test bents.
- The pile to cap connection is between a fixed and pinned head connection but is more accurately modeled as a fixed connection in FB Multipier. Models produced in FB Multipier using this assumption, will over predict the moment in the piles while underpredicting the deflection.
- P-y multipliers should not be neglected in modeling bridge bent piles spaced greater than 5 pile diameters apart. The use of these multipliers was required to calibrate the models in this thesis.
- The top two feet of soil provides little lateral resistance in lateral loading scenarios and should be disregarded during design modeling.

- Increasing lateral load on bents induces axial load in the bent piles. These loads become significant in battered pile bents, specifically for the interior piles and their connection to the bent cap. Pile batter induces rotation in the bent cap, creating large tensile forces at the pile to cap connection. Vertical pile bents experience lateral deflection with out rotation which provides smaller increases to axial demand than seen in the behavior of battered pile bents.
- All vertical pile bridge bents are preferred for use in standard ALDOT bridges due to better constructability and comparable performance to battered pile bents. Vertical pile bents also provide less axial demand at the pile to cap connection.
- Failure in bent caps due to lateral load in the weak direction is initiated at the pile to cap connection, typically as the piles try to pull out from the bent cap. Greater embedment into the bent cap provides greater resistance to lateral load by allowing the pile to cap connection to better develop moments in the pile head, thus preventing the axial failures typical of lesser embedment depths.

8.3 Recommendations for Future Work

- It is recommended that further research be done on the pile to cap connection detail, specifically in regard to the depth of pile embedment and it's effect on the failure mechanism for bents under lateral loads.

References

Abu-Farsakh, M. Y., Yu, X., Pathak, B., Alshibli, K., & Zhang, Z. (2011). Field Testing and Analyses of a Batter Pile Group Foundation Under Lateral Loading. *Transportation Research Record*, 42-55.

Brown, D. A., Morrison, C., & Reese, L. C. (1988). Lateral Load Behavior of Pile Group in Sand. *Journal of Geotechnical Engineering*, 1261-1276.

Brown, D. A., O'Neill, M. W., McVay, M., El Naggar, M. H., & Chakraborty, S. (2001). *Static and Dynamic Lateral Loading of Pile Groups.* Washington, D.C.: National Academy Press.

Campbell, J. (2015). *Experimental Testing and Analytical Modeling of Driven Steel Pile Bridge Bents.* Auburn, Alabama.

Coduto, D. P. (1999). *Geotechnical Engineering Principles and Practices.* Upper Saddle River, New Jersey: Prentice-Hall, Inc.

Eberhard, M. O., & Marsh, M. L. (1997). Lateral-Load Response of Two Reinforced Concrete Bents. *Journal of Structural Engineering*, 461-468.

Gerber, T. M., & Rollins, K. M. (2009). Behavior of a Nine-Pile Group With and Without a Pile Cap. *2009 International Foundation Congress and Equipment Expo*, (pp. 530-537).

Lawton, E. C., Pantelides, C. P., & Cook, C. R. (2001). *Soil-Pile-Structure Interaction of Bridge Bents Subjected to Lateral Loads.* Salt Lake City, Utah: The University of Utah.

Lin, S.-S., & Liao, J.-C. (2006). Lateral Response Evaluation of Single Piles Using Inclinometer Data. *Journal of Geotechnical and Geoenvironmental Engineering*, 1566-1573.

McCarthy, D. F. (2007). *Essentials of Soil Mechanics and Foundations Seventh Edition.* Upper Saddle River, New Jersey: Pearson Prentice Hall.

Miller, D. E. (2013). *Live-Load Response of In-Service Bridge Constructed with Precast, Prestressed Self-Consolidating.* Auburn, Alabama.

Ooi, P. K., & Ramsey, T. L. (2003). Curvature and Bending Moments from Inclinometer Data. *International Journal of Geomechanics*, 64-74.

Possiel, B. A. (2008). *Point of Fixity of Laterally Loaded Bridge Bents.* Raleigh, North Carolina: North Carolina State University.

Reese, L. C., & Wang, S.-T. (2006). *Verification of Computer Program LPile as a Valid Tool for Design of a Single Pile under Lateral Loading.*

Richards, P. W., Rollins, K. M., & Stenlund, T. E. (2011). Experimental Testing of Pile-to-Cap Connections for Embedded Pipe Piles. *Journal of Bridge Engineering*, 286-294.

Robertson, P. K., Davies, M. P., & Campanella, R. G. (1989). Design of Laterally Loaded Driven Piles Using the Flat Dilatometer. *Geotechnical Testing Journal*, 30-38.

Rollins, K. M., & Stenlund, T. E. (2010). *Laterally Loaded Pile Cap Connections.* Salt Lake City, Utah: Utah Department of Transportation.

Rollins, K. M., Olsen, K. G., Jensen, D. H., Garrett, B. H., Olsen, R. J., & Egbert, J. J. (2006). Pile Spacing Effects on Lateral Pile Group Behavior: Analysis. *Journal of Geotechnical and Geoenvironmental Engineering*, 1272-1283.

Rollins, K. M., Peterson, K. T., & Weaver, T. J. (1998). Lateral Load Behavior of Full-Scale Pile Group in Clay. *Journal of Geotechnical and Geoenvironmental Engineering*, 468-478.
Rollins, K. M., Sparks, A. E., & Peterson, K. T. (n.d.). Lateral Load Capacity and Passive Resistance of Full-Scale Pile Group and Cap. *Transportation Research Record*, 24-32.
Ruesta, P. F., & Townsend, F. C. (1997). Evaluation of Laterally Loaded Pile Group at Roosevelt Bridge. *Journal of Geotechnical and Geoenvironmental Engineering*, 1153-1161.